Sustainable underground reactive barrier to attenuate contaminants from agricultural drainage

A Dissertation Presented for the
Doctor of Philosophy
Degree
The University of Tennessee, Knoxville

Yuchuan Fan
December 2021

DEDICATION

This dissertation is dedicated to my Mom, Dad, and my girlfriend
for your endless love and support.

ACKNOWLEDGEMENTS

I would like to thank my main advisor, Dr. Jaehoon Lee, for his continued support. I appreciate his kindly support, attention and help. I am grateful for the resources he provided, which stem from countless hours of hard work reading papers and writing grants. The work in this dissertation would have been impossible without him.

There is not enough room to thank everyone who has positively impacted my time at UT. My success comes from working within a community of excellent scientists, both within and outside of my lab. Thank you to my committee members: Dr. Jie Zhuang, Dr. Michael Essington, Dr. Sindhu Jagadamma, and Dr. John Schwartz. Their thoughtful questions and suggestions greatly improved my dissertation research. Thank you to Galina, who keeps the Essington's lab running and analyzing collected water samples for me. Thank you Wesley Wright, who help me a lot of on constructing the field denitrifying bioreactor and technical help on laboratory experiments. Thank you to Melanie, who helped me order chemical staffs.

I am also grateful for the funding agencies, Chinese Scholarship Council, without their support, I would not have this great opportunity to have this wonderful journey (No. 201706350282).

Thank you to my family as well: Mom, and Dad. You kept me grounded and encouraged me. Special thanks to Mom and Dad, for cultivating my love of science and helping me to pursue my dreams. They saw the spark when I was young, and fanned it into a flame.

Finally, I would like to thank my girlfriend, Wen Liu. She has shown me faithful love and support through the ups and downs of graduate school. She believed in me though the entire process and move from China to accompany with me. During her own arduous trek through graduate courses at Agricultural Economic Department at UT, she continued to sacrifice her time and energy and support me. It has been rewarding to have a scientifically minded girlfriend with whom to share my exciting discoveries (as well as an abundance of boring details). I am eternally grateful to my supporter and cheerleader.

ABSTRACT

Denitrifying bioreactor (DNBR) has become a popular edge-of-field practice applied to reduce nitrate over the Mississippi river and to prevent a downstream hypoxic zone occurring at the Gulf of Mexico. Despite widespread field and laboratory studies, fewer investigations have been directed toward a systematic means of evaluating the nitrate removal performance achieved by various filling materials, abiotic factors, and other critical parameters. Our ultimate goal is to improve the nitrate removal by choosing the optimum fill materials and operate under optimal conditions, meanwhile, modeling the DNBR by critical variables. This study begins by establishing a global database. Forty filling materials were systematically categorized by natural carbon (NC), non-natural carbon (NNC), inorganic materials (IC), and multi-material (MM). The results showed that MM is the best option under a comprehensive consideration. Subsequently, based on this established database, a data-driven approach was adopted to study how nitrate removal rate (NRR) and nitrate removal efficiency (NRE) respond to various abiotic factors, including media age, hydraulic retention time, influent nitrate concentration, pH, dissolved organic carbon, dissolved oxygen content, temperature, and effective porosity. The results showed that HRT is the most

important abiotic factor for NRR. Then, biochar and silage leachate, two primary contributors of industrial and agricultural waste, were considered as amending materials to improve NRR and NRE in DNBR. The study showed that adding biochar and silage leachate together can significantly increase NRR. Following this, two nonlinear models were developed to describe the relationship between NRR, NRE, and hydraulic retention time (HRT). The results showed that the two models had a good performance (R^2>0.9). Moreover, C/N ratio affect NRE was also studied in the above experiments. We found the relationship between NRE and C/N ratio can be well explained by a nonlinear model. Taken together, these investigations provide an improved understanding of how to choose suitable filling materials and prepare optimal environmental conditions to enhance nitrate removal performance in DNBR for stakeholders and practitioners.

TABLE OF CONTENTS

LIST OF TABLES

LIST OF FIGURES

INTRODUCTION

Background

There is a need for cost-effective and proven best management practices to mitigate contaminants (e.g., excess nutrients, pathogens, and veterinary pharmaceuticals) in agricultural drainage. Typical concentrated animal feeding operations, such as dairy facilities, produce large quantities of manure which is stored in lagoons or holding ponds before being applied to nearby crop or pasture fields. Off-site movement of the manure, as well as other fertilizers through storm water runoff or percolation to groundwater, has been recognized as a major source of contamination of water bodies. This is especially true in areas with high rainfall and substantial topographic relief. Therefore, animal manure management is generating increased national and international concern, and many believe improved management practices are required. A major reason for this concern is the presence of chemicals of environmental concern (CEC) in the animal wastes (Soto et al. 2004; Tasho and Cho 2016). Veterinary antibiotics are the most commonly found CEC in manures because of their widespread use in livestock production, where they are used to treat sick animals (Landers et al. 2012). Current and past research has focused on identifying the presence of these antibiotics in the environment and their possible sources. Additionally, considerable research has focused on the possible effects that exposure to these chemicals can have on the health of humans and wildlife. However, little work has been done to develop a sustainable and cost-effective remediation system.

One technology that has been successfully employed for remediating agricultural chemicals, such as nitrate-nitrogen (NO_3-N) in groundwater, is the underground reactive

barrier, which is also known as denitrification beds, a denitrification wall, or a denitrifying bioreactor (DNBR) (Cameron and Schipper 2010; Schipper et al. 2010b). A DNBR is constructed by mixing an organic carbon (C) source (typically sawdust or woodchips) into soil below the water table in order to intercept groundwater flow (Fig. I-1). The increased and continuous supply of C to the denitrifiers enhances denitrification, such as the reduction of nitrate (NO_3) to N_2 after the production of a series of intermediate N oxide products, thus reducing the quantity of NO_3 in the discharge.

Abiotic factors

The performance of denitrifying bioreactor can be influenced by several abiotic factors, such as hydraulic retention time (HRT) (Gibert et al. 2008; Robertson 2010; Zulkhairi et al. 2010; Damaraju et al. 2015; Guo et al. 2017), influent nitrate concentration (C_{in}) (Schmidt and Clark 2012), dissolved oxygen (DO) (Gómez et al. 2002; Schmidt and Clark 2012), pH, temperature (Christensson et al. 1994; Xue et al. 1999; Rostron et al. 2001; Elefsiniotis and Li 2006; Robertson and Merkley 2009; Elgood et al. 2010; Vacková et al. 2011; Schmidt and Clark 2013; Damaraju et al. 2015; Hassanpour et al. 2017), dissolved organic carbon (DOC) (Maxwell et al. 2019b), porosity, and saturation level (Maxwell et al. 2019b, a; McGuire and Reid 2019). Due to the complex interaction that can occur among these various conditions when studying DNBRs, how the different abiotic factors influence the performance of DNBR is still not completely understood. Moreover, understanding the correlation between each abiotic factor and the performance of DNBR is highly important for designing and improving DNBR under various situations.

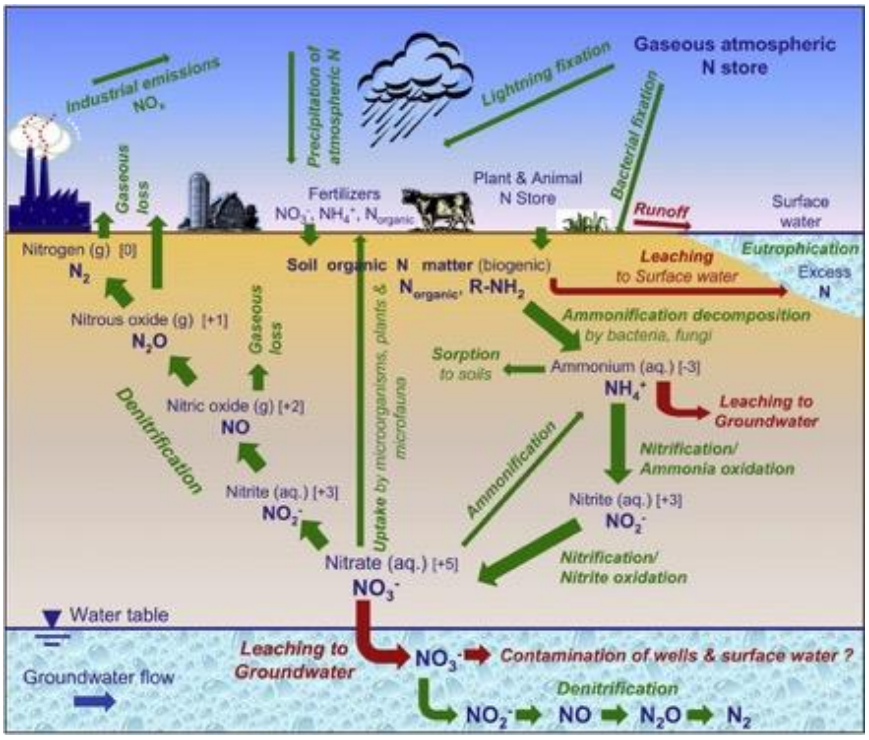

Figure I- 1 The schematic of N cycling in the agricultural system (Rivett et al. 2008)

Chemical treatment

DNBRs have been primarily focused on nitrate removal (Schipper et al. 2005; Gibert et al. 2008; Gottschall et al. 2016; Roser et al. 2018), but alternative CEC have also been studied, including phosphate (Bock et al. 2015; Gottschall et al. 2016; Hua et al. 2016), ammonium (Sakuma et al. 2008), herbicide (Ilhan et al. 2012), and veterinary antibiotics (Ilhan et al. 2012; Gottschall et al. 2016). However, the efficiencies of DNBRs for treating the various CEC are still uncertain and require further study.

Nitrate

Nitrogen (N) has an impact on the health of humans and our planet, and in fact, humans have altered the N cycle during the last 100 years (Onley 2017). Since the Haber-Bosch process was developed for the conversion of N_2 into ammonia, humans have increased the production of reactive N by approximately 100 Tg per year (Fields 2004). Further, the combustion of fossil fuels and the overuse of N fertilizers contributes to smog, low-lying ozone, the greenhouse gas effect, eutrophication, and drinking water contamination (Fields 2004). The World Health Organization (WHO) stipulated that the maximum NO_3 concentration in drinking water should be 50 mg L^{-1} (Organization 2008). The US EPA maximum permissible concentration for drinking water is 10 mg L^{-1} of NO_3^- N (EPA 2009). The permissible NO_3-N concentration in groundwater is 20 mg L^{-1} (PRC 1994) in China, while the maximum permissible concentration for nitrate in surface and central drinking water sources is less than 10 mg L^{-1} of NO_3-N (Zhang et al. 2013).

Fortunately, nature can self-remediate the impact of NO_3 on aquatic environments through the denitrification process, which transforms NO_3 to N_2 through the following

intermediaries: $NO_3 \rightarrow NO_2 \rightarrow NO \rightarrow N_2O \rightarrow N_2$ (Averill and Tiedje 1982). This processing can reduce the amount of NO_3 and nitrous oxides produced, which can then help to prevent eutrophication and global warming, as NO_3 increases algal blooms and N_2O is a potent greenhouse gas with a global warming potential 310 times greater than that of carbon dioxide. Denitrification is an important part of the N cycle (Fig. I-2). Several studies have demonstrated that DNBRs can be an effective approach to reduce NO_3 in aqueous environments by using the denitrification process (Volokita et al. 1996b; Tsai et al. 2004; Warneke et al. 2011; Gutierrez-Wing et al. 2012; Shen et al. 2015). In addition to denitrification, NO_3 depletion can also occur through two other pathways: (i) dissimilatory NO_3 reduction to ammonium (DNRA), and (ii) microbial assimilation or immobilization of inorganic N. DNRA typically occurs when NO_3 (electron acceptor) becomes limited, while denitrification dominates when organic C (electron donor) becomes limited (Kelso et al. 1997). However, several studies found DNRA as a potential NO_3 removal pathway in sub-surface systems (Bulger et al. 1989). In some environments, heterotrophic microorganisms can assimilate inorganic N for their growth causing a temporary reduction of NO_3 in the system. Stark and Hart (1997) reported that microorganism immobilized almost all the NO_3 produced in a natural forest landscape, resulting in a transient loss of NO_3 from the system. The availability of inorganic N and organic C, together with other biotic and abiotic factors, determines the dominance of one pathway over another. Measuring the NO_3 concentration of the effluent alone, as is commonly performed in practice, is insufficient to determine if denitrification occurred in the DNRA or if a portion of the NO_3 was immobilized in microbial biomass.

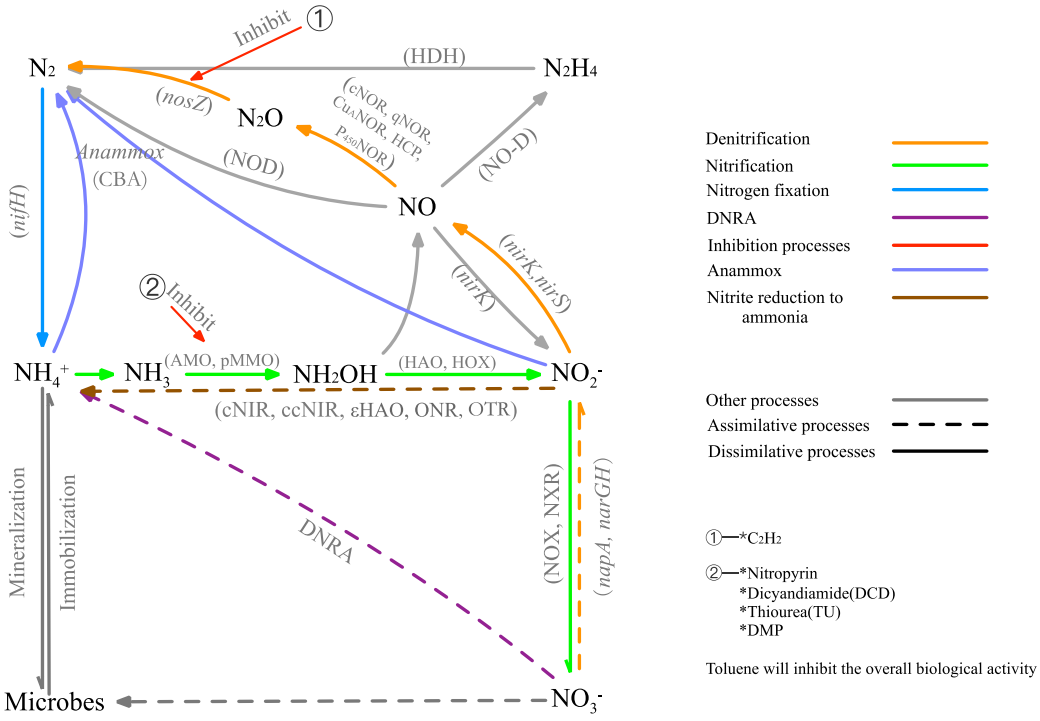

Yuchuan Fan 2019

Figure I- 2 The nitrogen (N) cycle in forest soil. The cycling of N in soil can be subdivided into (i) decomposition processes, (ii) assimilative processes, and (iii) dissimilative processes. Anammox, anaerobic ammonia oxidation; DNRA, dissimilatory nitrate reduction to ammonium. This diagram was adapted from Levy-Booth et al. (2014).

Phosphate

Phosphorus (P) is also a chemical of concern in drainage water, as it can trigger eutrophication in freshwater systems (Dils and Heathwaite 1999; Macrae et al. 2007), such as rivers, lakes, and wetlands (Sundareshwar et al. 2003; Søndergaard et al. 2007). Phosphorus transport from agricultural fields continues to be a focal point for addressing harmful algal blooms and nuisance algae in freshwater systems throughout the world. To date, large numbers of water samples in European countries detected P over detection limits (Holman et al. 2008). In the US, severe problems are also being encountered, especially in areas were P-sensitive water bodies are found, such as the Great Lakes, Chesapeake, Delaware Bay, Lake Okeechobee, and the Everglades (Daniel et al. 1998). Phosphate (PO_4), as previously indicated, is one of the significant nutrients that have been found in subsurface drainage waters. In agriculture fields, to guarantee sufficient nutrient supply for crop production, a solution concentration of above 3 mg L^{-1} is targeted, and a P concentration as high as 30 mg L^{-1} can be found in soil runoff (Withers et al., 2000). Furthermore, many studies have demonstrated that phosphorus loss from agricultural fields occurs predominantly in surface runoff (Sharpley et al., 1993; Heathwaite and Dils, 2000). Kladivko et al. (1991) measured agricultural subsurface drainage phosphate-phosphorus (PO_4-P) values in the 0.005 to 0.1 mg L^{-1} at an experimental field site in Indiana. Laubel et al. (1999) monitored storm event PO_4 in the range of 0.04 to 0.39 mg PO_4 L^{-1} at the subsurface drainage outlet for a small agricultural watershed in Denmark. Phosphate can also be discharged from subsurface drainage systems in local settings. Median PO_4-P values of 0.09 and 0.11 mg L^{-1} were measured by King et al. (2006) at two sites on a golf course located in Austin, Texas. In general,

drainage and subsurface PO_4-P concentrations above 0.5 mg L^{-1}, particularly in agricultural settings, would be considered unusual (Sims et al., 1998; Kinley et al., 2007). Indeed, total P concentrations≥0.02 mg L^{-1} are often considered problematic (Correll, 1998). In the United States, water quality standards for P are determined at the state level. However, only Illinois, Minnesota, and Wisconsin have set statewide numerical criteria for P levels or critical P concentrations for specific surface water bodies (USEPA, 2014). According to the USA EPA (1986), these levels were set at 1) no more than 0.1 mg L^{-1} for streams which do not empty into reservoirs, 2) no more than 0.05 mg L^{-1} for streams discharging into reservoirs, and 3) no more than 0.025 mg L^{-1} for reservoirs. Phosphorus removal has not been a focus of previous DNBR studies, and there remains a significant opportunity to engineer DNBR systems that can treat P and NO_3 simultaneously (Bock et al. 2015).

Antibiotics

Agriculture represents a large portion of the overall use of antibiotics worldwide. Animal production and aquaculture are relevant sources of environmental exposure to antibiotics and antibiotic-resistance development in soil (Gorbach 2001; Pruden et al. 2013; Wepking et al. 2017). Even though the veterinary antibiotics were changed from over-the-counter use to a marketing status requiring veterinary oversight at the beginning of 2017, some rebound in the reported sales volume in subsequent years. (FDA, 2020).

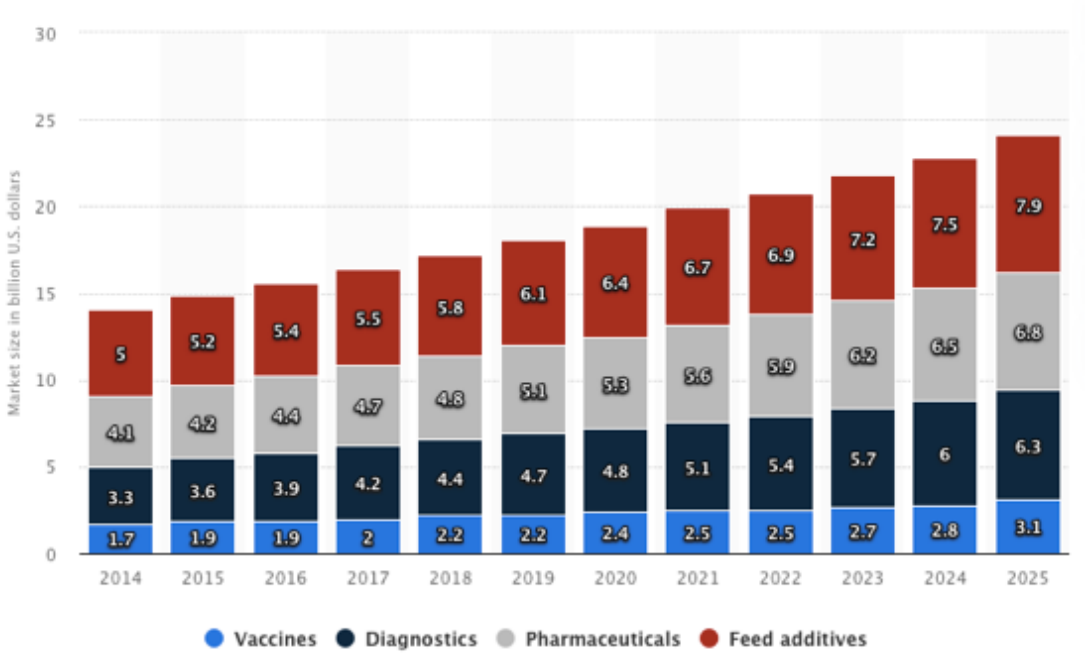

Figure I- 3 U.S. animal health market, by product, 2014 - 2025 (USD Billion)

Many of the antibiotics (40 to 95 %) are not entirely metabolized and are excreted in the urine and feces (Halling-Sørensen et al. 1998; Montforts et al. 1999; Tolls 2001; Winckler and Grafe 2001; Boxall et al. 2002; Halling-Sørensen et al. 2002; Vaclavik et al. 2004; Aga et al. 2005). The antibiotics contained in manure and are subsequently applied to soil and have the potential to contaminate surface water, via overland (runoff) and drain flow, as well as groundwater by leaching (Halling-Sørensen et al. 1998; Boxall et al. 2002; Kay et al. 2004; Kreuzig et al. 2005; Lee et al. 2014).

Before the veterinary antibiotics was banned in the United States, in agriculture, most livestock feedlots typically use large amounts of antibiotics for both disease prophylaxis and promoting growth because it ultimately improves animal productivity. As a result, the US animal health market has reported the antibiotics will have higher demand in the future (Fig. I-3). For example, Hamscher et al. (2003) reported that several types of antibiotics, including the tetracyclines and macrolides were detected in total amounts up to 12.5 mg kg^{-1} in pig-house dust which originates from feed, bedding, feces, and the animals themselves. Dewey et al. (1999) reported that 88% of 712 swine farms in the United States used antibiotics in feeds, and most (92%) antibiotics were fed on a continuous basis, especially to young growing swine. Kemper (2008) estimated that 11,200 Mg of antibiotics were used for nontherapeutic purposes for cattle, swine, and poultry, in the absence of disease, in the United States every year. The antibiotic treatment at nontherapeutic levels is considered to increase weight gain by the suppression of intestinal bacteria (Mitscher 1978), inhibition of subclinical infections, reduction in harmful microbial metabolites, and to enhanced nutrient uptake (Gaskins et al. 2002). The net gain achieved by feeding antibiotics to swine is estimated to be $45.5

million each year (Mathews Jr 2001). Although new legislative regulations targeting the administration of veterinary antibiotics in the United States have banned their use as prophylactics and for nontherapeutic purposes without the authorization of a veterinarian (U.S. Food and Drug Administration, 2015), environmental dispersal from therapeutic use will continue.

The legacy of veterinary antibiotics still exists in the agricultural system. The significant impact antibiotics have on soil can be illustrated by using sulfamethazine (SFM) as an example. The unmetabolized sulfa antibiotics in manure and urine may present a potential environmental hazard, especially when manure is applied directly to the soil surface. Our preliminary research with sulfur-based antibiotics showed that they were transported through soil in a nonequilibrium process and they were highly mobile in selected soils (Essington et al. 2010; Lee et al. 2014). This demonstrates that it is necessary to develop an innovative and cost-effective system to remediate these contaminants in order to protect water resources.

Filling materials

The carbon source used in DNBRs consists of natural organic carbon and synthetic biodegradable polymers. The use of natural organic carbon has been studied in detail during the last two decades. These sources include, maize cobs, wheat straw (Soares and Abeliovich 1998; Aslan and Türkman 2005), rice stalks, rice straw, cotton (Rocca et al. 2005; Della Rocca et al. 2006), woodchips (Schmidt and Clark 2012; Meffe et al. 2016), cardboard (Greenan et al. 2006), cornstalks (Greenan et al. 2006), corn stover, coniferous (Gibert et al. 2008), barley, willow (Gibert et al. 2008), leaves (Gibert et al. 2008), and

newspaper (Volokita et al. 1996b). Synthetic biodegradable polymers have also been studied. These include, polycaprolactone (PCL) (Boley et al. 2000; Honda and Osawa 2002; Walters et al. 2009), polyactic acid (PLA), polybutylene succinate (PBS), poly-3-hydroxybutyric acid (PHB) (Boley et al. 2000; Walters et al. 2009), and poly-3-hydroxybutyrate-co-hyroxyvelate (PHBV). Natural organic carbon sources remain the most common and frequently recommend filling material. From among all the natural organic carbon sources, the use of woodchips has been reported in many studies, because it is relatively inexpensive and readily available. In addition to using woodchips alone, adding an auxiliary material to improve the NO_3 removal rate has become increasingly popular. These additives to DNBRs include zero-valent iron (Su and Puls 2007), biochar (Bock et al. 2015; Bock et al. 2016), steel byproduct (Hua et al. 2016), and acetate (Roser et al. 2018). However, a cost-effective and sustainable treatment is still needed.

Many agricultural wastes have been used for heterotrophic denitrification, including maize cobs, wheat straw, and rice stalks (Li et al. 2017). The rate of heterotrophic denitrification is controlled by factors such as the concentrations of bioavailable C, oxygen (O_2), and NO_3-N (Seitzinger et al. 2006). Maize and wheat straw organic channel barriers (OCBs) were also capable of providing more labile C than wood media, which results in higher NO_3-N removal rates (Cameron and Schipper 2010). The findings of Greenan et al. (2006) highlighted that additional C substrates resulted in NO_3-N removal in the following ascending order: wood chips< wood chips and soil< cardboard< cornstalks.

In situ investigations have indicated that wood media annually consume less than 5% of the initial C mass within bioreactors (Robertson et al. 2000; Schipper and Vojvodic-Vukovic 2001; Robertson and Merkley 2009; Schmidt and Clark 2012). Small-

scale laboratory experiments demonstrate that alternative C substrates provide higher NO_3-N removal capacities than wood media and can be regarded as efficient C sources that rapidly release bioavailable C for the denitrification bacteria (Greenan et al. 2006). Denitrification bioreactors achieve mean NO_3-N mass removal rates in the range of 0.62-12.7 g N m^{-3} d^{-1} (Schipper et al. 2010a).

Until now, few studies have focused on the removal efficacy of different agrochemicals by active barriers. Further, it should be recognized that not all agrochemicals will be removed during reactor operation. Liu et al. (2015) reported that their OCBs composed of rice straw (RS) produced a higher mass removal rate of NH_4-N and NO_3-N than of PO_4-P, and the amount of RS in the barrier was positively correlated with NH_4-N and NO_3-N, while negatively correlated with PO_4-P removal. Some studies also reported that the woodchip filters of an on-farm treatment system for dirty dairy water also achieved a poor PO_4-P removal rate of 31% (Ruane et al. 2011).

Solid-phase denitrification relies on solid materials as a carbon source for biological denitrification and carriers for biofilm growth (Xie et al. 2017). This is a practical approach for nitrate removal from groundwater. The advantages of this are that the risks of overdosing are avoided, the process is simple to control and requires limited supervision, and produces a low amount of secondary organic pollution (Boley et al. 2000). The solid carbon materials can be divided into two classes; natural organic substances, such as woodchips, cotton, wheat straw, maize cobs, and reeds (Xie et al. 2017), and synthetic biodegradable polymers, which include PLA, PCL (Boley et al. 2000; Honda and Osawa 2002; Walters et al. 2009), PHB (Boley et al. 2000; Walters et al. 2009), and PBS and PHBV. In general, natural organic substances cannot offer

enough nutrition for microbes, and natural cellulose materials cannot support a long service life for NO_3 removal. For example, a small number of studies demonstrated that cracked newspaper and untreated short-staple cotton could be used as the carbon source for denitrification. However, the removal efficiency decreased with the fast consumption of these materials (Volokita et al. 1996a; Volokita et al. 1996b). As for synthetic biodegradable polymers, they are associated with a higher cost, a high amount of dissolved organic carbon and dark color in the effluent, and a relatively low overall denitrification efficiency (Healy et al. 2012). Due to these reasons, many researchers consider adopting mixed substrates. For example, blending biodegradable plastics with inexpensive organic substances (such as straw, cob, and bagasse) not only reduces cost but also improves the bed properties and biodegradability (Snaidr et al. 1997; Tokiwa et al. 2009).

Agricultural and Industrial waste

Biochar

Biochar is "a solid material obtained from thermochemical conversion of biomass in an oxygen-limited environment" as defined by the International Biochar Institute (IBI). It is a byproduct from industrial production and its characteristics, such as high pH and surface area, depends on the feedstock and temperature (Table 2). Biochar has been proven successful in reducing the mobility of N and P in agricultural soils (Clough and Condron 2010; Beck et al. 2011; Coumaravel et al. 2011; Nelson et al. 2011). Conversely, few studies have reported that biochar could be used in reducing NO_3, PO_4, and antibiotics in bioreactors. Speratti et al. (2018) studied the effects of biochar

feedstock (cotton residue, swine manure, eucalyptus sawmill residue, and sugarcane filtercake) and pyrolysis temperature (400, 500, and 600 °C) on leachate NO_3 concentrations when mixed with soil at 5% by weight. Their results indicated that filtercake and eucalyptus biochar functioned as the best treatments for retaining NO_3 in a Brazil Cerrado Arenosol soil. Further, Paetsch et al. (2018) compared the effect of in-situ aged and fresh biochar on the hydraulic conditions and microbial C in soil under drought conditions. They concluded that aged biochar could improve microbial C use under drought. Furthermore, biochar addition can ameliorate water regime, especially under drought conditions.

Silage leachate

Silage leachate is concentrated agricultural wastewater, and it requires management in livestock agriculture. Silage effluent can rapidly deplete DO, causing the death of fish and eutrophication when it reaches surface waters. It is corrosive to concrete and metal structures due to its acidity (pH≈4), making containment, handling, and disposal a challenge (Gebrehanna et al. 2014). In 2012, all haylage, grass silage, and green chop production amounted to 33 million tons, for corn silage 113 million tons, and for sorghum silage 6 million tons in the United States (NASS 2012). Further, many researchers had reported that other countries also produce large quantities of silage, such as New Zealand (Tikkisetty and Kuperus 2004) and China (Lujia et al. 2002). The storage of silage can often lead to the generation of wastewater in the form of leachate and runoff (Holly et al. 2018). If the ensiled crop moisture is high (>75-85%) (Gebrehanna et al. 2014) and sustained for a 30 to 60 d period, 90% of the silage effluent will occur within the first 20-

26 d (Savoie 1995). Moreover, silage leachate increases the nutrient concentrations (Faulkner et al. 2011) in the water systems, contaminating ground and surface waters (Holly et al. 2018). The chemical properties of silage leachate were initially reported by McDonald et al. (1991). They highlighted that the pH can be acidic, ranging from 3.5 to 5.5, and can contain 300 to 600 mg L^{-1} P, 800 to 3,700 mg L^{-1} of organic N, and 12,000 to 90,000 mg L^{-1} of five-day biological oxygen demand (BOD_5). Holly et al. (2018) also reported that intensively sampled sites of silage runoff had the following chemical characteristics; pH range from 4.21 to 6.36, BOD_5 from 1,008 to 4,011 mg L^{-1}, COD from 2,320 to 12,658 mg L^{-1}, total phosphorus (TP) from 21 to 98 mg L^{-1}, total kjeldahl nitrogen (TKN) from 53 to 416 mg L^{-1}, total ammoniacal nitrogen (TAN) from 18 to 129 mg L^{-1}, and total solids (TS) from 2,138 to 10,072 mg L^{-1}. For this reason, we performed a targeted literature review of the physicochemical properties of silage leachates (Table 3 and Appendix Table 2).

Research questions

A denitrifying bioreactor was systematically studied to evaluate the influence of filing materials and abiotic factors on performance. We also developed a predictive tool to model the influence of bioreactor properties on performance. A summary of each chapter and the research questions investigated is outlined below.

First, we established a global database from 63 peer-reviewed articles obtained from the web of science. Then, we performed a comprehensive systematic evaluation of the filling materials utilized in denitrifying bioreactors from the different perspectives,

including taxonomy, pollution swapping, cost analysis, and mechanisms to understand the optimal filling materials in denitrifying bioreactors.

Next, a diverse package of advanced tools was used to study how the abiotic factors impact nitrate removal performance.

In Chapter 3, agricultural (silage leachate) and industrial waste (biochar) were considered as an additive to the woodchip bioreactor to improve the nitrate removal performance. The nitrate removal performance was investigated under different nitrate loadings and hydraulic retention times.

In Chapter 4, two nonlinear models were developed to predict nitrate removal rate and nitrate removal efficiency based upon hydraulic retention time. The performance of two nonlinear models were also evaluated.

Finally, in Chapter 5, one nonlinear model was developed to predict nitrate removal efficiency relative to C/N ratio in inflow and outflow. The performance of the nonlinear model was evaluated, and the critical parameters were analyzed.

- Chapter 1: A systematic review highlighting the role of filling materials for nitrate removal in denitrifying bioreactors.
    - *Research Questions:*
        - *What filling materials have been studied in denitrifying bioreactors?*
        - *What is the nitrate removal performance for different filling materials?*
        - *What is the potential pollution generated by swapping different filling materials?*

        - *What is the cost of different filling materials?*
        - *What are the possible mechanisms of nitrate removal for different filling materials?*

- Chapter 2: The role of abiotic factors affecting nitrate removal in woodchip bioreactor.
    - *Research Questions:*
        - *How do different abiotic factors individually affect nitrate removal performance in woodchip bioreactors?*
        - *Do the study scales influence affect nitrate removal performance in woodchip bioreactors?*
        - *How do different abiotic factors affect nitrate removal performance in woodchip bioreactors?*
        - *Can nitrate removal performance be predicted with knowledge of the different abiotic factors?*
- Chapter 3: Effect of biochar and silage leachate on the performance of woodchip bioreactors in removing nitrate and veterinary antibiotics.
    - *Research Questions:*
        - *What is the nitrate removal performance in woodchip bioreactors amending with biochar and silage leachate under different hydraulic retention times?*
        - *What is the nitrate removal performance in woodchip bioreactors amending with biochar and silage leachate under different influent nitrate concentrations?*

        - *How is nitrate removal performance influenced by the different types of silage leachate?*
        - *What is the tylosin and sulfamethazine removal performance in woodchip bioreactors amending with biochar and silage leachate under different hydraulic retention times?*
- Chapter 4: Characterizing the role of hydraulic retention time on nitrate removal in denitrifying bioreactors.
    - *Research Questions:*
        - *Can models be developed to predict the nitrate removal rate and nitrate removal efficiency as a function of hydraulic retention time?*
        - *What model is better at describing the nitrate removal rate and nitrate removal efficiency with altering hydraulic retention time?*
        - *What is the relationship between abiotic factors and the model parameters?*
- Chapter 5: Evaluating the nitrate removal performance in denitrifying bioreactors by inflow and outflow C/N ratio.
    - *Research Questions:*
        - *What is the value of the inflow and outflow C/N ratio?*
        - *What model can be used to characterize the nitrate removal by inflow and outflow C/N ratio?*
        - *Can a predictive model be developed nitrate removal performance in bioreactors as a function of C/N ratio?*

References

Aga D S, O'Connor S, Ensley S, et al. 2005. Determination of the persistence of tetracycline antibiotics and their degradates in manure-amended soil using enzyme-linked immunosorbent assay and liquid chromatography−mass spectrometry[J]. Journal of Agricultural and Food Chemistry, 53(18): 7165-7171.

Aslan Ş, Türkman A. 2005. Combined biological removal of nitrate and pesticides using wheat straw as substrates[J]. Process Biochemistry, 40(2): 935-943.

Averill B, Tiedje J. 1982. The chemical mechanism of microbioal denitrification[J]. FEBS letters, 138(1): 8-12.

Beck D A, Johnson G R, Spolek G A. 2011. Amending greenroof soil with biochar to affect runoff water quantity and quality[J]. Environmental Pollution, 159(8): 2111-2118.

Bock E, Smith N, Rogers M, et al. 2015. Enhanced nitrate and phosphate removal in a denitrifying bioreactor with biochar[J]. Journal of Environmental Quality, 44(2): 605-613.

Bock E M, Coleman B, Easton Z M. 2016. Effect of biochar on nitrate removal in a pilot-scale denitrifying bioreactor[J]. Journal of Environmental Quality, 45(3): 762-771.

Boley A, Müller W R, Haider G. 2000. Biodegradable polymers as solid substrate and biofilm carrier for denitrification in recirculated aquaculture systems[J]. Aquacultural Engineering, 22(1): 75-85.

Boxall A B A, Blackwell P, Cavallo R, et al. 2002. The sorption and transport of a sulphonamide antibiotic in soil systems[J]. Toxicology Letters, 131(1): 19-28.

Bulger P R, Kehew A E, Nelson R A. 1989. Dissimilatory nitrate reduction in a waste-water contaminated aquifer[J]. Groundwater, 27(5): 664-671.

Cameron S G, Schipper L A. 2010. Nitrate removal and hydraulic performance of organic carbon for use in denitrification beds[J]. Ecological Engineering, 36(11): 1588-1595.

Christensson M, Lie E, Welander T. 1994. A comparison between ethanol and methanol as carbon sources for denitrification[J]. Water Science and Technology, 30(6): 83.

Clough T J, Condron L M. 2010. Biochar and the nitrogen cycle: Introduction[J]. Journal of Environmental Quality, 39(4): 1218-1223.

Coumaravel K, Santhi R, Kumar V, et al. 2011. Biochar-a promising soil additive-a review[J]. Agricultural Reviews, 32(2): 134-139.

Damaraju S, Singh U K, Sreekanth D, et al. 2015. Denitrification in biofilm configured horizontal flow woodchip bioreactor: effect of hydraulic retention time and biomass growth[J]. Ecohydrology & Hydrobiology, 15(1): 39-48.

Daniel T C, Sharpley A N, Lemunyon J L. 1998. Agricultural phosphorus and eutrophication: A symposium overview[J]. Journal of Environmental Quality, 27(2): 251-257.

Della Rocca C, Belgiorno V, Meriç S. 2006. An heterotrophic/autotrophic denitrification (HAD) approach for nitrate removal from drinking water[J]. Process Biochemistry, 41(5): 1022-1028.

Dewey C E, Cox B D, Straw B E, et al. 1999. Use of antimicrobials in swine feeds in the United States[J]. Swine health and production : the official journal of the American Association of Swine Practitioners, 1999 v.7 no.1(no. 1): pp. 19-25.
Dils R M, Heathwaite A L. 1999. The controversial role of tile drainage in phosphorus export from agricultural land[J]. Water Science and Technology, 39(12): 55-61.
Elefsiniotis P, Li D. 2006. The effect of temperature and carbon source on denitrification using volatile fatty acids[J]. Biochemical Engineering Journal, 28(2): 148-155.
Elgood Z, Robertson W D, Schiff S L, et al. 2010. Nitrate removal and greenhouse gas production in a stream-bed denitrifying bioreactor[J]. Ecological Engineering, 36(11): 1575-1580.
EPA U. 2009. National recommended water quality criteria[J]. United States Environmental Protection Agency', Office of Water, Office of Science and Technology.
Essington M E, Lee J, Seo Y. 2010. Adsorption of antibiotics by montmorillonite and kaolinite[J]. Soil Science Society of America Journal, 74(5): 1577-1588.
Faulkner J W, Zhang W, Geohring L D, et al. 2011. Nutrient transport within three vegetative treatment areas receiving silage bunker runoff[J]. Journal of Environmental Management, 92(3): 587-595.
Fields S. 2004. Global nitrogen: cycling out of control[J]. Environmental Health Perspectives, 112(10): A556.
Gaskins H R, Collier C T, Anderson D B. 2002. Antibiotics as growth promotants: Mode of action[J]. Animal Biotechnology, 13(1): 29-42.
Gebrehanna M M, Gordon R J, Madani A, et al. 2014. Silage effluent management: A review[J]. Journal of Environmental Management, 143: 113-122.
Gibert O, Pomierny S, Rowe I, et al. 2008. Selection of organic substrates as potential reactive materials for use in a denitrification permeable reactive barrier (PRB)[J]. Bioresource Technology, 99(16): 7587-7596.
Gómez M A, Hontoria E, González-López J. 2002. Effect of dissolved oxygen concentration on nitrate removal from groundwater using a denitrifying submerged filter[J]. Journal of Hazardous Materials, 90(3): 267-278.
Gorbach S L. 2001. Antimicrobial use in animal feed--time to stop[J]. The New England journal of medicine, 345(16): 1202-1203.
Gottschall N, Edwards M, Craiovan E, et al. 2016. Amending woodchip bioreactors with water treatment plant residuals to treat nitrogen, phosphorus, and veterinary antibiotic compounds in tile drainage[J]. Ecological Engineering, 95: 852-864.
Greenan C M, Moorman T B, Kaspar T C, et al. 2006. Comparing carbon substrates for denitrification of subsurface drainage water[J]. Journal of Environmental Quality, 35(3): 824-829.
Guo Y, Guo L, Sun M, et al. 2017. Effects of hydraulic retention time (HRT) on denitrification using waste activated sludge thermal hydrolysis liquid and acidogenic liquid as carbon sources[J]. Bioresource Technology, 224: 147-156.
Gutierrez-Wing M T, Malone R F, Rusch K A. 2012. Evaluation of polyhydroxybutyrate as a carbon source for recirculating aquaculture water denitrification[J]. Aquacultural Engineering, 51(Supplement C): 36-43.

Halling-Sørensen B, Nors Nielsen S, Lanzky P F, et al. 1998. Occurrence, fate and effects of pharmaceutical substances in the environment- A review[J]. Chemosphere, 36(2): 357-393.
Halling-Sørensen B, Sengeløv G, Tjørnelund J. 2002. Toxicity of tetracyclines and tetracycline degradation products to environmentally relevant bacteria, including selected tetracycline-resistant bacteria[J]. Archives of Environmental Contamination and Toxicology, 42(3): 263-271.
Hamscher G, Pawelzick H T, Sczesny S, et al. 2003. Antibiotics in dust originating from a pig-fattening farm: a new source of health hazard for farmers?[J]. Environmental Health Perspectives, 111(13): 1590-1594.
Hassanpour B, Giri S, Pluer W T, et al. 2017. Seasonal performance of denitrifying bioreactors in the Northeastern United States: Field trials[J]. Journal of Environmental Management, 202: 242-253.
Healy M G, Ibrahim T G, Lanigan G J, et al. 2012. Nitrate removal rate, efficiency and pollution swapping potential of different organic carbon media in laboratory denitrification bioreactors[J]. Ecological Engineering, 40: 198-209.
Holly M A, Larson R A, Cooley E T, et al. 2018. Silage storage runoff characterization: Annual nutrient loading rate and first flush analysis of bunker silos[J]. Agriculture, Ecosystems & Environment, 264: 85-93.
Holman I P, Whelan M J, Howden N J, et al. 2008. Phosphorus in groundwater—an overlooked contributor to eutrophication?[J]. Hydrological Processes: An International Journal, 22(26): 5121-5127.
Honda Y, Osawa Z. 2002. Microbial denitrification of wastewater using biodegradable polycaprolactone[J]. Polymer Degradation and Stability, 76(2): 321-327.
Hua G, Salo M W, Schmit C G, et al. 2016. Nitrate and phosphate removal from agricultural subsurface drainage using laboratory woodchip bioreactors and recycled steel byproduct filters[J]. Water Research, 102: 180-189.
Ilhan Z E, Ong S K, Moorman T B. 2012. Herbicide and antibiotic removal by woodchip denitrification filters: Sorption processes[J]. Water Air and Soil Pollution, 223(5): 2651-2662.
Kay P, Blackwell P A, Boxall A B A. 2004. Fate of veterinary antibiotics in a macroporous tile drained clay soil[J]. Environmental Toxicology and Chemistry, 23(5): 1136-1144.
Kelso B, Smith R V, Laughlin R J, et al. 1997. Dissimilatory nitrate reduction in anaerobic sediments leading to river nitrite accumulation[J]. Appl Environ Microbiol, 63(12): 4679-4685.
Kemper N. 2008. Veterinary antibiotics in the aquatic and terrestrial environment[J]. Ecological Indicators, 8(1): 1-13.
Kreuzig R, Höltge S, Brunotte J, et al. 2005. Test-plot studies on runoff of sulfonamides from manured soils after sprinkler irrigation[J]. Environmental Toxicology and Chemistry, 24(4): 777-781.
Landers T F, Cohen B, Wittum T E, et al. 2012. A review of antibiotic use in food animals: Perspective, policy, and potential[J]. Public Health Reports, 127(1): 4-22.

Lee J, Seo Y, Essington M E. 2014. Sorption and transport of veterinary pharmaceuticals in soil—A laboratory study[J]. Soil Science Society of America Journal, 78(5): 1531.
Levy-Booth D J, Prescott C E, Grayston S J. 2014. Microbial functional genes involved in nitrogen fixation, nitrification and denitrification in forest ecosystems[J]. Soil Biology and Biochemistry, 75: 11-25.
Li T Y, Li W Q, Feng C P, et al. 2017. In-situ biological denitrification using pretreated maize stalks as carbon source for nitrate-contaminated groundwater remediation[J]. Water Science and Technology-Water Supply, 17(1): 1-9.
Liu F, Wang Y, Xiao R L, et al. 2015. Influence of substrates on nutrient removal performance of organic channel barriers in drainage ditches[J]. Journal of Hydrology, 527: 380-386.
Lujia H, Guanghui T, Xiangyang L, et al. Straw resources and utilization in China[C]//Straw resources and utilization in China. 2003 ASAE Annual Meeting. American Society of Agricultural and Biological Engineers: 1
Macrae M, English M, Schiff S, et al. 2007. Intra-annual variability in the contribution of tile drains to basin discharge and phosphorus export in a first-order agricultural catchment[J]. Agricultural Water Management, 92(3): 171-182.
Mathews Jr K H 2001. Antimicrobial drug use and veterinary costs in US livestock production [M].
Maxwell B M, Birgand F, Schipper L A, et al. 2019a. Drying–rewetting cycles affect nitrate removal rates in woodchip bioreactors[J]. Journal of Environmental Quality, 48(1): 93-101.
Maxwell B M, Birgand F, Schipper L A, et al. 2019b. Increased duration of drying–rewetting cycles increases nitrate removal in woodchip bioreactors[J]. Agricultural & Environmental Letters, 4.
McDonald P, Henderson A, Heron S. 1991. The biochemistry of silage., 2nd edn.(Chalcombe Publications: Bucks, UK)[J].
McGuire P M, Reid M C. 2019. Nitrous oxide and methane dynamics in woodchip bioreactors: Effects of water level fluctuations on partitioning into trapped gas phases[J]. Environmental Science & Technology.
Meffe R, de Miguel A, Hernandez V M, et al. 2016. Soil amendment using poplar woodchips to enhance the treatment of wastewater-originated nutrients[J]. Journal of Environmental Management, 180: 517-525.
Mitscher L A 1978. Plant-derived antibiotics [M] //M. J. WEINSTEIN, G. H. WAGMAN, Journal of Chromatography Library. Elsevier: 463-477.
Montforts M H M M, Kalf D F, van Vlaardingen P L A, et al. 1999. The exposure assessment for veterinary medicinal products[J]. Science of The Total Environment, 225(1): 119-133.
NASS U 2012. Census of Agriculture, Ag Census Web Maps [M]. Available.
Nelson N O, Agudelo S C, Yuan W, et al. 2011. Nitrogen and Phosphorus Availability in Biochar-Amended Soils[J]. Soil Science, 176(5): 218-226.
Onley J R. 2017. Complete denitrification by the non-denitrifier anaeromyxobacter dehalogenans: The role of coupled biotic-abiotic reactions[J].

Organization W H 2008. Guidelines for drinking-water quality: incorporating first and second addenda to third edition, Vol. 1, Recommendations [M]. Geneva: WHO Press.
Paetsch L, Mueller C W, Kögel-Knabner I, et al. 2018. Effect of in-situ aged and fresh biochar on soil hydraulic conditions and microbial C use under drought conditions[J]. Scientific Reports, 8(1): 6852.
PRC S A o t 1994. China national standard: Quality standard for ground water. GB/T [M] //G. A. M. RESORUCES. Department of Geology and Mineral Resoruces; China: 14848-14893.
Pruden A, Larsson D G J, Amézquita A, et al. 2013. Management options for reducing the release of antibiotics and antibiotic resistance genes to the environment[J]. Environmental Health Perspectives, 121(8): 878-885.
Rivett M O, Buss S R, Morgan P, et al. 2008. Nitrate attenuation in groundwater: A review of biogeochemical controlling processes[J]. Water Research, 42(16): 4215-4232.
Robertson W D. 2010. Nitrate removal rates in woodchip media of varying age[J]. Ecological Engineering, 36(11): 1581-1587.
Robertson W D, Blowes D W, Ptacek C J, et al. 2000. Long-term performance of in situ reactive barriers for nitrate remediation[J]. Ground Water, 38(5): 689-695.
Robertson W D, Merkley L C. 2009. In-Stream bioreactor for agricultural nitrate treatment [J]. Journal of Environmental Quality, 38(1): 230-237.
Rocca C D, Belgiorno V, Meric S. 2005. Cotton-supported heterotrophic denitrification of nitrate-rich drinking water with a sand filtration post-treatment[J]. Water SA, 31(2): 229-236.
Roser M B, Feyereisen G W, Spokas K A, et al. 2018. Carbon dosing increases nitrate removal rates in denitrifying bioreactors at low-temperature high-flow conditions[J]. Journal of Environmental Quality, 47(4): 856-864.
Rostron W M, Stuckey D C, Young A A. 2001. Nitrification of high strength ammonia wastewaters: comparative study of immobilisation media[J]. Water Research, 35(5): 1169-1178.
Ruane E M, Murphy P N C, Healy M G, et al. 2011. On-farm treatment of dairy soiled water using aerobic woodchip filters[J]. Water Research, 45(20): 6668-6676.
Sakuma T, Jinsiriwanit S, Hattori T, et al. 2008. Removal of ammonia from contaminated air in a biotrickling filter–denitrifying bioreactor combination system[J]. Water Research, 42(17): 4507-4513.
Savoie P. 1995. Probability estimation of silage effluent from horizontal silos[J]. Canadian Agricultural Engineering, 37(1): 49-56.
Schipper L A, Barkle G F, Vojvodic-Vukovic M. 2005. Maximum rates of nitrate removal in a denitrification wall[J]. Journal of Environmental Quality, 34(4): 1270-1276.
Schipper L A, Robertson W D, Gold A J, et al. 2010a. Denitrifying bioreactors-An approach for reducing nitrate loads to receiving waters[J]. Ecological Engineering, 36(11): 1532-1543.

Schipper L A, Robertson W D, Gold A J, et al. 2010b. Denitrifying bioreactors—An approach for reducing nitrate loads to receiving waters[J]. Ecological Engineering, 36(11): 1532-1543.
Schipper L A, Vojvodic-Vukovic M. 2001. Five years of nitrate removal, denitrification and carbon dynamics in a denitrification wall[J]. Water Research, 35(14): 3473-3477.
Schmidt C A, Clark M W. 2012. Efficacy of a denitrification wall to treat continuously high nitrate loads[J]. Ecological Engineering, 42: 203-211.
Schmidt C A, Clark M W. 2013. Deciphering and modeling the physicochemical drivers of denitrification rates in bioreactors[J]. Ecological Engineering, 60: 276-288.
Seitzinger S, Harrison J A, Böhlke J K, et al. 2006. Denitrification across landscapes and waterscapes: A synthesis[J]. Ecological Applications, 16(6): 2064-2090.
Shen Z Q, Hu J, Wang J L, et al. 2015. Comparison of polycaprolactone and starch/polycaprolactone blends as carbon source for biological denitrification[J]. International Journal of Environmental Science and Technology, 12(4): 1235-1242.
Snaidr J, Amann R, Huber I, et al. 1997. Phylogenetic analysis and in situ identification of bacteria in activated sludge[J]. Applied and Environmental Microbiology, 63(7): 2884-2896.
Soares M I M, Abeliovich A. 1998. Wheat straw as substrate for water denitrification[J]. Water Research, 32(12): 3790-3794.
Søndergaard M, Jeppesen E, Lauridsen T L, et al. 2007. Lake restoration: successes, failures and long-term effects[J]. Journal of Applied Ecology, 44(6): 1095-1105.
Soto A M, Calabro J M, Prechtl N V, et al. 2004. Androgenic and estrogenic activity in water bodies receiving cattle feedlot effluent in Eastern Nebraska, USA[J]. Environmental Health Perspectives, 112(3): 346-352.
Speratti A B, Johnson M S, Sousa H M, et al. 2018. Biochar feedstock and pyrolysis temperature effects on leachate: DOC characteristics and nitrate losses from a Brazilian Cerrado Arenosol mixed with agricultural waste biochars[J]. Journal of Environmental Management, 211: 256-268.
Stark J M, Hart S C. 1997. High rates of nitrification and nitrate turnover in undisturbed coniferous forests[J]. Nature, 385: 61.
Su C, Puls R W. 2007. Removal of added nitrate in cotton burr compost, mulch compost, and peat: Mechanisms and potential use for groundwater nitrate remediation[J]. Chemosphere, 66(1): 91-98.
Sundareshwar P V, Morris J T, Koepfler E K, et al. 2003. Phosphorus Limitation of Coastal Ecosystem Processes[J]. Science, 299(5606): 563-565.
Tasho R P, Cho J Y. 2016. Veterinary antibiotics in animal waste, its distribution in soil and uptake by plants: A review[J]. Science of The Total Environment, 563-564: 366-376.
Tikkisetty B, Kuperus W. Environmentally friendly silage management[C]//Environmentally friendly silage management. Proceedings of SIDE Conference. South Island Dairy Event.
Tokiwa Y, Calabia B, Ugwu C, et al. 2009. Biodegradability of plastics[J]. International Journal of Molecular Sciences, 10(9): 3722.

Tolls J. 2001. Sorption of veterinary pharmaceuticals in soils: A review[J]. Environmental Science & Technology, 35(17): 3397-3406.
Tsai H-H, Ravindran V, Williams M D, et al. 2004. Forecasting the performance of membrane bioreactor process for groundwater denitrification[J]. Journal of Environmental Engineering and Science, 3(6): 507-521.
Vacková L, Srb M, Stloukal R, et al. 2011. Comparison of denitrification at low temperature using encapsulated Paracoccus denitrificans, Pseudomonas fluorescens and mixed culture[J]. Bioresource Technology, 102(7): 4661-4666.
Vaclavik E, Halling-Sørensen B, Ingerslev F. 2004. Evaluation of manometric respiration tests to assess the effects of veterinary antibiotics in soil[J]. Chemosphere, 56(7): 667-676.
Volokita M, Abeliovich A, Soares M I M. 1996a. Denitrification of groundwater using cotton as energy source[J]. Water Science and Technology, 34(1-2): 379.
Volokita M, Belkin S, Abeliovich A, et al. 1996b. Biological denitrification of drinking water using newspaper[J]. Water Research, 30(4): 965-971.
Walters E, Hille A, He M, et al. 2009. Simultaneous nitrification/denitrification in a biofilm airlift suspension (BAS) reactor with biodegradable carrier material[J]. Water Research, 43(18): 4461-4468.
Warneke S, Schipper L A, Matiasek M G, et al. 2011. Nitrate removal, communities of denitrifiers and adverse effects in different carbon substrates for use in denitrification beds[J]. Water Research, 45(17): 5463-5475.
Wepking C, Avera B, Badgley B, et al. 2017. Exposure to dairy manure leads to greater antibiotic resistance and increased mass-specific respiration in soil microbial communities[J]. Proceedings of the Royal Society B: Biological Sciences, 284(1851).
Winckler C, Grafe A. 2001. Use of veterinary drugs in intensive animal production[J]. Journal of Soils and Sediments, 1(2): 66.
Xie Y F, Zhang D J, Lou S, et al. 2017. Slowly released carbon source from composite materials system for removing nitrate pollution in groundwater[J]. Rsc Advances, 7(17): 10215-10220.
Xue Y, Kovacic D A, David M B, et al. 1999. In situ measurements of denitrification in constructed wetlands[J]. Journal of Environmental Quality, 28(1): 263-269.
Zhang X, Xu Z, Sun X, et al. 2013. Nitrate in shallow groundwater in typical agricultural and forest ecosystems in China, 2004–2010[J]. Journal of Environmental Sciences, 25(5): 1007-1014.
Zulkhairi M, Mohamed Yusoff M E, Abdul Rahman N, et al. 2010. The Effect of hydraulic retention time and volatile fatty acids on biohydrogen production from palm oil mill effluent under non-sterile condition[M]. City.

Appendices

Tables

Table I-1 Summary of different organic waste been used for heterotrophic denitrification

Organic substrate	System description	Initial NO_3^- N (mg dm^{-3})	Water velocity (m d^{-1})	HRT (d)	Overall NO_3^--N removal (%)	Denitrification rate (mg NO_3^--N dm^{-3} d^{-1} g_{sub}^{-1})	T (°C)	Reference
Cardboard	Batch	100	—	—	95.8	1.05	20	(Greenan et al. 2006)
Compost	Batch	32.2	—	—	92.7	0.026	22	(Gibert et al. 2008)
Coniferous	Batch	32.2	—	—	95.1	0.048	22	(Gibert et al. 2008)
Cornstalks	Batch	100	—	—	91.7	2.88	20	(Greenan et al. 2006)
Cotton	Column	19	0.16-0.86	—	85-97	0.064	27	(Rocca et al. 2005)
Cotton	Column	24.8	0.24-2.52	—	>99	0.50	23	(Della Rocca et al. 2006)
Cotton+Fe^0	Column	24.8	0.24-2.52	—	>99	0.62-0.73	23	(Della Rocca et al. 2006)
Cotton burr compost	Batch (shaked)	20	—	—	>99	0.91	23	(Su and Puls 2007)
Giant red	Batch	100	—	—	>99	3.33	20	(Ovez 2006)
Hardwood	Batch	32.2	—	—	98.7	0.035	22	(Gibert et al. 2008)
Leaves	Batch	32.2	—	—	93.9	0.217	22	(Gibert et al. 2008)
Liquorice	Batch	100	—	—	>99	6.20	20	(Ovez 2006)
Mixture	Batch	32.2	—	—	98.3	0.048	22	(Gibert et al. 2008)
Mulch	Batch	32.2	—	—	89.7	0.066	22	(Gibert et al. 2008)
Newspaper	Column	20-22.6	0.55-0.95	—	46 to >99	—	25	(Volokita et al. 1996)

Table I-1 continued

Seaweed (Gracilaria verrucosa)	Batch	100	—	—	>99	13.13	20	(Ovez 2006)
Softwood	Batch	32.2	—	—	98.7	0.067	22	(Gibert et al. 2008)
Softwood	Column	50	0.15	6.6	>96	0.034	22	(Gibert et al. 2008)
Softwood	Column	50	0.54	1.7	66	0.022	22	(Gibert et al. 2008)
Soil	Batch	32.2	—	—	73.2	0.001	22	(Gibert et al. 2008)
Wheat straw	Column	22.6	1.30	—	86	0.52	25	(Soares and Abeliovich 1998)
Wheat straw	Column	22.6	2.21	—	38	0.31	25	(Soares and Abeliovich 1998)
Wheat straw	Continuous reactor	22.6	0.34-2.06	—	60-100	—	31	(Aslan and Türkman 2005)
Willow	Batch	32.2	—	—	86.3	0.056	22	(Gibert et al. 2008)
Wood chips (*Quercus* sp.)	Batch	100	—	—	85.4	0.45	20	(Greenan et al. 2006)
Wood chips (+soybean oil)	Batch	100	—	—	80.1	0.76	20	(Greenan et al. 2006)

Table I-2 Biochar physicochemical properties (125 samples collected from literature, details in Appendix Table-S1)

	pH (H_2O)	CEC (molc m^{-2})	SSA (m^2 g^{-1})	PV (cm^3 g^{-1})	C (%)	N (%)	H (%)	O (%)	K (%)	P (%)	A_{sh} (%)
Min	3.73	0.12	0.70	0.002	20.19	0.04	0.35	0.70	16.90	0.0005	0.30
Max	12.30	2.58	642.00	1.323	95.30	10.21	16.70	46.80	31.40	2.3596	76.60
Median	8.70	0.64	19.15	0.038	68.27	1.40	2.99	13.68	22.20	0.1905	13.90
Mode	8.70	—	94.00	0.020	70.60	1.24	1.20	18.30	—	0.1870	1.10
Mean	8.65	0.98	81.38	0.235	64.64	1.75	3.23	18.05	23.60	0.4003	20.62
SE	1.76	0.81	138.17	0.419	17.63	1.58	2.22	13.43	4.15	0.6367	19.79
Q25th	7.42	0.39	4.35	0.020	51.06	0.95	1.53	7.42	19.90	0.1555	3.00
Q75th	9.90	1.72	65.03	0.144	78.00	1.94	4.31	26.20	26.70	0.2393	32.80

Note: PV means pore volume; A_{sh} means ash content
Details of the biochar characteristics can be seen in Appendix Table 1.

Table I-3 Silage leachate physicochemical properties (66 samples collected from literature, details in Appendix Table-S2)

	pH (H_2O)	NO_3-N (mg L^{-1})	NH_4-N (mg L^{-1})	Cl (mg L^{-1})	BOD_5 (mg L^{-1})	COD (mg L^{-1})	TOC (mg L^{-1})	TP (mg L^{-1})	TN (mg L^{-1})	SRP (mg L^{-1})	TKN (mg L^{-1})
Min	3.70	0.10	1.60	4.0	1451	30	6320	26	2750	0.1	4.1
Max	9.07	12.00	227.80	109.0	72500	80960	22970	1000	23000	67.0	270.0
Median	4.40	1.00	9.90	53.0	46400	6062	21400	48	3745	1.2	83.0
Mode	4.20	0.30		53.0	61800					31.0	
Mean	5.03	2.21	30.91	56.6	42859	19376	16897	329	5954	9.7	93.8
SE	1.35	2.87	46.04	30.0	24939	25000	7506	389	6460	15.4	91.0
Q25th	4.12	0.30	3.85	32.5	18267	3320	6320	34	3025	0.2	5.3
Q75th	5.49	3.60	46.15	78.0	62900	37380	22970	810	4093	15.4	188.0

Note: SRP means soluble reactive phosphorus; TKN means total kjeldahl nitrogen.

References for Table S-1

Aslan Ş, Türkman A. 2005. Combined biological removal of nitrate and pesticides using wheat straw as substrates[J]. Process Biochemistry, 40(2): 935-943.

Della Rocca C, Belgiorno V, Meriç S. 2006. An heterotrophic/autotrophic denitrification (HAD) approach for nitrate removal from drinking water[J]. Process Biochemistry, 41(5): 1022-1028.

Gibert O, Pomierny S, Rowe I, et al. 2008. Selection of organic substrates as potential reactive materials for use in a denitrification permeable reactive barrier (PRB)[J]. Bioresource Technology, 99(16): 7587-7596.

Greenan C M, Moorman T B, Kaspar T C, et al. 2006. Comparing carbon substrates for denitrification of subsurface drainage water[J]. Journal of Environmental Quality, 35(3): 824-829.

Ovez B. 2006. Batch biological denitrification using Arundo donax, Glycyrrhiza glabra, and Gracilaria verrucosa as carbon source[J]. Process Biochemistry, 41(6): 1289-1295.

Rocca C D, Belgiorno V, Meric S. 2005. Cotton-supported heterotrophic denitrification of nitrate-rich drinking water with a sand filtration post-treatment[J]. Water SA, 31(2): 229-236.

Soares M I M, Abeliovich A. 1998. Wheat straw as substrate for water denitrification[J]. Water Research, 32(12): 3790-3794.

Su C, Puls R W. 2007. Removal of added nitrate in cotton burr compost, mulch compost, and peat: Mechanisms and potential use for groundwater nitrate remediation[J]. Chemosphere, 66(1): 91-98.

Volokita M, Belkin S, Abeliovich A, et al. 1996. Biological denitrification of drinking water using newspaper[J]. Water Research, 30(4): 965-971.

CHAPTER I
A SYSTEMATIC REVIEW OF THE ROLE OF FILLING MATERIALS FOR NITRATE REMOVAL IN DENITRIFYING BIOREACTORS

This chapter is based on a manuscript draft by Yuchuan Fan et al.:

A version of this chapter was originally published by:

Yuchuan Fan, Jaehoon Lee, Jie Zhuang, Michael Essington, Sindhu Jagadamma, and John Schwartz. A systematic review of the role of filling materials for nitrate removal in denitrifying bioreactors.

My primary contributions to the work include (i) reviewing and summarizing relevant literature, (ii) compiling a global-wide database, (iii) gathering, analyzing, and summarizing data, (iv) initial writing of the manuscript, and (v) revising manuscript and coordinating revisions of the manuscript.

Abstract

Denitrifying bioreactors (DNBR) are widely used to reduce excess nitrate from agricultural drainage. Their performance depends on the physical and chemical properties of the filling materials. However, the effectiveness of different filling materials has never been quantitatively evaluated. In this study, 40 types of filling materials were summarized and global data was collected from 63 refereed articles, which include 216 independent DNBR units. The filling materials were classified into four groups: a) natural carbon (NC) such as woodchip; b) non-natural carbon (NNC) such as biodegradable polymers (e.g., polycaprolactone) and industrial by-products (e.g., biochar); c) inorganic material (IM) such as non-carbon materials (e.g., iron oxide); and d) multi-materials (MM) such as a mixture of the above materials. These materials are compared and evaluated using a meta-analysis method in terms of nitrate removal rate (NRR, g N m^{-3} d^{-1}) and nitrate removal efficiency (NRE, %). This study systematically reviewed the different filling material performance (NRR & NRE), potential mechanisms of nitrate removal, pollution swapping, and cost analysis. It indicated that MM as the optimal material for nitrate removal due to the low cost and wider scope of application. In MMs, adding auxiliary materials into woodchip-based DNBRs was promising for enhancing denitrification and maintaining

operation throughout an extended period. This comprehensive analysis can help optimize the design of DNBR to meet the practical requirements of users both environmentally and economically.

Introduction

Fugitive nitrogen (N) from excessive N fertilization is a severe problem in agricultural system around the world (Ju et al. 2009), causing eutrophication, algal blooms, fish kills, and potential damage to ecosystems. High N concentrations in surface and ground waters potentially increase the risk of methemoglobinemia (Tian et al. 2019), mutagenicity, teratogenicity, and birth defects in humans (Miao et al. 2020b). To solve this problem, the denitrifying bioreactor (DNBR) has been considered a sustainable and cost-effective approach to decrease N concentrations in surface and ground waters during the past two decades (Coleman et al. 2019). DNBRs have long lifespans (around 10 to 15 years) (Robertson et al. 2008; Long et al. 2011) and low investment costs (Christianson et al. 2013). DNBRs are also called denitrification beds, denitrification walls, or permeable reactive barriers (PRB) (Cameron and Schipper 2010; Schipper et al. 2010c). A DNBR is usually constructed by mixing an organic carbon (C) source (typically sawdust or woodchips) into natural soil and installing below the water table to intercept groundwater flow (Schipper et al. 2010b; Addy et al. 2016). Available C is released from the media to support denitrification, where nitrate (NO_3) is reduced to N_2 which proceeds through a series of intermediate N oxide products.

The conceptual designs of DNBRs range in size from laboratory to field scales in Fig 1.1. Lab-columns and bioreactors are widely adopted for laboratory scale studies with synthetic influents containing nitrate (Fig 1.1a & 1.1b) (Coleman et al. 2019; Yao et al. 2019). Field beds are always lined and placed into the upper 1-2 m of shallow groundwater in a trench on either side of a tile drain container to control the water level, with a by-pass pipe to remove excess water flow (Schipper et al. 2010b)

(Fig. 1.1c). Field walls are installed perpendicular to the groundwater flow path to intercept nitrate-laden groundwater (Fig. 1.1d) (Addy et al. 2016).

The types of filling materials used to improve DNBR function have been a topic of intensive study. In the initial stages of DNBR development, woody materials, such as tree bark, woodchip, and sawdust were used as major C sources (Blowes et al. 1994; Schipper and Vojvodic-Vukovic 1998; Schipper and Vojvodić-Vuković 2000; Van Driel et al. 2006; Healy et al. 2007). Later, agricultural wastes were used as natural carbon (NC) sources. These NC sources include maize cobs (Feyereisen et al. 2016; Sharrer et al. 2016), wheat straw (Soares and Abeliovich 1998; Aslan and Türkman 2005), rice straw (Liu et al. 2015), cotton (Rocca et al. 2005; Della Rocca et al. 2006), cornstalks (Greenan et al. 2006), corn stover (Feyereisen et al. 2016), conifers (Gibert et al. 2008), barley straw (Healy et al. 2012; Healy et al. 2015), leaves (Gibert et al. 2008), and green waste (Cameron and Schipper 2010; Cameron and Schipper 2012). Nevertheless, woody materials are still preferred due to their sustainability and longevity (Schipper et al. 2010b).

Many studies have focused on improving the woodchip-derived DNBR by adding auxiliary materials. These include, sand (Healy et al. 2007), steel by-product (Hua et al. 2016), biochar (Bock et al. 2015a; Bock et al. 2015b), seashell (Bruun et al. 2016), acetate (Roser et al. 2018), fly ash pellets (Li et al. 2018), mire flora, and potato (Kiani et al. 2020). In addition, non-natural carbon (NNC) sources have been investigated in the laboratory, achieving relatively high nitrate removal rates (NRR, g $N\ m^{-3}\ d^{-1}$). These NNC sources include synthetic C compounds, biochar (Bock et al. 2018b; Berger et al. 2019), and cardboard (Healy et al. 2012; Healy et al. 2015). Synthetic C compounds include polycaprolactone (PCL) (Boley et al. 2000; Honda and Osawa 2002; Walters et al. 2009), polylactic acid (PLA), polybutylene succinate

(PBS), poly-3-hydroxybutyric acid (PHB) (Boley et al. 2000; Walters et al. 2009), and poly-3-hydroxybutyrate-co-hydroxy valerate (PHBV). These materials can increase the NRR from approximately 0.02 (Pluer et al. 2019) up to 400 g N m^{-3} d^{-1} (Zhou et al. 2009). Studies have also used a mixture of multiple materials (MM), which includes various NC or other industrial and agricultural waste. For example, combinations of woodchips, sulfur particles, and zeolite (Li et al. 2017), or of woodchips, corncobs, and modified coconut coir (Roser et al. 2018) have generated a higher nitrate removal rates.

The nitrate removal mechanism is critical to the performance of DNBRs. Most studies focused on heterotrophic denitrification, which converts nitrate into nitrogen gas by denitrifying bacteria (Volokita et al. 1996; Warneke et al. 2011; Fenton et al. 2014; Shen et al. 2015). However, other mechanisms may be involved depending on fill types. Other mechanisms of nitrate removal include, autotrophic denitrification which relies on inorganic compounds (e.g. pyrite) (Xu et al. 2019), dissimilatory nitrate reduction to ammonium (DNRA) (Aalto et al. 2020), anaerobic ammonium oxidation (anammox) which combines nitrite and ammonium into nitrogen gas (Rambags et al. 2019), and chemical denitrification (chemodenitrification) (Liu et al. 2019a). The dominant nitrate reduction mechanism that occurs in a bioreactor is a function of the fill material type. However, few studies have addressed the relationship between filling material and nitrate removal mechanisms.

In this review, we compare the performances and removal mechanisms of various fill materials with the aim of help practitioners and researchers choose optimal materials as media in their DNBR. Overall, even though the filling materials were partly reviewed in previous studies (Griessmeier et al. 2019), they have not been quantitatively evaluated in a systematic manner. We review the nitrate removal

performance by various filling materials in DNBRs. The specific objectives were to develop a taxonomy of fill materials, evaluate the nitrate removal rate and efficiency of different fill materials, and summarize nitrate removal mechanisms, as well as the environmental and economic impacts of using DNBRs.

Materials and Methods

Data compilation

Data were compiled from published articles following the method described in the flow chart shown in Fig 1.2a. We found 14 articles related to "denitrification bed", 36 related to "denitrification wall", 83 related to "denitrifying bioreactor", and 69 related to "permeable reactive barrier" (Fig. 1.2a and 1.2b). There was a steady increase in the number of publications related to these topics during the past two decades (Fig. 1.2b). The most published articles were from the United States, followed by China, then New Zealand (Table 1.5). Research data used in this review were extracted from the articles using "GetData Graph Digitizer" software (Germany). In some cases, absent information was indirectly calculated. In total, we collected 10,179 sets of raw data from 63 peer-reviewed articles and compiled them in Microsoft Excel. In compiling information, we included the following for each wall, bed, or laboratory column bioreactor unit: author(s), year of publication, article title, journal title, site, number of measures (n), medium type, dimension, flow rate, medium age, hydraulic retention time (HRT), influent nitrate concentration (C_{in}), temperature, dissolved organic carbon (DOC) concentration, dissolved oxygen (DO), pH, effective porosity, nitrate removal rate (NRR), nitrate removal efficiency (NRE)

and the associated standard deviations (SD). Batch experiments are not included in the database due to the lack of a water flow component.

Filling materials

Fig. 1.3 shows the classification system used to define and distinguish different types of filling materials. The system categorized various filling materials of DNBRs into four main groups: natural carbon (NC), non-natural carbon (NNC), inorganic material (IM), and multi-material (MM). The proportion of the materials used in the DNBRs was 63.9% in NC, 4.6% in NNC, 1.4% in IM, and 28.2% in MM. The NC group consisted of materials from agricultural systems, including woodchips, wheat straw, rice straw, barley straw, corncobs, corn stalk, corn stover, cotton, green waste, leaves, lodge pine needles, and macrophyte residues. The use of woodchips represented the highest percentage (45.8%) in the NC group, which was further categorized into hardwood and softwood groups. The NNC group, which is mainly composed of artificial chemical and physical synthases, included biodegradable polymers (e.g., PHB, PCL, PBS), and wastes and other by-products (e.g., cardboard, biochar). The IM materials constituted only a small portion (1.4 %) of the DNBR filling materials. These included pyrite, sand, and amorphous iron oxides. The MM group was sub-grouped into “Woodchip+” (23.7%) and “Corncob+” (4.5%), as most of MM is woodchip- and corncob-derived. The soil was used in most studies as an additive into filling materials, but in the classification system, the soil is considered as an independent material or as a control category.

Meta-analysis of filling materials

A meta-analysis was conducted to analyze the nitrate removal response of NRR

and NRE among various filling materials. NRR (Peng et al. 2019) and NRE (Liu et al. 2015) was calculated using:

$$\mathrm{NRR} = \frac{V_T(N_{in}-N_{out})}{\mathrm{V_{BR}}\times t} \quad (1)$$

$$\mathrm{NRE} = \frac{N_{in}-N_{out}}{N_{in}} \quad (2)$$

Where V_T are influent water, N_{in} and N_{out} are the inflow and outflow nitrate concentrations (mg N L^{-1}), V_{BR} is the total volume of the DNBR (m^3), and *t* represents operation time (days).

Meta-analysis is a widely used tool to provide an indication of the comparable magnitude of differences in variables. in this case, the NNR and NNE aggregate from different studies (Addy et al. 2016). The effect size reflects the magnitude and direction of the treatment effect from each study (Israel and Richter 2011), including odds ratio, relative risk, risk difference, weighted mean difference (WMD), and standardized mean difference (SMD) (Lipsey and Wilson 2001; Wallace et al. 2017). In this study, we chose WMD as the effect size indicator because our data (NRR and NRE) were continuous variables with common units (g N m^{-3} d^{-1} or %). Thus, it was easier to interpret the findings using WMD (with units) compared to a unitless term, such as SMD (Israel and Richter 2011). The WMD is based on three parameters: (i) mean value (mean NRR and NRE), (ii) standard deviation (SD), and (iii) number of measurements (*n*). The above information may also be obtained for control treatments (NRR and NRE without a filling material in DNBR). However, the data collected from published articles did not always include control treatments, so we set the value of our control NRR (0.1 g N m^{-3} d^{-1}; SD, 0.01) after Addy et al. (2016). Also, the control NRE was set at 1%; SD, 0.01.

Each DNBR (wall, bed, laboratory column) is defined as one unit. Based on the database we established, we calculated the mean NRR and NRE values, the associated SD values, and *n* of each DNBR as a unit to make a meta-analysis. Then, filling materials categories were assigned (Main groups, Non-natural Carbon, Natural Carbon, Auxiliary, Woodchip+, Wood Source). The C/N ratio of the media and scale effects were also noted. Previous studies have reported a wide range of C/N ratios for media, so we classified the media C/N ratio into two categories, >100 and <100. To account for scaling effects on NRR and NRE, the DNBR systems were also divided into the lab- and field-scale categories. Details of the resulting groups and subgroups are summarized in Table 1. In addition, the lignocellulose index (LCI) was used as an indicator to describe C quality in natural C sources (e.g., woodchip). The LCI was calculated as (Feyereisen et al. 2016):

$$LCI = \frac{[lignin]}{[lignin]+ [cellulose]} \quad (3)$$

where the brackets represent % dry wt. composition.

We used a random-effects model, which accounts for the variation in methods between studies and sampling error within individual studies. The 95% confidence intervals (CIs) were corrected for bias and calculated by bootstrapping (sampling with replacement) with 999 iterations on the mean effect size. All meta-analysis was done by STATA (16, StataCorp, USA) software. Forest plots of our meta-analysis results were constructed in Microsoft Excel.

Results and Discussion

The performance of filling materials

The relationship between NRE and NRR

In general, NRR increased with increasing NRE as shown in Fig. 1.4 ($p < 0.05$). But NRR showed a greater uncertainty when NRE ranged from 90 to 100%. The reason could be denitrification is limited by nitrate concentration in influent water, or hydraulic retention time is too high, resulting in a low NRR value. Specifically, influent nitrate concentration is widely reported as an enzyme-substrate for denitrifying bacteria (Halaburka et al. 2017; Kouanda and Hua 2021). Thus, lower nitrate loading will limit the denitrification process. Moreover, greater HRT will limit the amount of treating water but increasing the denitrification reaction time. Thus, most researchers reported that NRR decreased with increasing HRT (Lepine et al. 2015), but NRE increased with increasing HRT (Hoover et al. 2015; Lepine et al. 2015). Up to now, NRR was reported more frequently than NRE in DNBR studies because NRR considers the total mass of N removal in a specific unit volume and time. However, NRE is prone to describe the potential nitrate removal ability or percentage rather than nitrate mass in the DNBR system. Although NRR was advocated to replace NRE in the past few years (Addy et al. 2016), we believe the two indicators (NRR & NRE) can evaluate the performance of DNBR from different perspectives. Therefore, both indicators should be taken into account in future research.

Nitrate removal by main groups

The NRR effect sizes were ranked in order of magnitude as NNC (329.45 g N m^{-3} d^{-1}) > MM (11.3 g N m^{-3} d^{-1}) > NC (7.89 g N m^{-3} d^{-1}) > IM (5.46 g N m^{-3} d^{-1}) > Soil (1.09 g N m^{-3} d^{-1}) (Fig. 1.5a). For NRE, the ranking order as NNC (78%) > IM (75%) > NC (59%) > MM (57%) > Soil (27%). The overall mean NRR and NRE for the fill material groups was 9.27 g N m^{-3} d^{-1} and 59%.

The NNC media showed the greatest NRR and NRE because NNC contains biodegradable polymers, which are easier to decompose than the C in the NC group, which contains a large number of recalcitrant C substances. In addition, biodegradable polymers were applied for concentrated nitrate-laden water, such as recirculated aquaculture systems (Boley et al. 2000) and wastewater (Walters et al. 2009). Therefore, a much greater NRR was showed than other fill materials. Conversely, the soil had the lowest NRR and NRE values. In most cases, the soil is a mixture of material with natural organic C in the DNBRs, and soil contains a large number of microorganisms that can be treated as a microbial inoculation. Even though NNC showed a very large NRR than other groups, it had a large variance which was mainly attributed to the biodegradable polymers were reported with a high value.

Nitrate removal by non-natural carbon materials

In terms of NNC, biodegradable polymers presented a very high NRR than waste and by-products of NNC (Fig. 1.5c). On the contrary, waste and by-product showed a greater NRE than the biodegradable polymers (Fig. 1.5d, $p < 0.05$). One of the possible reasons that polymer fill materials generate a greater NRR and lower NRE is that these DNBR studies use higher nitrate loading rates (38.8-95.2 mg L^{-1}) (Boley et

al. 2000; Honda and Osawa 2002; Zhou et al. 2009). Commonly, NRR increases with influent nitrate concentration (Pluer et al. 2016), but NRE decreases when inflow nitrate is not a limiting factor. These polymers can treat both nitrate and ammonium by simultaneous nitrification and denitrification in laboratory-scale bioreactors (Walters et al. 2009; Chu and Wang 2011). Combined, these processes generate higher NRR values than when traditional C sources are used (e.g., woodchip) which rely on heterotrophic denitrification alone.

Cardboard and biochar are classified into the "Waste & by-product" group, which are recycled as filling materials in DNBR, primarily due to their higher surface area and C content (Lehmann et al. 2011; Healy et al. 2012; Easton et al. 2015). Cardboard generates greater NRE values relative to woodchips and barley straw (Healy et al. 2012), although lower NRR values for cardboard have been reported (Healy et al. 2015). Biochar is a single filling material that generates a higher NRR than woodchips and amorphous iron oxides (Easton et al. 2015). The performance of biochar has been associated with an improved microorganism habitat (Lehmann et al. 2011) and increased nutrient retention capacity (Berger et al. 2019). This is why biochar is widely used as an auxiliary material into woodchip-derived DNBR for improving NRR (Bock et al. 2015b; Bock et al. 2018b). Nevertheless, compared with biodegradable polymers, cardboard and biochar fill has lower NRR performance. However, because of their lower cost, they are potential fill choices in real-world applications.

Nitrate removal by natural carbon materials

In the NC group, NRR effect sizes decrease in the following order: corncob (19.92 g N m^{-3} d^{-1}) > corn stover (13.58 g N m^{-3} d^{-1}) > macrophyte residue (12.74 g N

m^{-3} d^{-1}) > green waste (12.2 g N m^{-3} d^{-1}) > wheat straw (8.34 g N m^{-3} d^{-1}) > wood chip (6.89 g N m^{-3} d^{-1}) > barley straw (5.31 g N m^{-3} d^{-1}) > rice straw (4.8 g N m^{-3} d^{-1}) > pine needles (0.99 g N m^{-3} d^{-1}) (Fig. 1.5e). The NRE effect sizes were ranked in decreasing order, pine needles (98%) > leaves (91%) > macrophyte residue (81%) > barley straw (71%) > wood chip (60%) > corncob (52%) > wheat straw (47%) > green waste (47%) > rice straw (38%) > corn stover (28%) (Fig. 1.5f). These NC sources are popular as fill media due to their accessibility and low cost (Schipper et al. 2010b). Many studies have investigated the performance of NC materials in removing nitrate from agricultural drainage water. Healy et al. (2012) recorded the NRE for NC sources as lodge pine needles (75%), barley straw (74%), and lodge pine woodchip (70%). Cameron and Schipper (2010) compare several NCs and ranked the NRR from the highest to the lowest: corncobs (15-19.8 g N m^{-3} d^{-1}) > green waste (7.8-10.5 g N m^{-3} d^{-1}) > wheat straw (5.8-7.8 g N m^{-3} d^{-1}) > softwood (3.0-4.9 g N m^{-3} d^{-1}) > and hardwood (3.3-4.4 g N m^{-3} d^{-1}). The above NRR and NRE results are consistent with our results, with the exception of pine needles and corn stover. The performance of this N was significantly different in our evaluations, possibly due to the differences in hydraulic retention times and N loading rates.

Woodchips are the most reported NC material, with 99 NRR and 89 NRE citations. Woodchips generate intermediate NRR and NRE values which may be associated with low C release (0.13-0.53 mg g^{-1} L^{-1}) (Zhang et al. 2018) and low surface area (2.7 m^2 g^{-1}) (Healy et al. 2012) compared with the other NCs (Figs 1.5e and 1.5f). Most NCs showed a higher NRR than woodchips, but woody media is preferred due to its stability and sustainability (Addy et al. 2016) as well as cost, conductivity, longevity, and C/N (Schipper et al. 2010b).

Nitrate removal by Multi-materials

Our study showed that adding auxiliary materials into woodchip-derived DNBR (Woodchip+) increased NRR (Fig 1.6a, $p < 0.05$). However, this was not the case for corncob-derived (Corncob+) DNBR (Fig 1.6a, $p > 0.05$). Adding NCs into woodchip-derived DNBR (W+NCs) showed a greater NRR than the addition of NNCs and IMs (Fig 1.6c). However, adding auxiliary materials into woodchip- and corncob-derived DNBR did not increase NRE (Fig 1.6b & 1.6d).

The differing effect of adding auxiliary materials on woodchip and corncob NRR values is probably because corncob has a higher total C and total organic C than woodchip (Feyereisen et al. 2016). It is expected that NRR will increase with C content and lability, but this is not a linear relationship (Maxwell et al. 2019). Thus, adding an extra C source into corncob-derived DNBR (which has a higher C content and lability) may not have too much influence on the NRR and NRE compared with woodchip-derived DNBR which has a lower C content and lability. Furthermore, even though woodchip-derived DNBR has lower NRR compared with corncob-derived DNBR, woodchip-derived DNBR has been verified as a sustainable and stable DNBR by several previous studies (Robertson et al. 2008; Schipper et al. 2010b; Pluer et al. 2019); (Blowes et al. 1994; Healy et al. 2007; Feyereisen et al. 2016; Roser et al. 2018; Zhang et al. 2018; Coleman et al. 2019; Kijjanapanich and Yaowakun 2019; Pluer et al. 2019; Kiani et al. 2020).

There is no consensus about which auxiliary material is most effective for improving NRR and NRE. Our study indicates that adding NCs into woodchip-derived DNBR results in a greater NRR, relative to the addition of NNCs and IMs (Fig 1.6c). We inferred this result was probably due to more available C from the

addition of NCs. Research has also reported that adding NNCs (e.g., biochar) didn't increase the NRR (Coleman et al. 2019), while others reported that adding IMs (e.g. steel by-product) removes phosphate rather than nitrate (Hua et al. 2016). We also studied the performance of adding auxiliary materials into woodchip-derived DNBR. The NRR values of auxiliary materials in descending order was: sodium acetate (30.67 g N m^{-3} d^{-1}), potato (20.53 g N m^{-3} d^{-1}), fly ash pellet (19.08 g N m^{-3} d^{-1}), corncob (18 g N m^{-3} d^{-1}), mire flora (15.24 g N m^{-3} d^{-1}), steel (11.31 g N m^{-3} d^{-1}), biochar (10.38 g N m^{-3} d^{-1}), seashell (1.84 g N m^{-3} d^{-1}), flaxseed cake (1.6 g N m^{-3} d^{-1}), sand (1.5 g N m^{-3} d^{-1}), and filtralite (1.36 g N m^{-3} d^{-1}) (Fig 1.8). The descending order of NRE was: steel (90%), potato (86%), sodium acetate (84%), fly ash pellet (73%), mire flora (69%), biochar (53%), corncob (38%), and sand (36%) (Fig 1.8).

The results imply that the content and lability of C in auxiliary sources and blending choice have a large influence on the NRR of MM-derived DNBR. However, we found MM's application in field experiments was very rare. We expect that MM can be customized according to the local environment and the NRR and NRE goals. To achieve these goals, more diverse filling materials should be considered to make up for each component material's deficiencies. There is a great potential for combining various filling materials to increase NRR under wide environmental conditions, and a possible approach to keep the balance of the longevity and nitrate removal. Overall, MM-derived DNBR is the optimum choice that is able to operate in the long term, increase nitrate removal, and reduce environmental risks.

Nitrate removal by woodchip types

The NNR effect size of softwood was greater than that of hardwood ($p < 0.05$) (Fig 1.6e). However, the NRE effect size showed no significant difference between

hardwood and softwood (Fig 1.6f). The average NRR effect size of softwood and hardwood was 10.46 g N m^{-3} d^{-1} and 3.93 g N m^{-3} d^{-1} (Fig 1.6e). Previous studies showed softwood had a greater NRR than hardwood for the first ten months of DNBR operation long-term studies (0-15 years) (Cameron and Schipper 2010; Addy et al. 2016). This result was probably due to the indirect effects of wood density on C decomposition (Addy et al. 2016). Even though the higher density of the hardwood is expected to have a greater C supply than softwood, C is more easily released from softwood because of the low-density and greater oxygen infusion during decomposition (Cornwell et al. 2009).

Nitrate removal by media C/N ratio

In general, woodchips and cardboard materials have a high C/N ratio (>100), while the C/N ratio of single filling materials, such as barley straw, wheat straw, and corn stalk is below 100 (Table 2). As shown in Fig 1.6g, the materials with C/N ratios below 100 had a greater NRR than the materials with higher C/N ratios (>100). Fig 1.6f shows that the C/N ratio has no significant influence on NRE. The decrease in NRR from materials with higher C/N ratios is probably due to the influence of woodchips and cardboards. These materials have lower decomposition rates because the C source is mainly made of cellulose, hemicellulose, and lignin (Van der Lelie et al. 2012). Lignin is more recalcitrant than hemicellulose and cellulose (Janusz et al. 2017). Thus, the lignocellulose index (LCI) is greater. Table 2 showed that woodchips (hard and softwood) and cardboard have a greater LCI and C/N ratio than other plant materials. This may explain why these higher C/N ratio materials generated lower NRRs. Moreover, it has been observed that the C/N ratio decreases and LCI increase with time (Ghane et al. 2018). It has also been suggested that the C/N ratio is critical

for the longevity of the DNBR, and that LCI is a C quality indicator.

Nitrate removal by experiment scale

Fig 1.6i shows that the NRR effect size of the lab-scale and field-scale was 10.31 g N m^{-3} d^{-1} and 4.09 g N m^{-3} d^{-1}. This may attribute to greater control over experimental variables, such as stable higher temperatures (20 to 25 ℃), and higher nitrate loading (>10 mg L^{-1}) than present in natural agricultural drainage systems (Schipper et al. 2010b). Further, the activity of the dominant denitrifying bacteria might vary greatly with long-term exposure to synthetic wastewater, owing to their acclimation to stable wastewater properties (Miao et al. 2020b). The field influent water is also composed of solutions that have variable and complication compositions compared to the synthetic laboratory solutions. It has been reported that higher salinity will also inhibit nitrate removal (von Ahnen et al. 2019). Thus, our evaluation suggests that it is not advisable to compare the performance of denitrifying bioreactors at different scales.

Mechanisms of nitrate removal

Nitrate removal mechanisms are summarized in Fig. 1.7. The main mechanisms that occur in DNBRs are heterotrophic denitrification (HD), autotrophic denitrification (AD), dissimilatory nitrate reduction to ammonium (DNRA), and anaerobic ammonium oxidation (Anammox). The HD and AD mechanisms are the most commonly observed, while DNRA, Anammox, and Chemodentrification (CD) are uncommon.

The HD relies on organic C as the major electron donor for nitrate removal. The HD reaction is (where CH_2O represents organic C):

$$2NO_3^- + 2.5CH_2O + 2H^+ = N_2 + 3.5H_2O \quad (4)$$

Carlson et al. (2020) revealed that specific C sources favor different respiratory processes because respiratory and catabolic genes are differentially distributed across microbial genomes. However, some laboratory studies indicated that HD plays an important role in N_2O production, and the heterotrophic nitrate reduction likely stops at N_2O rather than N_2 ($2NO_3^- + 2CH_2O + 2H^+ = N_2O + 2CO_2 + 3H_2O$) (Wang et al. 2014).

The AD mechanism differs from HD in that inorganic compounds act as electron donors. These inorganic compounds include pyrite (Xu et al. 2019) (Eq. (5)), elemental sulfur (Zhou et al. 2011) (Eq. (6)), and zero-valent iron (ZVI) (Liu et al. 2019b) (Eq. (7)).

$$0.364FeS_2 + 0.116CO_2 + NO_3^- + 0.821H_2O + 0.023NH_4^+ \rightarrow 0.364Fe(OH)_3 + 0.023C_5H_7O_2N + 0.5N_2 + 0.729SO_4^{2-} + 0.48H^+ \quad (5)$$

$$1.06NO_3^- + 1.11S + 0.3CO_2 + 0.785H_2O \rightarrow 0.5N_2 + 1.11SO_4^{2-} + 1.16H^+ + 0.06C_5H_7O_2N \quad (6)$$

$$NO_3^- + 4Fe^0 + 10H^+ \rightarrow NH_4^+ + 4Fe^{2+} + 3H_2O \quad (7)$$

The DNRA mechanism has been reported to occur in DNBRs (Gibert et al. 2008; Li et al. 2017; Aalto et al. 2020). The DNRA reaction is (Kuypers et al. 2018).

$$NO_3^- + 2CH_2O + 2H^+ = NH_4^+ + 2CO_2 + H_2O \quad (8)$$

This mechanism is competitive with denitrification, especially at higher concentrations of electron donors (Carlson et al. 2020) or limited nitrate (Kelso et al.

1997). Thus, DNRA is favored when the C dosage is high and is likely to occur in DNBRs with MM, NC, or NNC due to the extra C dosage.

Chemodenitrification (CD) is the reduction of NO_3^- via a chemical process (e.g., Fe (II) oxidation) (Parkes et al. 2007):

$$10Fe^{2+} + 2NO_3^- + 12H^+ = 10Fe^{3+} + N_2 + 6H_2O \quad (9)$$

Based on our review of the literature, the CD has not been reported in DNBR studies. This is partially due to the fact that chemical denitrification requires a catalyst. For example, it was found that nitrate cannot be directly reduced by Fe(II) without a catalyst (Hansen et al. 2001), such as Cu^{2+}, iron oxides and hydroxides, or microbial surfaces (Coby and Picardal 2005; Rancourt et al. 2005).

Compared with the above mechanisms, the most economical approach for nitrate removal is Anammox (Mulder et al. 1995). Anammox bacteria have been confirmed as a type of chemoautotrophic bacteria, which use CO_2 as the C source (Kimura et al. 2011):

$$NH_4^+ + 1.32NO_2^- + 0.066HCO_3^- + 0.13H^+ \rightarrow 1.02N_2 + 0.26NO_3^- + 0.066CH_2O_{0.5}N_{0.15} + 2.03H_2O \quad (10)$$

Anammox process is facilitated by the bacteria that belong to phylum *Planctomycetes* (van Teeseling et al., 2015). To date, seven anammox genera (*Brocadia*, *Kuenenia*, *Scalindua*, *Brasilis*, *Jettenia*, *Anammoxoglobus*, *Anammoximicrobium*) and about 22 anammox species have been identified in wastewater treatment systems, marine ecosystems, terrestrial ecosystems, and lab bioreactors (Miao et al. 2019). In addition, anammox bacteria are sensitive to

environmental conditions, such as oxygen (Egli et al. 2001), temperature (Tomaszewski et al. 2017), and pH (Strous et al. 1999). The Anammox process may be dominant in systems where denitrification occurs under limited C conditions (Rambags et al. 2019). Li et al. (2015) found that both NH_4-N and total nitrogen removal efficiencies exceeded 90% when the chemical oxygen demand (COD) is 100 mg L^{-1}. In contrast, Anammox accounted for only 69% of total N removal when COD concentrations reached 300 mg L^{-1}. Although organic compounds may adversely impact Anammox, a low COD concentration or suitable COD/N ratio may support the occurrence of both Anammox and denitrification (Ni et al. 2012; Miao et al. 2015), which could subsequently increase NRE.

Although many studies reported Anammox in natural and artificial environments (Cao et al. 2020), very little research has been conducted on this topic in connection with DNBR. Based on our review, Rambags et al. (2019) were the first to report that Anammox occurred in DNBR with woodchip, coconut husk, and gravel fill materials. A prerequisite of Anammox is the presence of both NO_3 and NH_4. However, DNBR is used to treat agricultural drainage water without NH_4. Thus, it is a challenge to involve the Anammox mechanism in DNBR systems. If Anammox was to occur in DNBR systems, the processing can be a practical pathway to the remove of nitrate from agricultural drainage water without consuming too much available C. The process may also limit the production of nitrous oxide, compared with denitrification. Further studies are needed to investigate what types of media and environment will cause Anammox to occur in DNBR without NH_4.

Pollution swapping

Previous studies of DNBR indicate the production of many substances, including

chemical oxygen demand (COD) (Rivas et al. 2020), ammonium (NH_4), phosphorus (PO_4) (Rivas et al. 2020), methane (CH_4) (Elgood et al. 2010), carbon dioxide (CO_2) (Bock et al. 2018a) and nitrous oxide (N_2O) (Elgood et al. 2010). For most of the NC group, such as woodchips, dissolved organic carbon (DOC) and soluble phosphorus are two concerns, especially during the start-up phase (Sharrer et al. 2016; Rivas et al. 2020). Sharrer et al. (2016) reported that approximately 20-30 mg P kg^{-1} was released, and the bulk of this was released within the first 24h of DNBR operation (Sharrer et al. 2016). Rivas et al. (2020) also reported that elevated DOC and dissolved P occurred in the effluent during the start-up phase. Another issue is the incomplete denitrification of NO_3 and the production of N_2O (attributed to heterotrophic denitrification) (Wang et al. 2014). Some researchers reported that adding biochar can reduce N_2O losses (Bock et al. 2015a). Also, other NC sources, like maize cobs, will lead to increased C and N_2O in the effluent, as well as substantial C consumption by non-denitrifiers (Warneke et al. 2011).

NNC materials are high-risk materials that may cause second pollution or pose environmental risks. For example, cardboard was reported to emit greenhouse gas emission of CH_4 (296 g CO_2-eq m^{-2} d^{-1}) (Healy et al. 2015). Also, biodegradable polymers have the problem of producing color in the effluent (Warneke et al. 2011).

For the IM materials, elemental sulfur serves as an electron donor for the AD process. It is low soluble, non-toxic, and stable under normal conditions. The primary shortcoming in S oxidation is the production of sulfate and acid (Li et al. 2017) (Eq. (11)):

$$1.1S+NO_3^-+0.76H_2O+0.4CO_2+0.08NH_4^+ \rightarrow 0.08C_5H_7O_2N+1.1SO_4^{2-}+0.5N_2+1.28H^+ \quad (11)$$

The acidity produced in the process may be by adding limestone, but this process enhances the hardness of the treated water (Zhou et al. 2011). Zero valent iron (ZVI) also serves as an electron donor for the AD process. The undesirable pollutant is ammonium, and the abiotic reaction is illustrated in Eq. (7) (Liu et al. 2019b).

The MM group of fill materials may face all of the issues described above. It is concerning that the addition of extra C sources may excessively increase the release of organic C from bioreactors, while the addition of activated C substantially reduces organic C losses while maintaining denitrification (Pluer et al. 2020).

Cost analysis

Filling materials occupy about 13% to 55% of the total cost of establishing a DNBR in the field (Christianson et al. 2012). Therefore, the cost of the filling materials is an important factor to be considered in DNBR construction. However, the cost of filling materials is difficult to evaluate due to the large uncertainty in the source. Even though our meta-analysis presented that NNC, IM, and MM have greater NNR or NRE than NC (Fig 1.5a and 1.5b), considering the real application, most of NCs were applied due to their lower cost than NNC, IM, and MM. For example, biodegradable polymers cost from $3-10 per kilogram of PBS, PLA, and PCL (Chu and Wang 2011) which limited its application in agricultural practices. Thus, in terms of economic evaluation, NC is the best material comparing the NNC, NC, IM, and MM categories because almost all NC can be easily obtained from proximate cropland or forestland. Some researchers have reported that it costs more for organic electron donors (e.g., methanol, acetic acid) than for inorganic electron donors (Table 3). This is because methanol and acetic acid organic C sources are commercial chemicals that are more expensive than the NC source. Inorganic electron donors for

nitrate removal, elemental sulfur, sulfides, ZVI, pyrite, and thiocyanate have a relatively lower cost (Table 3)

From our perspective, we suggest that MM is the optimum media because its auxiliary materials have a wide choice to reduce cost and achieve a circular economy by considering agricultural and industrial wastes. So far, the use of agricultural solid waste in DNBRs has been well documented (Schipper et al. 2010a; Warneke et al. 2011; Healy et al. 2012; Tangsir et al. 2017). But little is known about industrial waste. Recent studies point out that utilizing industrial waste in DNBRs not only contributed toward a circular economy but also enhanced nitrogen removal (Kiani et al. 2020). In fact, this strategy has been investigated by a few studies, such as those using biochar (Bock et al. 2018b; Berger et al. 2019; Povilaitis and Matikienė 2020) or fly ash pellets (Li et al. 2018) as auxiliary materials. Our meta-analysis also demonstrated that adding biochar or fly ash pellets into woodchip-derived DNBR can significantly increase NRR and NRE relative to woodchips alone (Fig 1.8). Furthermore, organic liquid hazardous waste was recently proposed to reduce nitrate and dispose of organic liquid wastes simultaneously, exhibiting lower environmental stress and fewer non-renewable inputs required than the traditional process (Miao et al. 2020a). But little progress has been made with using organic liquid waste in DNBRs. Therefore, we suggest that reutilizing industrial and agricultural waste into DNBR is a win-win strategy that should bring more attraction to producers to improve nitrate removal and reduce environmental risks.

Conclusions

The NRR increased with NRE from a holistic review, but a greater uncertainty of NRR at a high NRE range (90-100%). The NRR and NRE by different filling materials in DNBR vary. We point out the nitrate removal is associated with wood types, media C/N ratio, and study scale. Importantly, the ranking order of nitrate removal performance by NRR and NRE is not consistent for the filling materials. Thus, both indexes should be considered in future studies. This review summarizes the filling materials (40 types) into four main groups: natural carbon (NC), non-natural carbon (NNC), inorganic material (IM), and multi-material (MM). Our meta-analysis did a comparative assessment among the filling materials and indicated that NNC has the highest nitrate removal (NRE & NRR). However, we suggest MM as the optimum material for nitrate removal due to the low cost and wider application. In MMs, adding auxiliary into woodchip-based DNBR was a promising choice for enhancing denitrification and keeping a long-term operation.

Acknowledgements

This work was partially supported by the Chinese Government Scholarship, Chinese Scholarship Council (CSC No. 201706350282), which is funding to Yuchuan Fan. We thank Wen Liu for help at data collection.

References

Aalto S L, Suurnäkki S, von Ahnen M, et al. 2020. Nitrate removal microbiology in woodchip bioreactors: A case-study with full-scale bioreactors treating aquaculture effluents[J]. Science of The Total Environment: 138093.

Addy K, Gold A J, Christianson L E, et al. 2016. Denitrifying Bioreactors for Nitrate Removal: A Meta-Analysis[J]. Journal of Environmental Quality, 45(3): 873-881.

Aslan Ş, Türkman A. 2005. Combined biological removal of nitrate and pesticides using wheat straw as substrates[J]. Process Biochemistry, 40(2): 935-943.

Berger A W, Valenca R, Miao Y, et al. 2019. Biochar increases nitrate removal capacity of woodchip biofilters during high-intensity rainfall[J]. Water Research, 165: 115008.

Blowes D W, Robertson W D, Ptacek C J, et al. 1994. Removal of agricultural nitrate from tile-drainage effluent water using in-line bioreactors[J]. Journal of Contaminant Hydrology, 15(3): 207-221.

Bock E, Smith N, Rogers M, et al. 2015a. Enhanced Nitrate and Phosphate Removal in a Denitrifying Bioreactor with Biochar[J]. Journal of Environmental Quality, 44(2): 605-613.

Bock E M, Coleman B, Easton Z M. 2015b. Effect of Biochar on Nitrate Removal in a Pilot-Scale Denitrifying Bioreactor[J]. Journal of Environmental Quality, 45(3): 762-771.

Bock E M, Coleman B S L, Easton Z M. 2018a. Effect of biochar, hydraulic residence time, and nutrient loading on greenhouse gas emission in laboratory-scale denitrifying bioreactors[J]. Ecological Engineering, 120: 375-383.

Bock E M, Coleman B S L, Easton Z M. 2018b. Performance of an under-loaded denitrifying bioreactor with biochar amendment[J]. Journal of Environmental Management, 217: 447-455.

Boley A, Müller W R, Haider G. 2000. Biodegradable polymers as solid substrate and biofilm carrier for denitrification in recirculated aquaculture systems[J]. Aquacultural Engineering, 22(1): 75-85.

Bruun J, Hoffmann C C, Kjaergaard C. 2016. Nitrogen Removal in Permeable Woodchip Filters Affected by Hydraulic Loading Rate and Woodchip Ratio[J]. Journal of Environmental Quality, 45(5): 1688-1695.

Cameron S G, Schipper L A. 2010. Nitrate removal and hydraulic performance of organic carbon for use in denitrification beds[J]. Ecological Engineering, 36(11): 1588-1595.

Cameron S G, Schipper L A. 2012. Hydraulic properties, hydraulic efficiency and nitrate removal of organic carbon media for use in denitrification beds[J]. Ecological Engineering, 41: 1-7.

Cao S, Du R, Zhou Y. 2020. Coupling anammox with heterotrophic denitrification for enhanced nitrogen removal: A review[J]. Critical Reviews in Environmental Science and Technology: 1-34.

Carlson H K, Lui L M, Price M N, et al. 2020. Selective carbon sources influence the end products of microbial nitrate respiration[J]. The ISME Journal: 1-12.

Christianson L, Tyndall J, Helmers M. 2013. Financial comparison of seven nitrate reduction strategies for Midwestern agricultural drainage[J]. Water Resources and Economics, 2-3: 30-56.

Christianson L E, Bhandari A, Hailers M J. 2012. A Practice-Oriented Review Of Woodchip Bioreactors For Subsurface Agricultural Drainage[J]. Applied Engineering in Agriculture, 28(6): 861-874.
Chu L, Wang J. 2011. Nitrogen removal using biodegradable polymers as carbon source and biofilm carriers in a moving bed biofilm reactor[J]. Chemical Engineering Journal, 170(1): 220-225.
Coby A J, Picardal F W. 2005. Inhibition of NO3- and NO2- Reduction by Microbial Fe(III) Reduction: Evidence of a Reaction between NO2− and Cell Surface-Bound Fe2+[J]. Applied and Environmental Microbiology, 71(9): 5267-5274.
Coleman B S L, Easton Z M, Bock E M. 2019. Biochar fails to enhance nutrient removal in woodchip bioreactor columns following saturation[J]. Journal of Environmental Management, 232: 490-498.
Cornwell W K, Cornelissen J H, Allison S D, et al. 2009. Plant traits and wood fates across the globe: rotted, burned, or consumed?[J]. Global Change Biology, 15(10): 2431-2449.
Della Rocca C, Belgiorno V, Meriç S. 2006. An heterotrophic/autotrophic denitrification (HAD) approach for nitrate removal from drinking water[J]. Process Biochemistry, 41(5): 1022-1028.
Easton Z M, Rogers M, Davis M, et al. 2015. Mitigation of sulfate reduction and nitrous oxide emission in denitrifying environments with amorphous iron oxide and biochar[J]. Ecological Engineering, 82: 605-613.
Egli K, Fanger U, Alvarez P J J, et al. 2001. Enrichment and characterization of an anammox bacterium from a rotating biological contactor treating ammonium-rich leachate[J]. Archives of Microbiology, 175(3): 198-207.
Elgood Z, Robertson W D, Schiff S L, et al. 2010. Nitrate removal and greenhouse gas production in a stream-bed denitrifying bioreactor[J]. Ecological Engineering, 36(11): 1575-1580.
Fenton O, Healy M G, Brennan F, et al. 2014. Permeable reactive interceptors: blocking diffuse nutrient and greenhouse gases losses in key areas of the farming landscape[J]. The Journal of Agricultural Science, 152(S1): 71-81.
Feyereisen G W, Moorman T B, Christianson L E, et al. 2016. Performance of agricultural residue media in laboratory denitrifying bioreactors at low temperatures[J]. Journal of Environmental Quality, 45(3): 779-787.
Ghane E, Feyereisen G W, Rosen C J, et al. 2018. Carbon Quality of Four-Year-Old Woodchips in a Denitrification Bed Treating Agricultural Drainage Water[J]. Transactions of the ASABE, 61(3): 995-1000.
Gibert O, Pomierny S, Rowe I, et al. 2008. Selection of organic substrates as potential reactive materials for use in a denitrification permeable reactive barrier (PRB)[J]. Bioresource Technology, 99(16): 7587-7596.
Greenan C M, Moorman T B, Kaspar T C, et al. 2006. Comparing carbon substrates for denitrification of subsurface drainage water[J]. Journal of Environmental Quality, 35(3): 824-829.
Griessmeier V, Leberecht K, Gescher J. 2019. NO3- removal efficiency in field denitrification beds: key controlling factors and main implications[J]. Environmental Microbiology Reports, 11(3): 316-329.
Halaburka B J, LeFevre G H, Luthy R G. 2017. Evaluation of Mechanistic Models for Nitrate Removal in Woodchip Bioreactors[J]. Environmental Science & Technology, 51(9): 5156-5164.

Hansen H C B, Guldberg S, Erbs M, et al. 2001. Kinetics of nitrate reduction by green rusts—effects of interlayer anion and Fe(II):Fe(III) ratio[J]. Applied Clay Science, 18(1): 81-91.
Healy M G, Barrett M, Lanigan G J, et al. 2015. Optimizing nitrate removal and evaluating pollution swapping trade-offs from laboratory denitrification bioreactors[J]. Ecological Engineering, 74: 290-301.
Healy M G, Ibrahim T G, Lanigan G J, et al. 2012. Nitrate removal rate, efficiency and pollution swapping potential of different organic carbon media in laboratory denitrification bioreactors[J]. Ecological Engineering, 40: 198-209.
Healy M G, Rodgers M, Mulqueen J. 2007. Denitrification of a nitrate-rich synthetic wastewater using various wood-based media materials[J]. Journal of Environmental Science and Health Part A, 41(5): 779-788.
Honda Y, Osawa Z. 2002. Microbial denitrification of wastewater using biodegradable polycaprolactone[J]. Polymer Degradation and Stability, 76(2): 321-327.
Hoover N L, Bhandari A, Soupir M L, et al. 2015. Woodchip denitrification bioreactors: Impact of temperature and hydraulic retention time on nitrate removal[J]. Journal of Environmental Quality, 45(3): 803-812.
Hua G, Salo M W, Schmit C G, et al. 2016. Nitrate and phosphate removal from agricultural subsurface drainage using laboratory woodchip bioreactors and recycled steel byproduct filters[J]. Water Research, 102: 180-189.
Israel H, Richter R R. 2011. A guide to understanding meta-analysis[J]. journal of orthopaedic & sports physical therapy, 41(7): 496-504.
Janusz G, Pawlik A, Sulej J, et al. 2017. Lignin degradation: microorganisms, enzymes involved, genomes analysis and evolution[J]. Fems Microbiology Reviews, 41(6): 941-962.
Ju X-T, Xing G-X, Chen X-P, et al. 2009. Reducing environmental risk by improving N management in intensive Chinese agricultural systems[J]. Proceedings of the National Academy of Sciences, 106(9): 3041-3046.
Kelso B, Smith R V, Laughlin R J, et al. 1997. Dissimilatory nitrate reduction in anaerobic sediments leading to river nitrite accumulation[J]. Appl Environ Microbiol, 63(12): 4679-4685.
Kiani S, Kujala K, T. Pulkkinen J, et al. 2020. Enhanced nitrogen removal of low carbon wastewater in denitrification bioreactors by utilizing industrial waste toward circular economy[J]. Journal of Cleaner Production, 254: 119973.
Kijjanapanich P, Yaowakun Y. 2019. Enhancement of Nitrate-Removal Efficiency Using a Combination of Organic Substrates and Zero-Valent Iron as Electron Donors[J]. Journal of Environmental Engineering, 145(4): 10.
Kimura Y, Isaka K, Kazama F. 2011. Effects of inorganic carbon limitation on anaerobic ammonium oxidation (anammox) activity[J]. Bioresource Technology, 102(6): 4390-4394.
Kouanda A, Hua G. 2021. Determination of Nitrate Removal Kinetics Model Parameters in Woodchip Bioreactors[J]. Water Research: 116974.
Kuypers M M M, Marchant H K, Kartal B. 2018. The microbial nitrogen-cycling network[J]. Nature Reviews Microbiology, 16: 263.
Lehmann J, Rillig M C, Thies J, et al. 2011. Biochar effects on soil biota – A review[J]. Soil Biology & Biochemistry, 43(9): 1812-1836.

Lepine C, Christianson L, Sharrer K, et al. 2015. Optimizing hydraulic retention times in denitrifying woodchip bioreactors treating recirculating aquaculture system wastewater[J]. Journal of Environmental Quality, 45(3): 813-821.
Li R, Feng C P, Xi B D, et al. 2017. Nitrate removal efficiency of a mixotrophic denitrification wall for nitrate-polluted groundwater in situ remediation[J]. Ecological Engineering, 106: 523-531.
Li S, Cooke R A, Huang X, et al. 2018. Evaluation of fly ash pellets for phosphorus removal in a laboratory scale denitrifying bioreactor[J]. Journal of Environmental Management, 207: 269-275.
Lipsey M W, Wilson D B. 2001. Practical meta-analysis[M]. City: Sage Publications, Inc.
Liu F, Wang Y, Xiao R, et al. 2015. Influence of substrates on nutrient removal performance of organic channel barriers in drainage ditches[J]. Journal of Hydrology, 527: 380-386.
Liu T, Chen D, Luo X, et al. 2019a. Microbially mediated nitrate-reducing Fe(II) oxidation: Quantification of chemodenitrification and biological reactions[J]. Geochimica et Cosmochimica Acta, 256: 97-115.
Liu X W, Xu J, Huang J L, et al. 2019b. Bacteria-supported iron scraps for the removal of nitrate from low carbon-to-nitrogen ratio wastewater[J]. Rsc Advances, 9(6): 3285-3293.
Long L M, Schipper L A, Bruesewitz D A. 2011. Long-term nitrate removal in a denitrification wall[J]. Agriculture Ecosystems & Environment, 140(3-4): 514-520.
Maxwell B M, Birgand F, Schipper L A, et al. 2019. Increased duration of drying–rewetting cycles increases nitrate removal in woodchip bioreactors[J]. Agricultural & Environmental Letters, 4.
Miao L, Wang S, Cao T, et al. 2015. Optimization of three-stage Anammox system removing nitrogen from landfill leachate[J]. Bioresource Technology, 185: 450-455.
Miao L, Yang G Q, Tao T, et al. 2019. Recent advances in nitrogen removal from landfill leachate using biological treatments - A review[J]. Journal of Environmental Management, 235: 178-185.
Miao S, Jin C, Liu R, et al. 2020a. Carbon harvesting from organic liquid wastes for heterotrophic denitrification: Feasibility evaluation and cost and emergy optimization[J]. Resources, Conservation and Recycling, 160: 104782.
Miao S, Jin C, Liu R, et al. 2020b. Microbial community structures and functions of hypersaline heterotrophic denitrifying process: Lab-scale and pilot-scale studies[J]. Bioresource Technology: 123244.
Mulder A, van de Graaf A A, Robertson L A, et al. 1995. Anaerobic ammonium oxidation discovered in a denitrifying fluidized bed reactor[J]. Fems Microbiology Ecology, 16(3): 177-183.
Ni S-Q, Ni J-Y, Hu D-L, et al. 2012. Effect of organic matter on the performance of granular anammox process[J]. Bioresource Technology, 110: 701-705.
Parkes S D, Jolley D F, Wilson S R. 2007. Inorganic nitrogen transformations in the treatment of landfill leachate with a high ammonium load: A case study[J]. Environmental Monitoring and Assessment, 124(1-3): 51-61.
Peng W, Pivato A, Garbo F, et al. 2019. Stabilization of solid digestate and nitrogen removal from mature leachate in landfill simulation bioreactors packed with aged refuse[J]. Journal of Environmental Management, 232: 957-963.

Pluer W T, Geohring L D, Steenhuis T S, et al. 2016. Controls influencing the treatment of excess agricultural nitrate with denitrifying bioreactors[J]. Journal of Environmental Quality, 45(3): 772-778.
Pluer W T, Morris C K, Walter M T, et al. 2019. Denitrifying bioreactor response during storm events[J]. Agricultural Water Management, 213: 1109-1115.
Pluer W T, Walter M T, Steinschneider S. 2020. Understanding Complex Flow Pathways within Lab-Scale Denitrifying Bioreactors with a Conservative Tracer[J]. Transactions of the ASABE, 63(2): 417-427.
Povilaitis A, Matikienė J. 2020. Nitrate removal from tile drainage water: The performance of denitrifying woodchip bioreactors amended with activated carbon and flaxseed cake[J]. Agricultural Water Management, 229: 105937.
Rambags F, Tanner C C, Schipper L A. 2019. Denitrification and anammox remove nitrogen in denitrifying bioreactors[J]. Ecological Engineering, 138: 38-45.
Rancourt D G, Thibault P-J, Mavrocordatos D, et al. 2005. Hydrous ferric oxide precipitation in the presence of nonmetabolizing bacteria: Constraints on the mechanism of a biotic effect[J]. Geochimica et Cosmochimica Acta, 69(3): 553-577.
Rivas A, Barkle G, Stenger R, et al. 2020. Nitrate removal and secondary effects of a woodchip bioreactor for the treatment of subsurface drainage with dynamic flows under pastoral agriculture[J]. Ecological Engineering, 148: 105786.
Robertson W D, Vogan J L, Lombardo P S. 2008. Nitrate removal rates in a 15-year-old permeable reactive barrier treating septic system nitrate[J]. Ground Water Monitoring and Remediation, 28(3): 65-72.
Rocca C D, Belgiorno V, Meric S. 2005. Cotton-supported heterotrophic denitrification of nitrate-rich drinking water with a sand filtration post-treatment[J]. Water SA, 31(2): 229-236.
Roser M B, Feyereisen G W, Spokas K A, et al. 2018. Carbon Dosing Increases Nitrate Removal Rates in Denitrifying Bioreactors at Low-Temperature High-Flow Conditions[J]. Journal of Environmental Quality, 47(4): 856-864.
Schipper L, Vojvodic-Vukovic M. 1998. Nitrate removal from groundwater using a denitrification wall amended with sawdust: Field trial[J]. Journal of Environmental Quality, 27(3): 664-668.
Schipper L A, Cameron S C, Warneke S. 2010a. Nitrate removal from three different effluents using large-scale denitrification beds[J]. Ecological Engineering, 36(11): 1552-1557.
Schipper L A, Robertson W D, Gold A J, et al. 2010b. Denitrifying bioreactors-An approach for reducing nitrate loads to receiving waters[J]. Ecological Engineering, 36(11): 1532-1543.
Schipper L A, Robertson W D, Gold A J, et al. 2010c. Denitrifying bioreactors—An approach for reducing nitrate loads to receiving waters[J]. Ecological Engineering, 36(11): 1532-1543.
Schipper L A, Vojvodić-Vuković M. 2000. Nitrate removal from groundwater and denitrification rates in a porous treatment wall amended with sawdust[J]. Ecological Engineering, 14(3): 269-278.
Sharrer K L, Christianson L E, Lepine C, et al. 2016. Modeling and mitigation of denitrification ‘woodchip’ bioreactor phosphorus releases during treatment of aquaculture wastewater[J]. Ecological Engineering, 93: 135-143.
Shen Z Q, Hu J, Wang J L, et al. 2015. Comparison of polycaprolactone and starch/polycaprolactone blends as carbon source for biological

denitrification[J]. International Journal of Environmental Science and Technology, 12(4): 1235-1242.
Soares M I M, Abeliovich A. 1998. Wheat straw as substrate for water denitrification[J]. Water Research, 32(12): 3790-3794.
Strous M, Kuenen J G, Jetten M S M. 1999. Key physiology of anaerobic ammonium oxidation[J]. Applied and Environmental Microbiology, 65(7): 3248-3250.
Tangsir S, Moazed H, Naseri A A, et al. 2017. Investigation on the performance of sugarcane bagasse as a new carbon source in two hydraulic dimensions of denitrification beds[J]. Journal of Cleaner Production, 140: 1176-1181.
Tian H, Liang X, Gong Y, et al. 2019. Health Risk Assessment of Nitrate Pollution in Shallow Groundwater: A Case Study in China[J]. prevention, 8: 9.
Tomaszewski M, Cema G, Ziembińska-Buczyńska A. 2017. Influence of temperature and pH on the anammox process: A review and meta-analysis[J]. Chemosphere, 182: 203-214.
Van der Lelie D, Taghavi S, McCorkle S M, et al. 2012. The metagenome of an anaerobic microbial community decomposing poplar wood chips[J]. Plos One, 7(5): e36740.
Van Driel P, Robertson W, Merkley L. 2006. Denitrification of agricultural drainage using wood-based reactors[J]. Transactions of the ASABE, 49(2): 565-573.
Volokita M, Belkin S, Abeliovich A, et al. 1996. Biological denitrification of drinking water using newspaper[J]. Water Research, 30(4): 965-971.
von Ahnen M, Aalto S L, Suurnäkki S, et al. 2019. Salinity affects nitrate removal and microbial composition of denitrifying woodchip bioreactors treating recirculating aquaculture system effluents[J]. Aquaculture, 504: 182-189.
Wallace B C, Lajeunesse M J, Dietz G, et al. 2017. OpenMEE: Intuitive, open-source software for meta-analysis in ecology and evolutionary biology[J]. Methods in Ecology and Evolution, 8(8): 941-947.
Walters E, Hille A, He M, et al. 2009. Simultaneous nitrification/denitrification in a biofilm airlift suspension (BAS) reactor with biodegradable carrier material[J]. Water Research, 43(18): 4461-4468.
Wang Q, Jiang G, Ye L, et al. 2014. Heterotrophic denitrification plays an important role in N2O production from nitritation reactors treating anaerobic sludge digestion liquor[J]. Water Research, 62: 202-210.
Warneke S, Schipper L A, Matiasek M G, et al. 2011. Nitrate removal, communities of denitrifiers and adverse effects in different carbon substrates for use in denitrification beds[J]. Water Research, 45(17): 5463-5475.
Xu B K, Shi L S, Zhong H, et al. 2019. The performance of pyrite-based autotrophic denitrification column for permeable reactive barrier under natural environment[J]. Bioresource Technology, 290: 10.
Yao Z B, Wang C L, Song N, et al. 2019. Development of a hybrid biofilm reactor for nitrate removal from surface water with macrophyte residues as carbon substrate[J]. Ecological Engineering, 128: 1-8.
Zhang W, Ruan X H, Bai Y, et al. 2018. The characteristics and performance of sustainable-releasing compound carbon source material applied on groundwater nitrate in-situ remediation[J]. Chemosphere, 205: 635-642.
Zhou H, Zhao X, Wang J. 2009. Nitrate removal from groundwater using biodegradable polymers as carbon source and biofilm support[J]. International Journal of Environment and Pollution, 38(3): 339-348.

Zhou W, Sun Y, Wu B, et al. 2011. Autotrophic denitrification for nitrate and nitrite removal using sulfur-limestone[J]. Journal of Environmental Sciences, 23(11): 1761-1769.

Appendices

Tables

Table 1.1 Ranges of data within categories for the parameters assessed by meta-analysis.

Groups		Categories (Bioreactor units)
1	Main Groups	1.1 Natural carbon (138)
		1.2 Non-natural carbon[§] 10)
		1.3 Inorganic material[£] (3)
		1.4 Multi-material[†] (61)
		1.5 Soil (4)
2	Non-natural Carbon[§]	2.1 Biodegradable polymers (5)
		2.2 Waste and by-products (5)
3	Natural Carbon	3.1 Woodchip (99)
		3.2 Barley straw (6)
		3.3 Wheat straw (3)
		3.4 Maize cobs (10)
		3.5 Corn stover (2)
		3.6 Green waste (4)
		3.7 Rice straw (8)
		3.8 Pine needles (3)
		3.9 Macrophyte residue (3)
4	Auxiliary	4.1 Woodchip (99)
		4.2 Woodchip+[¶] (53)
		4.3 Corncob (10)
		4.4 Corncob+[¶] (10)
5	Woodchip+[¶]	5.1 W+NCs[ß] (5)
		5.2 W+NNCs (35)
		5.3 W+IMs (12)
6	Wood Source	6.1 Hardwood (38)
		6.2 Softwood (35)
7	Scales	7.1 Lab (67)
		7.2 Field (32)
8	C/N Ratio	8.1 <100 (42)
		8.2 >100 (103)

§ Non-natural carbon includes biochar, cardboard, and biodegradable polymers;
£ Inorganic material includes pyrite, sand, and amorphous iron oxide.
† Multi-materials include mixed materials which more than one;
¶ Woodchip+ represents the woodchip-derived bioreactor mix with other materials; corncob+ represents the corncob-derived bioreactor mix with other materials;
ß W represents woodchip.

Table 1.2 Ranges of data within categories for the parameters assessed by meta-analysis. List of agricultural waste chemical properties and C/N ratio, the data comes from (Worasuwannarak et al. 2007; Guo et al. 2012; Healy et al. 2012; Wang et al. 2012; Ma et al. 2016; Janusz et al. 2017; Ghane et al. 2018)

Plant material	Chemical properties				
	Chemical composition (% dry wt)				C/N ratio
	Cellulose	Hemicelluloses	Lignin	LCI (%)	
Softwood	23-42	12-32	27-32	30.2-57	223.8-496
Hardwood	38-51	17-40	21-31	25.4-57	223.8-496
Barley straw	33.25	20.36	17.13	24.2	65.7
Rice straw	32	35.7	22.3	24.8	55.25
Wheat straw	34.2	23.68	13.88	19.3	81.1
Corn stalks	61.2	19.3	6.9	7.9	41.5
Corncob	50.5	31	15	15.5	35
Cereal	45-55	26-32	16-21	18.4-19.4	n.a.
Cardboard	20	20	16.6	28.6	208

n.a.=not available.

References for Table 1.2

Di Capua F, Pirozzi F, Lens P N L, et al. 2019. Electron donors for autotrophic denitrification[J]. Chemical Engineering Journal, 362: 922-937.

Ghane E, Feyereisen G W, Rosen C J, et al. 2018. Carbon Quality of Four-Year-Old Woodchips in a Denitrification Bed Treating Agricultural Drainage Water[J]. Transactions of the ASABE, 61(3): 995-1000.

Guo R, Li G, Jiang T, et al. 2012. Effect of aeration rate, C/N ratio and moisture content on the stability and maturity of compost[J]. Bioresource Technology, 112: 171-178.

Healy M G, Ibrahim T G, Lanigan G J, et al. 2012. Nitrate removal rate, efficiency and pollution swapping potential of different organic carbon media in laboratory denitrification bioreactors[J]. Ecological Engineering, 40: 198-209.

Janusz G, Pawlik A, Sulej J, et al. 2017. Lignin degradation: microorganisms, enzymes involved, genomes analysis and evolution[J]. Fems Microbiology Reviews, 41(6): 941-962.

Ma Y, Hummel M, Määttänen M, et al. 2016. Upcycling of waste paper and cardboard to textiles[J]. Green Chemistry, 18(3): 858-866.

Wang X, Yang G, Feng Y, et al. 2012. Optimizing feeding composition and carbon–nitrogen ratios for improved methane yield during anaerobic co-digestion of dairy, chicken manure and wheat straw[J]. Bioresource Technology, 120: 78-83.

Worasuwannarak N, Sonobe T, Tanthapanichakoon W. 2007. Pyrolysis behaviors of rice straw, rice husk, and corncob by TG-MS technique[J]. Journal of Analytical and Applied Pyrolysis, 78(2): 265-271.

Table 1.3 Price, utilization, and cost of organic and inorganic electron donors for biological denitrification

(1)	Electron donor	Price (USD/kg e^- donor)	Specific substrate utilization (kg e^- donor/kg $N\text{-}NO_3^-$)	Cost (USD/kg $N\text{-}NO_3^-$)
Organic§	Methanol (CH_3OH)	0.7-0.9	2.5	1.8-2.3
	Acetic acid (CH_3COOH)	2.2	3.6	7.9
Inorganic§	Chemical sulfur (S^0_{chem})	0.1	2.6	0.26
	Sulfide (S^{2-})	0.13	1.9	0.25
	Thiosulfate ($S_2O_3^{2-}$)	0.21-0.26	6.5	1.4-1.7
	Ferrous iron ($Fe^{2+)}$	0.3	19.9	6
	Zero-valent iron (Fe^0)	0	10	0
	Pyrite (FeS_2)	0.4	2.9	1.2
	Sulfite (SO_3^{2-})	0.18	n.a.	n.a.
	Manganese (Mn^{2+})	0.2-0.21	9.8	2.0-2.1
	Thiocyanate (SCN^-)	0	2.6	0

n.a.=not available.

§ The price, specific substrate utilization, and cost data of methanol, acetic acid, and inorganic compounds come from Di Capua et al. (2019)

Table 1.4 Summary of filling materials types in denitrifying bioreactor

No	Natural carbon (NC)	No	Non-natural carbon (NNC)	No	Inorganic material (IM)	No	Multi-material (MM)
NC_1	Woodchip	NNC_1	Cardboard	IM_1	Sand	MM_1	Sand + Grow bark
NC_2	Corn stover	NNC_2	Biochar	IM_2	Amorphous iron oxide	MM_2	Sand+Grow bark+Woodchip
NC_3	Barley straw	NNC_3	Polyhydroxybutyrate (PHB)	IM_3	Pyrite	MM_3	Woodchip+Sulfur particles+zeolite
NC_4	Rice straw	NNC_4	Polycaprolactone (PCL)			MM_4	Corn cobs+Modified coconut coir
NC_5	Green waste	NNC_5	Polybutylene succinate (PBS)			MM_5	Corn cobs+Modified coconut coir+Modified biochar
NC_6	Maize cobs					MM_6	Corn cobs+Plastic biofilm carrier
NC_7	Wheat straw					MM_7	Sugarcane bagasses+Soil
NC_8	Lodge pine needles					MM_8	Sulfur+Coral stone
NC_9						MM_9	Woodchip+Steel
NC_{10}						MM_{10}	Woodchip+Biochar
						MM_{11}	Woodchip+Sodium acetate
						MM_{12}	Woodchip+Flaxseed cake

Table 1.4 continued

	MM_{13}	Woodchip+Filtralite
	MM_{14}	Woodchip+Seashell
	MM_{15}	Woodchip+Sand
	MM_{16}	Woodchip+Corn cobs
	MM_{17}	Woodchip+Fly ash pellet
	MM_{18}	Woodchip+Mire flora
	MM_{19}	Woodchip+Potato

Figures

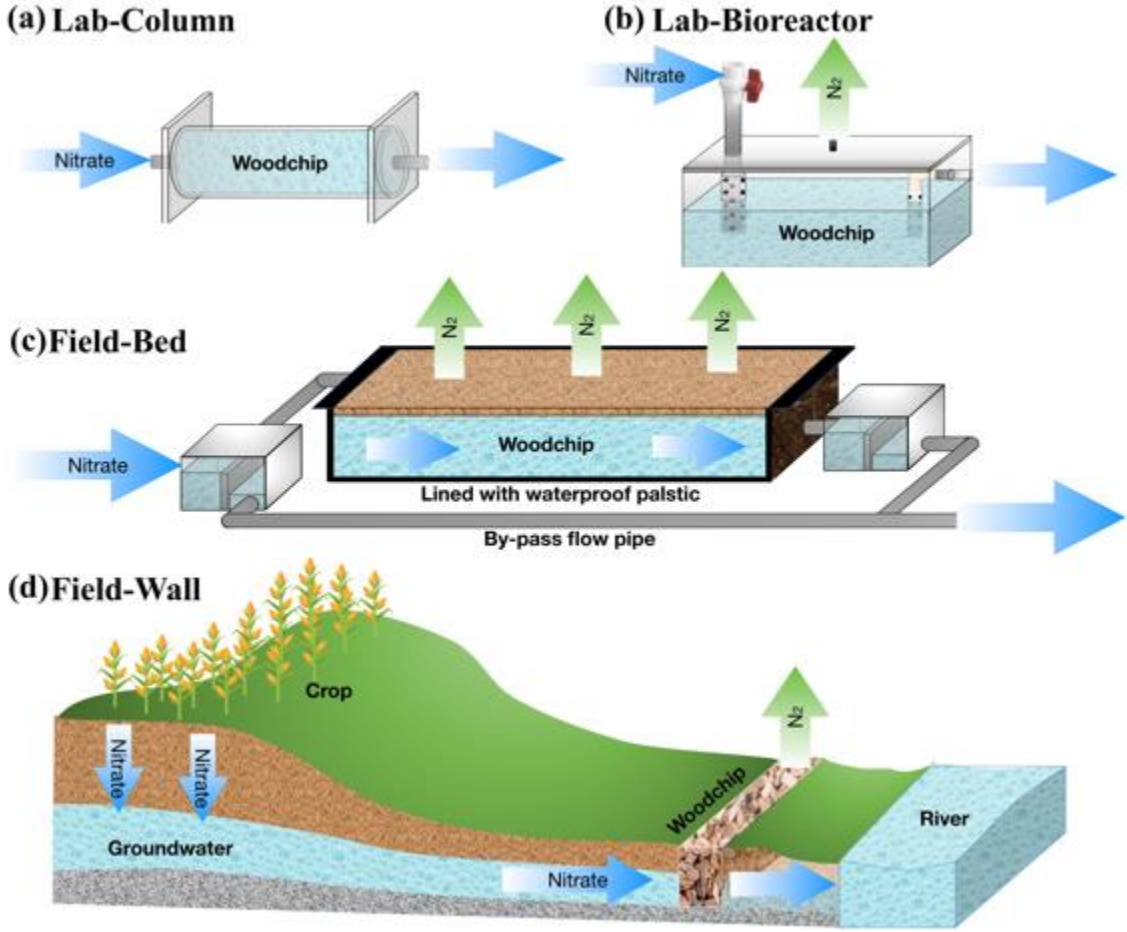

Figure 1.1 Conceptual scheme of four denitrifying bioreactors, including **(a)** lab columns, **(b)** lab bioreactors, **(c)** field beds, and **(d)** field walls.

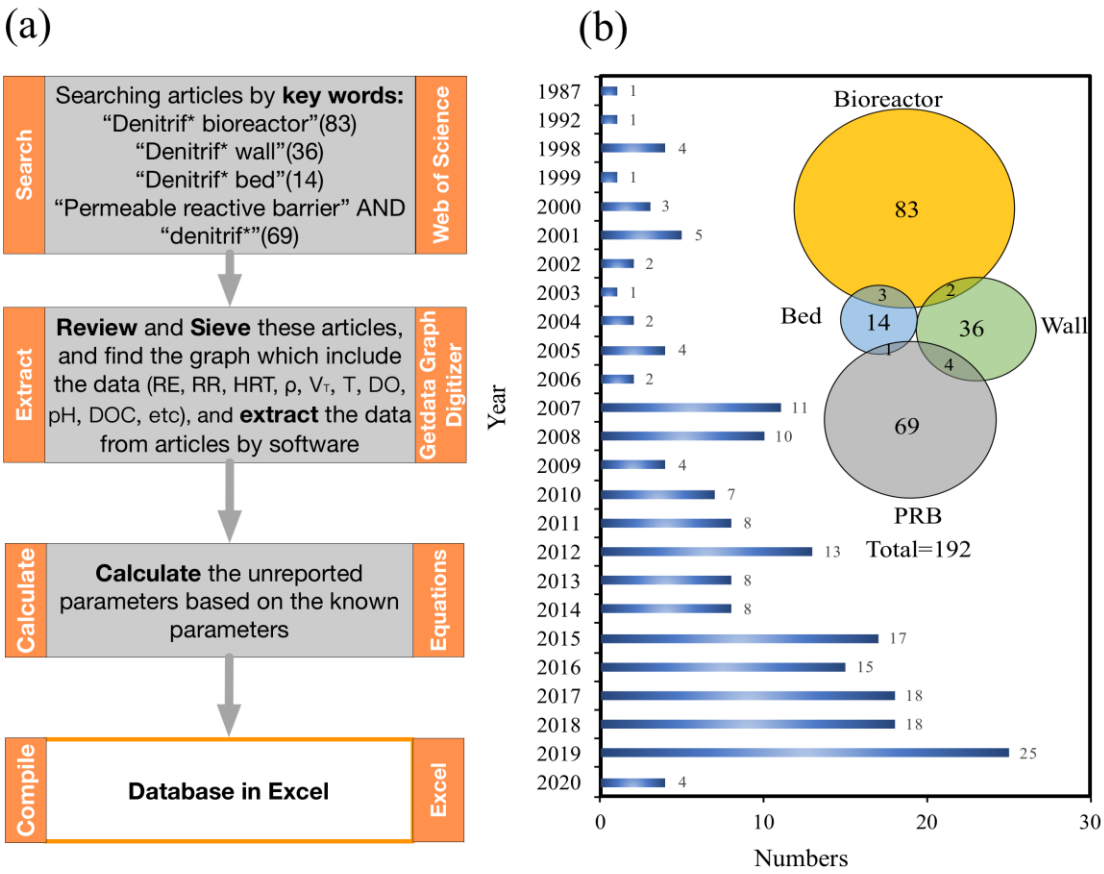

Figure 1.2 (a) Flow chart of the data compilation; (b) The number of the published DNBR articles over the year. We found 14 articles related to "denitrification bed", 36 related to "denitrification wall", 83 related to "denitrifying bioreactor", and 69 related to "permeable reactive barrier".

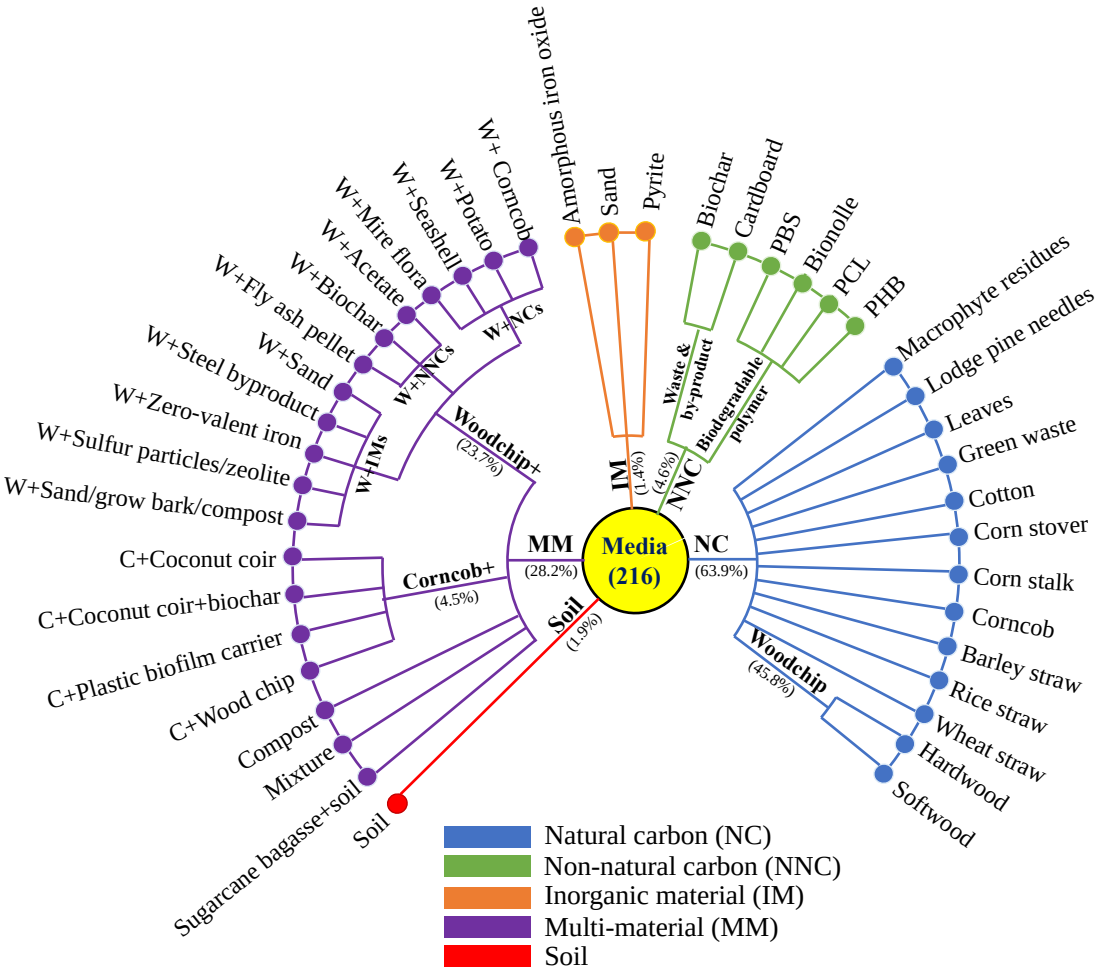

Figure 1.3 The taxonomy of filling materials in denitrifying bioreactors. The filling materials contain 216 bioreactor studies which come from 63 peer-reviewed articles. Filling materials are major classified into five groups, including natural carbon (NC), non-natural carbon (NC), inorganic material (IM), multi-material (MM), and soil, respectively. In the NC group, the single woodchip can be categorized by hardwood and softwood. In the MM groups, including woodchip-derived DNBR (Woodchip+), corncob-derived DNBR (Corncob+), and others. W represents woodchip, C represents corncob, Woodchip+ represents woodchip plus auxiliary carbon source, Corncob+ represents corncob plus auxiliary carbon source. Soil as a control group. The numbers in the bracket represent the percentage of involved studies.

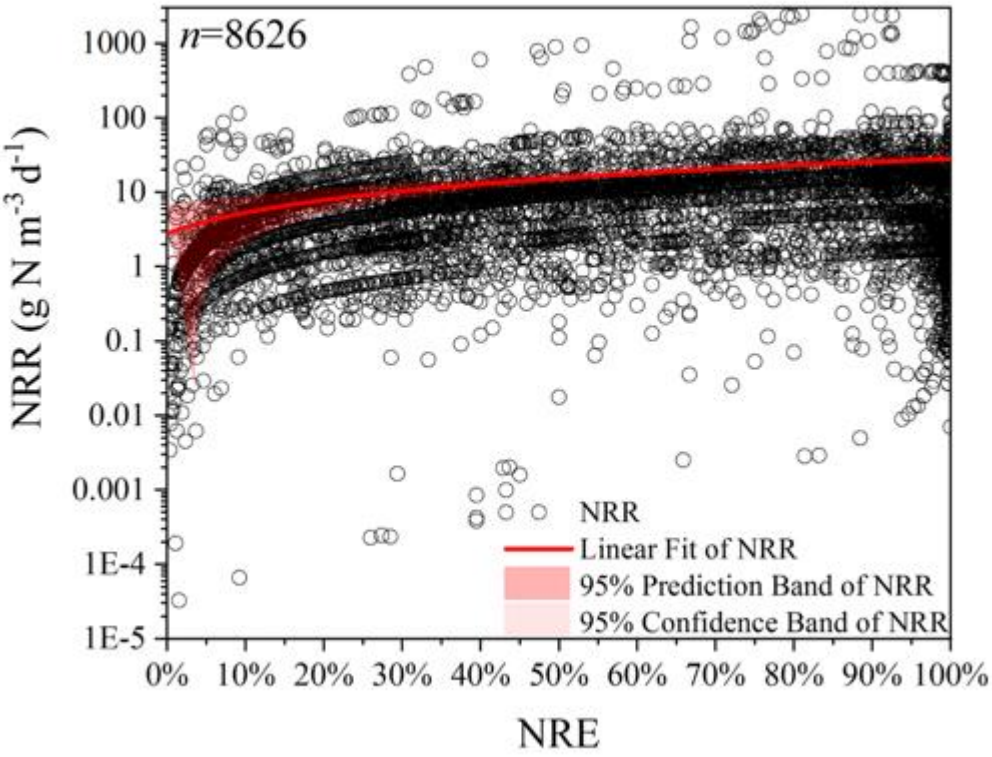

Figure 1.4 The nitrate removal rate (NRR) versus nitrate removal efficiency (NRE), all the data contained five filling materials in DNBR, including natural carbon (NC), non-natural carbon (NNC), inorganic material (IM), multi-material (MM), and soil, respectively. The red line was fitted by a linear equation with 95% confidence band and 95% prediction band. n represents the number of the data.

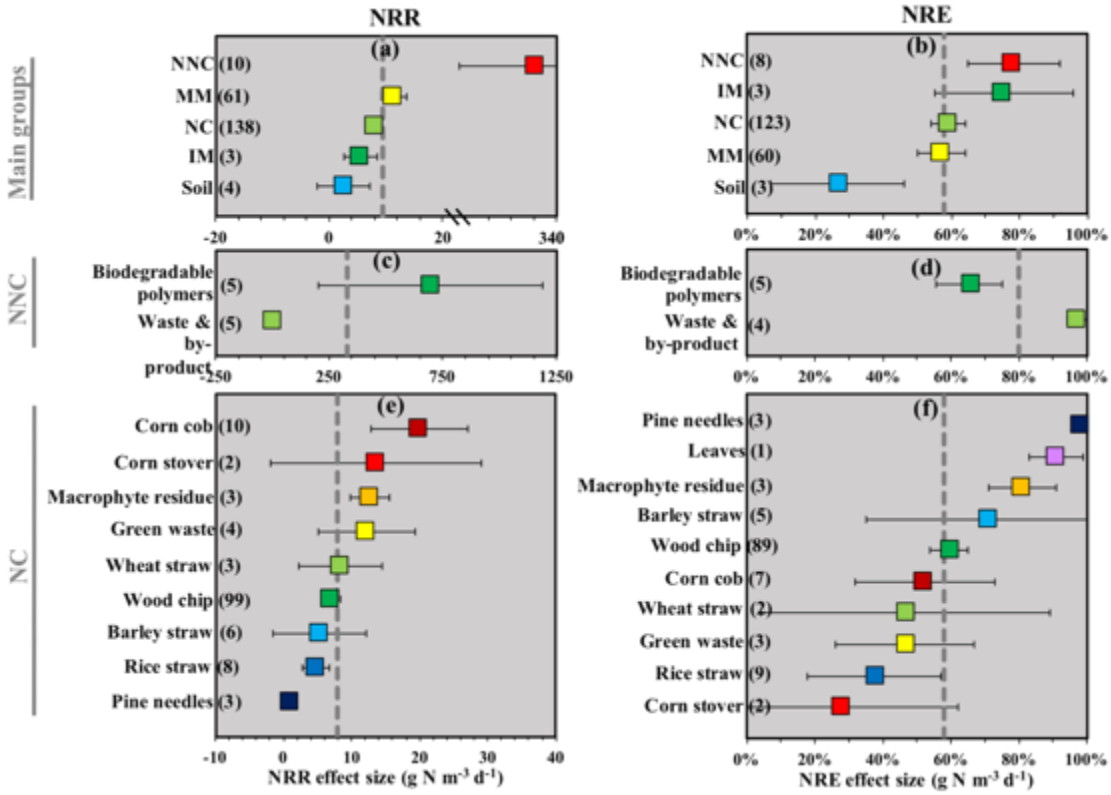

Figure 1.5 Mean nitrate removal rate (NRR) by categories of (a) main groups, (c) non-natural carbon (NNC), and (e) natural carbon (NC). Mean nitrate removal efficiency (NRE) by categories of (b) main groups, (d) non-natural carbon (NNC), and (f) natural carbon (NC). The bracketed number represents the number of DNBR units in that category that were used in the analysis.

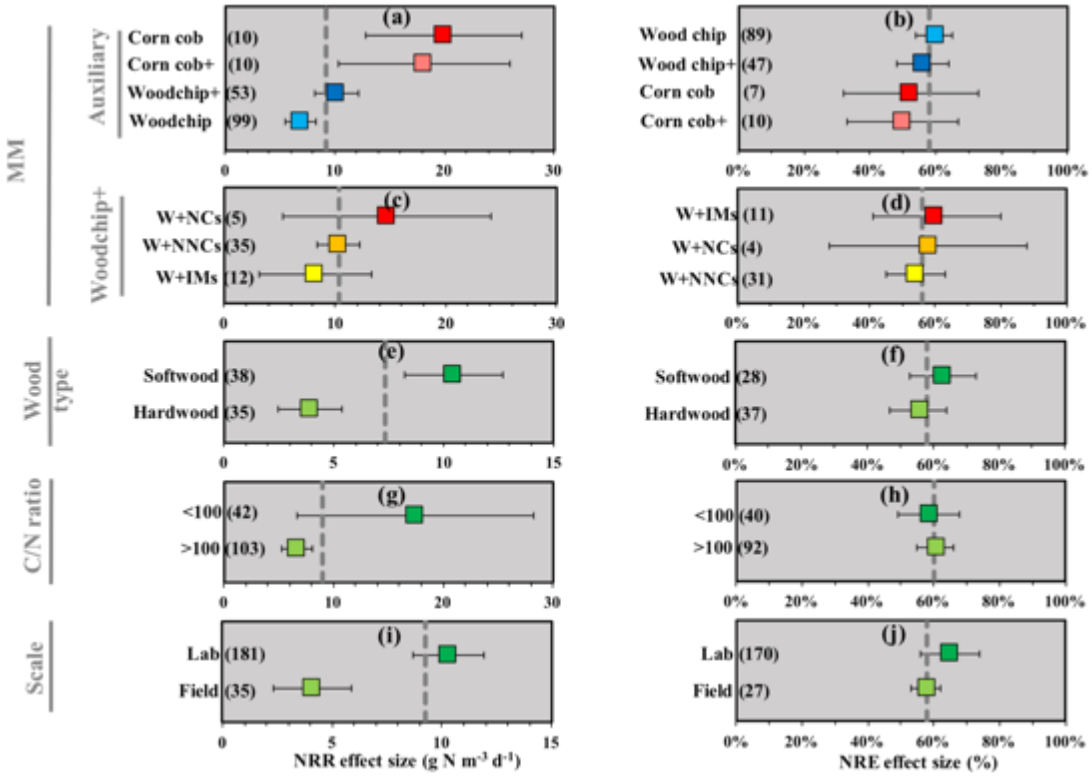

Figure 1.6 Mean nitrate removal rate (NRR) effect size by categories of **(a)** auxiliary materials, **(c)** woodchip+, **(e)** wood type, **(g)** C/N ratio, and **(i)** scale. Mean nitrate removal efficiency (NRE) by categories of **(b)** auxiliary materials, **(d)** woodchip+, **(f)** Wood type, **(h)** C/N ratio, and **(j)** scale. The bracketed number represents the number of DNBR units in that category that were used in the analysis.

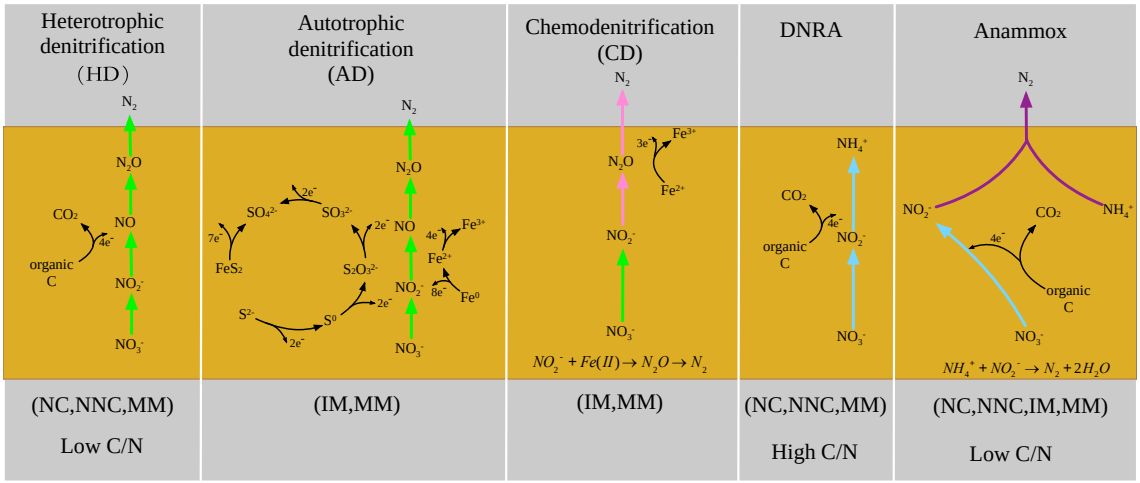

Figure 1.7 Schematic of mechanisms for various fill materials (natural carbon, non-natural carbon, multi-material, inorganic carbon) in the denitrifying bioreactor. These mechanisms include heterotrophic denitrification (HD), autotrophic denitrification (AD), chemodenitrification (CD), dissimilatory nitrate reduction to ammonia (DNRA), and anaerobic ammonium oxidation (Anammox).

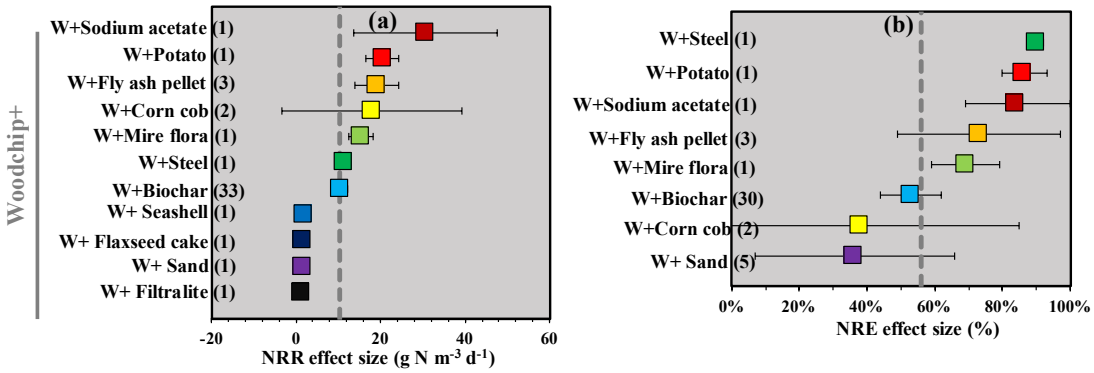

Figure 1.8 (a)Mean nitrate removal rate (NRR) effect size by adding various types of auxiliary materials; (b) Mean nitrate removal efficiency (NRE) effect size by adding various types of auxiliary materials.

CHAPTER II
A SYSTEMATIC REVIEW OF THE ROLE OF ABIOTIC FACTORS FOR NITRATE REMOVAL IN WOODCHIP BIOREACTORS

This chapter is based on a manuscript draft by Yuchuan Fan et al.:

A version of this chapter was originally published by:

Yuchuan Fan, Jaehoon Lee, Jie Zhuang, Michael Essington, Sindhu Jagadamma, and John Schwartz. The role of abiotic factors affecting nitrate removal in woodchip bioreactor.

My primary contributions to the work include (i) reviewing and summarizing relevant literature, (ii) gathering, analyzing, and summarizing data, (iii) initial writing of the manuscript, and (iv) revising manuscript and coordinating revisions of the manuscript.

Abstract

Woodchip bioreactors (WBR) are extensively used to reduce nitrate from agricultural drainage. However, the relative importance of abiotic factors for the removal is unclear. In this study, we identified eight abiotic factors, including media age, hydraulic retention time (HRT), influent nitrate concentration (C_{in}), temperature, dissolved organic carbon (DOC), dissolved oxygen (DO), pH, and effective porosity of WBR-filling materials. Based on a database that included 10,179 sets of data from 63 peer-reviewed articles, the nitrate removal rate (NRR) and nitrate removal efficiency (NRE) corresponding to the eight abiotic factors by different categories were systematically summarized. The results presented in Chapter 2 showed that abiotic factors have different interrelationships at lab and field scales, and it was confirmed that pH, DO, HRT, DOC, effective porosity, and media age were the most factors affecting nitrate removal in lab studies. In contrast, temperature, HRT, pH, and effective porosity were the most factors in field studies. Further, a structural equation model (SEM) successfully constructs a framework to explain how the various abiotic factors, directly and indirectly, affect NRE and NRR (RMSEA=0.008, NFI=0.998). This review provided greater insights regarding the different contribution of eight abiotic factors for NRR and NRE.

Introduction

Nitrate exports by stormwater and agricultural runoff is a global issue (Padilla et al. 2018), causing eutrophication, the death of fish, algal bloom, and other ecological problems. Thus, many field practices have been developed to remediate the high levels of nitrate present in agricultural drainage, such as constructed wetland, riparian buffer, tile drainage, and denitrifying bioreactor (DNBR). Among them, DNBR is considered as a sustainable (Robertson et al. 2008; Long et al. 2011) and low-cost technology to remove nitrate from agricultural drainage (Christianson et al. 2013). DNBR is a barrier (or bed) that intercepts agricultural drainage to remove nitrate removal (Schipper et al. 2010a). There are a variety of porous materials used to fill the DNBR, including natural carbon (e.g. woodchip and corncobs), non-natural carbon (e.g. biochar, cardboard), and inorganic materials (e.g. pyrite) (Fan et al., 2021). Among them, woodchip bioreactors (WBR) are extensively used in practice due to their relatively easy local access and low-cost, given that they can be sustained for 10-15 years without any maintenance (Robertson et al. 2008; Long et al. 2011).

Nitrate removal rate (NRR) and nitrate removal efficiency (NRE) are reported to range from 0.02 to 166.9 g N m^{-3} d^{-1} (Pluer et al. 2019) and 6.5 to 99.8% (Coleman et al. 2019). Such a wide range of nitrate removal is caused by the variation in abiotic factors. These abiotic factors include media age (Addy et al. 2016), hydraulic retention time (HRT) (Gibert et al. 2008; Robertson 2010; Zulkhairi et al. 2010; Damaraju et al. 2015; Guo et al. 2017), influent nitrate concentration (N_{in}) (Schmidt and Clark 2012), dissolved oxygen (DO) (Gómez et al. 2002; Schmidt and Clark 2012), pH (Roser et al. 2018), temperature (Schmidt and Clark 2013; Damaraju et al. 2015; Hassanpour et al. 2017), dissolved organic carbon (DOC) (Maxwell et al. 2019b), effective porosity (Healy et al. 2012), and saturation level (Maxwell et al. 2019b, a; McGuire and Reid 2019). In contrast, other factors such as grain size and wood species have

been reported to have no impact on nitrate removal (Van Driel et al. 2006; Cameron and Schipper 2010).

In addition to the contribution of abiotic factors on the wide range of denitrification rates, the experimental scale also influences the degree of nitrate removal. It has been reported that the average NRR at a laboratory scale is 2.5-fold higher with respect to the field scale (Fan et al., 2021). This is probably due to more abiotic factors contributing to field experiments than laboratory experiments. However, there is little known regarding the mechanisms governing nitrate removal by different key abiotic factors at different scales. Although previous literature reviews had reported the rates of nitrate removal (Schipper et al. 2010a; Christianson et al. 2012) and analyzed a small number of abiotic factors through quantitative assessment by meta-analysis (Addy et al. 2016), only influent N, HRT, medium age, and temperature were studied. Furthermore, the relationship between different abiotic factors has been rarely investigated. In this study, eight abiotic factors were identified and summarized based on our established global-wide database.

This study aimed to identify the most important abiotic factors and assess the impacts of the eight abiotic factors on nitrate removal. The specific objectives of this study were to: (i) improve our understanding of how NRR and NRE correspond to the identified eight abiotic factors, independently; (ii) compare the correlation of eight abiotic factors on laboratory and field scales; and (iii) uncover how the eight abiotic factors, directly and indirectly, influence NRR and NRE in DNBR.

Materials and methods

Nitrate removal indexes

Nitrate removal rate (NRR) and nitrate removal efficiency (NRE) are commonly used to quantitatively evaluate the performance of the WBR (Liu et al. 2015; Li et al. 2017). NRR

indicates a daily reduction of nitrate concentration while NRE reflects the overall reduction of nitrate mass, ranging from 0 to 100%. They can be calculated with the following equations:

$$NRR = \frac{M_{in} - M_{out}}{HRT \times V_T} \quad (1)$$

$$NRE = \frac{M_{in} - M_{out}}{M_{in}} \quad (2)$$

where M_{in} represents the influent nitrate mass (g), M_{out} represents the effluent nitrate mass, HRT represents the hydraulic retention time (d), and V_T represents the total volume of the WBR (m^3).

Database

This study is based on our database (Fan et al., 2021), which was established by searching the keywords "denitrif* bed", "denitrif* wall", "denitrif* bioreactor", and "permeable reactive barrier" from Web of Science, respectively. A database including 10,179 sets of data from 63 peer-reviewed articles was established. Moreover, we browsed these articles and found 14 related to "denitrification bed", 36 papers related to "denitrification wall", 83 related to "denitrifying bioreactor", and 69 related to "permeable reactive barrier". A total of 192 papers were reviewed and were distributed around the world (Fig 2.1). An overview of the obtained data and the calculation process is reported in Fan et al., 2021.

Abiotic factors

We categorized abiotic factors into two groups: an even range and uneven range. For the even range, such as temperature, DO, pH, and effective porosity, the interval values were evenly categorized. For the uneven range, such as media age, HRT, C_{in}, and DOC were based

on the data's characteristics. According to the characteristics of the abiotic factors, a large variance at the initial stage occurs. For instance, the NRR declines sharply in the first year (Addy et al. 2016) and we therefore set a shorter time interval at the first year, including the 1st Month, 2nd Month, and 3rd Month, respectively. Similarly, NRR dramatically decreases with HRT at low HRT, thus we classified the HRT categories into 0-5, 5-10, 10-20, 20-50, 50-100, 100-500, and 500-3000, respectively. All the details of these categories are provided in Table 1.

The quantitative relationship between the temperature and the reaction coefficient was described using the following equation (Ghane et al. 2015).

$$NRR_{T_i} = NRR_{T_0} \times \theta^{(T_i - T_0)} \quad (3)$$

where NRR_{Ti} represents nitrate removal rate at a temperature T_i (g N m^{-3} d^{-1}), NRR_{T0} represents nitrate removal rate at a temperature T_0 (g N m^{-3} d^{-1}), θ represents the temperature coefficient (-) at T_0, T_i represents the temperature of the medium at a different time (°C). This equation is usually valid in the temperature range from 4 to 30°C, defined as the *mesophilic* range, in which most of the aerobic systems are involved. The interpretation of the coefficient θ is made such that, if θ is equal to, for example, 1.02, the value of the reaction rate increases by 2% ((1.02-1.00) × 100) for each 1°C increment in temperature (Von Sperling 2007).

Principal component and Pearson correlation analyses

Principal component analysis (PCA) was conducted (Origin2020, OriginLab Inc, USA) to reduce the dimensionality of the eight abiotic factors and classify them into several principal components. The dataset had passed through Bartlett's test with a *p*-value of < 0.001 (SPSS, IBM Inc, USA), which indicated the feasibility of PCA analysis. The principal components'

eigenvalues were all above 1, which indicated that the new variables were significant and maximized variance.

The relationship between abiotic factors and nitrate removal indices (NRR & NRE) in lab and field studies were evaluated by the Pearson correlation coefficient (PCC), which was also performed using Origin (2020, OriginLab Inc, USA) software.

Structural equation model

We fit a structural equation model (SEM) to infer the relative importance of eight abiotic factors for NRR and NRE. SEM was performed by IBM SPSS Amos (26, IBM Inc, USA). The SEM analysis was conducted following the steps: 1) specific problem situation 2) propose theoretical hypothesis 3) determine the model structure 4) data collection 5) estimation of the model parameters 6) model fitting and evaluation 7) model readjustment 8) model result analysis (Fig 2.2). Model evaluation adopted Normed Fit Index (NFI) and Root Mean Square Error of Approximation (RMSEA) as indicators to evaluate the fitting degree of the model. MacCallum et al. (1996) have used 0.01, 0.05, and 0.08 for RMSEA to indicate excellent, good, and mediocre fit, respectively. A NFI value between 0.90 and 0.95 is considered marginal, above 0.95 is good, while below 0.90 is considered to be a poor-fitting model (Bollen and Long 1993). In SEM, the standardized path coefficients (SPC) indicate the direct effect of a variable assumed to be a cause on another variable assumed to be an effect.

Results and discussions

Effect of abiotic factors on NRR and NRE

Media age

The mean NRR was found to decrease from 11.3 at the first month to 1.6 g N m^{-3} d^{-1} at 3-15 years (Fig 2.3A). NRE also decreased with media age, ranging from 62% at the first month to

30% at 3 years (Fig. 2.3B). However, an inconsistent result was found at 3-15 years, where NRE increased to 53%. This could possibly be due to lower influent nitrate concentrations during the 3–15-year period, resulting in a low NRR but a high NRE. Regarding NRR, Fig 2.3A illustrates that NRR underwent a gradual and steady decrease during the first three years, while the mean was then relatively stable (1.6 g N m^{-3} d^{-1}) from 3-15 years. However, the mean NRE did not decrease steadily. Interestingly, the NRE was observed to remain at around 53% within 15 years. Our results were consistent with previous studies which reported that the first year of NRR was significantly higher than the second and third years (Addy et al. 2016). The reason for the higher NRR at the beginning is most likely due to more DOC loss from the filling materials (Schipper et al. 2010b; Healy et al. 2012; Fenton et al. 2014) and, consequently, low DOC loss leads to a low NRR at 3-15 years. Several studies also showed that DOC decreased over the time due to an increase in woodchip carbon recalcitrance over time (Ghane et al. 2018).

Hydraulic retention time (HRT)

With increasing HRT, the NRR decreased from 14.9 to 0.4 g N m^{-3} d^{-1} (Fig 2.4A) and the NRE increased from 40% to 84% (Fig 2.4B). As presented in Fig 2.4A and 2.4B, the HRT corresponding to the maximum NRR and NRE occurred at 0-5 hours and at 500-3000 hours. The HRT of 10-20 hours had a higher NRR than the HRT of 5-10 hours, which is probably due to HRT in this range having a higher probability to result in a greater NRR. Those findings are consistent with previous studies which showed NRR decreased with HRT, while NRE increased with HRT. A plethora of literature reported an exponential decrease in NRR with HRT (Robertson 2010; David et al. 2016; Pluer et al. 2019; Povilaitis and Matikienė 2020), and this phenomenon could be described by the First-order or Zero-order model (Robertson 2010). This could be explained by more substrate being released and consumed

under the longer HRTs. These results were similar to the findings of Zulkhairi et al. (2010) who revealed that denitrifying bacteria had a short contact time with the surfaces of carbon sources at lower HRTs. Therefore, nitrite accumulation is attributable to the short HRT, which results in increased nitrite accumulation and a decreased NRE because of the low contact time for microbial activity and wash-out of bacteria (Damaraju et al. 2015). Moreover, it is widely accepted that a higher HRT corresponds to a higher NRE. Currently, there is no consensus regarding whether the change of NRE with HRT is exponential (Tangsir et al. 2017; Rivas et al. 2020), or proportional (Lepine et al. 2015), and thus requires further study.

Influent nitrate concentration (N_{in})

We found that the mean NRR and NRE did not increase with N_{in} after 20 mg N L^{-1} (Fig 2.5A and 2.5B), and the mean NRE decreased with N_{in}. In other words, N_{in} between 10-20 mg N L^{-1} showed a higher mean NRR than the other N_{in} values. Furthermore, NRE did not increase with N_{in} when N_{in} was over 10 mg N L^{-1}. This result is inconsistent with previous individual studies given that it is widely accepted that higher N_{in} potentially lead to a greater NRR when the electron donors are sufficiently supplied (Rivett et al. 2008; Lepine et al. 2015) and lower N_{in} with a significantly lower NRR compared with greater N_{in} based on a meta-analysis (Addy et al. 2016). According to Rivas et al. (2020), inflow NO_3-N increased from 0.5 kg to 4 kg and resulted in an increase in NRR from 0.7 to 1.5 g N m^{-3} d^{-1}. However, according to the horizontal woodchip column studies by Damaraju et al. (2015), when influent loads exceed approximately 140 g N L^{-1} d^{-1} in a reactor, the load reduction performance begins to decline greatly. Ruan et al. (2009) noted that, as the nitrate loading rate increased from 0.1 to 1.2 kg m^{-3} d^{-1}, NRR consequently increased from 0.05 to 0.55 before decreasing to 0.4 kg m^{-3} d^{-1}. Previous studies suggested that if the N_{in} values increase too much it will affect the denitrification process by

halting the production of N_2 gas and causing the accumulation of N_2O (Blackmer and Bremner 1978). It has been shown that N_{in} must occur above a certain limit for NRR to increase, but this threshold remains unclear. Additionally, low N_{in} can also affect the NRR by increasing the ratio of N_2O:N_2 (Magalhaes et al. 2003) and delaying the reduction of N_2O to N_2 by soil microorganisms (Blackmer and Bremner 1978), which means N_2O is accumulated to stop the denitrification process.

Temperature

There is a clear trend of increased NRR when the temperature is increased from 0 to 25 ˚C, before it decreases when it is raised from 25 to 30 ˚C (Fig 2.6A). However, NRE increased when the temperature was raised from 0 to 15 ˚C, then decreased when raise from 15 to 30 ˚C (Fig 2.6B). Theoretically, the optimal temperature for denitrification is 25-35 ˚C, while denitrification can still occur between 2 and 50 ˚C. Fig 2.6A and 2.6B present the values of temperature reported in peer-reviewed articles that ranged from 0 to 30 ˚C, and the optimum temperature for NRR and NRE was determined to be 20-25 ˚C and 10-15 ˚C. This is not consistent with observed denitrification in soils, and the probable reason is the temperatures for the lab and field denitrifying bioreactor studies were mostly in the range of 0-25 ˚C. Table 2 lists the temperature coefficients (θ) reported in previous studies, which range from 1.01 to 1.14, with a mean of 1.08. According to our dataset, θ was 1.09 based on the mean NRR at 0-2 ˚C and 20-22 ˚C (Fig 2.6A). Thus, our study indicated that an average 1˚C increment of temperature in the *mesophilic* range contributes 9% to NRR increasing.

Effluent dissolved organic carbon (DOC)

Fig 2.7A demonstrates that the mean NRR decreased with DOC from 0-5 to 5-10 mg L^{-1}, then increased with DOC from 5-10 to 50-100 mg L^{-1}. Lastly, NRR decreased with DOC from 50-100 to 200-500 mg L^{-1}. Similarly, Fig 2.7B highlights that the mean NRE decreased with DOC from 0-5 to 5-10 mg L^{-1}, then increased with DOC from 5-10 to 200-500 mg L^{-1}. These results indicate that a start-up phenomenon occurred when effluent DOC was within 0-5 mg L^{-1}. Start-up phenomena were commonly reported at denitrifying bioreactors where the NRE or NRR showed a greater value when the bioreactor was at an initial stage. However, this high NRE or NRR then decreased with time. This effect was probably due to more DOC being released at the beginning. On the other hand, higher DOC concentrations supply enough electrons for nitrate reduction. Therefore, previous researchers have considered improving the NRR and NRE by adding additional carbon sources in a direct way, such as adding biochar (Bock et al. 2015) and acetate (Roser et al. 2018), or in an indirect way by drying-rewetting (Maxwell et al. 2019b). However, a lower DOC (0-5 mg L^{-1}) with a higher NRR and NRE may indicate that DOC is fully utilized within the WBR. Furthermore, a higher DOC is not only beneficial for denitrification, but also for dissimilatory nitrate reduction (DNRA), which will compete with denitrification. DNRA could occur when the DOC is so high that it affects the C/N ratio, raising it above 7.7 (van den Berg et al. 2015). Thus, this demonstrates that effluent DOC cannot serve as a direct indicator for NRR and NRE, simply because increasing DOC may not absolutely increase NRR, but it does seem to be a guarantee for NRE.

Effluent dissolved oxygen (DO)

Our database showed that denitrification mainly occurs at a DO concentration of <2 mg L^{-1} (Fig 2.8A). Furthermore, NRR decreased with DO in the range 0-2 mg L^{-1}, and a DO at 0-0.5 showed the maximum mean NRR. However, there was no clear trend between NRE and DO (Fig 2.8B). Thus far, the threshold required for DO to inhibit NRR is not clear (Warneke et al. 2011). In addition, it is widely accepted that anaerobic conditions are favorable for denitrification. When the DO concentration is greater than 5 mg L^{-1}, the probability for denitrification to occur is low because it indicates strong aerobic conditions (Knoll et al. 2020). The reason is that a large DO concentration promotes nitrification, but too much DO will then inhibit the denitrification process (Li et al. 2012). Furthermore, the reduction of oxygen to water is the first reaction (ΔG=-78.5, Eh=+334) in the redox reaction sequence in saturated zones, followed by a nitrate reduction reaction (ΔG=-72.3, Eh=+231) (Rivett et al. 2008). Organic carbon tends to act as an electron donor preferentially for the free oxygen (O_2). Nitrate will be the favorable electron acceptor until free oxygen is consumed. Therefore, the lower oxygen concentration in WBRs benefits the reduction of nitrate to inert nitrogen gas. Thus, our result indicated that the most appropriate DO for NRR in WBR is in the range 0-0.5 mg L^{-1}, which is consistent with the previous study of (Li et al. 2012).

Effluent pH

Fig 2.9A and 2.9B illustrates that the pH range of the WBR is from 4.0 to 8.0, which is consistent with the preferred range of heterotrophic denitrifiers (Rust et al. 2000). Notably, If pH values are less than 5, denitrification is inhibited and nitrite or N_2O tends to accumulate to stop the denitrification chain (Brady and Weil 2016). If pH values are larger than 8, denitrification activity decreases (Rust et al. 2000). Normally, the combination of CO_2 and OH which has been released from denitrification yields HCO_3. If the balance is broken, the pH can rise due to the OH production rate increasing above that of CO_2 (Rivett et al. 2008), and the

upper limit of pH for denitrification can reach up to 8.3 (Rust et al. 2000). Damaraju et al. (2015) showed that the pH variation was in the range of 6.5-7.5, which was favorable for the effective function of denitrifying bacteria. Povilaitis and Matikienė (2020) conducted their WBR study with activated carbon and flaxseed cake, which highlighted that the pH ranged from 7 to 7.5 and produced higher NRE. However, our study suggests that the mean NRE is lower (56%) while the mean NRR is higher (9.1 g N m^{-3} d^{-1}) when pH was 7-8 (Fig 2.9B).

Effective porosity (ρ)

As Fig 2.10A and 2.10B shows, the effective porosity (ρ, or called drainable porosity) of WBR varied from 0.3 to 0.8. The greatest mean NRR, 10.8 g N m^{-3} d^{-1}, was found at a ρ between 0.6-0.7 (Fig 2.10A). Regarding NRE, the greatest mean NRE, 67%, was found at ρ between 0.6-0.7 (Fig 2.10A). Only a few studies addressed the impact of ρ on NRR or NRE and this is probably due to ρ being hard to accurately maintain in woodchip filled bioreactors. However, ρ is important given that ρ determines the effective volume of the WBR. Thus, ρ can influence the saturated hydraulic conductivity (Flint and Selker 2003), which has an indirect influence on the HRT. However, the relationship between nitrate removal (NRR & NRE) and ρ is complicated, so further investigation is required to improve our understanding of this relationship.

Comparison of lab- and field-scale

Fig 2.11A and 2.11B reports a higher Pearson correlation coefficient (r) in lab-scale experiments with respect to their field-scale counterparts, indicating that lab studies reflected a strong linear relationship between abiotic factors and nitrate removal than field studies. This is probably due to the more stable environmental conditions that can be controlled in lab studies compared with field studies, and thus fewer variances contributed to a higher r values in lab studies. Regrading the lab studies, HRT, N_{in}, DO, pH, and media age showed a negative

relationship with NRE while temperature, DOC, and effective porosity showed a significant positive relationship with NRE. In addition, temperature, DOC, DO, pH, and effective porosity showed a relatively high r with NRE, being 0.55, 0.49, -0.59, -0.52, and 0.41, respectively ($p < 0.05$). Moreover, N_{in}, temperature, and effective porosity showed a significant positive relationship with NRR. HRT, DOC, DO, pH, and media age showed a significant negative relationship with NRR. Furthermore, HRT, DO, and effective porosity showed a significant linear relationship with NRR, and the r values were -0.53, -0.54, and 0.4, respectively ($p < 0.05$). In the field studies, the r was much smaller with respect to the laboratory studies. The highest r value was between NRE and pH, as well as NRR and effective porosity. In comparison, the negative and positive relationship between nitrate removal (NRR & NRE) and abiotic factors were almost consistent in both scales.

Fig 2.12A and 2.12B illustrated that the total percentages of variances for lab studies (69.4%) are larger than field studies (48.0%). Thus, the abiotic factors in lab studies can be easier to use given that fewer new variables are required. It should be noted that the loadings plot of the abiotic factors reveals the relationships between these variables in the space of the first two components. For lab scale studies, HRT and DO had similar variances while DOC and temperature were also similar. Furthermore, PC1 explained 41.8% of the variance and this was mainly attributed to effective porosity, pH, DO, HRT, DOC, and temperature. PC2 explained 27.6% of the variance. However, in the field studies, pH and effective porosity had similar variances. Media age and DO were also similar. PC1 explained 41.8% of the variance and was mainly attributed to HRT, media age, DO, pH, and effective porosity. PC2 explained 17.2% of the variance, with temperature and DO being the major contributions. Overall, the length of the arrows indicated that pH, DO, HRT, DOC, effective porosity, and media age were the most influential abiotic factors in lab studies. In contrast, temperature, HRT, pH, and effective porosity were the most influential abiotic factors in field studies. This is

probably due to a large seasonal change in the field conditions (Hassanpour et al. 2017). Surprisingly, we found that DOC is a significant abiotic factor in lab-studies, rather than field-studies, as shown by the thinner arrow for DOC in the loadings plot generated from the in field-scale studies (Fig 2.12A-B). A further novel finding is that pH and effective porosity have similar loadings in the field-scale studies, which is also consistent with their stronger relationship observed in correlation analysis (r=0.64, p<0.05) (Fig 2.12B). We assume this is probably due to a higher effective porosity, leading to a larger pore volume in WBRs, and in turn increases the pH in the reactors.

SEM explain the impacts of abiotic factors on nitrate removal

Fig 2.13 reveals how the eight abiotic factors affect NRR and NRE by different pathways. Specifically, the SEM indicated that N_{in} (^{adj}r=0.43, p<0.001) and ρ (^{adj}r=0.3, p<0.001) represent those parameters which have the largest impact on NRR, which was probably due to them being necessary parameters to calculate NRR (Eq. 1). Interestingly, it demonstrated that pH (^{adj}r=-0.57, p <0.001) also has a significant impact on NRE, which is consistent with our correlation analysis (r=-0.428; p <0.05). Contrary to our expectations, other abiotic factors presented a low ^{adj}r with NRE. However, correlation analysis showed a derived factor that was determined to be better related to NRE (Fig 2.13), which was nitrate reduction (C_{rd}, mg N L^{-1}; r=0.5; p <0.05). This is likely due to C_{rd} being part of the equation to calculate NRE.

In the previous discussions, the relationship of media age, HRT, C_{in}, temperature, DOC, DO, pH, and ρ with NRR were investigated in WBRs. However, the abiotic factors that affect NRR in WBRs were not only related directly, but a more complicated causal relationship was found in this SME analysis. For instance, medium age was found to have a negative effect on temperature (^{adj}r = -0.29, r = -0.118, p < 0.001) and DOC (^{adj}r = -0.37, r = -0.354, p < 0.001). This is probably due to temperature being a time-varying parameter, especially in the field, and reduced carbon bioavailability in a higher medium age. C_{in} had a direct effect on pH (^{adj}r = -

0.46, r = 0.182, $p < 0.001$) because nitrous oxide dissolved in the water will cause acidification (Winterdahl et al. 2014). In addition, HRT had a direct effect on (^{adj}r = -0.23, r = -0.409, $p < 0.001$) because a lower HRT is associated with a higher flux of water flow through the WBR in unit time, increasing the effect of pH. Some of the abiotic factors, conversely, had an effect loop. For instance, it was detected that ρ influenced temperature (^{adj}r = -0.57, r = -0.387, $p < 0.001$) and HRT (^{adj}r = -0.47, r = 0.07, $p < 0.001$), while HRT had an effect on temperature (^{adj}r = 0.25, r = -0.176, $p < 0.001$). On the whole, this indicated that ρ had both a direct and an indirect effect on temperature, which was possibly due to ρ governing the pore volume, which is a buffer zone for heat exchange.

Conclusions

This study systematically identified that nitrate removal rate (NRR) and nitrate removal efficiency (NRE) were impacted by eight mainly abiotic factors, including media age, hydraulic retention time (HRT), influent nitrate concentration (C_{in}), temperature, dissolved organic carbon (DOC), dissolved oxygen (DO), pH, and effective porosity. NRR and NRE, corresponding to the above eight abiotic factors independently, were presented in this study by a global-wide database. Specifically, the NRR and NRE decreased with the media age. Similarly, NRR decreased with HRT and, in contrast, NRE increased with HRT significantly. An influent nitrate concentration of 10 mg L^{-1} is a threshold value for the performance of nitrate removal, along with a lower NRR but a higher NRE below 10 mg L^{-1}, and vice versa. We found that the optimal temperature for NRR is in the range of 20-25 ℃, while a temperature range of 10-15 ℃ results in a higher NRE. The overall temperature coefficient is 1.09, which means the NRR increases by 9% (=1.09-1.00=0.09) for each increment of 1℃ in the temperature. Further, our data indicate that an effluent DOC in the range of 0-5 mg C L^{-1} and 30-200 mg L^{-1} respond

to a higher NRR and NRE. In terms of DO, denitrification mainly occurs below 2 mg L^{-1} in DNBRs, and the optimal DO for NRR is 0-5 mg L^{-1}. It was found that the optimal pH for NRR is in the range of 7-8, but NRE is lowest within this range. For the effective porosity, NRR reached a maximum at 0.6-0.7 while NRE reached a maximum at 0.4-0.5. Overall, NRR and NRE respond to abiotic factors that were not always kept consistent. Thus, this suggests that nitrate removal indicators should be carefully selected by different abiotic factors.

The results of Pearson correlation and principal component analysis demonstrated that pH, DO, HRT, DOC, effective porosity, and media age were the most influential abiotic factors in lab studies. In contrast, temperature, HRT, pH, and effective porosity were the most influential abiotic factors in field studies. Therefore, to define the critical parameters for nitrate removal prediction, different input parameters should be considered under different scales.

Finally, the SEM also successfully constructed a framework to explain how the various abiotic factors, directly and indirectly, affect NRR and NRE (RMSEA=0.008, NFI=0.998). This complicated framework can provide greater insights into how the NRR and NRE are affected by various abiotic factors.

References

Addy K, Gold A J, Christianson L E, et al. 2016. Denitrifying Bioreactors for Nitrate Removal: A Meta-Analysis[J]. Journal of Environmental Quality, 45(3): 873-881.

Blackmer A, Bremner J. 1978. Inhibitory effect of nitrate on reduction of N2O to N2 by soil microorganisms[J]. Soil Biology and Biochemistry, 10(3): 187-191.

Bock E, Smith N, Rogers M, et al. 2015. Enhanced Nitrate and Phosphate Removal in a Denitrifying Bioreactor with Biochar[J]. Journal of Environmental Quality, 44(2): 605-613.

Bollen K A, Long J S. 1993. Testing structural equation models[M]. City: Sage.

Brady N C, Weil R R. 2016. The nature and properties of soils[M]. City: Pearson.

Cameron S G, Schipper L A. 2010. Nitrate removal and hydraulic performance of organic carbon for use in denitrification beds[J]. Ecological Engineering, 36(11): 1588-1595.

Christianson L, Tyndall J, Helmers M. 2013. Financial comparison of seven nitrate reduction strategies for Midwestern agricultural drainage[J]. Water Resources and Economics, 2-3: 30-56.

Christianson L E, Bhandari A, Hailers M J. 2012. A Practice-Oriented Review Of Woodchip Bioreactors For Subsurface Agricultural Drainage[J]. Applied Engineering in Agriculture, 28(6): 861-874.

Coleman B S L, Easton Z M, Bock E M. 2019. Biochar fails to enhance nutrient removal in woodchip bioreactor columns following saturation[J]. Journal of Environmental Management, 232: 490-498.

Damaraju S, Singh U K, Sreekanth D, et al. 2015. Denitrification in biofilm configured horizontal flow woodchip bioreactor: effect of hydraulic retention time and biomass growth[J]. Ecohydrology & Hydrobiology, 15(1): 39-48.

David M B, Gentry L E, Cooke R A, et al. 2016. Temperature and Substrate Control Woodchip Bioreactor Performance in Reducing Tile Nitrate Loads in East-Central Illinois[J]. Journal of Environmental Quality, 45(3): 822-829.

Fenton O, Healy M G, Brennan F, et al. 2014. Permeable reactive interceptors: blocking diffuse nutrient and greenhouse gases losses in key areas of the farming landscape[J]. The Journal of Agricultural Science, 152(S1): 71-81.

Flint L E, Selker J S. 2003. Use of porosity to estimate hydraulic properties of volcanic tuffs[J]. Advances in Water Resources, 26(5): 561-571.

Ghane E, Fausey N R, Brown L C. 2015. Modeling nitrate removal in a denitrification bed[J]. Water Research, 71: 294-305.

Ghane E, Feyereisen G W, Rosen C J, et al. 2018. Carbon Quality of Four-Year-Old Woodchips in a Denitrification Bed Treating Agricultural Drainage Water[J]. Transactions of the ASABE, 61(3): 995-1000.

Gibert O, Pomierny S, Rowe I, et al. 2008. Selection of organic substrates as potential reactive materials for use in a denitrification permeable reactive barrier (PRB)[J]. Bioresource Technology, 99(16): 7587-7596.

Gómez M A, Hontoria E, González-López J. 2002. Effect of dissolved oxygen concentration on nitrate removal from groundwater using a denitrifying submerged filter[J]. Journal of Hazardous Materials, 90(3): 267-278.

Guo Y, Guo L, Sun M, et al. 2017. Effects of hydraulic retention time (HRT) on denitrification using waste activated sludge thermal hydrolysis liquid and acidogenic liquid as carbon sources[J]. Bioresource Technology, 224: 147-156.

Hassanpour B, Giri S, Pluer W T, et al. 2017. Seasonal performance of denitrifying bioreactors in the Northeastern United States: Field trials[J]. Journal of Environmental Management, 202: 242-253.

Healy M G, Ibrahim T G, Lanigan G J, et al. 2012. Nitrate removal rate, efficiency and pollution swapping potential of different organic carbon media in laboratory denitrification bioreactors[J]. Ecological Engineering, 40: 198-209.
Knoll L, Breuer L, Bach M. 2020. Nation-wide estimation of groundwater redox conditions and nitrate concentrations through machine learning[J]. Environmental Research Letters.
Lepine C, Christianson L, Sharrer K, et al. 2015. Optimizing hydraulic retention times in denitrifying woodchip bioreactors treating recirculating aquaculture system wastewater[J]. Journal of Environmental Quality, 45(3): 813-821.
Li R, Feng C P, Xi B D, et al. 2017. Nitrate removal efficiency of a mixotrophic denitrification wall for nitrate-polluted groundwater in situ remediation[J]. Ecological Engineering, 106: 523-531.
Li Y F, Liu J Y, Zhang Y 2012. Startup of Denitrification Bioreactor and Influence of Temperature and DO for Treatment [M] //H. LI, Y. F. LIU, M. GUO, et al., Sustainable Development of Urban Environment and Building Material, Pts 1-4: 913-918.
Liu F, Wang Y, Xiao R, et al. 2015. Influence of substrates on nutrient removal performance of organic channel barriers in drainage ditches[J]. Journal of Hydrology, 527: 380-386.
Long L M, Schipper L A, Bruesewitz D A. 2011. Long-term nitrate removal in a denitrification wall[J]. Agriculture Ecosystems & Environment, 140(3-4): 514-520.
MacCallum R C, Browne M W, Sugawara H M. 1996. Power analysis and determination of sample size for covariance structure modeling[J]. Psychological methods, 1(2): 130.
Magalhaes C, Moreira R, Wiebe W, et al. Salinity and inorganic nitrogen effects on nitrification and denitrification rates in inter-tidal sediments and rocky biofilms: Douro River Estuary, Portugal[C]//Salinity and inorganic nitrogen effects on nitrification and denitrification rates in inter-tidal sediments and rocky biofilms: Douro River Estuary, Portugal. Proceedings of the 7th International Specialised IWA Conference on Diffuse Pollution and Basin Management, Dublin. 6.73-76.79
Maxwell B M, Birgand F, Schipper L A, et al. 2019a. Drying–rewetting cycles affect nitrate removal rates in woodchip bioreactors[J]. Journal of Environmental Quality, 48(1): 93-101.
Maxwell B M, Birgand F, Schipper L A, et al. 2019b. Increased duration of drying–rewetting cycles increases nitrate removal in woodchip bioreactors[J]. Agricultural & Environmental Letters, 4.
McGuire P M, Reid M C. 2019. Nitrous oxide and methane dynamics in woodchip bioreactors: Effects of water level fluctuations on partitioning into trapped gas phases[J]. Environmental Science & Technology.
Padilla F M, Gallardo M, Manzano-Agugliaro F. 2018. Global trends in nitrate leaching research in the 1960–2017 period[J]. Science of The Total Environment, 643: 400-413.
Pluer W T, Morris C K, Walter M T, et al. 2019. Denitrifying bioreactor response during storm events[J]. Agricultural Water Management, 213: 1109-1115.
Povilaitis A, Matikienė J. 2020. Nitrate removal from tile drainage water: The performance of denitrifying woodchip bioreactors amended with activated carbon and flaxseed cake[J]. Agricultural Water Management, 229: 105937.
Rivas A, Barkle G, Stenger R, et al. 2020. Nitrate removal and secondary effects of a woodchip bioreactor for the treatment of subsurface drainage with dynamic flows under pastoral agriculture[J]. Ecological Engineering, 148: 105786.

Rivett M O, Buss S R, Morgan P, et al. 2008. Nitrate attenuation in groundwater: A review of biogeochemical controlling processes[J]. Water Research, 42(16): 4215-4232.
Robertson W D. 2010. Nitrate removal rates in woodchip media of varying age[J]. Ecological Engineering, 36(11): 1581-1587.
Robertson W D, Vogan J L, Lombardo P S. 2008. Nitrate removal rates in a 15-year-old permeable reactive barrier treating septic system nitrate[J]. Ground Water Monitoring and Remediation, 28(3): 65-72.
Roser M B, Feyereisen G W, Spokas K A, et al. 2018. Carbon Dosing Increases Nitrate Removal Rates in Denitrifying Bioreactors at Low-Temperature High-Flow Conditions[J]. Journal of Environmental Quality, 47(4): 856-864.
Ruan Y J, Luo G Z, Tan H X, et al. 2009. Nitrate and phosphate removal in sulphur-coral stone autotrophic denitrification packed-bed reactors[J]. Canadian Journal of Civil Engineering, 36(5): 923-932.
Rust C M, Aelion C M, Flora J R. 2000. Control of pH during denitrification in subsurface sediment microcosms using encapsulated phosphate buffer[J]. Water Research, 34(5): 1447-1454.
Schipper L A, Robertson W D, Gold A J, et al. 2010a. Denitrifying bioreactors-An approach for reducing nitrate loads to receiving waters[J]. Ecological Engineering, 36(11): 1532-1543.
Schipper L A, Robertson W D, Gold A J, et al. 2010b. Denitrifying bioreactors—An approach for reducing nitrate loads to receiving waters[J]. Ecological Engineering, 36(11): 1532-1543.
Schmidt C A, Clark M W. 2012. Efficacy of a denitrification wall to treat continuously high nitrate loads[J]. Ecological Engineering, 42: 203-211.
Schmidt C A, Clark M W. 2013. Deciphering and modeling the physicochemical drivers of denitrification rates in bioreactors[J]. Ecological Engineering, 60: 276-288.
Tangsir S, Moazed H, Naseri A A, et al. 2017. Investigation on the performance of sugarcane bagasse as a new carbon source in two hydraulic dimensions of denitrification beds[J]. Journal of Cleaner Production, 140: 1176-1181.
van den Berg E M, van Dongen U, Abbas B, et al. 2015. Enrichment of DNRA bacteria in a continuous culture[J]. The ISME Journal, 9(10): 2153-2161.
Van Driel P W, Robertson W D, Merkley L C. 2006. Upflow reactors for riparian zone denitrification[J]. Journal of Environmental Quality, 35(2): 412-420.
Von Sperling M. 2007. Activated Sludge and Aerobic Biofilm Reactors[M]. City: IWA Publishing.
Warneke S, Schipper L A, Bruesewitz D A, et al. 2011. Rates, controls and potential adverse effects of nitrate removal in a denitrification bed[J]. Ecological Engineering, 37(3): 511-522.
Winterdahl M, Bishop K, Erlandsson M 2014. Acidification, Dissolved Organic Carbon (DOC) and Climate Change [M] //B. FREEDMAN, Global Environmental Change. Springer Netherlands; Dordrecht: 281-287.
Zulkhairi M, Mohamed Yusoff M E, Abdul Rahman N, et al. 2010. The Effect of Hydraulic Retention Time and Volatile Fatty Acids on Biohydrogen Production from Palm Oil Mill Effluent under Non-Sterile Condition[M]. City.

Appendices

Figures

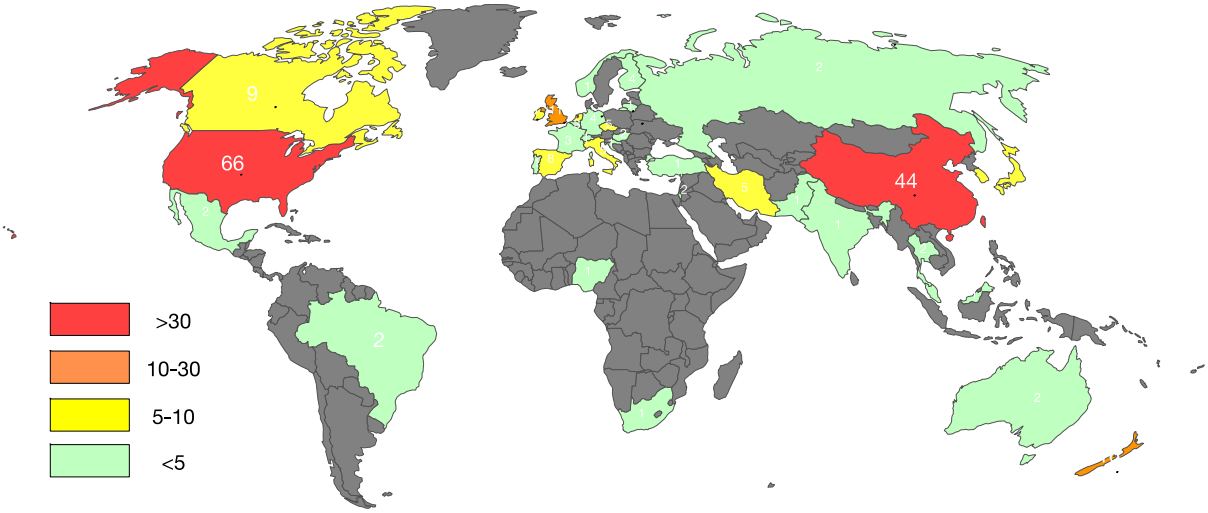

Figure 2.1 Global distribution of peer-reviewed papers related to denitrifying bioreactors.

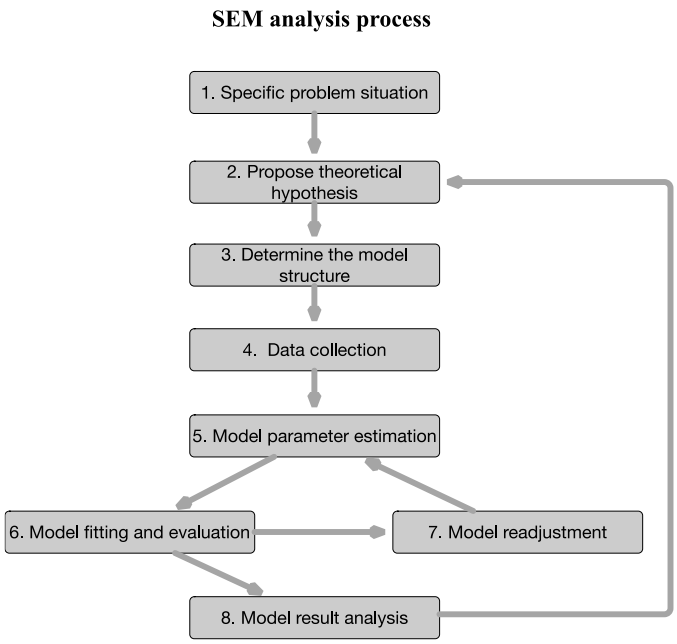

Figure 2.2 (A) SEM analysis process flow chart.

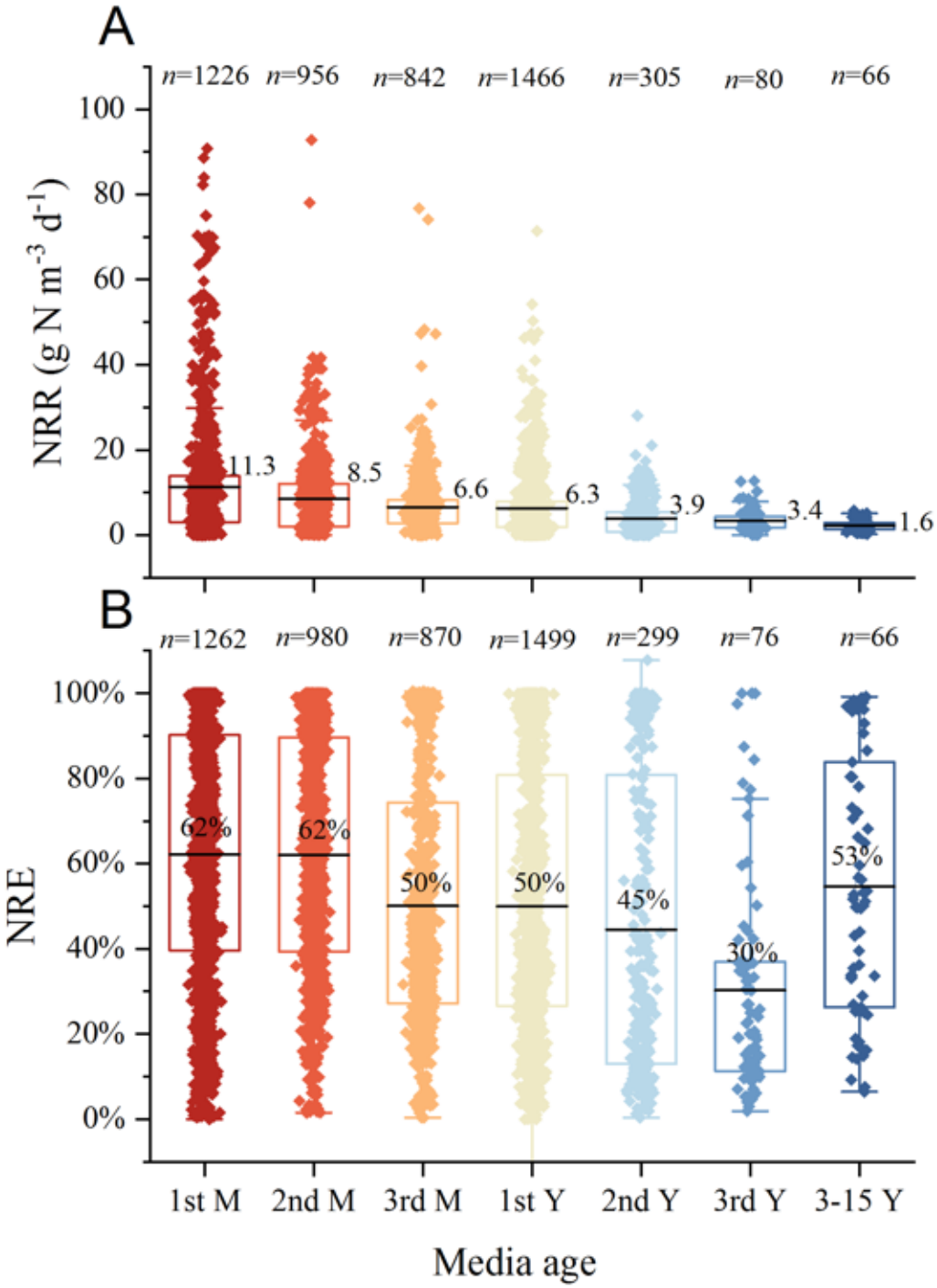

Figure 2.3 (A) Nitrate removal rate (NRR, g N m^{-3} d^{-1}) and (B) nitrate removal efficiency (NRE, %) respond to the medium age. *n* represents the number of data points. M represents month, Y represents year. Error bar represents standard error.

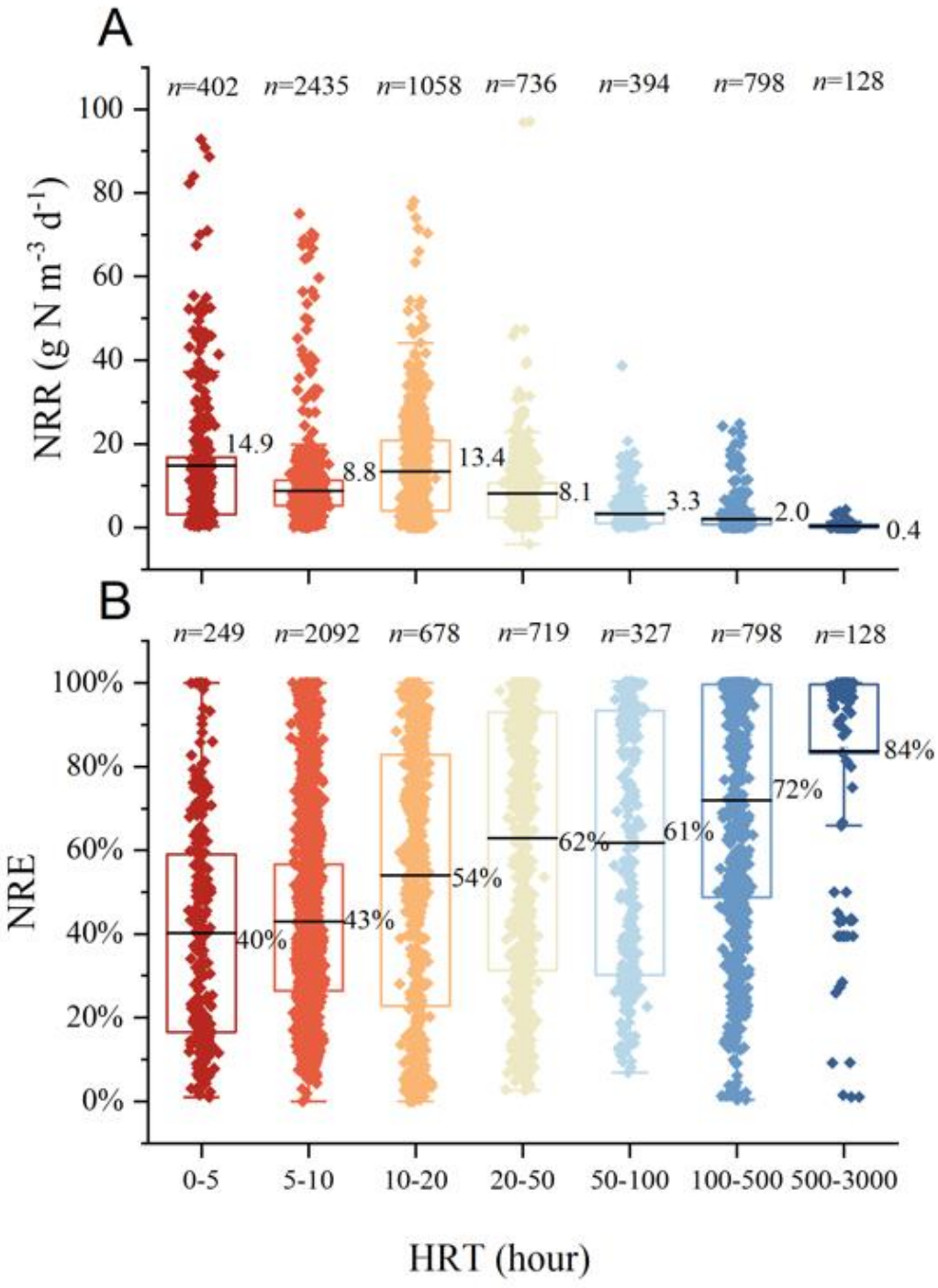

Figure 2.4 Nitrate removal rate (NRR, g N m^{-3} d^{-1}) and (B) nitrate removal efficiency (NRE, %) respond to the hydraulic retention time (HRT). *n* represents the number of data points. Error bar represents standard error.

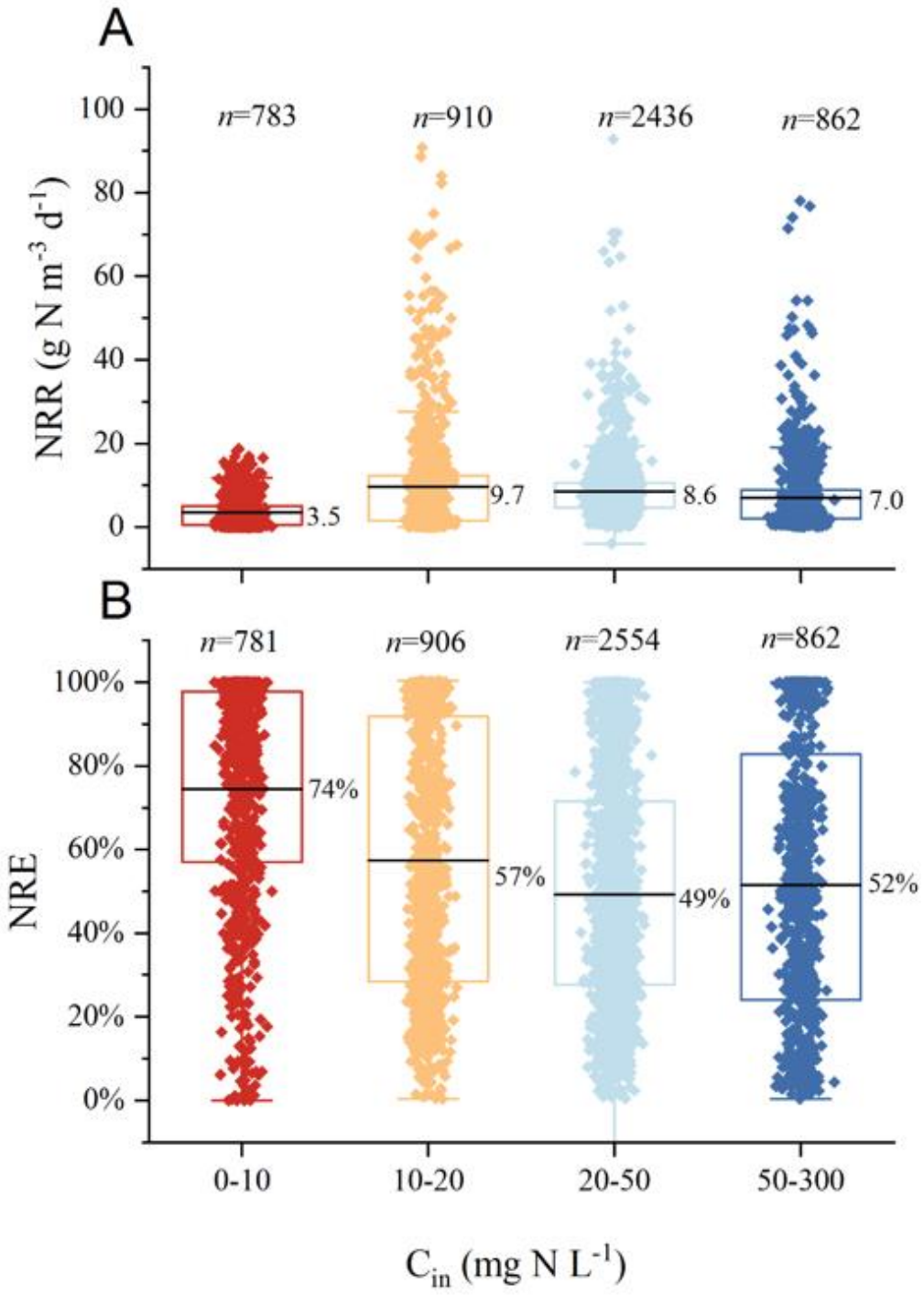

Figure 2.5 Nitrate removal rate (NRR, g N m^{-3} d^{-1}) and (B) nitrate removal efficiency (NRE, %) respond to the influent nitrate concentration (C_{in}). *n* represents the number of data points. Error bar represents standard error.

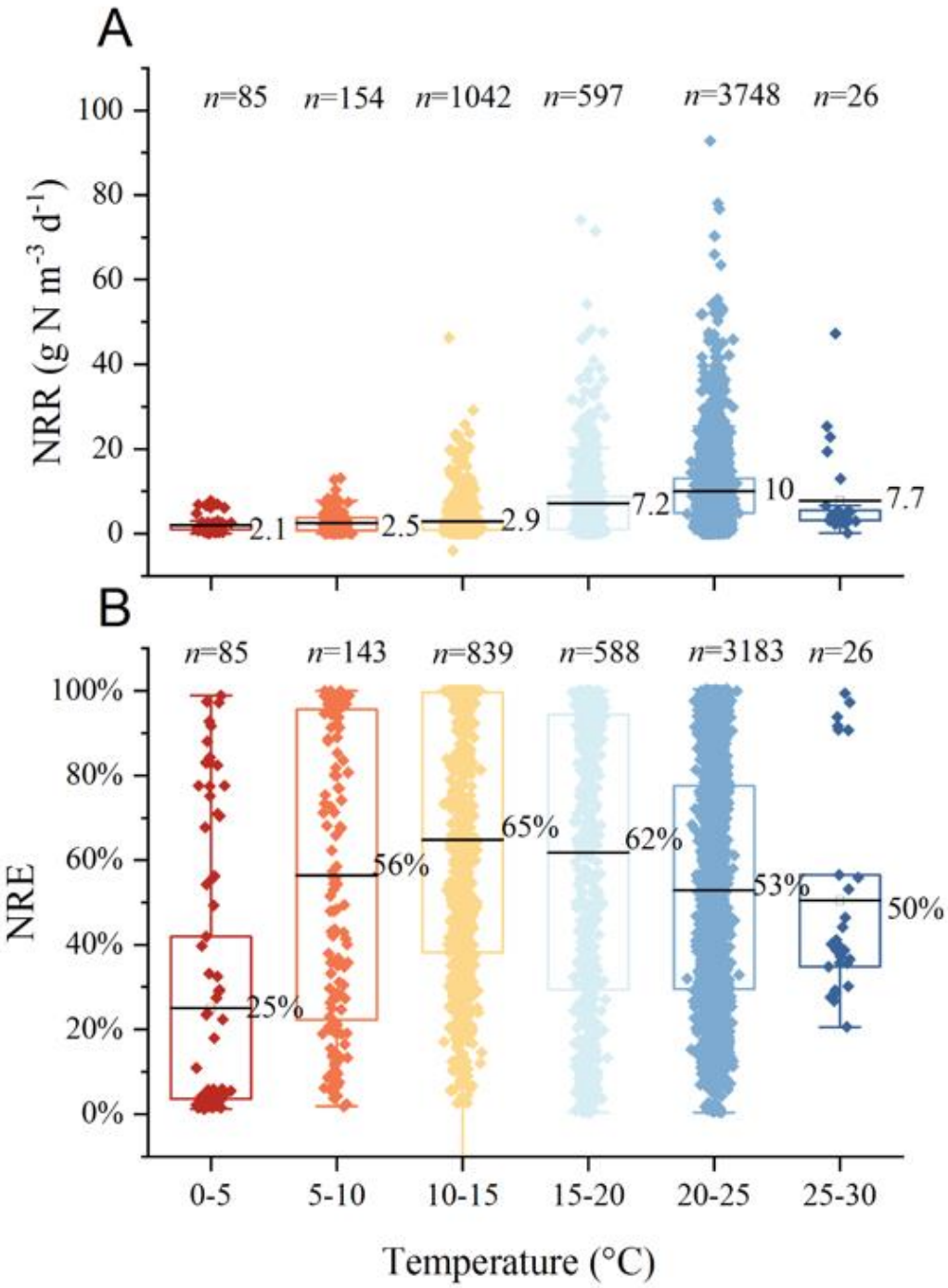

Figure 2.6 Nitrate removal rate (NRR, g N m^{-3} d^{-1}) and (B) nitrate removal efficiency (NRE, %) respond to the temperature. *n* represents the number of data points. Error bar represents standard error.

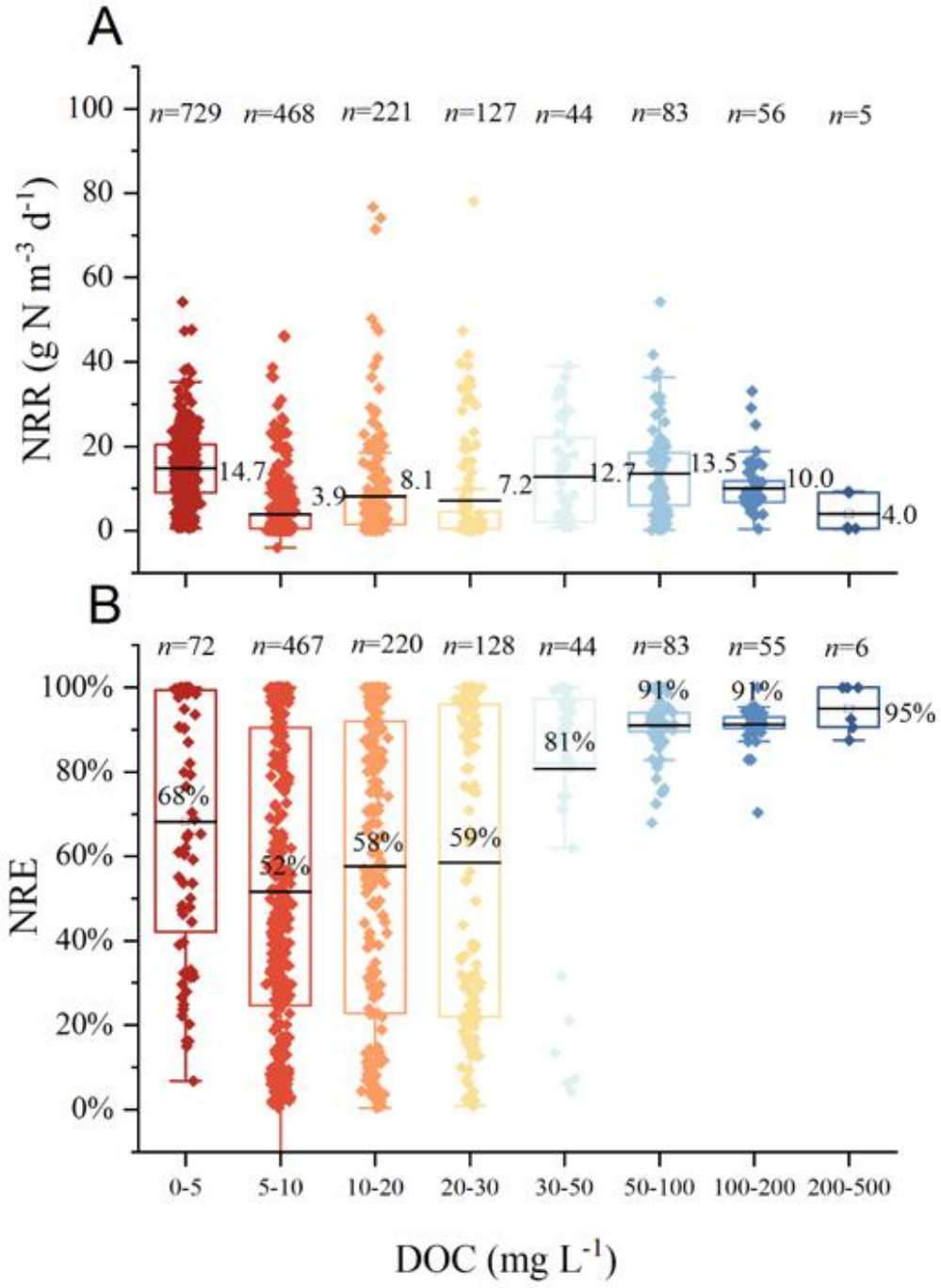

Figure 2.7 Nitrate removal rate (NRR, g N m^{-3} d^{-1}) and (B) nitrate removal efficiency (NRE, %) respond to the dissolved organic carbon (DOC). *n* represents the number of data points. Error bar represents standard error.

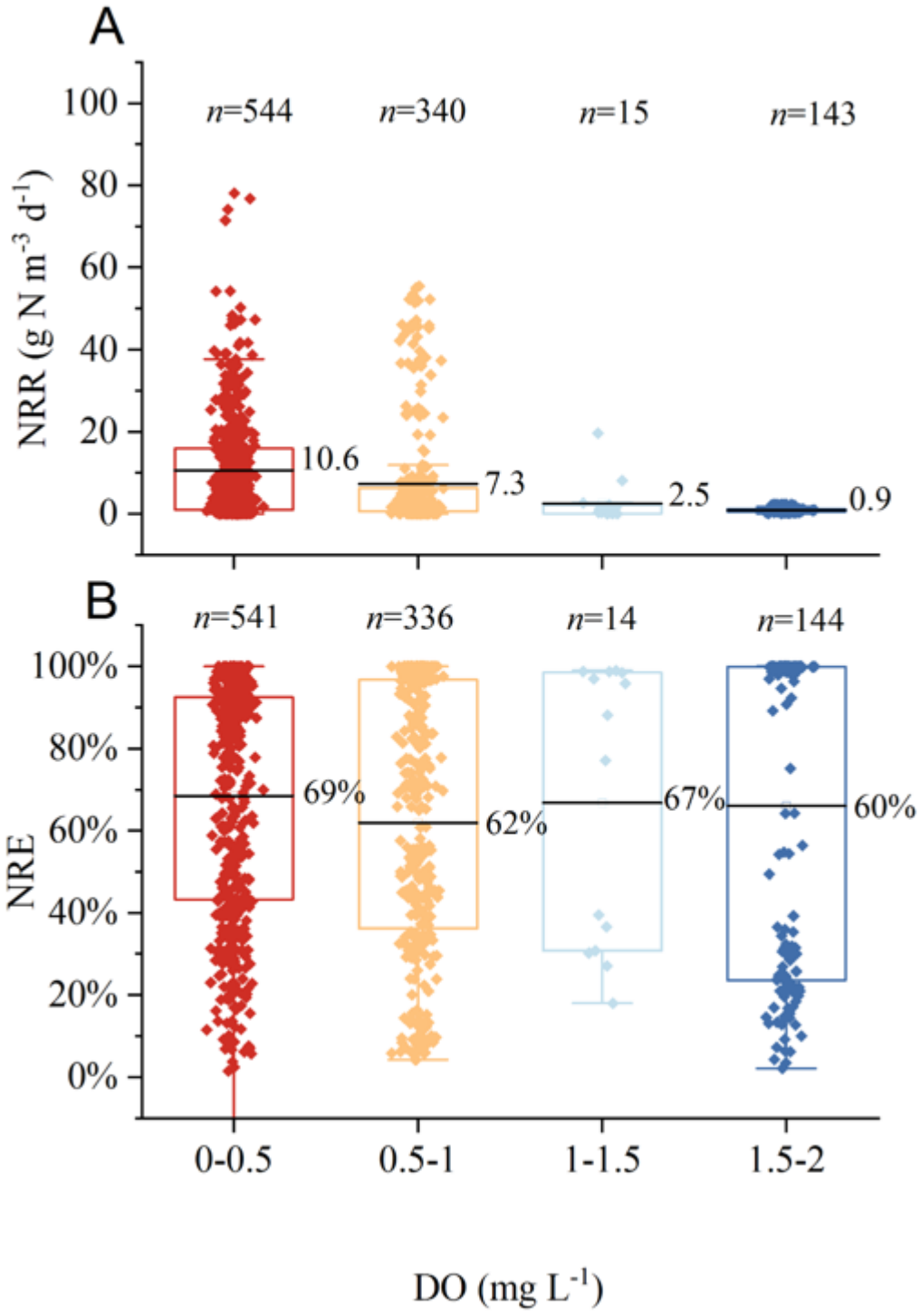

Figure 2.8 Nitrate removal rate (NRR, g N m^{-3} d^{-1}) and (B) nitrate removal efficiency (NRE, %) respond to the dissolved oxygen (DO). *n* represents the number of data points. Error bar represents standard error.

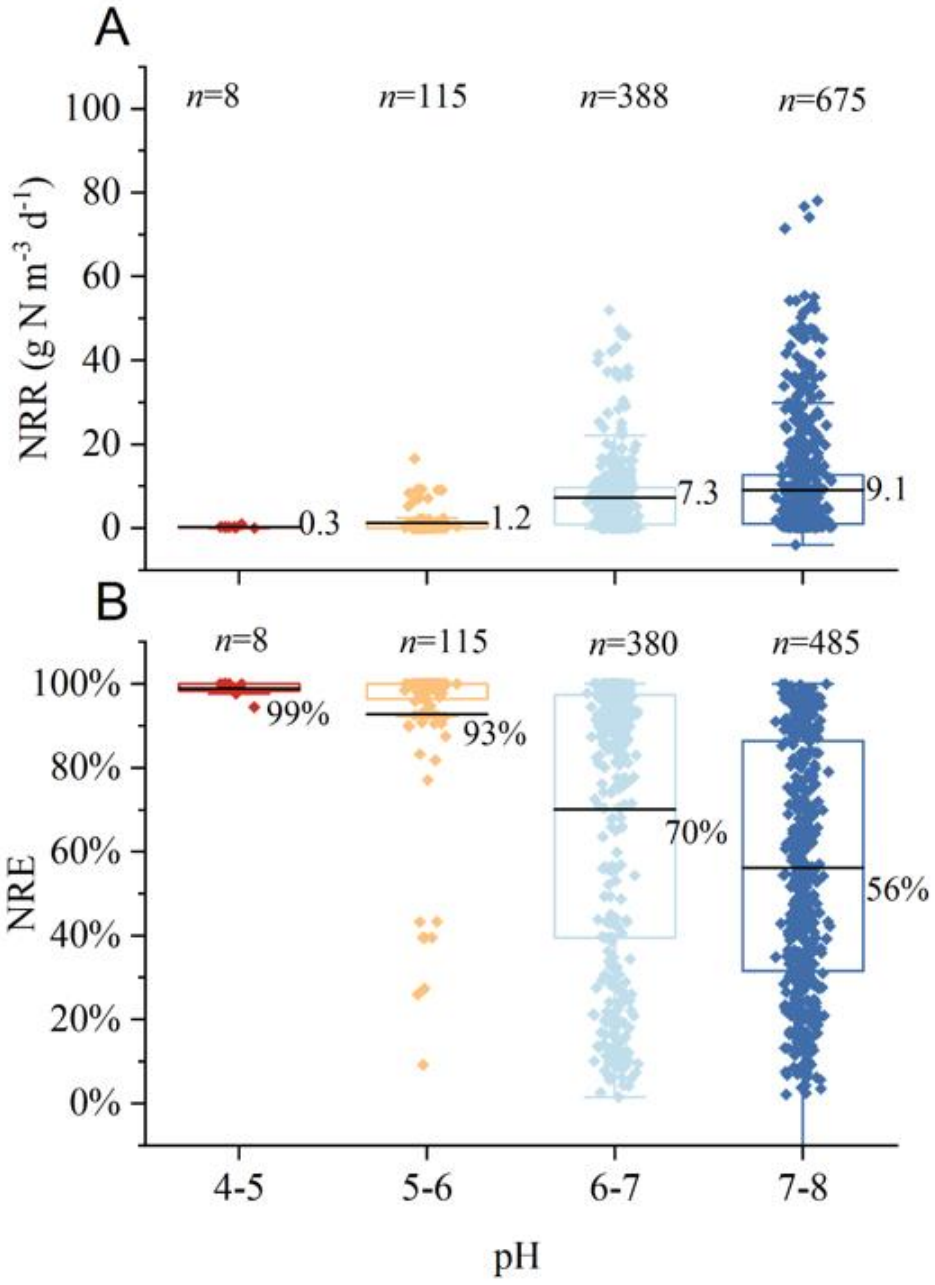

Figure 2.9 Nitrate removal rate (NRR, g N m^{-3} d^{-1}) and (B) nitrate removal efficiency (NRE, %) respond to the pH of solution. pH is classified as 4-5, 5-6. 6-7, and 7-8, respectively. *n* represents the number of data points. Error bar represents standard error.

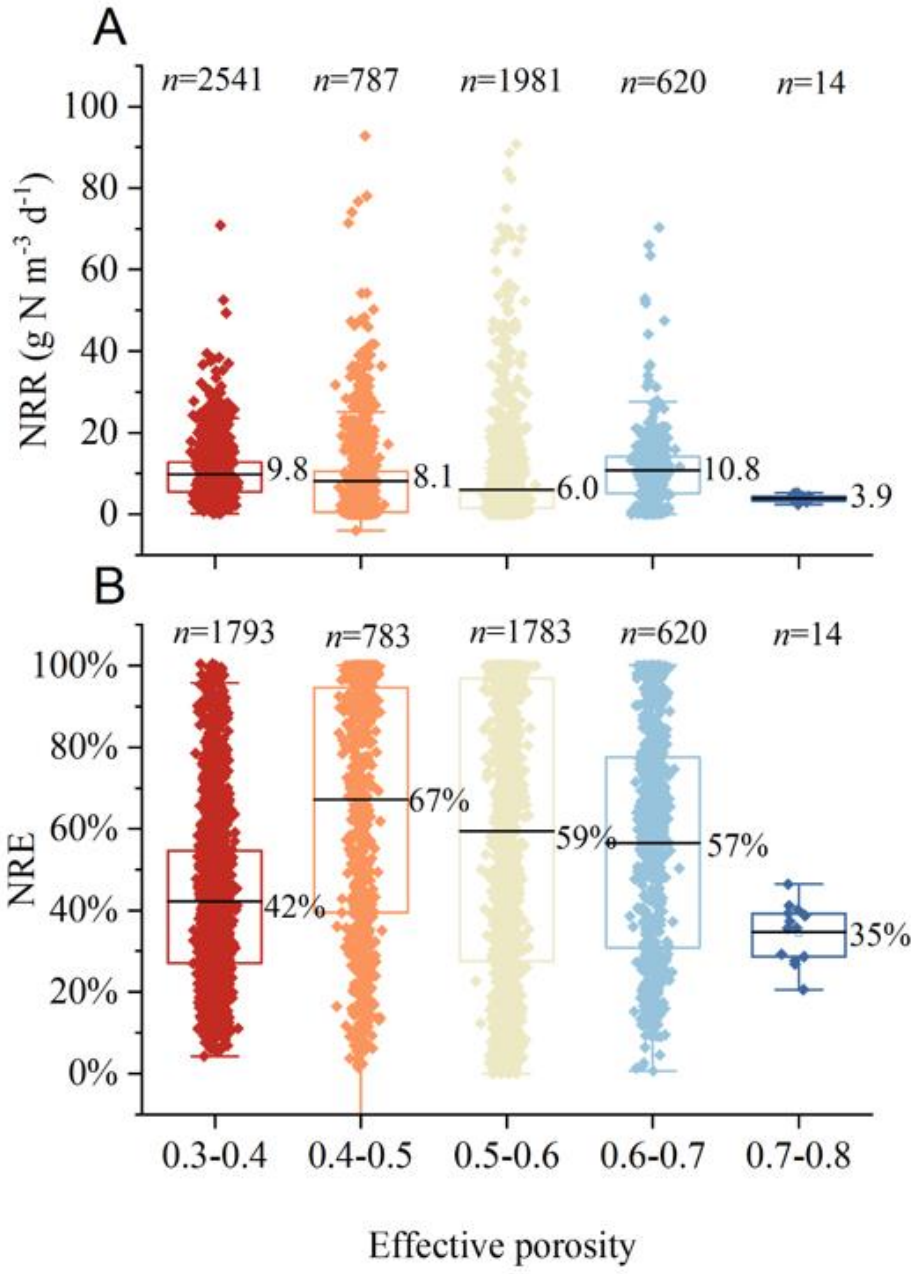

Figure 2.10 Nitrate removal rate (NRR, g N m^{-3} d^{-1}) and (B) nitrate removal efficiency (NRE, %) respond to the effective porosity. Effective porosity is classified as 0.3-0.4, 0.4-0.5. 0.5-0.6, 0.6-0.7, and 0.7-0.8, respectively. *n* represents the number of data points. Error bar represents standard error.

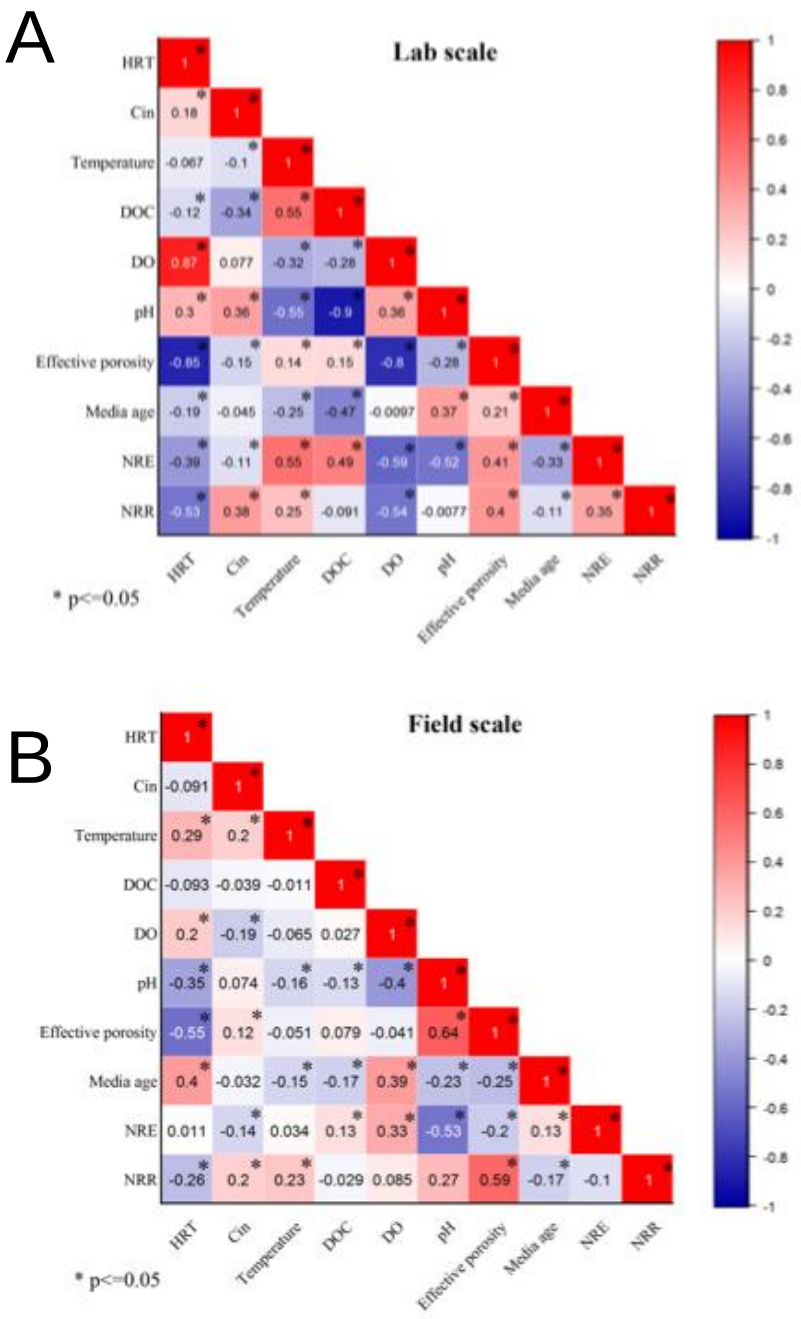

Figure 2.11 Pearson correlation of effluent dissolved organic carbon (DOC, mg C L^{-1}), effluent dissolved oxygen (DO, mg L^{-1}), effluent pH, influent nitrate concentration (C_{in}, mg N L^{-1}), temperature (℃), effective porosity, media age (days), hydraulic retention time (HRT, hours), nitrate reduction (C_{rd}, mg N L^{-1}), nitrate removal efficiency (NRE, %), and nitrate removal rate (NRR, g N m^{-3} d^{-1}) in lab (A) and field (B) scale. The dataset has missing data, and the specific total data number of HRT, C_{in}, temperature, DOC, DO, pH, porosity, and medium age are 5888, 5151, 5814, 1733, 1045, 1192, 5859, and 5086, respectively. * represents significant level ($p<0.05$).

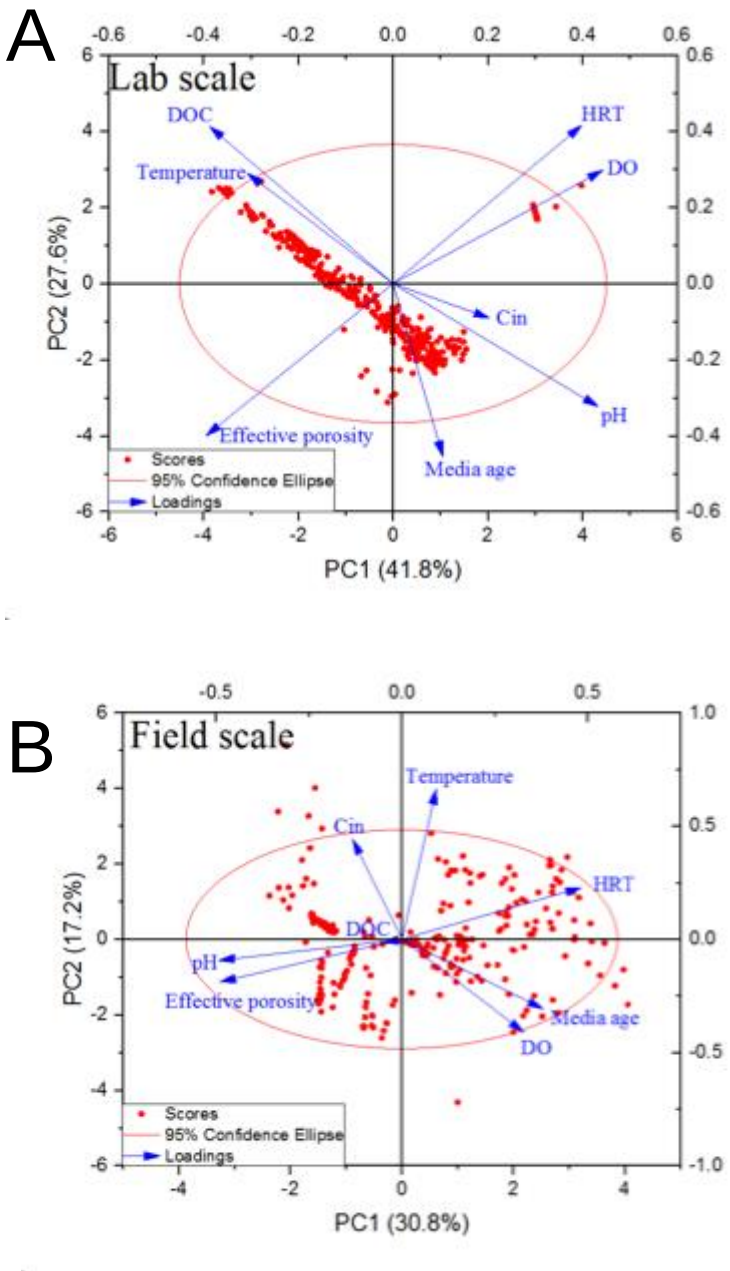

Figure 2.12 Principal component analysis of eight abiotic factors in lab (A) and field scale (B), which include dissolved organic carbon (DOC, mg C L^{-1}), dissolved oxygen (DO, mg L^{-1}), pH, influent nitrate concentration (C_{in}, mg N L^{-1}), temperature (°C), effective porosity, media age (d), hydraulic retention time (HRT, hours). They are analyzed by three categories, including total dataset, lab dataset, and filed dataset. The dataset has been tested by Bartlett's test (SPSS, IBM Inc, USA), which indicated that the dataset could be analyzed by principal component analysis. The dataset has missing data, and the specific total data number of HRT, C_{in}, temperature, DOC, DO, pH, porosity, and medium age are 5888, 5151, 5814, 1733, 1045, 1192, 5859, and 5086, respectively. * represents significant level ($p<0.05$).

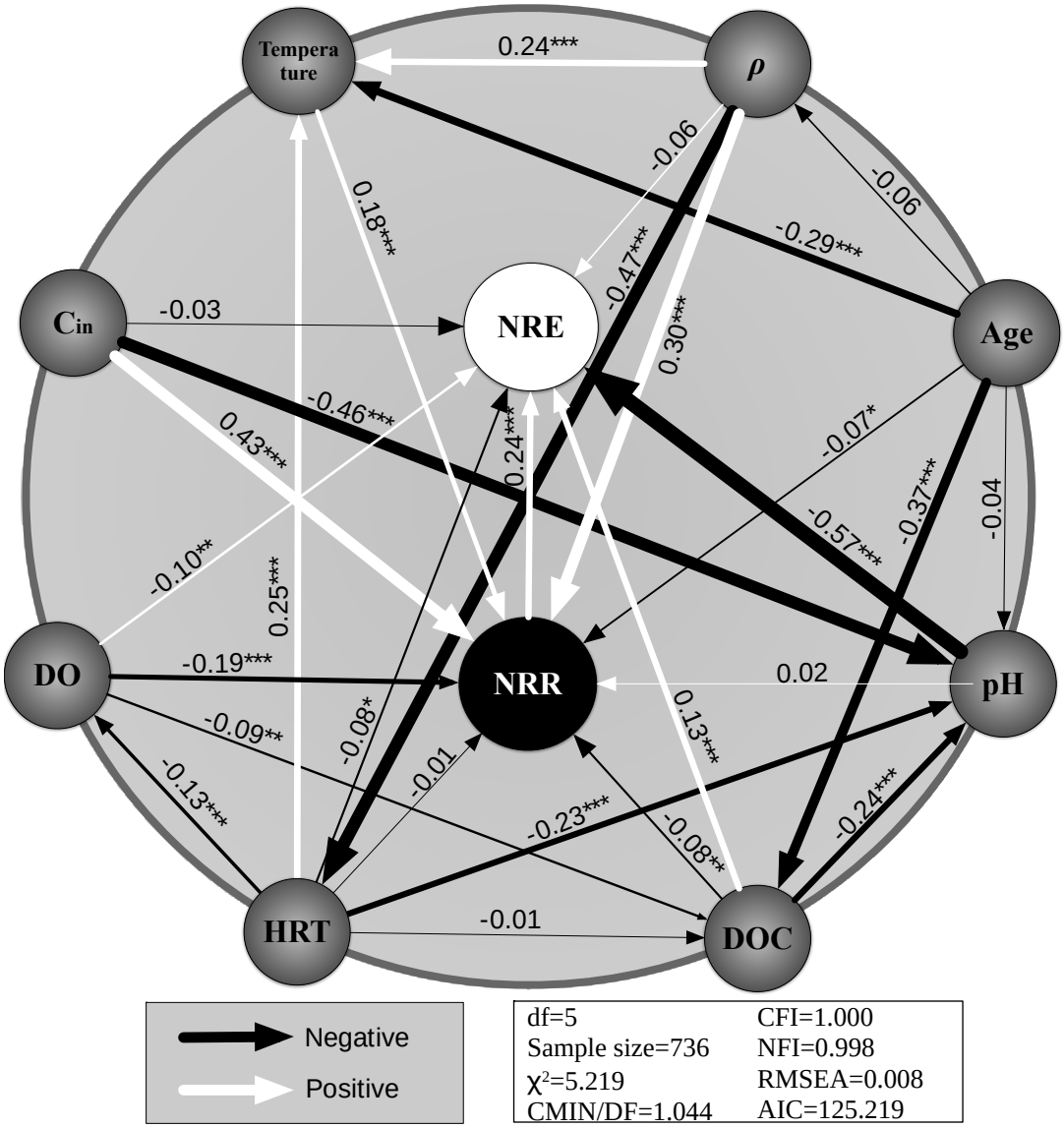

Figure 2.13 Structural equation model for controlling the removal rate and removal efficiency in woodchip-derived denitrifying bioreactors. Boxes indicate variables. HRT represents hydraulic retention time (hours), DO represents effluent dissolved oxygen (mg L^{-1}), Age represents medium age (d), DOC represents effluent dissolved organic carbon (mg C L^{-1}), C_{in} represents influent nitrate concentration (mg N L^{-1}), RE represents removal efficiency (%), RR represents removal rate (g N m^{-3} d^{-1}). An arrow represents a causal relationship (P<0.05). Arrow direction indicates the direction of effect. Arrow width indicates effect size. A black arrow denotes positive relationship, and a white arrow a negative relationship. Numbers above arrows are standardized path coefficient. The data is collected from six peer-reviewed articles. The degree of freedom (df), sample size, χ^2, CMIN/DF, CFI, NFI, RMSEA, and AIC are shown in the lower right.

CHAPTER III
EFFECT OF BIOREACTOR AND SILAGE LEACHATE ON THE PERFORMANCE OF WOODCHIP BIOREACTOR IN REMOVING NTIRATE AND VETERINARY ANTIBIOTICS

This chapter is based on a manuscript draft by Yuchuan Fan et al.:

A version of this chapter was originally prepared by:

Yuchuan Fan, Jaehoon Lee, Jie Zhuang, Michael Essington, Sindhu Jagadamma, and John Schwartz. Effect of biochar and silage leachate on the performance of woodchip bioreactor in removing nitrate and veterinary antibiotics.

My primary contributions to the work include (i) designing and implementing experiments, (ii) assay troubleshooting and refinement, (iii) initial writing of the manuscript, and (iv) revising manuscript and coordinating revisions of the manuscript.

Abstract

The removal of nitrates in denitrifying bioreactors is highly variable due to the fill properties, hydraulic retention time (HRT), and nitrate loading concentrations. We hypothesized that amending a woodchip bioreactor (W) with biochar (B) and silage leachate (S) could improve the nitrate removal performance. Twelve, lab-scale bioreactors were constructed to test the nitrate removal performance under different fill (W, W+B, W+S, W+B+S), HRT (0.5, 1, 2, 3, 4, 6, 8, 12, 24 hr), and nitrate loading concentration (5.4±0.3; 15.9±0.4; 33±1.5). We observed that adding biochar and silage leachate into the woodchip bioreactor together resulted in the greatest nitrate removal efficiency (NRE) and nitrate removal rate (NRR) values under all HRTs, nitrate loadings, and fill materials (W, W+B, W+S, W+B+S), which verified our hypothesis. However, at greater HRT (> 8 h), these improvements became less apparent. Moreover, adding silage leachate into the woodchip bioreactor also significantly increased nitrate removal rate (NRR) and nitrate removal efficiency (NRE). This effect was not observed when biochar was added, however, except at high values of HRT (≥8 h). According to our results of structural equation modeling, we attributed the biochar-improved denitrification to the decreases in dissolved oxygen, saturated hydraulic conductivity, and pH value, and increase in TOC after the addition of silage leachate. We found that the addition of biochar could increase the removal efficiency (RE) of sulfamethazine and tylosin at low loading concentrations (< 2 mg L^{-1}), while no effects on RE were observed at high loading concentrations (25 mg L^{-1}). Overall, the results showed

that adding biochar and silage leachate into woodchip bioreactors represents a promising and cost-effective approach to improving nitrate and veterinary antibiotics removal from agricultural drainage.

Introduction

The integrated crop-livestock agricultural system is believed to be a sustainable approach to improve soil quality, increase yield, produce a diversity of foods, and improve land use efficiency (Hilimire 2011; Asai et al. 2018). For example, manure can be applied to fields for crop nutrient acquisition (Hilimire 2011). It has been demonstrated that manure containing a range of partially metabolized (40 to 95%) veterinary antibiotics which has become a global agro-ecological issue (Kuppusamy et al. 2018). Further, the overuse of nitrate fertilizer in cropland areas has also become a global issue resulting in eutrophication and algal blooms in surface waters, and has potentially damaged human health (Padilla et al. 2018). Therefore, there is an need to attenuate nitrate and veterinary antibiotics before they get into water bodies and adversely affect human health and the environment.

Among the strategies employed to mitigate surface water contamination, woodchip bioreactors (WBs) have proven to be an effective, inexpensive, and sustainable management practice to remove nitrate by filling with woodchip (Pluer et al. 2019; Povilaitis and Matikienė 2020). Furthermore, woodchips have also been shown to offer the added benefit of retaining antibiotics to reduce pollution of surface water and groundwater in batch experiments (Ilhan et al. 2012). However, few studies have investigated the efficacy of WB in removing antibiotics given that WB has been primarily reported as a tool useful for nitrate removal, rather than other chemicals. Additionally, there is a large degree of variation in nitrate removal, as the nitrate removal rate (NRR) ranges from 0.51 to 166.91 g N m^{-3} d^{-1} (Pluer et al. 2019) and nitrate removal efficiency (NRE) ranges from 6.5 to 99.8% (Coleman et al. 2019). Our previous meta-analysis indicated that adding auxiliary materials into WB can significantly increase NRE (Fan

et al., 2021). The auxiliary materials include zero-valent iron (ZVI) (Su and Puls 2007), biochar (Bock et al. 2015; Bock et al. 2016), steel byproduct (Hua et al. 2016), and acetate (Roser et al. 2018). Among them, biochar is the most used material (Bock et al. 2015; Bock et al. 2016; Bock et al. 2018b, a; Berger et al. 2019; Coleman et al. 2019; Tian et al. 2019; Povilaitis and Matikienė 2020). These combinations, termed woodchip/biochar bioreactor (WBB), have the effect of decreasing dissolved oxygen (DO) in pore water, increasing water holding capacity, and providing electrons for denitrification (Berger et al. 2019; Tian et al. 2019). However, the inconsistent performance of woodchip/biochar bioreactor (WBB) has been reported (Bock et al. 2015; Bock et al. 2016; Bock et al. 2018b; Berger et al. 2019; Coleman et al. 2019). Therefore, further studies are needed to clarify the biochar-mediated alterations on physical and chemical properties of the WBB media to maximize NRR and NRE. Few studies have investigated the efficacy of WB in removing antibiotics given that WB has been primarily reported as a tool useful for nitrate removal, rather than other chemicals. Biochar had been reported to remove veterinary antibiotics (Teixidó et al. 2011; Yang et al. 2019). However, it is unclear whether addition of biochar into WBs can remove veterinary antibiotics.

In recent years, auxiliary materials have been studied for their ability to increase nitrate removal in WBB. Tian et al. (2019) added ZVI into the WBB in order to enhance nitrate removal from stormwater and found that biochar/ZVI removed 30.6-95.7% of nitrate from the influent with respect to -6.1-89.6% in the control group (i.e., without biochar and ZVI). Povilaitis and Matikienė (2020) modified WBB with flaxseed cake. Their results indicated that the auxiliary material substantially increased the release of organic carbon, but they could not demonstrate any increase in nitrate removal. Overall, there is uncertainty regarding the impact of adding additional carbon sources into WBB on nitrate removal. Nonetheless, the most frequently reported carbon source used as an additive could improve the capacity of the WBB to remove nitrates, but they were limited due to the high cost of auxiliary materials. For

example, the cost of ZVI varies from $20 to $77 per pound (Gavaskar et al. 2005). Thus, there is a lack of feasible and low-cost choice of filling materials for improving the nitrate removal in WBBs.

To increase the feasibility of applying WBB in the field, low-cost materials or agricultural waste should be considered as auxiliary materials. This paper proposes mixing silage leachate, which is a liquid C source from agricultural waste, into WBB. Silage leachate is widely reported in concentrated agricultural wastewater, and its reuse is a critical issue for livestock agriculture. Silage leachate reaching watercourses can rapidly deplete DO, causing the death of fish and eutrophication (Faulkner et al. 2011; Gebrehanna et al. 2014). It is corrosive to concrete and metal structures due to its acidity (pH≈4) (Faulkner et al. 2011), rendering its containment, handling, and disposal a significant challenge (Gebrehanna et al. 2014; Holly et al. 2018). In 2019, 133 million tons of corn for silage, 18 million tons of alfalfa haylage and greenchop, and 4 million tons of sorghum for silage were produced in the United States (NASS 2020). Moreover, many researchers have reported that other countries also produce large volume of silage, including New Zealand (Tikkisetty and Kuperus 2004) and China (Lujia et al. 2002). The storage of silage is often a significant source of wastewater in the forms of leachate and runoff (Holly et al. 2018). If the ensiled crop moisture is high (>75-85%) (Gebrehanna et al. 2014), and is sustained for a period of between 30 to 60 days, 90% of silage effluent will occur within the first 20-26 days (Savoie 1995). However, silage leachate consists of an abundant carbon source which may reach up to 22,970 mg L^{-1} (Arnold et al., 2000), so it could potentially serve as an additional carbon source for WBB. Thus, we hypothesized that adding silage leachate into WBB would be a win-win strategy. Adding silage leachate will enhance the removal of nitrate, lower the cost, and reduce environmental contamination. We expect that the combination of these unique filling materials could improve nitrate and veterinary antibiotics removal in denitrifying bioreactors.

The objective of this study was to compare the performances of woodchip (W), woodchip with biochar (W+B), woodchip with silage leachate (W+S), and woodchip with biochar and silage leachate together (W+B+S) in bioreactors for the removal of nitrate and veterinary antibiotics. We linked the nitrate removal capacity to biochar-mediated and leachate-mediated alterations in terms of the physical and chemical properties of the bioreactor. Furthermore, we investigated the removal efficacy of nitrate and veterinary antibiotics under various hydraulic retention times, influent concentrations, and silage leachate type.

Materials and Methods

The lab-bioreactor system

As shown in Fig 3.1, twelve laboratory-scale bioreactors were constructed. The bioreactor was a polypropylene tank, which consisted of a cap and body parts. The bioreactor cap included a water valve, cover sheet, and influent pipe. The bottom of the influent pipe was drilled evenly with holes to prevent an uneven distribution of inflow water to the bioreactor. A vent is centered on the cover sheet, which is used to release gas emissions (e.g., N_2, CO_2). The body of the bioreactor is 18 cm in width, 12 cm in height, and 30 cm in length, which includes a PVC influent protector, effluent tube, and outlet. When the cap and body were combined, the inflow pipe was inserted into the PVC protector to prevent clogging, and a seal strip was placed in the middle to create an anaerobic environment. Each type of media treatment consisted of three replicates, and six of these bioreactors were used to fill the woodchip (W, Bioreactor-1). The other six bioreactors were filled with woodchip and biochar (W+B, Bioreactor-2). A plastic filter with 100 even holes (5 mm in diameter) was installed vertically at the center of the bioreactor as a stand to hold biochar (Fig 3.1). Below the effluent outlet is a saturation zone which is filled with woodchip or woodchip plus biochar. A one-cm coarse sand layer

(predominantly 2-3 mm in grain size) was created over the saturation zone. To inoculate the saturation zones, a 50 g/L soil solution was prepared by mixing 50 g riverbank sandy loam (4% clay, 21% silt, and 75% sand) with 1 L of tap water, then added to the saturation zone of each bioreactor cell.

The woodchip was a local garden mulch woodchip. The woodchips were sieved through a 50 mm-mesh sieves to remove any residual soil and root, then washed 3 times with tap water and dried in the oven at 80 ^{o}C for 24 h. Finally, the woodchip was stored in a sealed plastic container until use.

The biochar was obtained from Proton Power, Inc. (Lenoir City, TN, USA). This company uses fast biomass pyrolysis to produce liquid biofuel and hydrogen, and biochar is a byproduct of the process. For this study, wood chips were obtained from whole logs using a brush chipper (Vermeer BC1000XL, Pella, IA, USA). Wet wood crumbles (mostly 5–10 mm in diameter) were generated using a Forest Concepts 6.4-mm M24ci Crumbler (Forest Concepts, LLC, Auburn, Washington, USA) and were then pyrolyzed using a Proton Power CHyP engine. While biochar can be obtained by pyrolysis performed at relatively low temperatures (300 ^{o}C), which preferably do not exceed 900 ^{o}C (Chen et al. 2017), the chars used in this study were prepared in a modified fast pyrolysis process, with a higher peak temperature (1,110 ^{o}C) and short residence time. The continuous process conveys feedstock using an auger, which requires the correlation of the volumetric displacement per revolution with bulk density. This correlation is used to maintain the desired mass throughput. Depending on the density, the residence time window was between 3 min and 5 min, during which the temperature was rapidly increased from ambient to the peak temperature. This fast pyrolysis regime was selected to maximize the liquid product yield and to improve the quality of the solid product (Inguanzo et al. 2001; Yahya et al. 2015). The biochar was collected in a sealed metal bin to prevent oxidation, allowed to cool, and stored for further use.

Silage leachate was collected from the silage bunker at the University of Tennessee dairy farm located at the East Tennessee AgResearch and Education Center (ETREC), Little River Animal and Environmental Unit (LRAEU). Given that the concentrations of the chemicals present in the silage leachate are mainly dependent on the rainfall and the silage type, we collected silage leachate at two different times. The first collection (i.e., fresh silage leachate) was performed while rainfall was occurring; the second collection (i.e., old silage leachate) was performed five days after rainfall had stopped. The old silage leachate was more concentrated in DOC than the fresh silage leachate. Since DOC is one of the most important factors affecting denitrification, we diluted both of the silage leachate into the same TOC (400 mg L^{-1}) using deionized water. The detailed chemical properties of the two different silage leachate after dilution are provided in Table 1.

Bioreactor characteristics

To calculate the total volume (V_T) and pore volume (PV) of the bioreactor, we employed a weighing method using a bench-scale balance. Initially, the masses of the bioreactor (W_1), the bioreactor with saturated water (W_2), the bioreactor with dry woodchip (W_3), and the filled bioreactor with saturated water (W_4) were obtained. Subsequently, water was discharged until no more water flowed out and the mass of the filled bioreactor was obtained once more (W_5). The total (η) and drainable porosity ($ß$) can be calculated using,

$$V_T = W_2 - W_1 \tag{1}$$

$$PV = W_3 - W_2 \tag{2}$$

$$h = \frac{W_4 - W_3}{V_T} \tag{3}$$

$$b = \frac{W_4 - W_5}{V_T} \tag{4}$$

Flow velocities (Q/A) were plotted as a function of the hydraulic gradient (Δh/L) observed in the constant head permeameter tests and saturated hydraulic conductivity (K_s) values were obtained from the slopes of linear fits to the experimental data (Christianson et al. 2010; Feyereisen and Christianson 2015). Bulk density was computed as follows (Christianson et al. 2010):

$$r_b = r_w(1- h) \quad (5)$$

where η is the porosity (dimensionless), ρ_b is the bulk density (g cm^{-3}), and ρ_w (g cm^{-3}) is the woodchip density which was measured equal to 0.267 g cm^{-3}.

The K_s values of our bioreactors ranged from 0.071 to 0.16 cm/s, which are lower than in previous studies which reported woody media in the range 0.35-11.6 cm/s for sawdust to 61-mm chips, respectively (Cameron and Schipper 2010). This was probably due to the small size of the effluent hose (diameter in 1 cm), which may limit the K_s.

Experimental set up

We conducted five laboratory experiments to study how different media (W, W+B, W+S, W+B+S), HRT, nitrate loading concentration, and type of silage leachate impacted NRE and NRR. The details of the experimental design are presented in Table 3.

Sampling and analysis methods

The influent was sampled from the prepared synthetic solution, and the effluents were manually sampled from the outflow water. Each outflow sample consisted of one pore volume water of the bioreactor. All samples were filtered with 0.22-μm membrane filters before storage at 4 ^oC. Filtered subsamples were preserved in vials and prepared for measuring NO_3-N, NH_4-N, NO_2-N, PO_4-P, sulfamethazine, and tylosin concentrations within 48 h after the manual sampling. Similarly, filtered subsamples were preserved in glass vials by acidification with HCl before total organic carbon (TOC) analysis.

Sulfamethazine and tylosin concentrations were determined by a high-pressure liquid chromatography (HPLC) system coupled with ultraviolet detection (Hewlett-Packard series 1100, Hewlett-Packard, Palo Alto, CA). This procedure was described by Essington et al. (2010) and Lee et al. (2014). NO_3-N, NH_4-N, NO_2-N, and PO_4-P were measured by a continuous flow analyzer (San, Skalar Inc, Dutch). TOC was measured by the total organic carbon analyzer (Shimadzu Inc, Japan).

The pH and DO were measured using an Orion Star pH/DO portable multi-parameter meter (A326, ThermoFisher Inc., USA). The temperature was measured with a thermocouple sensor. This system was connected to a data logger (CR800, Campell Inc, USA).

Data processing and calculation

Chemical removal indicators

To quantitatively describe the removal of nitrate and veterinary antibiotics, removal efficiency (RE, %) and removal rate (RR, g m^{-3} d^{-1}) were calculated using:

$$RE = \frac{C_{in}^{i} - C_{out}^{i}}{C_{in}^{i}} \tag{6}$$

$$RR = \frac{M_{in}^{i} - M_{out}^{i}}{HRT \times V_T} \tag{7}$$

where superscript *i* represents nitrate, tylosin, or sulfamethazine; C_{in} and C_{out} represent inflow chemical concentration and outflow chemical concentration. HRT represents hydraulic retention time (day) and V_T represents the total volume of the bioreactor (m^3).

N mass balance calculation

To compare the difference of N amount and type between the influent and effluent water, we measured the concentrations of different N species in Exp#1 and Exp#4 to calculate the mass of NO_3-N, NH_4-N, and NO_2-N using:

$$M_i = \sum_{j=1}^{n=3} V_j \times N_j \quad (8)$$

where *i* represents different species of N, including NO_3-N, NH_4-N, and NO_2-N; *j* represents the sampling time; *M* represents the mass of nitrogen (mg); *V* represents the volume of collecting water (L); and *N* represents the N concentration (mg L^{-1}).

Statistical analysis

A four-way mixed-model ANOVA was used to determine the direct and interaction effects of media, hydraulic retention time, influent nitrate concentration, and silage leachate type on the nitrate removal rate and nitrate removal efficiency (SPSS 27; IBM Corporation, Meadville, PA, USA). In addition, a one-way ANOVA was used to determine the significant difference of NRE and NRR values among the different media and hydraulic retention time. A *p*-value < 0.5 was required for a difference to be deemed statistically significant.

The effect sizes of pH, DO, TOC, and K_s were quantified with a structural equation modeling (AMOS 26; IBM Corporation, Meadville, PA, USA). We followed the procedures of developing and modifying a structural equation model described in previous studies (Li et al. 2019; Li et al. 2021). Briefly, there are three steps to build a structural equation modeling: (1) propose an *a priori* model based on experience or background information; (2) test whether important pathways were left out (modification indices ≥4) and if the existing pathways were significant ($p \leq 0.05$); (3) revise the *a priori* model by adding missing pathways and dropping insignificant pathways in consideration of model fit and scientific rationality. Multivariate

normality was assessed by considering Kurtosis values ≤7. Path coefficients were tested by maximum likelihood estimation. Standardized path coefficients were reported as effect sizes based on standard deviation units, ranging from 0 to 1. For NRR and NRE, we assumed that pH, DO, TOC, and K_s had direct effects on NRR and NRE according to previous findings by Tian et al. (2019) and Berger et al. (2019). Those assumptions led to the *a priori* model.

Given that a restricted size of data was input into the structural equation modeling, the interpretation of data related to the same type of biochar and woodchip may be limited. To generalize those conclusions into more universal concepts, a larger-scale study may be required in the future.

Results

Physical and chemical properties of bioreactor

As presented in Fig 3.2A and 3.2B, biochar addition significantly ($p < 0.05$) affected the saturated hydraulic conductivities (K_s) of bioreactors and effluent dissolved oxygen (DO). The addition of biochar produced a 35% reduction in K_s with respect to the woodchip bioreactor (Fig 3.2A). Given that denitrifying bioreactors use a passive technology, the water flow rate is determined by the K_s. Thus, adding biochar decreases the water flow rate, and inversely increases the hydraulic retention time (HRT). Further, both biochar and dosing silage leachate decreased effluent DO values (Fig 3.2B). In all bioreactors, effluent DO values decreased from 7.93±0.2 (influent) to 3.11±2.0 (W), 2.92±2.2 (W+B), 2.61±2.1 (W+S), and 2.37±2.0 mg L^{-1} (W+B+S) (Fig 3.2B).

Adding biochar and silage leachate significantly ($p < 0.05$) altered the effluent chemical properties, including pH and TOC (Fig 3.2C and 3.2D). Biochar addition (W+B) significantly ($p < 0.05$) increased effluent pH from X to 6.83±0.2 when compared with W. Conversely, silage leachate addition (W+S) significantly ($p < 0.05$) decreased effluent pH to 6.57±0.17.

Adding biochar and silage leachate together into the WB led to a neutral pH with no significant difference with respect to W ($p > 0.05$) (Fig 3.2C). In addition, addition of biochar and silage leachate could significantly increase the TOC, and the two auxiliary materials have synergistic effect on the increase of TOC (Fig 3.2D).

Effect of adding biochar and silage leachate

Fig 3.3 shows the NRE and NRR of the different bioreactors (W, W+B, W+S, and W+B+S) tested in the study. The mean value of NRE for W+B+S, (76%) was significantly greater than the other treatments: W+S (63%), W+B (57%), and W (53%) (Fig 3.3A). There was no significant difference in NRE between W, W+B, and W+S ($p > 0.05$). The W+B+S treatment also showed the greatest mean value (24.7 g N m^{-3} d^{-1}) compared to other treatments: W+S (17.4 g N m^{-3} d^{-1}), W+B (14.4 g N m^{-3} d^{-1}), and W (12.8 g N m^{-3} d^{-1}) (Fig 3.3A). Similarly, there was no significant difference in NRE among W, W+B, and W+S ($p > 0.05$) (Fig 3.3B).

The structural equation modeling (SEM) was used to explain the causal relationship between biochar and silage leachate addition among the bioreactor physicochemical properties. The goodness-of-fit indices suggested an optimal fit of our physical and chemical properties of bioreactors (CMIN/DF = 4.916, GFI = 0.939, CFI = 0.957, RMSEA = 0.143, Fig 3.4A). This SEM indicated that biochar addition mainly affected the physical properties (effect size = -0.97) rather than the chemical properties (effect size = -0.003). The model also showed that the physical properties exerted a positive effect on DO (effect size = 0.33) and K_s (effect size = 0.93). Conversely, silage leachate addition mainly affected the chemical properties (effect size = -1.00), rather than the physical properties (effect size = -0.23), with a positive effect on pH (effect size = 0.38) and a negative effect on TOC (effect size = -0.34).

To disaggregate the chemical (e.g., pH and TOC) and physical factors (e.g., K_s and DO) on nitrate removal indices, we tested the model for NRE and NRR (Fig 3.4B-C). The goodness-of-fit indices indicated an optimal fit of our measured physical and chemical data on NRE

(CMIN/DF = 1.983, GFI = 0.988, CFI = 0.987, RMSEA = 0.072, Fig 3.4B). K_s had a positive effect on DO (effect size = 0.16), but a negative effect on TOC (effect size = -0.44). Similarly, pH had a positive effect on DO (effect size = 0.61), but a negative effect on TOC (effect size = -0.45). DO showed a positive effect on TOC (effect size = 0.61). Finally, DO had a negative effect (effect size = -0.27) and TOC a positive effect (effect size = 0.46) on NRE.

The goodness-of-fit indices indicated an optimal fit of our measured physical and chemical data on NRR (CMIN/DF = 3.337, GFI = 0.993, CFI = 0.992, RMSEA = 0.111, Fig 3.4C). The effect size between chemical and physical factors was the same as that presented in Fig 3.4B. In contrast, DO and TOC had a positive effect (effect size = 0.71) and TOC a negative effect (effect size = -0.21) on NRR. Furthermore, K_s (effect size = -0.43) and pH (effect size = -0.77) showed direct negative effects on NRR.

Effect of hydraulic retention time

The NRE and NRR values obtained for different HRT and media are shown in Fig 3.5. The results show that the addition of biochar and silage leachate into the woodchip bioreactor (i.e., W+B+S) increased the values of NRE and NRR. Adding silage leachate alone into the woodchip bioreactor (i.e., W+S) also increased NRE and NRR, but the effect was significantly lower ($p < 0.05$) than adding biochar and silage leachate when HRT was low (≤4 h). However, adding biochar into woodchip bioreactor did not result in any significant increase of NRE and NRR, except for HRT at high values of 8 and 12 h. In addition, there were no differences in terms of NRE and NRR for different media when HRT was greater than 24 h, due to the limitation of nitrate concentration. Overall, adding silage leachate alone (W+S) or biochar and silage leachate together (W+B+S) into the woodchip bioreactor increased NRE and NRR at low HRT (≤ 4 h). In comparison, adding biochar alone into the woodchip significantly increased NRE and NRR at high HRTs (8 and 12 h). The addition of biochar and silage leachate had significant effects on NRR and NRE ($p < 0.01$), which with an interaction effect between

biochar and silage leachate having a further impact on NRE ($p < 0.001$) when HRT was below 4 h.

Effect of influent nitrate concentration

Influent nitrate concentration had significant effects on NRE and NRR ($p < 0.05$) (Fig 3.6A and 3.6B). The relationships between NRE and HRT and NRR and HRT were linear. The NRE decreased with influent nitrate concentration, while the NRR increased with influent nitrate concentration. In addition, a greater difference in terms of NRE and NRR occurred among different media at greater influent NO_3-N concentrations. Moreover, the fitted linear regression model showed no significant difference between W and W+B ($p < 0.05$) relative to both NRE and NRR.

Effect of silage leachate type

Adding old silage leachate (OS) into the media of W+B+S resulted in a significant increase in NRE compared with adding fresh silage leachate (FS). However, using different types of silage leachate did not significantly affect the NRE (Fig 3.7). Fig 3.8 indicates that adding FS produced less ammonium in the effluent water compared with adding OS. This implied that adding FS into the woodchip bioreactor could improve the total N removal with respect to the addition of OS.

Removal of sulfamethazine and tylosin removal

The removal efficiency of the two veterinary antibiotics (SMT and TYL) with various media (W, W+B, W+S, W+B+S) at different HRT values (1, 4, 6, 8, 12, and 24 h) and influent nitrate concentrations are presented in Fig 3.9. The media type and HRT had significant ($p < 0.05$) effects on the removal efficiency (RE) of SMT and TYL when influent concentration were low (0.34 ± 0.17 mg SMT L^{-1} and 1.86 ± 0.29 mg TYL L^{-1}) (Fig 3.9A and 3.9C). When influent antibiotic concentrations were high (24.5 mg SMT L^{-1} and 25.7 mg TYL L^{-1}), the HRT

had a significant ($p < 0.001$) impact on the RE of SMT and TYL while media had no significant effect on the RE of SMT and TYL ($p > 0.05$) (Fig 3.9B and 3.9D). The RE of SMT and TYL increased with increasing HRT. Moreover, W+B+S had the highest RE for SMT and TYL at low influent concentrations (Fig 3.9A and 3.9C).

Discussion

Effect of biochar on chemical removal in bioreactors

This study found that adding biochar into the woodchip bioreactor did not improve NRE and NRR at low HRT (≤4 h) (Fig 3.5B) and that different influent nitrate concentrations did not influence NRE or NRR (Fig 3.6B). However, biochar addition resulted in a significant increase in NRE when HRT was above 8 h (Fig 3.5A and 3.5B); although influent nitrate concentrations did not influence NRE (Fig 3.6A). Thus, these results suggest that the inconsistent biochar impacts observed in different previous studies might be caused by different HRTs.

The greater NRE observed in biochar-amended bioreactors was primarily attributed to changes in the physical properties (e.g., K_s and DO), consistent with previous studies (Tian et al. 2019). The lower K_s could indirectly increase NRE by leading to a greater HRT. However, the HRT was not dependent on K_s as the flow rate was artificially controlled by peristaltic pumps rather than water head. In some cases (2-6 h), our study showed that biochar addition resulted in a higher NRE than woodchip bioreactors at the same HRT. In addition, biochar decreased the DO by increasing the small water-filled pore volume to produce an anaerobic environment that is favorable to reproduction of denitrifying bacteria. Apart from decreasing K_s and DO, a previous study reported that biochar addition was able to increase porosity and water saturation (Tian et al. 2019). However, our study did not show any significant difference

between W and W+B in terms of total porosity and effective porosity ($p > 0.05$, Table 2). This was likely due to a low biochar fraction (10%, v/v).

Altering the chemical properties, such as increasing pH and released DOC, slightly increased nitrate removal. This study showed that biochar can increase the average pH (Fig 3.2C), without producing a significant increase on effluent TOC (Fig 3.2D). The suitable pH range for heterotrophic denitrifiers was in the range of 4.0 to 8.0 (Rust et al. 2000). As such, the minor pH variation elicited by adding biochar may not have a significant impact on denitrification. Overall, the chemical effects on nitrate removal may be somewhat limited.

In addition to altering the physical and chemical properties, adding biochar into woodchip bioreactors could promote denitrification by providing extra electron donors for denitrifying bacteria (Tian et al. 2019) and increased microbial biomass (Berger et al. 2019). The redox-facile hydro/quinone groups in biochar could make biochar both an electron donor and acceptor (Saquing et al. 2016). Thus, biochar can release stored electrons to support autotrophic denitrification. Moreover, the larger surface area and amount of micro-pore volume can provide a favorable environment for denitrifying bacteria. previous research reported that adding biochar did not affect the relative abundance of denitrifying genes (Berger et al. 2019). Therefore, further studies are required to quantify the contribution of biochar on biological activities.

NO_3-N adsorption onto biochar or soil clay minerals might contribute to nitrate removal in WBB bioreactors. It was reported that NO_3 adsorbs onto various modified biochar (Zhang et al. 2012; Wang et al. 2015), but it is rarely reported on unmodified biochar (Zhang et al. 2020). In this study, our biochar is unmodified, thus nitrate adsorption onto the biochar might be very limited in our bioreactor. Similarly, nitrate is a conservative anion, no adsorption onto soil clay minerals that was added into the bioreactors.

Considering all the aforementioned mechanisms, the physical properties appear to be the factors most important for increasing nitrate removal in woodchip bioreactors. The addition of biochar did not result in significant modifications to the chemical properties (e.g., pH) and uncertainty remains in terms of altering the biological properties (i.e., no effect on the relative abundance of denitrifying genes) (Berger et al. 2019).

Except for increasing nitrate removal, adding biochar could offer further benefits, such as the capacity to remove ammonium (Fig 3.8), veterinary antibiotics (Fig 3.9), and decrease the exhaustion rate of woodchips when HRT is less than 5 h (Berger et al. 2019). The increase in sulfamethazine and tylosin removal after adding biochar may be due to adsorption (Yang et al. 2019). Numerous studies have reported that modified biochar is a sustainable adsorbent (Mohan et al. 2014) for removing several classes of chemicals, such as phosphate (Zhang et al. 2020), pesticides (Safaei Khorram et al. 2016), and metals (Inyang et al. 2016). Therefore, adding biochar into the woodchip bioreactor could serve as a potential framework to remediate water quality in addition to nitrate removal.

Effect of silage leachate on nitrate removal in bioreactors

Silage leachate, a polluted water from agricultural systems, has been shown as a cost-effective addition to increase nitrate removal rate for woodchip bioreactors in this study. The addition of silage leachate significantly increased the average NRE by approximately 19% compared with the woodchip bioreactor (Fig 3.3A). It was determined that the addition of silage leachate increased the released TOC, prompting denitrification activities, as the average effluent TOC in W+S was 1.73 fold-times greater than in W (Fig 3.2D). We found that the silage type might not have significant effects on NRE in the woodchip bioreactor (Fig 3.7). This could be explained by the fact that all our silage leachate was diluted to the same TOC (approximately 400 mg L^{-1}) before being added. This suggests that, when the TOC is constant, other components (e.g., PO_4-P, NH_4-N, NO_2-N) of silage leachate may not affect NRE.

However, the different amounts of NH_4-N in old silage leachate and fresh silage leachate may lead to a different fraction of NH_4-N in the effluent. We observed that compared to adding fresh silage leachate, when adding old silage leachate, the proportion of NH_4-N in total N in effluent was increased 20% (Fig 3.8). The NH_4-N was increased after adding silage leachate could be as an evident of occurring dissimilatory nitrate reduction in the ammonium (DNRA) process. Previous studies have reported that DNRA occurred in woodchip bioreactors with a high carbon dosage (Gibert et al. 2008; Li et al. 2017; Aalto et al. 2020) and this high carbon dosage could result in a greater C/N ratio, which has been reported as the dominant condition for DNRA to compete with denitrification (Tiedje 1982; van den Berg et al. 2015). In this study, the C/N ratio for fresh silage leachate and old silage leachate were 1,932 and 13,890, respectively, which were relatively high. Even though the silage leachate dosing amount was 10% of pore water, it would dramatically increase the C/N ratio of water within the bioreactor. Previous studies have indicated that with a C/N ratio over 7.7, up to 90% of all nitrate was converted to ammonium (van den Berg et al. 2015). Therefore, a higher C/N ratio in the silage leachate could have resulted in the DNRA. Our study indicated that adding fresh silage leachate does not decrease NRE but may reduce the accumulation of ammonium in effluent. Even though the accumulation of ammonium in effluent can be mitigated by adding fresh silage leachate, the optimal silage leachate dosing required to improve the total N removal efficiency, rather than the nitrate removal efficiency, should be studied in the future.

Regarding NRR as the nitrate removal indicator, adding silage leachate significantly affects NRR when HRT is in the range of 0.5 to 12 h. However, a greater HRT (> 12 h) may result in a lower difference of NRR among the treatments. Besides, adding silage leachate did not elicit any significant increase in tylosin and sulfamethazine removal efficiency, it probably indicated that the removal mechanism of two veterinary antibiotics may not attributed to microbial activities.

Effect of biochar and silage leachate interaction on nitrate removal in bioreactors

We found that adding biochar and silage leachate together could significantly increase NRE and NRR at different HRT (Fig 3.5A and 3.5B). This indicates that biochar and silage leachate addition had a synergistic effect on NRE and NRR. This result might be explained by the fact that greater TOC was released in W+B+S (Fig 3.2D). This observation might support the explanation that biochar could trap DOC in pore water, or in the thin film near its surface, which can be utilized by the microbial community (Ulrich et al. 2017). A lot of DOC from silage leachate may be trapped into biochar, thus the greater TOC observed in effluent was probably coming from the DOC previously trapped by biochar. Hence, a higher DOC near the surface of the biochar and woodchip could prompt denitrification activities (Hartz et al. 2017).

In addition to a greater TOC, a low average DO (2.37 mg L^{-1}, Fig 3.2B) may also contribute to denitrification. The low DO in the bioreactor was probably attributed to the low DO of the old silage leachate (1.43 mg L^{-1}), and biochar addition can also facilitate a low DO as previously suggested. Thus, the low DO concentration in W+B+S might increase the growth of denitrifying bacteria. Furthermore, the average pH of W+B+S was 6.72, which was not significant different than the pH in W, which was 6.78 (Fig 3.2C), likely due to the pH neutralization as a result of the biochar and silage leachate addition. All the aforementioned chemical and physical properties may contribute to the greater degree of nitrate removal. The different substrates in the woodchip bioreactor may result in a different microbial activities and communities (Hellman et al. 2021). However, in this study, the microbial analysis for the different media is lacking, and we expected that W+B+S would be associated with a greater microbial biomass than W, W+B, and W+S.

With the exception of nitrate, it was found that adding biochar and silage leachate together may increase tylosin removal efficiency at a low influent concentration (e.g., 1.86±0.29 mg TYL L^{-1}). Conversely, no increase in sulfamethazine removal efficiency was

observed at higher HRT and greater influent concentrations compared to other treatments (W, W+B, W+S). In light of this, further studies are required to investigate the effect of different biochar fractions, as well as various silage leachate dosing strategies, on the removal of nitrate and veterinary antibiotics.

Conclusions

Our results showed that adding biochar and silage leachate together can significantly increase NRR compared with the woodchip bioreactor. Our structural equation model explained that this enhancement of nitrate removal was most likely attributed to the altered physical properties induced by biochar addition (K_s) and chemical properties by silage addition (DO). Thus, adding biochar and silage leachate into a woodchip bioreactor can further benefit the increasing TOC and decreasing DO by providing a favorable environment for denitrifying bacteria. It was also observed that the treatment of adding biochar and silage leachate showed the greatest NRR and NRE at various HRTs and nitrate loadings. Adding either biochar or silage leachate alone into the woodchip bioreactor could also increase nitrate removal, but that the ultimate determinants were HRT and influent nitrate concentration. We determined that biochar addition could increase sulfamethazine and tylosin removal efficiency (RE) at low influent concentrations (<2 mg L^{-1}), while there was no effect at high influent concentrations (e.g., 25 mg L^{-1}). In light of these findings, future work should evaluate the long-term performance of woodchip bioreactors amended with different biochar fractions and silage leachate in removing nitrate and other pollutants under field conditions.

References

Aalto S L, Suurnäkki S, von Ahnen M, et al. 2020. Nitrate removal microbiology in woodchip bioreactors: A case-study with full-scale bioreactors treating aquaculture effluents[J]. Science of The Total Environment: 138093.

Asai M, Moraine M, Ryschawy J, et al. 2018. Critical factors for crop-livestock integration beyond the farm level: A cross-analysis of worldwide case studies[J]. Land Use Policy, 73: 184-194.

Berger A W, Valenca R, Miao Y, et al. 2019. Biochar increases nitrate removal capacity of woodchip biofilters during high-intensity rainfall[J]. Water Research, 165: 115008.

Bock E, Smith N, Rogers M, et al. 2015. Enhanced nitrate and phosphate removal in a denitrifying bioreactor with biochar[J]. Journal of Environmental Quality, 44(2): 605-613.

Bock E M, Coleman B, Easton Z M. 2016. Effect of biochar on nitrate removal in a pilot-scale denitrifying bioreactor[J]. Journal of Environmental Quality, 45(3): 762-771.

Bock E M, Coleman B S L, Easton Z M. 2018a. Effect of biochar, hydraulic residence time, and nutrient loading on greenhouse gas emission in laboratory-scale denitrifying bioreactors[J]. Ecological Engineering, 120: 375-383.

Bock E M, Coleman B S L, Easton Z M. 2018b. Performance of an under-loaded denitrifying bioreactor with biochar amendment[J]. Journal of Environmental Management, 217: 447-455.

Cameron S G, Schipper L A. 2010. Nitrate removal and hydraulic performance of organic carbon for use in denitrification beds[J]. Ecological Engineering, 36(11): 1588-1595.

Chen Y, Zhang X, Chen W, et al. 2017. The structure evolution of biochar from biomass pyrolysis and its correlation with gas pollutant adsorption performance[J]. Bioresource Technology, 246: 101-109.

Christianson L, Castelló A, Christianson R, et al. 2010. Technical Note: Hydraulic property determination of denitrifying bioreactor fill media[J]. Applied Engineering in Agriculture, 26: 849-854.

Coleman B S L, Easton Z M, Bock E M. 2019. Biochar fails to enhance nutrient removal in woodchip bioreactor columns following saturation[J]. Journal of Environmental Management, 232: 490-498.

Essington M E, Lee J, Seo Y. 2010. Adsorption of antibiotics by montmorillonite and kaolinite[J]. Soil Science Society of America Journal, 74(5): 1577-1588.

Faulkner J W, Zhang W, Geohring L D, et al. 2011. Nutrient transport within three vegetative treatment areas receiving silage bunker runoff[J]. Journal of Environmental Management, 92(3): 587-595.

Feyereisen G W, Christianson L E. 2015. HYDRAULIC FLOW CHARACTERISTICS OF AGRICULTURAL RESIDUES FOR DENITRIFYING BIOREACTOR MEDIA[J]. Applied Engineering in Agriculture, 31(1): 89-96.

Gavaskar A, Tatar L, Condit W. 2005. Cost and performance report nanoscale zero-valent iron technologies for source remediation [J].

Gebrehanna M M, Gordon R J, Madani A, et al. 2014. Silage effluent management: A review[J]. Journal of Environmental Management, 143: 113-122.

Gibert O, Pomierny S, Rowe I, et al. 2008. Selection of organic substrates as potential reactive materials for use in a denitrification permeable reactive barrier (PRB)[J]. Bioresource Technology, 99(16): 7587-7596.

Hartz T, Smith R, Cahn M, et al. 2017. Wood chip denitrification bioreactors can reduce nitrate in tile drainage[J]. California Agriculture, 71(1): 41-47.

Hellman M, Hubalek V, Juhanson J, et al. 2021. Substrate type determines microbial activity and community composition in bioreactors for nitrate removal by denitrification at low temperature[J]. Science of The Total Environment, 755: 143023.
Hilimire K. 2011. Integrated crop/livestock agriculture in the United States: A review[J]. Journal of Sustainable Agriculture, 35(4): 376-393.
Holly M A, Larson R A, Cooley E T, et al. 2018. Silage storage runoff characterization: Annual nutrient loading rate and first flush analysis of bunker silos[J]. Agriculture, Ecosystems & Environment, 264: 85-93.
Hua G, Salo M W, Schmit C G, et al. 2016. Nitrate and phosphate removal from agricultural subsurface drainage using laboratory woodchip bioreactors and recycled steel byproduct filters[J]. Water Research, 102: 180-189.
Ilhan Z E, Ong S K, Moorman T B. 2012. Herbicide and Antibiotic Removal by Woodchip Denitrification Filters: Sorption Processes[J]. Water Air and Soil Pollution, 223(5): 2651-2662.
Inguanzo M, Menendez J, Fuente E, et al. 2001. Reactivity of pyrolyzed sewage sludge in air and CO2[J]. Journal of Analytical and Applied Pyrolysis, 58: 943-954.
Inyang M I, Gao B, Yao Y, et al. 2016. A review of biochar as a low-cost adsorbent for aqueous heavy metal removal[J]. Critical Reviews in Environmental Science and Technology, 46(4): 406-433.
Kuppusamy S, Kakarla D, Venkateswarlu K, et al. 2018. Veterinary antibiotics (VAs) contamination as a global agro-ecological issue: A critical view[J]. Agriculture, Ecosystems & Environment, 257: 47-59.
Lee J, Seo Y, Essington M E. 2014. Sorption and transport of veterinary pharmaceuticals in soil—A laboratory study[J]. Soil Science Society of America Journal, 78(5): 1531.
Li L, Konkel J, Jin V L, et al. 2021. Conservation management improves agroecosystem function and resilience of soil nitrogen cycling in response to seasonal changes in climate[J]. Science of The Total Environment, 779: 146457.
Li L, Wilson C B, He H, et al. 2019. Physical, biochemical, and microbial controls on amino sugar accumulation in soils under long-term cover cropping and no-tillage farming[J]. Soil Biology and Biochemistry, 135: 369-378.
Li R, Feng C P, Xi B D, et al. 2017. Nitrate removal efficiency of a mixotrophic denitrification wall for nitrate-polluted groundwater in situ remediation[J]. Ecological Engineering, 106: 523-531.
Lujia H, Guanghui T, Xiangyang L, et al. Straw resources and utilization in China[C]//Straw resources and utilization in China. 2003 ASAE Annual Meeting. American Society of Agricultural and Biological Engineers: 1
Mohan D, Sarswat A, Ok Y S, et al. 2014. Organic and inorganic contaminants removal from water with biochar, a renewable, low cost and sustainable adsorbent – A critical review[J]. Bioresource Technology, 160: 191-202.
NASS U 2020. Crop Production 2019 Summary [M]: 122.
Padilla F M, Gallardo M, Manzano-Agugliaro F. 2018. Global trends in nitrate leaching research in the 1960–2017 period[J]. Science of The Total Environment, 643: 400-413.
Pluer W T, Morris C K, Walter M T, et al. 2019. Denitrifying bioreactor response during storm events[J]. Agricultural Water Management, 213: 1109-1115.
Povilaitis A, Matikienė J. 2020. Nitrate removal from tile drainage water: The performance of denitrifying woodchip bioreactors amended with activated carbon and flaxseed cake[J]. Agricultural Water Management, 229: 105937.

Roser M B, Feyereisen G W, Spokas K A, et al. 2018. Carbon dosing increases nitrate removal rates in denitrifying bioreactors at low-temperature high-flow conditions[J]. Journal of Environmental Quality, 47(4): 856-864.
Rust C M, Aelion C M, Flora J R. 2000. Control of pH during denitrification in subsurface sediment microcosms using encapsulated phosphate buffer[J]. Water Research, 34(5): 1447-1454.
Safaei Khorram M, Zhang Q, Lin D, et al. 2016. Biochar: A review of its impact on pesticide behavior in soil environments and its potential applications[J]. Journal of Environmental Sciences, 44: 269-279.
Saquing J M, Yu Y-H, Chiu P C. 2016. Wood-Derived Black Carbon (Biochar) as a Microbial Electron Donor and Acceptor[J]. Environmental Science & Technology Letters, 3(2): 62-66.
Savoie P. 1995. Probability estimation of silage effluent from horizontal silos[J]. Canadian Agricultural Engineering, 37(1): 49-56.
Su C, Puls R W. 2007. Removal of added nitrate in cotton burr compost, mulch compost, and peat: Mechanisms and potential use for groundwater nitrate remediation[J]. Chemosphere, 66(1): 91-98.
Teixidó M, Pignatello J J, Beltrán J L, et al. 2011. Speciation of the ionizable antibiotic sulfamethazine on black carbon (Biochar)[J]. Environmental Science and Technology, 45(23): 10020-10027.
Tian J, Jin J, Chiu P C, et al. 2019. A pilot-scale, bi-layer bioretention system with biochar and zero-valent iron for enhanced nitrate removal from stormwater[J]. Water Research, 148: 378-387.
Tiedje J M. 1982. Denitrification[J]. Methods for Soil Analysis, 2: 1011-1024.
Tikkisetty B, Kuperus W. Environmentally friendly silage management[C]//Environmentally friendly silage management. Proceedings of SIDE Conference. South Island Dairy Event.
Ulrich B A, Vignola M, Edgehouse K, et al. 2017. Organic Carbon Amendments for Enhanced Biological Attenuation of Trace Organic Contaminants in Biochar-Amended Stormwater Biofilters[J]. Environmental Science & Technology, 51(16): 9184-9193.
van den Berg E M, van Dongen U, Abbas B, et al. 2015. Enrichment of DNRA bacteria in a continuous culture[J]. The ISME Journal, 9(10): 2153-2161.
Wang Z, Guo H, Shen F, et al. 2015. Biochar produced from oak sawdust by Lanthanum (La)-involved pyrolysis for adsorption of ammonium (NH4+), nitrate (NO3−), and phosphate (PO43−)[J]. Chemosphere, 119: 646-653.
Yahya M A, Al-Qodah Z, Ngah C Z. 2015. Agricultural bio-waste materials as potential sustainable precursors used for activated carbon production: A review[J]. Renewable and Sustainable Energy Reviews, 46: 218-235.
Yang W, Feng T, Flury M, et al. 2019. Effect of sulfamethazine on surface characteristics of biochar colloids and its implications for transport in porous media[J]. Environmental Pollution, 256: 113482.
Zhang M, Gao B, Yao Y, et al. 2012. Synthesis of porous MgO-biochar nanocomposites for removal of phosphate and nitrate from aqueous solutions[J]. Chemical Engineering Journal, 210: 26-32.
Zhang M, Song G, Gelardi D L, et al. 2020. Evaluating biochar and its modifications for the removal of ammonium, nitrate, and phosphate in water[J]. Water Research, 186: 116303.

Appendices

Tables

Table 3.1 The chemical properties of silage leachate before dosing

Silage leachate type	HRT (h)	NO_3-N (mg/L)	NH_4-N (mg/L)	NO_2-N (mg/L)	TN (mg/L)	PO_4 (mg/L)	TC (mg/L)	TOC (mg/L)
Old	1	0.03	5.6	n/d	35.77	19.33	444.51	418.17
Old	6	0.13	49.93	n/d	77.7	0.04	416.1	411.98
Fresh	6	0.25	44.76	n/d	66.87	0.85	501	413.4

Table 3.2 Physical properties of each bioreactor

No	Biochar (g)	Silage leachate (v/v)	Woodchip (g)	PV (ml)	η (%)	ß (%)	ρ_b (g cm^{-3})	K_s (cm s^{-1})
T1	0	0	1500	3114	63.55%	42.67%	0.097	0.146
T2	0	0	1500	3067	62.59%	44.06%	0.100	0.152
T3	0	0	1500	3078	62.82%	47.20%	0.099	0.141
T4	78.4	0	1350	3079	62.84%	45.55%	0.099	0.1057
T5	78.4	0	1350	3079	62.84%	48.27%	0.099	0.0931
T6	78.4	0	1350	2908	59.35%	42.80%	0.109	0.1025
T7	0	10%	1500	3363	68.63%	43.12%	0.084	0.1217
T8	0	10%	1500	3315	67.65%	40.65%	0.086	0.1596
T9	0	10%	1500	3314	67.63%	45.73%	0.086	0.1377
T10	78.4	10%	1350	3222	65.76%	43.55%	0.091	0.0953
T11	78.4	10%	1350	2920	59.59%	43.82%	0.108	0.0708
T12	78.4	10%	1350	3088	63.02%	48.06%	0.099	0.0853

PV represents pore volume;

η represents total porosity;

ß represents secondary porosity (or effective porosity);

ρ_b represents bulk density;

K_s represents hydraulic conductivity

Table 3.3 Experimental set up

Experiments	Concentration	Media	Silage leachate type	HRT
Exp#1	Nitrate: 6.8 TYL: 0.36±0.18 SMT:1.89±0.32	W; W+B; W+S; W+B+S	Old	1, 6
Exp#2	Nitrate: 6.8 TYL: 25.7 SMT: 24.5	W; W+B; W+S; W+B+S	Old	4, 8, 12, 24
Exp#3	Nitrate: 6.8	W; W+B; W+S; W+B+S	Old	0.5, 1, 2, 3, 4
Exp#4	Nitrate: 6.8	W+S; W+B+S	Fresh	6
Exp#5	Nitrate: 5.4±0.3; 15.9±0.4; 33±1.5	W; W+B; W+S; W+B+S	Old	6

Note: HRT represents hydraulic retention time; TYL represents tylosin; SMT represents sulfamethazine; W represents woodchip, B represents biochar, S represents silage leachate.

Figures

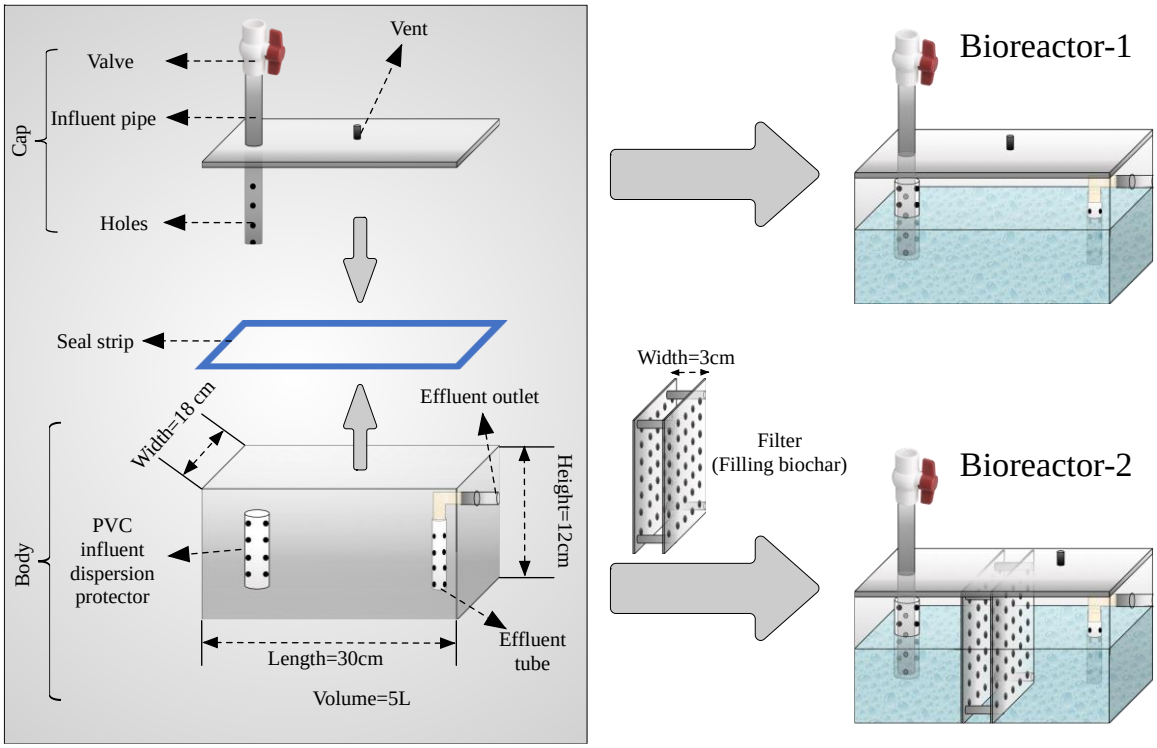

Figure 3.1 Schematic of lab-bioreactor setup. Bioreactor-1 was filled up with a woodchip, and Bioreactor-2 was filled up with woodchip and biochar together, and the biochar was held by the plastic filter in the middle of the bioreactor.

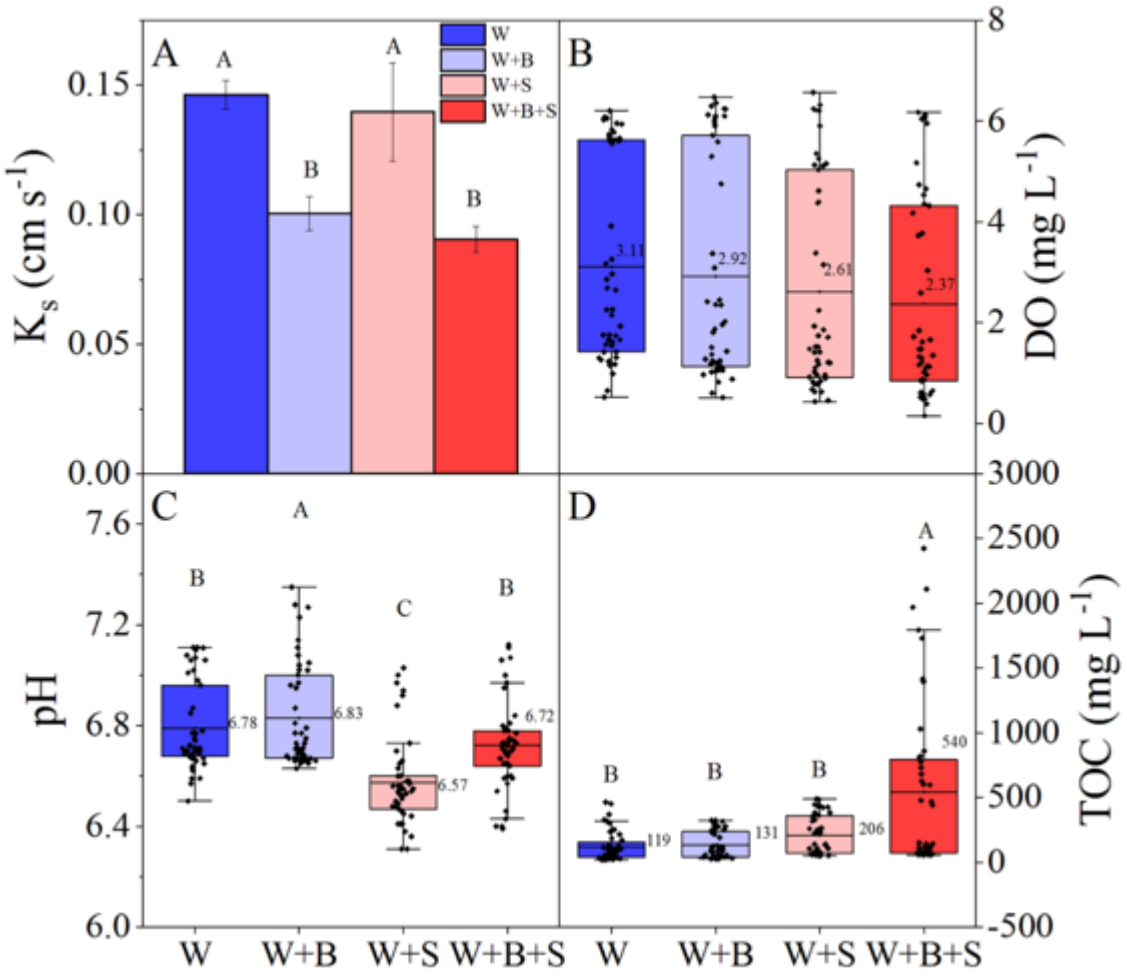

Figure 3.2 (A) Saturated hydraulic conductivity (Ks) values of different fill-materials bioreactors, including W, W+B, W+S, and W+B+S. W represents woodchip bioreactor; B represents biochar; S represents silage leachate. (B) The observed data of effluent dissolved oxygen, (C) effluent pH, and (D) effluent total organic carbon (TOC) at different bioreactors. All the chemical and physical properties data were measured under the same influent nitrate concentration (6.8 mg N L^{-1}), but various hydraulic retention time (0.5, 1, 2, 3, 4, 6, 8, 12, 24 h) and media (W, W+B, W+S, W+B+S). Different letters indicate significant differences within media ($p < 0.05$). The error bars are standard deviation.

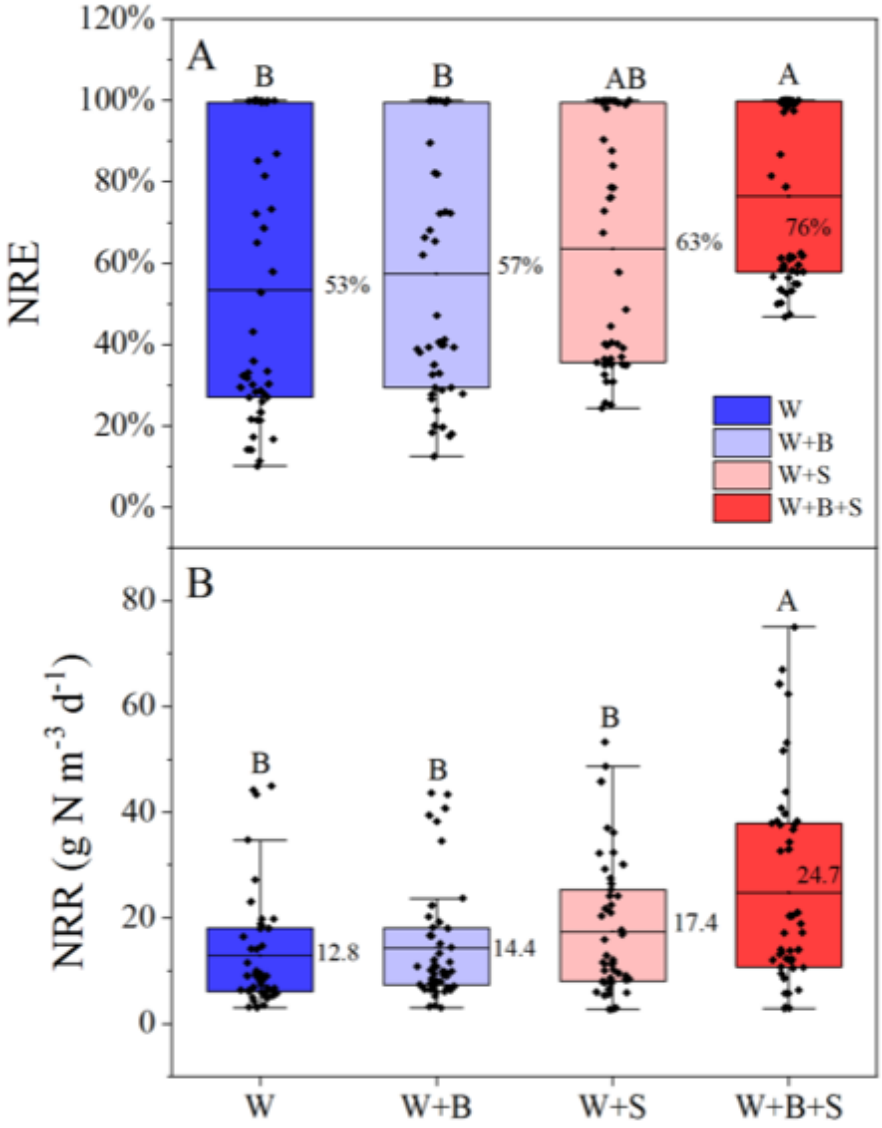

Figure 3.3 (A) Nitrate removal efficiency (NRE) and (B) nitrate removal rate (NRR) in different bioreactors, including W, W+B, W+S, and W+B+S. W represents woodchip bioreactor; B represents biochar; S represents silage leachate. All the NRE and NRR were calculated based on the experiment which conducted at the same influent nitrate concentration (6.8 mg N L^{-1}), but various hydraulic retention time (0.5, 1, 2, 3, 4, 6, 8, 12, 24 h) and media (W, W+B, W+S, W+B+S). Different letters indicate significant differences within media ($p < 0.05$). The error bars are standard deviation.

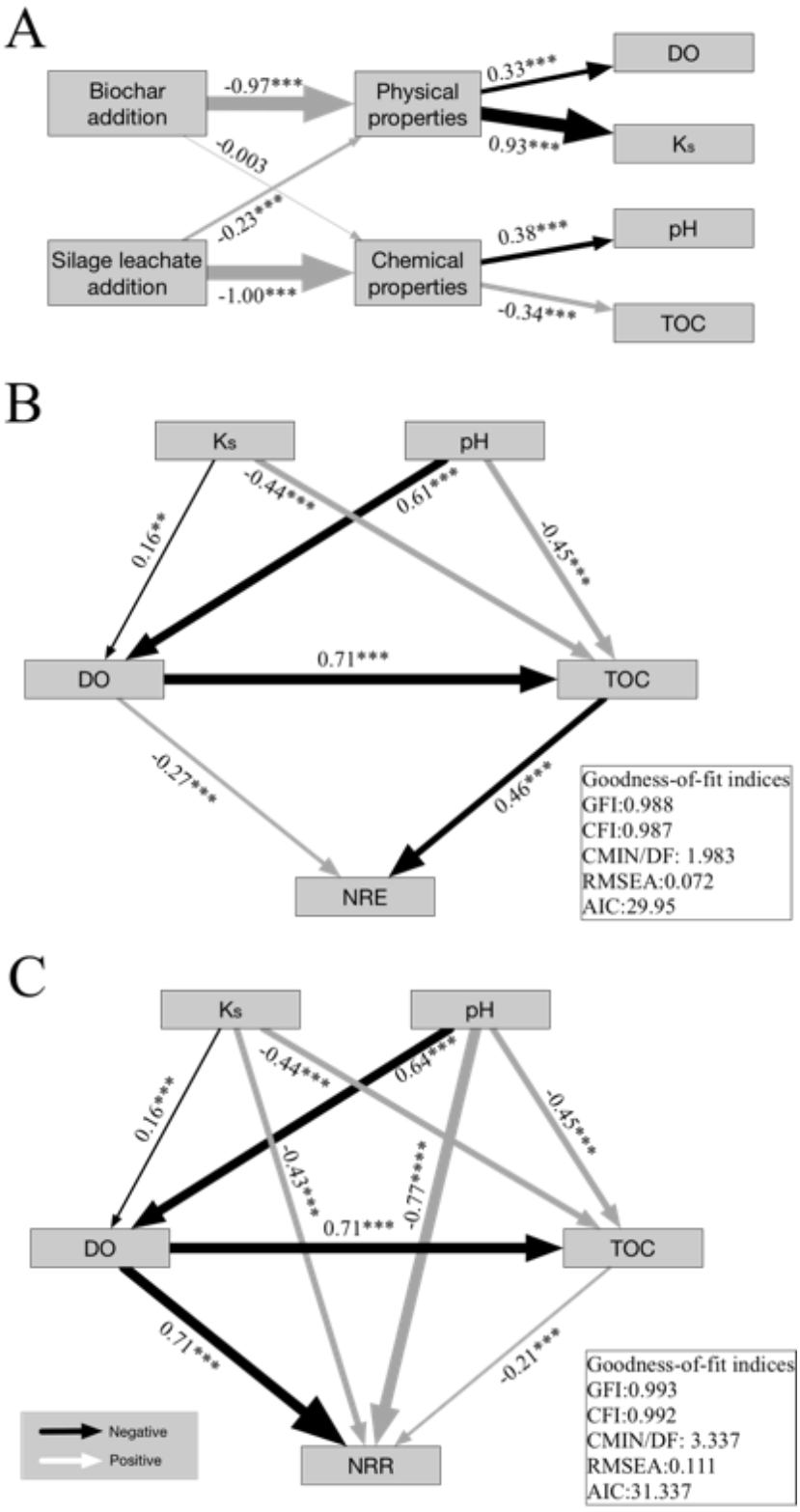

Figure 3.4 (A) Structural equation model for biochar and silage leachate addition effects on physical and chemical factors of bioreactor and effluent. DO: dissolved oxygen; Ks: saturated hydraulic conductivity; TOC: total organic carbon; (B) Structural equation model for physical and chemical factors effects on NRE, and (C) NRR. NRE: nitrate removal efficiency; NRR: nitrate removal rate. All the chemical (pH, TOC), physical properties (DO, Ks), and nitrate

removal (NRE and NRR) data were measured under the same influent nitrate concentration (6.8 mg N L-1), but various hydraulic retention time (0.5, 1, 2, 3, 4, 6, 8, 12, 24 h) and media (W, W+B, W+S, W+B+S). Arrows represent causal relationships. Arrow direction indicates the direction of causation. Arrow width indicated effect size. Black arrows denote positive relationships and gray arrows negative relationships. Number close to arrows are standardized path coefficients, i.e., effect sizes. Following with symbols *, **, *** represent significant, highly significant, and extremely significant, respectively. Goodness-of-fit indices are attached.

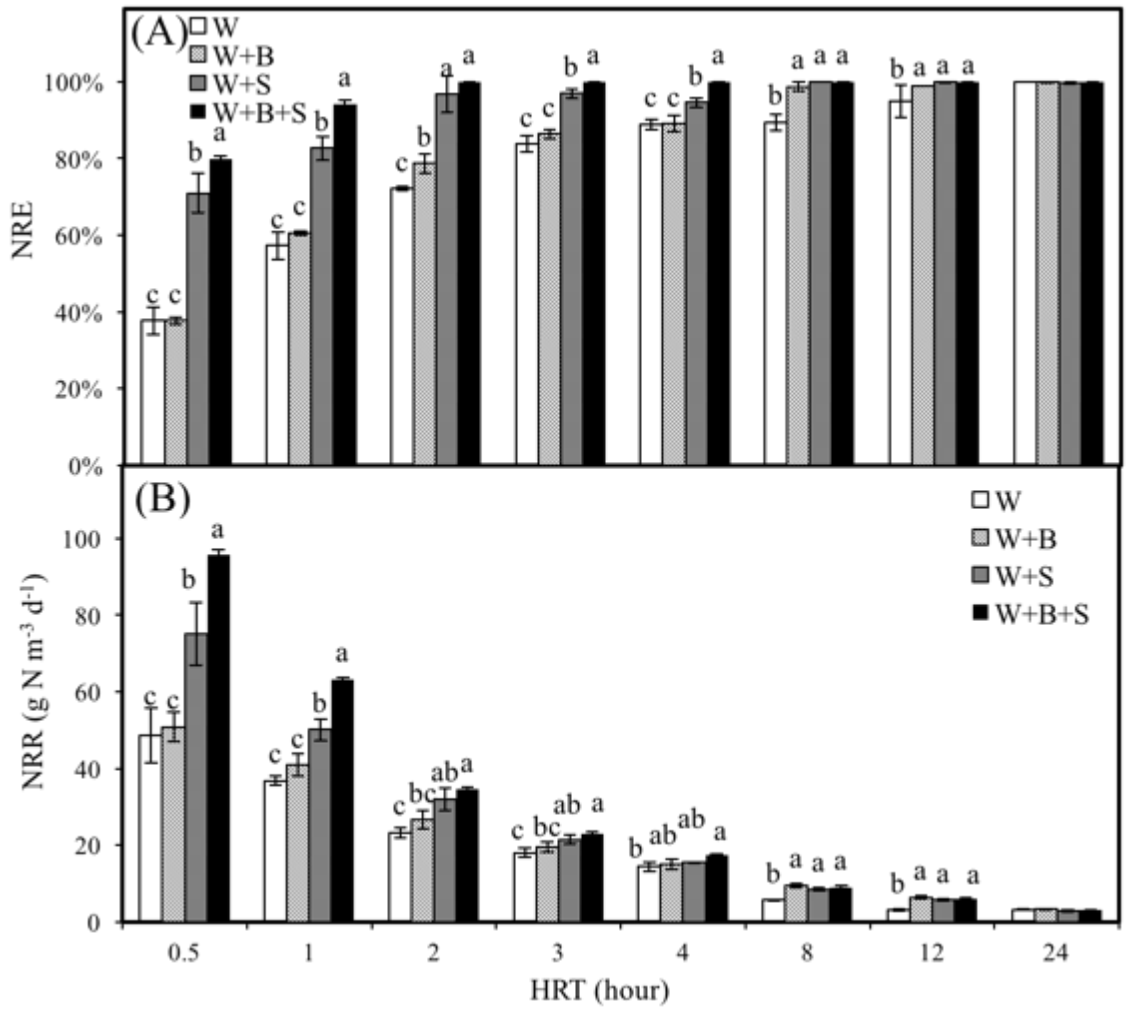

Figure 3.5 (A) Nitrate removal efficiency (NRE) for different hydraulic retention times (HRT) at various media, including W, W+B, W+S, and W+B+S. W represents woodchip bioreactor; B represents biochar; S represents silage leachate. (B) Nitrate removal efficiency (NRE) for different hydraulic retention times (HRT) at various media. Different letters indicate significant differences within media ($p < 0.05$). The error bars are standard deviation.

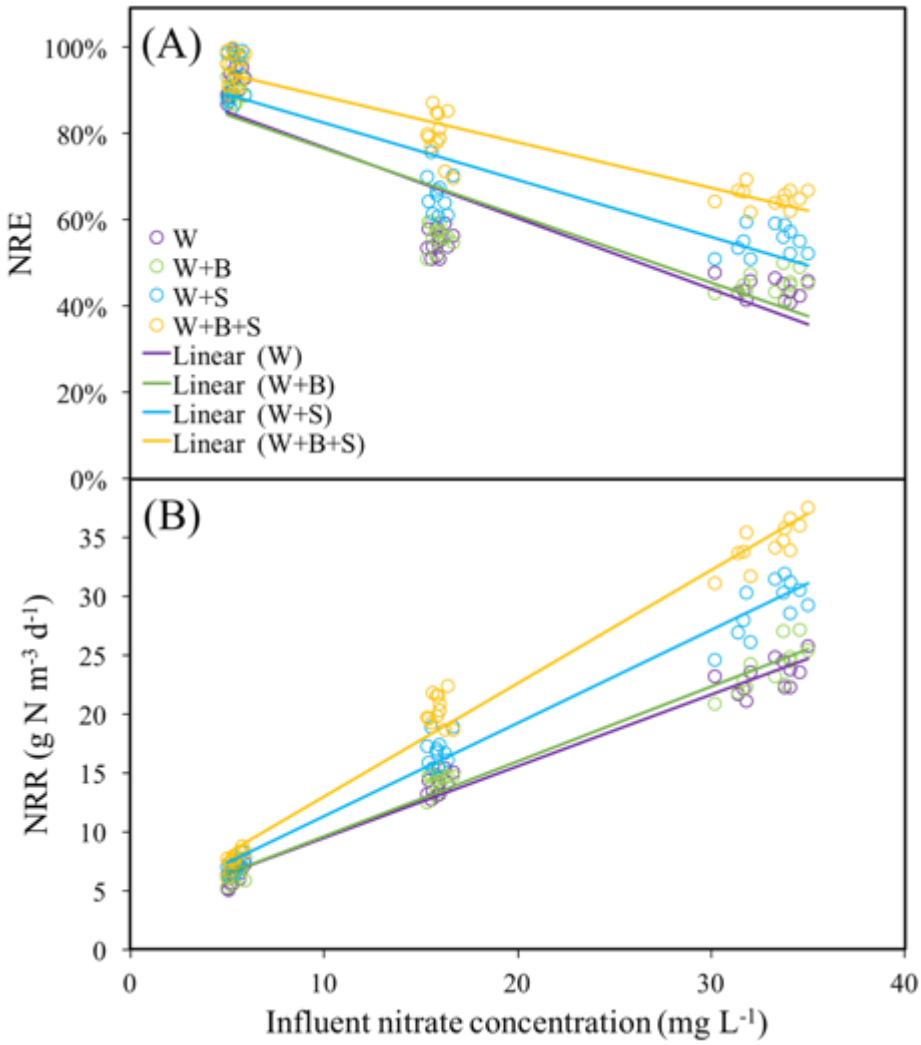

Figure 3.6 (A) Nitrate removal efficiency (NRE) for various media (W, W+B, W+S, W+B+S) changed with influent nitrate concentration at 6h-HRT. (B) Nitrate removal efficiency (NRE) for various media (W, W+B, W+S, W+B+S) changed with influent nitrate concentration at 6h-HRT. W represents woodchip bioreactor; B represents biochar; S represents silage leachate.

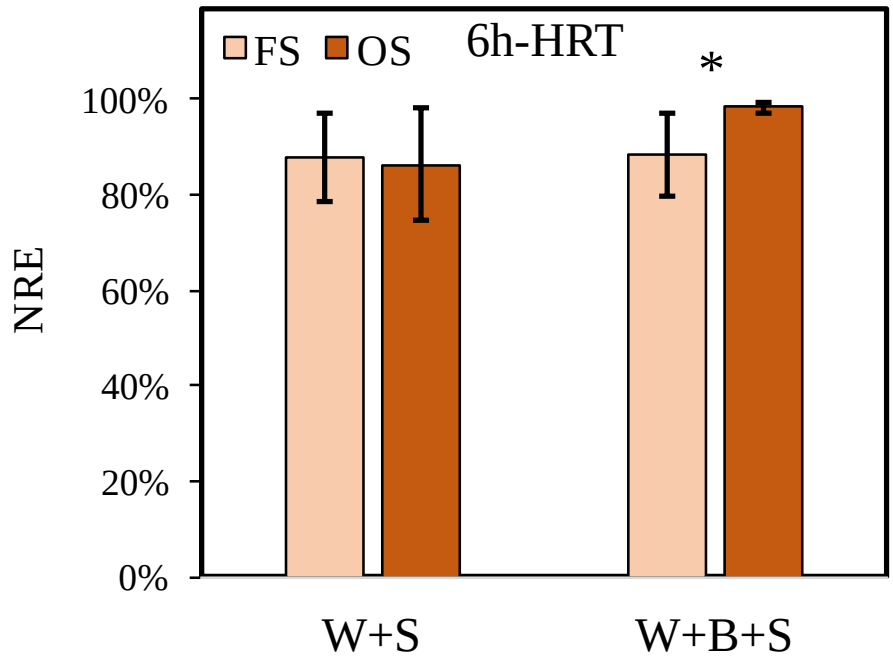

Figure 3.7 The nitrate removal efficiency (NRE) at media of W+S and W+B+S by adding different silage leachate (OS and FS). OS represents old silage leachate; FS represents fresh silage leachate; W represents woodchip; S represents silage leachate; B represents biochar. The error bars are standard deviation. * represents significant difference ($p < 0.05$).

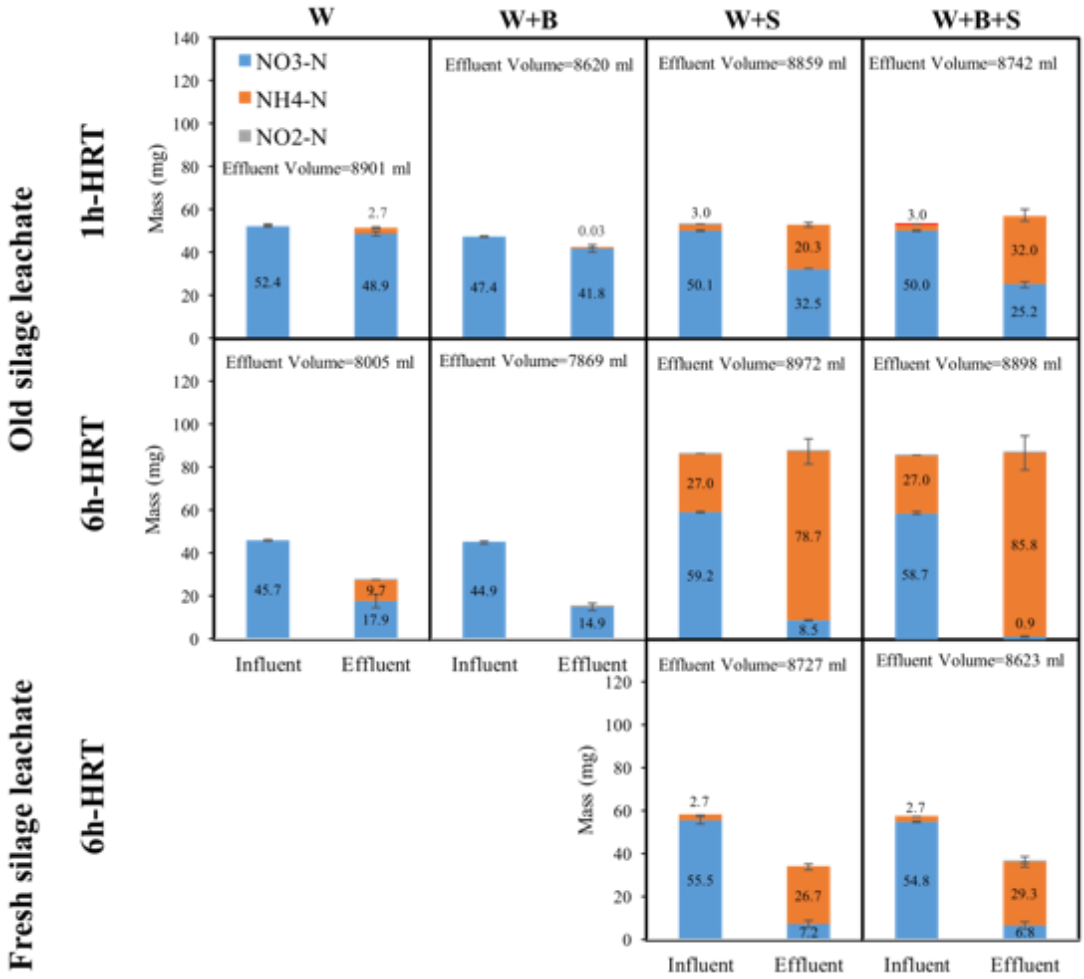

Figure 3.8 The mass of different species of N (NO_3-N, NH_4-N, NO_2-N) in influent and effluent under two hydraulic retention times (HRT, 1 and 6 h) and four different media (W, W+B, W+S, W+B+S). W represents woodchip bioreactor; B represents biochar; S represents silage leachate. Silage leachate was collected from UT dairy farm which is located at East Tennessee AgResearch and Education Center (ETREC) at Little River Animal and Environmental Unit (LRAEU). Fresh silage leachate was collected from the silage bunker when rainfall is occurring, the old silage leachate was collected after five days when rainfall is stopped. Both of the silage leachate addition were diluted into around 400 mg L^{-1} of TOC by deionized water. Influent volume is equal to effluent volume around 8622 ± 381 ml.

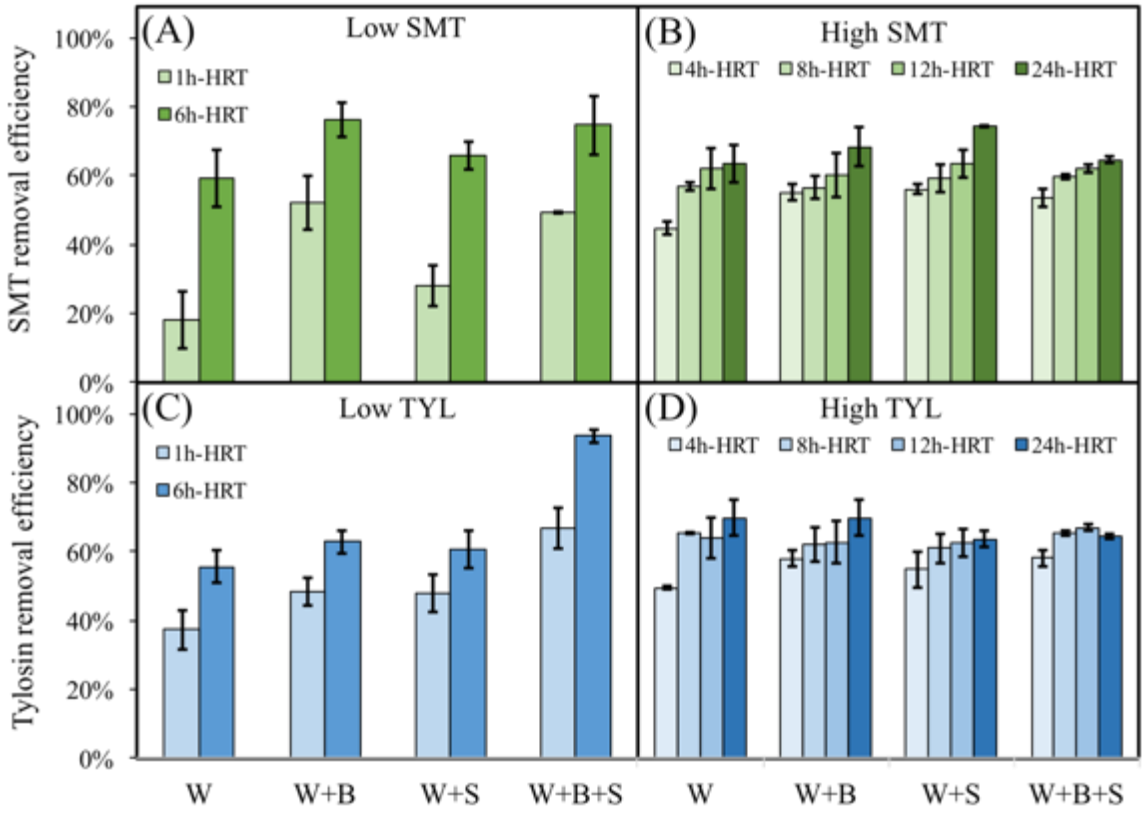

Figure 3.9 (A) Sulfamethazine (SMT) removal efficiency at a low influent concentration (0.34 ± 0.17 mg SMT L^{-1}) under two hydraulic retention times (HRT, 1 and 6 h) and various media (W, W+B, W+S, W+B+S). (B) SMT removal efficiency at a high influent concentration (24.5 mg SMT L^{-1}) under four hydraulic retention times (HRT, 4, 8, 12, 24 h) and various media (W, W+B, W+S, W+B+S). (C) Tylosin (TYL) removal efficiency at a low influent concentration (1.86 ± 0.29 mg TYL L^{-1}) under two hydraulic retention times (HRT, 1 and 6 h) and various media (W, W+B, W+S, W+B+S). (D) TYL removal efficiency at a high influent concentration (25.7 mg TYL L^{-1}) under four hydraulic retention times (HRT, 4, 8, 12, 24 h) and various media (W, W+B, W+S, W+B+S). W represents woodchip bioreactor; B represents biochar; S represents silage leachate.

CHAPTER IV
CHARACTERIZING THE ROLE OF HYDRAULIC RETENTION TIME ON NITRATE REMOVAL IN DENITRIFYING BIOREACTORS

This chapter is based on a manuscript draft by Yuchuan Fan et al.:

A version of this chapter was originally prepared by:

Yuchuan Fan, Jaehoon Lee, Jie Zhuang, Michael Essington, Sindhu Jagadamma, and John Schwartz. Characterizing the role of hydraulic retention time on nitrate removal in denitrifying bioreactors.

My primary contributions to the work include (i) designing and implementing experiments, (ii) developing models, (iii) initial writing of the manuscript, and (iv) revising manuscript and coordinating revisions of the manuscript.

Abstract

The use of inorganic N fertilizers in the agricultural system has adversely impacted human health and the environment. Denitrifying bioreactors (DNBRs) are a cost-effective and sustainable practice commonly used at the edge of the field to remove nitrate from runoff and agriculture. Hydraulic retention time (HRT, hours) is considered to be one of the most important variables for nitrate removal rate (NRR, g N m^{-3} d^{-1}) and nitrate removal efficiency (NRE, %). In this study, nitrate reduction per length of flow path in DNBRs (N_{rd}, mg N L^{-1} m^{-1}) was first defined in order to then characterize the nitrate removal by two developed two nonlinear models; Mitscherlich model (MT) and the Michaelis-Menten model (MM). This study is the first to utilize nonlinear models to relate NRR and NRE to HRT. To verify the models, eight experiments were conducted under different scales (lab and field), media (woodchip, woodchip+biochar, woodchip+silage leachate, woodchip+biochar+silage leachate), and influent nitrate concentration (6.8-70 mg N L^{-1}). The results showed that the MT model had a better performance than the MM model since the MT model produced a lower RMSE and greater R^2 than the MM model. In addition, the MT model could precisely characterize the N_{rd}, NRR, and NRE changes with HRT. With the application of the MT model, the optimal HRT (HRT_O) can be theoretically calculated, which may potentially aid designers and practitioners when designing and operating the denitrifying bioreactors.

Introduction

Excess nitrate in agricultural drainage is an issue experienced frequently across the globe (Padilla et al. 2018; Knoll et al. 2020). To prevent the anthropogenic nitrate flow into water bodies, the denitrifying bioreactor (DNBR) is widely applied in the field. The DNBR intercepts nitrate-contaminated water and converts nitrate into inert nitrogen gas by a biological denitrification process(Schipper et al. 2010). The results of numerous studies indicate that DNBRs can be operated for more than 15 years without maintenance (Schipper et al. 2010; Long et al. 2011).

Previous studies reported significant variability in nitrate removal rate (NRR, g N m^{-3} d^{-1}) and nitrate removal efficiency (NRE, %) for DNBRs, ranging from 0.51 to 166.9 g N m^{-3} d^{-1} (Pluer et al. 2019; von Ahnen et al. 2021) and 6.5 to 99.8% (Coleman et al. 2019). This large variation in NRR and NRE has been attributed to several abiotic factors, such as pH, dissolved organic carbon (DOC), dissolved oxygen (DO), HRT, temperature, media age, effective porosity, and influent nitrate concentration (Citing my Chapter 2). Numerous studies have explored various models to predict nitrate removal as a function of the abiotic factors. In particular, Halaburka et al. (2017) developed a multispecies reactive transport model with Michaelis-Menten kinetics to predict effluent nitrate concentrations in the experimental columns as a function of DO and DOC. Kouanda and Hua (2021) conducted laboratory bioreactors using fresh, composted, and aged woodchips to predict nitrate removal as a function of influent nitrate concentration using the Michaelis-Menten model. Conversely, Nordström and Herbert (2019) used temperature and influent nitrate concentration to estimate effluent nitrate concentration in a woodchip bioreactor using a combination of the Eyring equation and Michaelis-Menten model. Jaynes et al. (2016) used a dual-porosity transport model to simulate the nitrate concentration in a woodchip bioreactor. Ghane et al. (2015) developed a non-Darcy transport model with Michaelis-Menten kinetics to describe nitrate removal as a function of

effective porosity, nitrate concentration, temperature, and bed length. Overall, the aforementioned studies focused primarily on the impact of influent nitrate concentration on nitrate removal, rather than other abiotic factors.

Even though influent nitrate concentration continues to be the most commonly used variable to simulate nitrate removal, other factors that may contribute to nitrate removal have been underestimated. Especially hydraulic retention time (HRT), our recent study indicated that HRT was the most critical abiotic factor for NRR (Fan et al., 2021). Some previous studies have also suggested that HRT is a crucial parameter in the operation of denitrification reactor (von Ahnen et al. 2021). Numerous studies reported the relationship between nitrate removal (NRR and NRE) and HRT. Regarding NRR, some studies indicated that NRR decreased with HRT (Robertson 2010; David et al. 2016; Pluer et al. 2019; Povilaitis and Matikienė 2020) while others reported that NRR increased at first then decreased with HRT (von Ahnen et al. 2021). It is still not clear why the relationship between NRR and HRT may differ under certain conditions. In light of this, some studies focused on quantifying the NRR as a function of HRT through various models. For instance, Robertson (2010) found that the First-order model better fits the NRR response to HRT than the Zero-order model. However, the First-order model is not insufficient to describe how NRR relates to HRT, because studies indicate that NRR does not decrease with HRT in a linear fashion (Povilaitis and Matikienė 2020). Even though it is widely accepted that higher a NRE corresponds to a greater HRT, there is no consensus regarding whether the relationship between NRE and HRT occurs in an exponential (Tangsir et al. 2017; Rivas et al. 2020) or proportional manner (Lepine et al. 2015). Therefore, there are gaps in quantifying the relationship between nitrate removal (NRR and NRE) and HRT.

To develop a reasonable and reliable model to explain the relationship between nitrate removal (NRR and NRE) and HRT, nitrate reduction per bioreactor length (N_{rd}, mg N L^{-1} m^{-1}) was first defined as a dependent variable. This new variable reflects the average reduction in

nitrate concentration per unit length given that many studies reported that influent nitrate concentration typically decreased with distance within the DNBRs, irrespective of whether they were field or laboratory studies (Robertson 2010; Warneke et al. 2011). In addition, N_{rd} can be also used to calculate NRR and NRE with other input parameters (effective porosity, influent nitrate concentration, and bioreactor length). Thus, describing the relationship between N_{rd} and HRT can be an alternative approach to understand the relationship between nitrate removal (NRR and NRE) and HRT.

To describe how N_{rd} changes with HRT, we investigated a series of common nonlinear models, including Michaelis-Menten (Michaelis and Menten 1913), Mitsscherlich (Mitscherlich 1919), Gompertz (Gompertz 1825), Logistic (Verhulst 1838), Bertalanffy (Von 1957), Richards (Richards 1959), and Korf models (Kivisite 1988). In this study, we adopted the Michaelis-Menten (MM) and Mitscherlich (MT) models to describe the relationship between N_{rd} and HRT because the main characteristics of the N_{rd} response curve, which are the convex shape and with an upper limit. Laboratory and field studies were conducted under various environmental conditions with different influent nitrate concentrations, filling materials, bioreactor types, and experimental scales to evaluate the two nonlinear models. We did not consider woodchip variety (Cameron and Schipper 2010), age (Robertson 2010), and particle size (Van Driel et al. 2006; Cameron and Schipper 2010) since these parameters have already been shown to have no significant effect on nitrate removal rate after the early stages of the DNBR operation. The primary objectives of this study were: (1) to develop nonlinear models to explore the relationship between nitrate removal indicators (NRR and NRE) and HRT, and (2) to determine the optimal HRT and evaluate the performance of the models. The results will allow for a prediction of nitrate removal as a function of HRT and provide insight into optimal HRT (HRT_O) which may in turn aid researchers and practitioners in improving the performance of DNBR.

Materials and Methods

Experimental setup

Twelve laboratory bioreactors (B1) were designed to fill four different filling materials, including woodchips only (W) and W amended with (10% v/v) biochar (W+B), silage leachate (W+S), and biochar and silage leachate (W+B+S). 10% (v/v) biochar was filled in the middle of the bioreactor with the aid of a filter stand (Width=3 cm) and placed in direct contact with the woodchip (Table 1). A 2 cm deep covering of coarse sand (diameter<0.5 cm) was added to the surface of the woodchip to prevent the woodchip floating. As for the filling materials, the woodchips came from the campus mulch. The biochar was obtained from a local company (Proton Power, Inc.). The silage leachate was collected from the UT dairy farm located at the East Tennessee AgResearch and Education Center (ETREC) at Little River Animal and Environmental Unit (LRAEU). The details of the laboratory bioreactors, biochar, and silage leachate are described in Chapter 3.

Three PVC columns (B2), each with a length of 90 cm and an internal diameter of 10 cm, were used to construct horizontal bioreactors (Fig. 1). The total volume of the column is 7 L and is filled only with woodchip (Sugar maple, *Acer saccharum*) obtained from the University of Tennessee at Knoxville. The size of the woodchip ranged from 1 to 6 cm. 2.7 kg woodchip was compacted into the column. The top inlet hose was connected with a peristaltic pump (FH100M, Fisher Inc, USA) and the outflow hose connected with a collecting bucket. A prepared solution was pumped to the column at flow rates of 66.7, 33.3, 16.7, 11.1, 8.3, 5.6, 3.7, and 2.8 ml min^{-1}. Tap water was added to each column to soak the woodchip for 48 h before determining the pore volume (4025±141 ml) and porosity of each bioreactor. Drainable porosity (ρ_e) was determined after draining each bioreactor for one hour (Kouanda and Hua 2021), and the resulting porosities were 56.9, 56.7, and 53.6%, respectively.

Two field-scale bioreactors were constructed at East Tennessee AgResearch and Education Center (ETREC) at Little River Animal and Environmental Unit (LRAEU) (35°46'14.0"N 83°50'44.9"W). The field barriers used a mixture of sawdust (95%) and sand & soil (5% in volume). The bottom and side of the reactive barriers were lined with commercial-grade geosynthetics to prevent groundwater intrusion. The reactive barriers are 1.5 m deep, 2.74 m wide, and 4.5 m long and receive a discharge from the cropped field in the Unit. The surface of the barriers is covered with a mixture of gravel and soil to hold the fill material in place. There were a total of 12 monitoring wells with different depths (Deep: 1.1 m; Medium: 0.6 m; Low: 0.3 m) in the barrier to collect water samples. Temperature sensors were attached to the monitoring wells (Fig. 1). The inflow water was provided by submersible pumps which were installed at the bottom of a wetland with a maximum flow rate of 10 gallons per minute. Given that the flow rate is affected by clogging of the aquatic plants, a wide range of HRT occurred, ranging from 2 to 50 hours. One of the auto-samplers (ISCO, Teledyne Inc, USA) was placed in front of the two field bioreactors while the other two were placed after the two bioreactors. Following collection, the water was filtered through a 0.22-μm membrane filter. 2 mL of filtered samples were injected into vials and stored in the refrigerator at 4 ℃ before measuring NO_3-N (San, Skalar Inc, Dutch).

In addition to the laboratory and field experiments, published data was obtained from Easton et al. (2015) and Pluer et al. (2016) to test the models. The details of the two experiments are reported in Table 1.

Calculate nitrate removal rate and maximum nitrate removal rate by hydraulic retention time

Many studies have reported that the NRR (g m^{-3} d^{-1}) can be calculated using the following equation (Rivas et al. 2020):

$$\mathrm{NRR} = \frac{V_T(N_{in}-N_{out})}{V_{WB}\times t} \quad (1)$$

where C_{rd} represents the nitrate reduction (mg L^{-1}); V_t the amount of water (L); V_{WB} the total volume of the denitrifying bioreactor(m^3); and t the hydraulic retention time (d^{-1}).

To calculate NRR as a function of HRT, we replaced V_t, t, and V_{WB} in Eq. (1) as follows (Povilaitis and Matikienė 2020):

$$\boldsymbol{f} = \frac{\boldsymbol{V_t}}{\boldsymbol{t}} \quad (2)$$

$$\mathbf{V_{WB}} = \frac{\boldsymbol{PV}}{\boldsymbol{\rho_e}} \quad (3)$$

$$\mathrm{HRT} = 24 \cdot 1000 \cdot \frac{PV}{f} \quad (4)$$

where HRT represents the hydraulic retention time (hours); f the flow rate (L d^{-1}); PV the pore volume of the denitrifying bioreactor (m^3); and ρ_e the effective porosity of denitrifying bioreactor. Substituting Eqs (2), (3), and (4) into Eq (1),

$$\mathrm{NRR} = \frac{24\cdot(N_{in}-N_{out})\cdot\rho_e}{HRT} \quad (5)$$

To calculate the theoretical maximum nitrate removal rate (NRR_{TM}, g N m^{-3} d^{-1}), we assumed the nitrate was totally removed within the bioreactor. Thus, N_{out} = 0 and,

$$\mathrm{NRR_{TM}} = \frac{24\cdot N_{in}\cdot\rho_e}{HRT} \quad (6)$$

Nitrate reduction per length

We calculated NRR as a function of HRT using Eq. (5), indicating that NRR is determined by N_{in}, N_{out}, and ρ_e. Among these parameters, ρ_e is always constant for a specific

DNBR, while N_{out} is dependent on many factors, and one of the controlling factors is the length of the DNBR. In most studies, the flow in DNBR is treated as plug flow (Ghane et al. 2019), and nitrate removal will change along the length of the DNBR (Ghane et al. 2015). To exclude the influence of the length of the bioreactor, here we normalized (N_{in} - N_{out}) by the length of the bioreactor and define this new indicator (N_{rd}) as:

$$\mathrm{N_{rd}} = \frac{N_{in}-N_{out}}{L_B} \tag{7}$$

where L_B represents the length of the denitrifying bioreactor (m). This index can reflect the ability of the DNBR to reduce nitrate reduction per meter. To consider this index, we substituted Eq (7) into Eq (5),

$$\mathrm{NRR} = \frac{24 \cdot N_{rd} \cdot L_B \cdot \rho_e}{HRT} \tag{8}$$

Therefore, according to the above conversion, the NRR can be calculated with N_{rd}, L_B, ρ_e, and HRT.

Developing a model to characterize N_{rd} by HRT

Characterizing N_{rd} by the Michaelis-Menten (MM) model:

$$\mathrm{N_{rd-MM}} = \frac{N_{max-MM} \cdot HRT}{k+HRT} \tag{9}$$

where $N_{max\text{-}MM}$ represents the maximum N_{rd}, *y*-intercept is zero; when *x* value is *k*, the *y* value is half of $N_{max\text{-}MM}$.

Characterizing N_{rd} with the Mitscherlich (ML) model:

$$\mathrm{N_{rd-MT}} = N_{max-MT}(1 - ae^{-bHRT}) \tag{10}$$

where $N_{max\text{-}MT}$ represents the maximum N_{rd}, when a>1, the *x*-intercept is positive when 0<a<1, the *x*-intercept is negative.

Both of the two nonlinear models predict N_{rd} increases with HRT. The nonlinear models have a similar trend, as well as with an asymptote (maximum N_{rd}). Conversely, the significant difference is that starting point of the MM model is (0,0) while the ML model is (*ln*a/b, 0).

Developing a model to characterize NRR by HRT

To characterize how NRR changes with HRT, the Michaelis-Menten and Mitscherlich models were developed by substituting Eq (9) and Eq (10) into Eq (8), respectively:

$$\mathrm{NRR_{MM}} = \frac{24 \cdot N_{max-MM} \cdot L_B \cdot \rho_e}{(k+HRT)} \tag{11}$$

$$\mathrm{NRR_{MT}} = \frac{24 \cdot N_{max-MT} \cdot (1-ae^{-bHRT}) L_B \cdot \rho_e}{HRT} \tag{12}$$

To determine how NRR changed with HRT in the NRR-MM model, we took the derivative of $\mathrm{NRR_{MM}}$:

$$\mathrm{NRR'_{MM}} = -\frac{24 \cdot N_{max-MM} \cdot L_B \cdot \rho_e}{(k+HRT)^2} < 0 \tag{13}$$

which shows that $\mathrm{NRR_{MM}}$ decreases with increasing HRT and the parameter *k*.

To determine how NRR changed with HRT in the NRR-MT model, we took the derivative of $\mathrm{NRR_{MT}}$:

$$\mathrm{NRR'_{MT}} = \frac{24 \cdot N_{max-MT} (abHRT+a-e^{bHRT}) e^{-bHRT}}{HRT^2} \tag{14}$$

In Eq (14), $N_{max\text{-}MT}$, e^{-bHRT}, and HRT^2 are all above zero. Thus, the negative or positive value of NRR'_{Mit} is determined by ($abHRT$+a-e^{bHRT}). Therefore, we defined this part as follows:

$$f(HRT) = abHRT + a - e^{bHRT} \tag{15}$$

To determine the positive or negative value of f(HRT), we took the derivative of f(HRT):

$$f'(HRT) = b(a - e^{bHRT}) \tag{16}$$

The value of f' (HRT) is evaluated as follows:

$$\begin{cases} f'(HRT) > 0, \ HRT < \frac{lna}{b} \\ f'(HRT) = 0, \ HRT = \frac{lna}{b} \\ f'(HRT) < 0, \ HRT > \frac{lna}{b} \end{cases} \tag{17}$$

So when HRT=(lna)/b,

$$f_{max}(HRT) = alna \tag{18}$$

The value of $f_{\max}(HRT)$ is evaluated as follows:

$$\begin{cases} f_{max}(HRT) \le 0, 0 < a \le 1 \\ f_{max}(\mathrm{HRT}) > 0, \quad a > 1 \end{cases} \tag{19}$$

When $0<a\le1$, $f_{max}(HRT)\le0$, so $NRR'_{MT}<0$, NRR_{MT} decreases with HRT.

When $a>1$, $f_{max}(HRT)>0$, so $NRR'_{MT}>0$, a turning point exists when NRR_{MT} changes with HRT. Hence, this turning point corresponds to the optimal HRT (HRT_O) and the maximum NRR (NRR_{max}). The lambert W function (also known as the omega function or product logarithm) was used to solve the analytical solution of $f(HRT_O)=0$, namely of the inverse relation of the function $f(w)=we^w$. Converting $f(HRT_O)=0$ into the format of $f(w)=we^w$, HRT_O can be solved by the lambert function as demonstrated by the following equations (Corless et al. 1996):

$$\begin{cases} HRT_{O_1} = \frac{-1-W_0(-\frac{1}{ae})}{b}, & -\frac{1}{b} < HRT_{O_1} < 0 \\ HRT_{O_2} = \frac{-1-W_{-1}(-\frac{1}{ae})}{b}, & HRT_{O_2} > 0 \end{cases} \tag{20}$$

where W_0 represents the upper branch of the lambert W function ($y>-1$); W_{-1} represents the lower branch of the lambert W function ($y<-1$). HRT_{O1} and HRT_{O2} represent the first and second analytical solutions of the HRT_O. Note that HRT can only be predicted using HRT_{O2} because it is a positive number. The NRR_{MT} that corresponds to HRT_O ($NRR_{max\text{-}MT}$) is:

$$\mathrm{NRR}_{\mathrm{max-MT}} = \frac{24 \cdot N_{max-MT} \cdot b \cdot L_B \cdot \rho_e \cdot (1-ae-b^{-1-w_{-1}(-\frac{1}{ae})})}{[-1-w_{-1}(-\frac{1}{ae})]} \tag{21}$$

Developing a model to characterize NRE by HRT

NRE values can be calculated by the following equations (Liu et al. 2015),

$$\mathrm{NRE} = \frac{N_{\mathrm{in}}-N_{\mathrm{out}}}{N_{in}} \tag{22}$$

where NRE_{MM} represents the NRE values predicted by the MM model; NRE_{MT} represents the NRE values predicted by the MT model.

To characterize how NRE changes with HRT, the Michaelis-Menten model and Mitscherlich model were developed by substituting Eq (9) and Eq (7) into Eq (22), and substituting Eq. (10) and Eq (7) into Eq. (22),.

$$\mathrm{NRE_{MM}} = \frac{N_{max-MM} \cdot HRT \cdot L_B}{N_{in}(k+HRT)} \quad (23)$$

$$\mathrm{NRE_{MT}} = \frac{N_{max-MT}(1-ae^{-bHRT})L_B}{N_{in}} \quad (24)$$

Model evaluation and parameter estimation

The root-mean-squared error (RMSE) and coefficient of determination (R^2) were used to evaluate the performance of each model. RMSE and R^2 were calculated as follows:

$$\mathrm{RMSE} = \sqrt{\sum_{i=1}^{n} \frac{(y_i - x_i)^2}{n}} \quad (25)$$

$$\mathrm{R^2} = 1 - \frac{\sum_{i=1}^{n}(y_i - x_i)^2}{\sum_{i=1}^{n}(y_i - \bar{y}_i)^2} \quad (26)$$

where y_i is the simulated NRE, x_i is the actual NRE, and n is the measured number.

Parameter estimation was performed using the least-square method of the Excel solver function. In addition, the correlation between the measured parameters and those predicted by the MT and MM models was evaluated by the Pearson correlation coefficient, which and was computed using Origin software (2020, OriginLab Inc, USA).

HRT_O and $HRT_{90\%}$ were adopted to represent the optimal HRT according to the MT model; HRT_O was calculated by Eq. (20) and $HRT_{90\%}$ was the HRT at which 90% of the nitrate was removed.

Results and discussion

N_{rd} changes with HRT

Nitrate reduction per length (N_{rd}) was first evaluated in this study. Fig. 3 shows that N_{rd} changes with HRT as a function of media (W, W+B, W+S, and W+B+S), influent nitrate concentrations (5.4±0.3, 15.9±0.4, and 33±1.5 mg N L^{-1}), and scales (lab-, field-scale). N_{rd} was found to increase with HRT, and this upward curve was associated with media and influent nitrate concentration. For instance, as shown in Fig. 3a-d, the treatment of W+S and W+B+S

presented a maximum N_{rd} when HRT was approximately 4 h and 2 h, while W and W+B showed a greater HRT at 12 h. This implies that the nitrate removal performance of W+S and W+B+S was better than W and W+B. Moreover, there was no significant difference in the maximum N_{rd} of 26 mg N L^{-1} m^{-1} across the four media, which was mainly constrained by the influent nitrate concentration at 6.8 mg N L^{-1}, rather than the HRT (Fig. 3a-d). As for the laboratory columns which utilized the media of W under LN (Fig. 3e), N_{rd} quickly increased to the maximum value of 7.7 mg N L^{-1} m^{-1} after 4h-HRT. Regarding MN and HN (Fig. 3f and 3g), N_{rd} rose from 2.5 to 24.1 mg N L^{-1} m^{-1}, and 3.6 to 56.2 mg N L^{-1} m^{-1}, respectively. In addition to the difference in maximum N_{rd}, the increasing rate of N_{rd} decreased from LN to HN. In contrast, field bioreactors showed a low N_{rd} in the range 0-2 mg N L^{-1} m^{-1} (Fig. 3h). N_{rd} data obtained from Easton et al. (2015) and Pluer et al. (2016) are presented in Fig. 3i and 3j. The curve in Fig. 3i was similar to Fig. 3a, which both showed N_{rd} increasing with HRT as a parabolic growth. In contrast, Fig. 3j showed N_{rd} increasing with HRT in a linear fashion, but this was probably due to the limited HRT (2-12 h) that cannot predict an upper limit of N_{rd}.

All of the HRT-induced changes in N_{rd} were fitted with the MM and MT models. The results indicated that the N_{rd} changed with HRT and this can be characterized by the MM and MT models under different media, influent nitrate concentrations, and scales (R^2>0.702). The other reference data also indicated that HRT-induced changes in N_{rd} can be characterized rather well using the MM and MT models (R^2>0.933).

NRE changes with HRT

As presented in Fig. 4, all figures showed that NRE increased with HRT, with the exception of Fig. 4j. Regarding different media (W, W+B, W+S, and W+B+S), NRE changed with HRT in different manners. W+B+S showed a greater initial NRE (79.9%) than W (37.6%), W+B (37.6%), and W+S (70.9%). Table 4 highlights that the N_{max} calculated from the MT ($N_{max\text{-}MT}$) and MM ($N_{max\text{-}MM}$) models showed no difference among the media. On the

other hand, the MT model predicts differences in $HRT_{90\%}$, which were 3.78, 3.29, 1.46, and 0.8 for W, W+B, W+S, and W+B+S. Similar results were also observed using the MM model (Table 5). Further, the increasing rate of increase in NRE observed with increasing HRT decreased with increasing influent nitrate concentration. Also, the NRE values were decreased with increasing N, although the nitrate removal amount increased with increasing N (Fig. 4h). Similarly, the $HRT_{90\%}$ increased from 2.07 to 30.49 when influent nitrate concentration increased from 6.9 to 70 mg N L^{-1}. In support of these findings, Easton et al. (2015) showed that NRE increased with HRT, which was also similar to the lab-scale results. However, Pluer et al. (2016) showed that NRE fluctuated with HRT, which was probably due to the large variation of influent nitrate concentration.

The MT and MM models could fit the actual NRE as a function of HRT (R^2>0.933). In most cases, we found that the MT model produced a greater R^2 than the MM model (Fig. 4a-j). However, we found that the values of the fitted parameters presented a significant difference between the NRE and NRR models. For example, discrepancies in $N_{max\text{-}MM}$ and *k* were observed between NRE and NRR data in Pluer et al. (2016) (Table 3). This could be explained by the HRTs being in the range of 2 to 12 h, which presented a linear relationship between N_{rd} and HRT. This resulted in significant uncertainty given that there was no upper limit in N_{max}.

NRR changes with HRT

Fig. 5 shows that NRR changed with HRT as a function of media, influent nitrate concentration, and scales. In most cases, NRR rapidly decreased with increasing HRT, followed by a slow decrease with further increases in HRT. In addition, it was found that the degree of NRR decrease was associated with media, influent nitrate concentration, and scales. W+B+S presented a greater initial NRR (95.7 g N m^{-3} d^{-1}) than W (75.1 g N m^{-3} d^{-1}), W+B

(50.8 g N m^{-3} d^{-1}), and W+S (48.6 g N m^{-3} d^{-1}). Surprisingly, LN showed a greater NRR than MN and HN when HRT was 1 h (Fig. 5e-g). We suspect that the high nitrate loading at low HRT would inhibit the denitrification process. Previous studies have reported that a large N_{in} will affect the denitrification process (Blackmer and Bremner 1978; Damaraju et al. 2015). In addition, it was found that adding influent nitrate concentration would change the relationship between NRR and HRT. As such, Fig. 5g shows that NRR increased with HRT in the range 1 to 4 h, then decreased with HRT. HRT_O was predicted to be 2.73 and this is reported in Table 4. In addition, the field experiment also highlighted that the turning point in NRR (Fig. 5h), as shown in Table 4, was 9.76 h. Easton et al. (2015) and Pluer et al. (2016) reported that NRR decreased with HRT, which was similar to the lab-scale results.

The MM model predicted the NRR changes associated with HRT very well, except for two cases. The first was the condition using woodchip as media with HN (33±1.5 mg N L^{-1}) (Fig. 5g), while the other was at the field bioreactor (Fig. 5h). Conversely, the MT model was able to show a turning point that corresponded with higher R^2 values than those obtained with the MM model in these two particular cases. As such, it indicated that the MT model performs better than the MM model in predicting NRR as a function of HRT. Furthermore, we also found that the variation in NRR was significantly higher in the field experiments relative to the laboratory experiments (Fig. 5h), and the temperature variability was probably the reason for a lower R^2 for field experiments.

NRR_{TM} changes with HRT

Fig. 6 shows that the theoretical maximum nitrate removal rate (NRR_{TM}) decreases with HRT under different influent nitrate concentration (N_{in}) and effective porosity (ρ_e). This is an ideal condition where the nitrate is assumed to be removed entirely in a denitrifying bioreactor. The curve shifted from the left to the right position when N_{in} and ρ_e were increasing, indicating that the value of NRR_{TM} was increasing.

We suspect that if the nitrate is completely removed, the actual NRR would be closer to NRR_{TM}, which leads to the dynamic change of NRR being closer to a downward curve than NRR_{TM}. That is, NRR will decrease with the increase of HRT. Therefore, this theory might explain why the relationship between NRR and HRT has been primarily reported as a downward trend (Robertson 2010; David et al. 2016; Pluer et al. 2019; Povilaitis and Matikienė 2020). It may also be used to explain some opposite examples, such as the upward trend that occurred (von Ahnen et al. 2021), which was probably due to the NRR being lower than the NRR_{TM}. The low NRRs may be due to the lower HRT and higher nitrate concentrations in influent, as indicated in Fig. 5g.

Model evaluation, parameter estimation, and correlation

Fig. 7 summarizes all the RMSE and R^2 values obtained for predicting NRR and NRE. The MT model presented a significantly lower RMSE ($p < 0.05$) and a relatively greater R^2 than the MM model in characterizing NRR and NRE. Overall, these results suggest that the MT model will perform better than the MM model.

Tables 3 and 4 summarize all of the model parameters, including $N_{max\text{-}MT}$, $N_{max\text{-}MM}$, HRT_O, $HRT_{90\%}$, *a*, *b*, and *k* under different scales, media, and N loading. Fig. 8 shows the correlation among these parameters. For the MT model, the shape parameters *a* and *b* were not observed to be correlated with the other parameters (Fig. 8a). This observation was also similar in the NRE model (Fig. 8b), which implies that parameters *a* and *b* are independent. In the MM model, a significant relationship was observed between parameter *k* and $N_{max\text{-}MM}$ ($p < 0.05$) in NRR and NRE (Fig. 8a and 8b). As expected, the parameters N_{in}, $N_{max\text{-}MT}$, and $N_{max\text{-}MM}$ were significantly correlated with each other ($r>0.96$, $p<0.05$) (Fig. 8a and 8b). Indeed, N_{max} is one of the essential parameters considered by both the MT and MM models. In comparison, the value of N_{max} obtained from the MT and MM models differed, as $N_{max\text{-}MM}$ was significantly greater than $N_{max\text{-}MT}$ (Fig. 8c). In addition, we found that $N_{max\text{-}MT}$ was highly correlated

(R^2=0.985) with N_{in}. The linear regression coefficient was 1.02, which indicates that the N_{max-MT} values were almost equal to N_{in} (Fig. 8d). Similarly, N_{max-MM} was also highly correlated (R^2=0.905) with N_{in}, but N_{max-MM} was greater than N_{in} (Fig. 8e). These results indicate that the value of N_{max} was associated with N_{in}.

Overall, this study successfully developed nonlinear models to describe the relationship between nitrate removal (NRR and NRE) and HRT through an intermediate variable, nitrate reduction per bioreactor length (N_{rd}). The results indicate that the MT model performs better than the MM model, especially for predicting NRR. In particular, the MT model was able to show that NRR changed with HRT under two different conditions: (1) NRR decreased with HRT exponentially; (2) or NRR increased with HRT initially, but then decreased with HRT exponentially. Unfortunately, the MM model was only able to satisfy the first condition.

Model application and limitations

The MT model is not only able to characterize NRR and NRE changes on the basis of HRT, but it also provides an approach to predict the optimal HRT (HRT_O). The minimum prerequisites to estimate the HRT_O are: (1) The DNBR experiment was operated under different HRTs; and (2) the influent nitrate concentration and temperature do not undergo significant variation. Moreover, if the experiment was conducted under a wide range of HRTs, the N_{rd} will benefit from obtaining accurate parameters. After the parameters were obtained, they can be used to judge whether the HRT_O exists, as mentioned previously in the Materials and Methods (Eq. (19)), when $0<a\leq1$, it indicates that the theoretical HRTo should be close to zero. Indeed, HRT_O cannot be zero under the actual operation of a denitrifying bioreactor. In this situation, we assume that the hydraulic gradient and hydraulic conductivity will determine the minimum HRT_O. For example, von Ahnen et al. (2021) operated a denitrifying bioreactor at different HRTs (1.82, 3.64, 5.46, and 7.28 h), and the reported HRT_O was 1.82. Therefore, the smaller

the HRT, the greater the NRR. Furthermore, when a>1, it indicates that the HRT_O exists. Meanwhile, HRT_O can be calculated by Eq. (20), and the corresponding maximum HRT can be calculated by Eq. (21). As shown in Fig. 9, HRT_O was determined by shape parameters a and b. Specifically, HRT_O increased with parameter a and decreased with parameter b. In addition, we found that parameters a and b had an interaction with HRT_O. When the value for parameter b was at low, HRT_O increased with parameter a rapidly, and vice versa. When the value for parameter a was high, HRT_O increased with parameter b rapidly, and vice versa.

Even though the two nonlinear models considered many abiotic factors, the temperature was not considered in this study. It is well known that denitrification is a biological process that is affected by temperature (Hassanpour et al. 2017; Nordström and Herbert 2019). Many of models have considered the temperature sensitivity by an index Q_{10} (Vacková et al. 2011; Nordström and Herbert 2019), the relative change in reaction rate by a 10°C change in temperature. Therefore, further studies are required to assess the influence of temperature on the the model and verify its potentiality in field experiments.

Conclusions

This study aimed to characterize the role of hydraulic retention time on nitrate removal by performing eight experiments which were conducted under different scales (lab and field), media (woodchip, woodchip+biochar, woodchip+silage leachate, woodchip+biochar+silage leachate), and influent nitrate concentration (6.8-70 mg N L^{-1}).

Nitrate reduction per length (N_{rd}) was firstly defined and was shown to be an excellent indicator to describe nitrate removal. Two nonlinear models were developed to characterize the N_{rd}, nitrate removal efficiency (NRE), nitrate removal rate (NRR), and theoretical maximum NRR (NRR_{TM}) as a function of HRT: the Mitscherlich model (MT) and the

Michaelis-Menten model (MM). The results showed that N_{rd}, NRR, and NRE could be well fitted by the MT and MM models. In contrast, the MT model produced a lower RMSE and higher R^2 than the MM model, which indicates that MT performed better than the MM model. In addition, these results indicate that the relationship between NRR and HRT is associated with media, influent nitrate concentration, and scales. The MT model revealed that this change in relationship between NRR and HRT could be determined by fitted shape parameter *a*, which may be larger or smaller than 1. Further, the optimal HRT (HRT_O) can be predicted by shape parameters *a* and *b* from the MT model, which is informative for users of denitrifying bioreactors (DNBRs) when aiming to optimize the nitrate removal performance. Overall, this study provides a powerful tool to quantitatively characterize nitrate removal on the basis of changes in HRT.

References

Blackmer A, Bremner J. 1978. Inhibitory effect of nitrate on reduction of N2O to N2 by soil microorganisms[J]. Soil Biology and Biochemistry, 10(3): 187-191.

Cameron S G, Schipper L A. 2010. Nitrate removal and hydraulic performance of organic carbon for use in denitrification beds[J]. Ecological Engineering, 36(11): 1588-1595.

Coleman B S L, Easton Z M, Bock E M. 2019. Biochar fails to enhance nutrient removal in woodchip bioreactor columns following saturation[J]. Journal of Environmental Management, 232: 490-498.

Corless R M, Gonnet G H, Hare D E, et al. 1996. On the LambertW function[J]. Advances in Computational mathematics, 5(1): 329-359.

Damaraju S, Singh U K, Sreekanth D, et al. 2015. Denitrification in biofilm configured horizontal flow woodchip bioreactor: effect of hydraulic retention time and biomass growth[J]. Ecohydrology & Hydrobiology, 15(1): 39-48.

David M B, Gentry L E, Cooke R A, et al. 2016. Temperature and Substrate Control Woodchip Bioreactor Performance in Reducing Tile Nitrate Loads in East-Central Illinois[J]. Journal of Environmental Quality, 45(3): 822-829.

Easton Z M, Rogers M, Davis M, et al. 2015. Mitigation of sulfate reduction and nitrous oxide emission in denitrifying environments with amorphous iron oxide and biochar[J]. Ecological Engineering, 82: 605-613.

Ghane E, Fausey N R, Brown L C. 2015. Modeling nitrate removal in a denitrification bed[J]. Water Research, 71: 294-305.

Ghane E, Feyereisen G W, Rosen C J. 2019. Efficacy of bromide tracers for evaluating the hydraulics of denitrification beds treating agricultural drainage water[J]. Journal of Hydrology, 574: 129-137.

Gompertz B. 1825. On the Nature of the Function Expressive of the Law of Human Mortality, and on a New Mode of Determining the Value of Life Contingencies[J]. Philosophical Transactions of the Royal Society of London, 115(2): 513-583.

Halaburka B J, LeFevre G H, Luthy R G. 2017. Evaluation of Mechanistic Models for Nitrate Removal in Woodchip Bioreactors[J]. Environmental Science & Technology, 51(9): 5156-5164.

Hassanpour B, Giri S, Pluer W T, et al. 2017. Seasonal performance of denitrifying bioreactors in the Northeastern United States: Field trials[J]. Journal of Environmental Management, 202: 242-253.

Jaynes D B, Moorman T B, Parkin T B, et al. 2016. Simulating Woodchip Bioreactor Performance Using a Dual-Porosity Model[J]. Journal of Environmental Quality, 45(3): 830-838.

Kivisite A K. 1988. Mathematical functions of forest growth.[J]. Estonian Agricultural Academy: 108.

Knoll L, Breuer L, Bach M. 2020. Nation-wide estimation of groundwater redox conditions and nitrate concentrations through machine learning[J]. Environmental Research Letters.

Kouanda A, Hua G. 2021. Determination of Nitrate Removal Kinetics Model Parameters in Woodchip Bioreactors[J]. Water Research: 116974.

Lepine C, Christianson L, Sharrer K, et al. 2015. Optimizing hydraulic retention times in denitrifying woodchip bioreactors treating recirculating aquaculture system wastewater[J]. Journal of Environmental Quality, 45(3): 813-821.

Liu F, Wang Y, Xiao R, et al. 2015. Influence of substrates on nutrient removal performance of organic channel barriers in drainage ditches[J]. Journal of Hydrology, 527: 380-386.

Long L M, Schipper L A, Bruesewitz D A. 2011. Long-term nitrate removal in a denitrification wall[J]. Agriculture Ecosystems & Environment, 140(3-4): 514-520.
Michaelis L, Menten M L. 1913. Die kinetik der invertinwirkung[J]. Biochem. z, 49(333-369): 352.
Mitscherlich E A. 1919. Problems of plant growth[J]. Landwirtschaftliche jahrbucher, 53:: 167~182.
Nordström A, Herbert R B. 2019. Identification of the temporal control on nitrate removal rate variability in a denitrifying woodchip bioreactor[J]. Ecological Engineering, 127: 88-95.
Padilla F M, Gallardo M, Manzano-Agugliaro F. 2018. Global trends in nitrate leaching research in the 1960–2017 period[J]. Science of The Total Environment, 643: 400-413.
Pluer W T, Geohring L D, Steenhuis T S, et al. 2016. Controls influencing the treatment of excess agricultural nitrate with denitrifying bioreactors[J]. Journal of Environmental Quality, 45(3): 772-778.
Pluer W T, Morris C K, Walter M T, et al. 2019. Denitrifying bioreactor response during storm events[J]. Agricultural Water Management, 213: 1109-1115.
Povilaitis A, Matikienė J. 2020. Nitrate removal from tile drainage water: The performance of denitrifying woodchip bioreactors amended with activated carbon and flaxseed cake[J]. Agricultural Water Management, 229: 105937.
Richards F J. 1959. A FLEXIBLE GROWTH FUNCTION FOR EMPIRICAL USE[J]. Journal of Experimental Botany, 10(29): 290-300.
Rivas A, Barkle G, Stenger R, et al. 2020. Nitrate removal and secondary effects of a woodchip bioreactor for the treatment of subsurface drainage with dynamic flows under pastoral agriculture[J]. Ecological Engineering, 148: 105786.
Robertson W D. 2010. Nitrate removal rates in woodchip media of varying age[J]. Ecological Engineering, 36(11): 1581-1587.
Schipper L A, Robertson W D, Gold A J, et al. 2010. Denitrifying bioreactors—An approach for reducing nitrate loads to receiving waters[J]. Ecological Engineering, 36(11): 1532-1543.
Tangsir S, Moazed H, Naseri A A, et al. 2017. Investigation on the performance of sugarcane bagasse as a new carbon source in two hydraulic dimensions of denitrification beds[J]. Journal of Cleaner Production, 140: 1176-1181.
Vacková L, Srb M, Stloukal R, et al. 2011. Comparison of denitrification at low temperature using encapsulated Paracoccus denitrificans, Pseudomonas fluorescens and mixed culture[J]. Bioresource Technology, 102(7): 4661-4666.
Van Driel P, Robertson W, Merkley L. 2006. Denitrification of agricultural drainage using wood-based reactors[J]. Transactions of the ASABE, 49(2): 565-573.
Verhulst P. 1838. Correspondence Mathematique et Physique 10[J].
von Ahnen M, Dalsgaard J, Pedersen P B. 2021. Effect of different C/N ratios and hydraulic retention times on denitrification in saline, recirculating aquaculture system effluents[J]. Aquacultural Engineering, 94: 102170.
Von B L. 1957. Quantitative laws in metabolism and growth[J]. The Quarterly Review of Biology, 32(Volume 32, Number 3): 217-231.
Warneke S, Schipper L A, Bruesewitz D A, et al. 2011. Rates, controls and potential adverse effects of nitrate removal in a denitrification bed[J]. Ecological Engineering, 37(3): 511-522.

Appendices

Tables

Table 4.1 Experimental set up

No	Bioreactor type	Scale	Media	N loading (mg N L^{-1})	HRT
Exp1	B1	Lab	W	6.8	0.5, 1, 2, 3, 4, 8, 12, 24
Exp2	B1	Lab	W+B	6.8	0.5, 1, 2, 3, 4, 8, 12, 24
Exp3	B1	Lab	W+S	6.8	0.5, 1, 2, 3, 4, 8, 12, 24
Exp4	B1	Lab	W+B+S	6.8	0.5, 1, 2, 3, 4, 8, 12, 24
Exp5	B2	Lab	W	6.9	1, 2, 4, 6, 8, 12, 18, 24
Exp6	B2	Lab	W	23.7	1, 2, 4, 6, 8, 12, 18, 24
Exp7	B2	Lab	W	70.0	1, 2, 4, 6, 8, 12, 18, 24
Exp8	B3	Field	W	2.8-11.4	Range in 2-50
Easton et al. (2015)	B1	Lab	W	15	3,6,12, 18, 24, 30, 36, 42,48,54,60, 66, 72, 96, 120
Pluer et al. (2016)	B1	Lab	W	2.5-20	2, 4, 6, 8, 10, 12

Note: B1 represents tank bioreactor; W represents woodchip; B represents biochar, F represents flaxseed; HRT represents hydraulic retention time.

Table 4.2 Compare and contrast the two nonlinear models to predict NRR and NRE

Models	Equation	Maximum	HRT_O
NRE_{MM}	$\frac{N_{max-MM} \cdot HRT \cdot L_B}{N_{in}(k + HRT)}$	$\rightarrow \frac{N_{max-MM} \cdot L_B}{N_{in}}$	$\rightarrow \infty$
NRE_{MT}	$\frac{N_{max-MT}(1-ae^{-bHRT})L_B}{N_{in}}$	$\rightarrow \frac{N_{max-MT} \cdot L_B}{N_{in}}$	$\rightarrow \infty$
NRR_{MM}	$\frac{24 \cdot N_{max-MM} \cdot L_B \cdot \rho_e}{(k + HRT)}$	$\rightarrow \frac{24 \cdot N_{max-MM} \cdot L_B \cdot \rho_e}{k}$	$\rightarrow 0$
NRR_{MT}	$\frac{24 \cdot N_{max-MT} \cdot (1-ae^{-bHRT})L_B \cdot \rho_e}{HRT}$	$\frac{24 \cdot N_{max-MT} \cdot b \cdot L_B \cdot \rho_e \cdot (1 - ae - b^{-1-w_{-1}(-\frac{1}{ae})})}{[-1 - w_{-1}(-\frac{1}{ae})]}$	$\begin{cases} \rightarrow 0, & a \leq 1 \\ \frac{-1 - w_{-1}(-\frac{1}{ae})}{b}, & a > 1 \end{cases}$

Note: HRT_O represents the optimal HRT corresponding to the maximum values of NRR or NRE. $w_{-1}(x)$ represents weber function.

Table 4.3 Fitting parameters of the two nonlinear models which are used to describe the relationship between NRE and HRT

No	Mitscherlich Model				Michaelis-Menten Model		
	$N_{max\text{-}MT}$	a	b	$HRT_{90\%}$	$N_{max\text{-}MM}$	k	$HRT_{90\%}$
Exp1	6.830	0.750	0.340	3.78	29.008	1.229	3.61
Exp2	7.001	0.764	0.403	3.29	29.891	1.089	3.21
Exp3	6.475	0.510	1.131	1.46	26.755	0.223	1.54
Exp4	6.491	0.589	2.038	0.80	26.717	0.138	0.85
Exp5	7.717	0.963	0.779	2.07	8.276	0.750	3.84
Exp6	27.313	0.982	0.025	15.84	73.498	46.51	22.11
Exp7	74.665	1.011	0.061	30.49	121.782	26.593	35.90
Exp8	8.981	1.066	0.046	4.53	3.674	48.602	23.57
Easton et al. (2015)	25.120	0.904	0.044	46.08	29.620	16.858	49.82
Pluer et al. (2016)	638.625	0.999	0.001	—	6547.132	6522.89	—

Table 4.4 Fitting parameters of the two nonlinear models which are used to describe the relationship between NRR and HRT

No	Mitscherlich Model				Michaelis-Menten Model		
	$N^{*}_{max\text{-}MT}$	a	b	HRT_O	$N^{*}_{max\text{-}MM}$	k	HRT_O
Exp1	5.038	0.939	1.072	→0	6.229	0.858	→0
Exp2	6.820	0.968	0.772	→0	6.793	0.956	→0
Exp3	6.41	0.797	1.217	→0	7.346	0.509	→0
Exp4	6.416	1.068	2.463	0.17	7.490	0.340	→0
Exp5	7.021	0.910	0.714	→0	8.333	1.121	→0
Exp6	31.802	0.980	0.021	→0	26.251	12.517	→0
Exp7	66.661	1.013	0.062	2.73	152.972	42.009	→0
Exp8	14.742	1.026	0.025	9.76	5.53×10^{10}	2.07×10^{11}	→0
Easton et al. (2015)	26.233	0.882	0.038	→0	24.432	11.12	→0
Pluer et al. (2016)	700.133	0.998	0.001	→0	29.051	20.73	→0

Figures

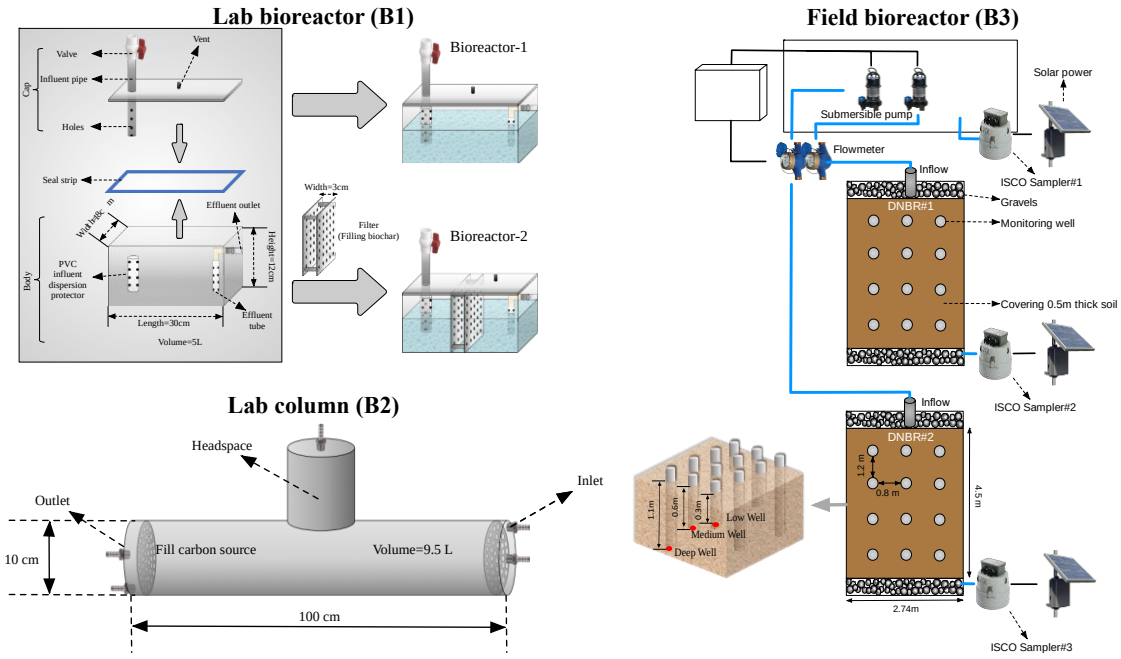

Figure 4.1 B1 was a schematic diagram of a lab bioreactor, and details can be seen in Chapter 3. B2 was a schematic diagram of the lab column. B3 was a plan view of field bioreactors. B1 and B2 were constructed in the Soil Physics lab at the University of Tennessee. Field bioreactors were constructed at East Tennessee AgResearch and Education Center (ETREC) at Little River Animal and Environmental Unit (LRAEU) (35°46'14.0"N 83°50'44.9"W).

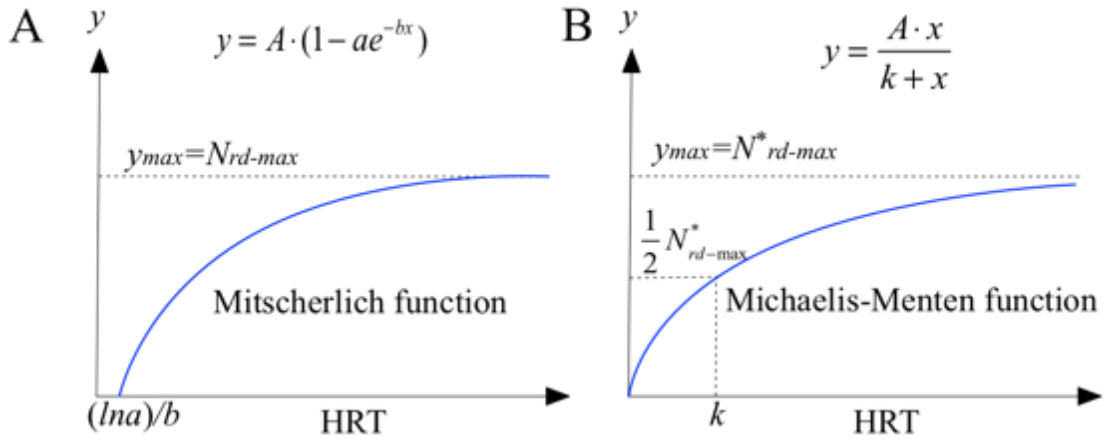

Figure 4.2 A) A schematic figure of nitrate reduction per length (N_{rd}) changed with hydraulic retention time (HRT) by Mitscherlich function; B) N_{rd} changed with HRT by Michaelis-Menten function.

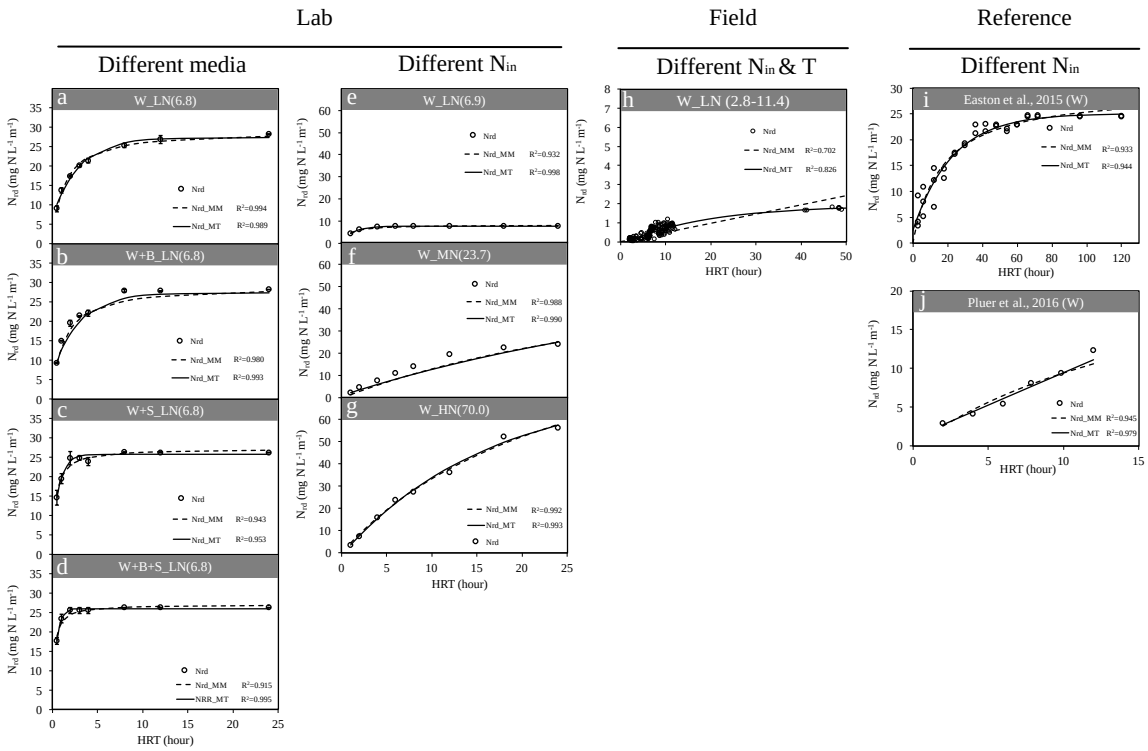

Figure 4.3 Nitrate reduction per bioreactor length (N_{rd}) values changed with different hydraulic retention time (HRT) under different fill-materials, including a) woodchip (W), b) woodchip+biochar (W+B), c) woodchip+silage leachate (W+S), and d) woodchip+biochar+silage leachate (W+B+S); Similarly, N_{rd} changed with HRT under different influent nitrate concentrations, including e) low nitrate concentration (LN, 5.4±0.3 mg N L^{-1}), f) medium nitrate concentration (MN, 15.9±0.4 mg N L^{-1}), and g) high nitrate concentration (HN, 33±1.5 mg N L^{-1}); h) N_{rd} changed with HRT at field bioreactors with low nitrate concentration (LN, 2.8-11.4 mg N L^{-1}); In addition, other refereed articles reported that N_{rd} changed with HRT under different influent nitrate concentrations, including i) Easton et al. (2015) (15 mg N L^{-1}), and j) Pluer et al. (2016) (2.5 to 20 mg N L^{-1}). N_{in} represents the influent nitrate concentration, T represents temperature. The error bars are standard deviations. All the data were fitted with MM, and MT models, respectively. R^2 was shown from 0.702 to 0.998., and

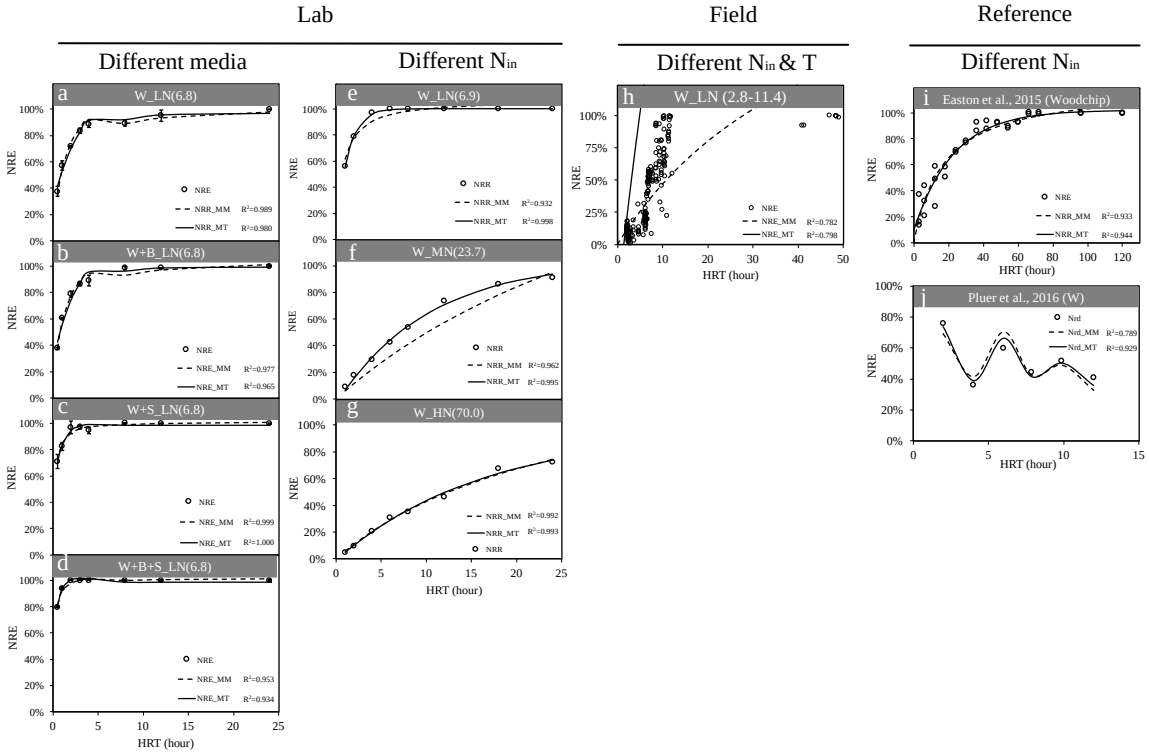

Figure 4.4 Nitrate removal efficiency (NRE) values changed with different hydraulic retention time (HRT) under different fill-materials, including a) woodchip (W), b) woodchip+biochar (W+B), c) woodchip+silage leachate (W+S), and d) woodchip+biochar+silage leachate (W+B+S); Similarly, NRE changed with HRT under different influent nitrate concentrations, including e) low nitrate concentration (LN, 5.4±0.3 mg N L^{-1}), f) medium nitrate concentration (MN, 15.9±0.4 mg N L^{-1}), and g) high nitrate concentration (HN, 33±1.5 mg N L^{-1}); h) NRE changed with HRT at field bioreactors with low nitrate concentration (LN, 2.8-11.4 mg N L^{-1}); In addition, other refereed articles reported that NRE changed with HRT under different influent nitrate concentrations, including i) Easton et al. (2015) (15 mg N L^{-1}), and j) Pluer et al. (2016) (2.5 to 20 mg N L^{-1}). N_{in} represents the influent nitrate concentration, T represents temperature. The error bars are standard deviations. All the data were fitted with MM, and MT models, respectively. R^2 was shown from 0.782 to 1.000.

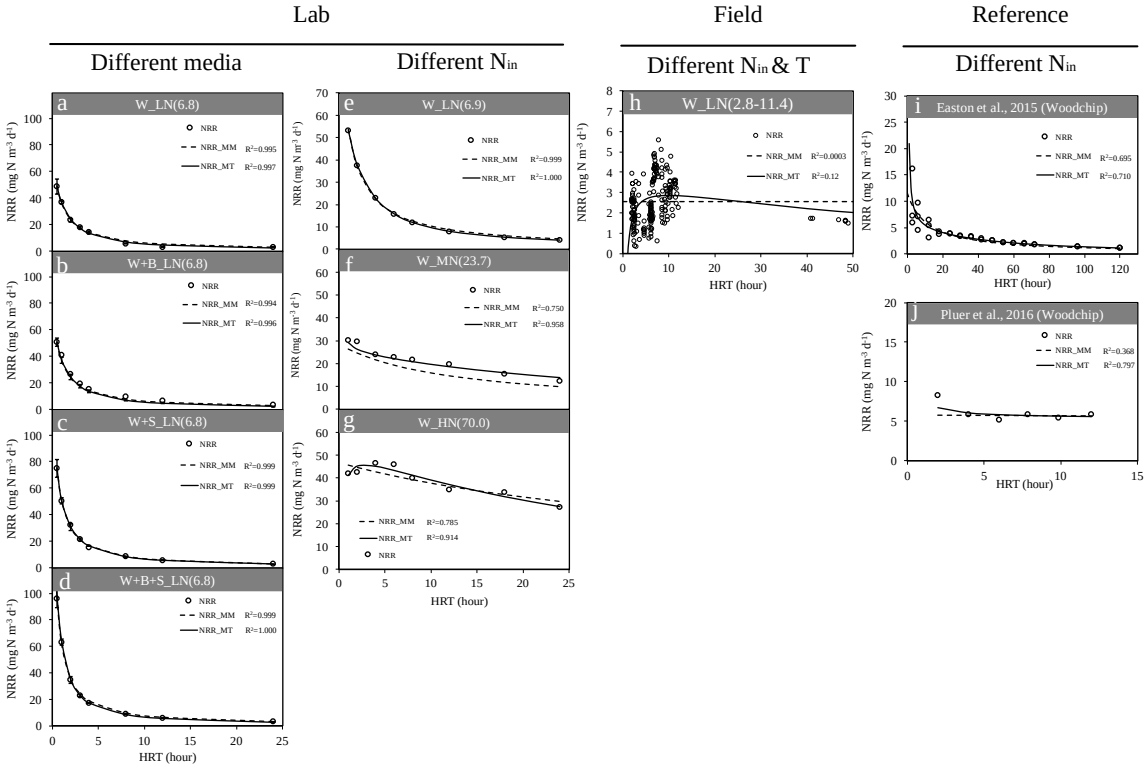

Figure 4.5 Nitrate removal rate (NRR) values changed with different hydraulic retention time (HRT) under different fill-materials, including a) woodchip (W), b) woodchip+biochar (W+B), c) woodchip+silage leachate (W+S), and d) woodchip+biochar+silage leachate (W+B+S); Similarly, NRR changed with HRT under different influent nitrate concentrations, including e) low nitrate concentration (LN, 5.4±0.3 mg N L^{-1}), f) medium nitrate concentration (MN, 15.9±0.4 mg N L^{-1}), and g) high nitrate concentration (HN, 33±1.5 mg N L^{-1}); h) NRR changed with HRT at field bioreactors with low nitrate concentration (LN, 2.8-11.4 mg N L^{-1}); In addition, other refereed articles reported that NRR changed with HRT under different influent nitrate concentrations, including i) Easton et al. (2015) (15 mg N L^{-1}), and j) Pluer et al. (2016) (2.5 to 20 mg N L^{-1}). N_{in} represents the influent nitrate concentration, T represents temperature. The error bars are standard deviations. All the data were fitted with MM, and MT models, respectively. R^2 was shown from 0.003 to 1.000.

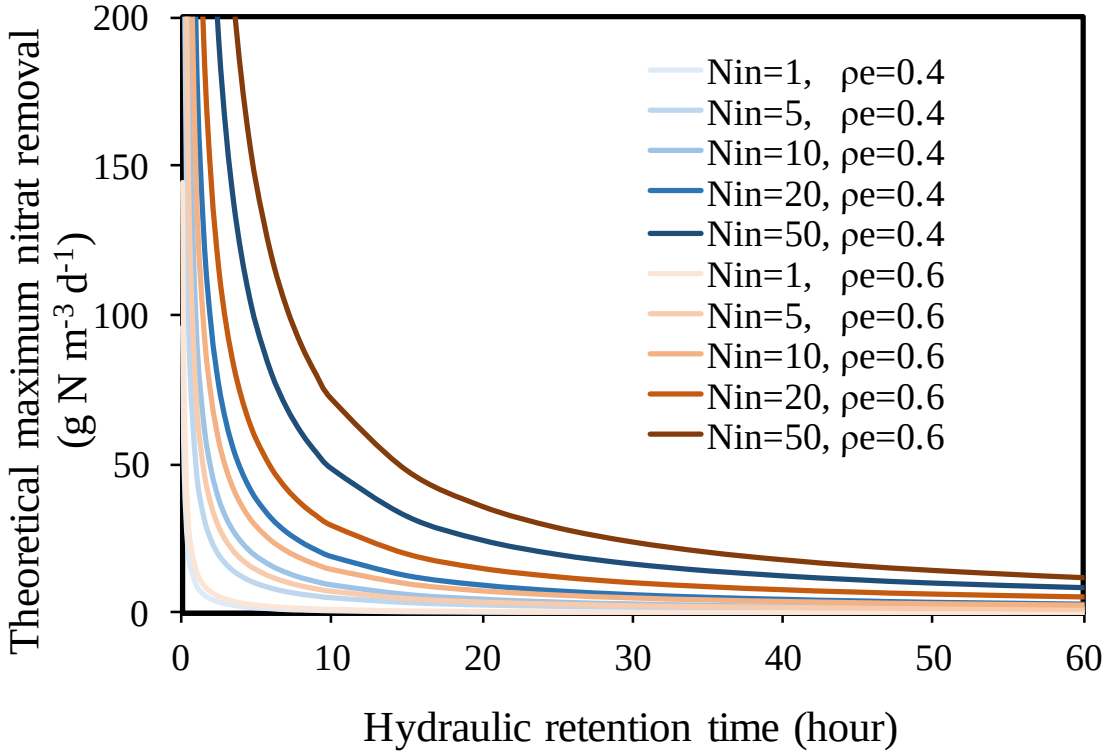

Figure 4.6 Theoretical maximum nitrate removal rate changed with hydraulic retention time at different influent nitrate concentrations, including 1, 5, 10, 20, 50, 100, 200, and 300 mg N L^{-1}, respectively. The effective porosity is assumed to be 0.5.

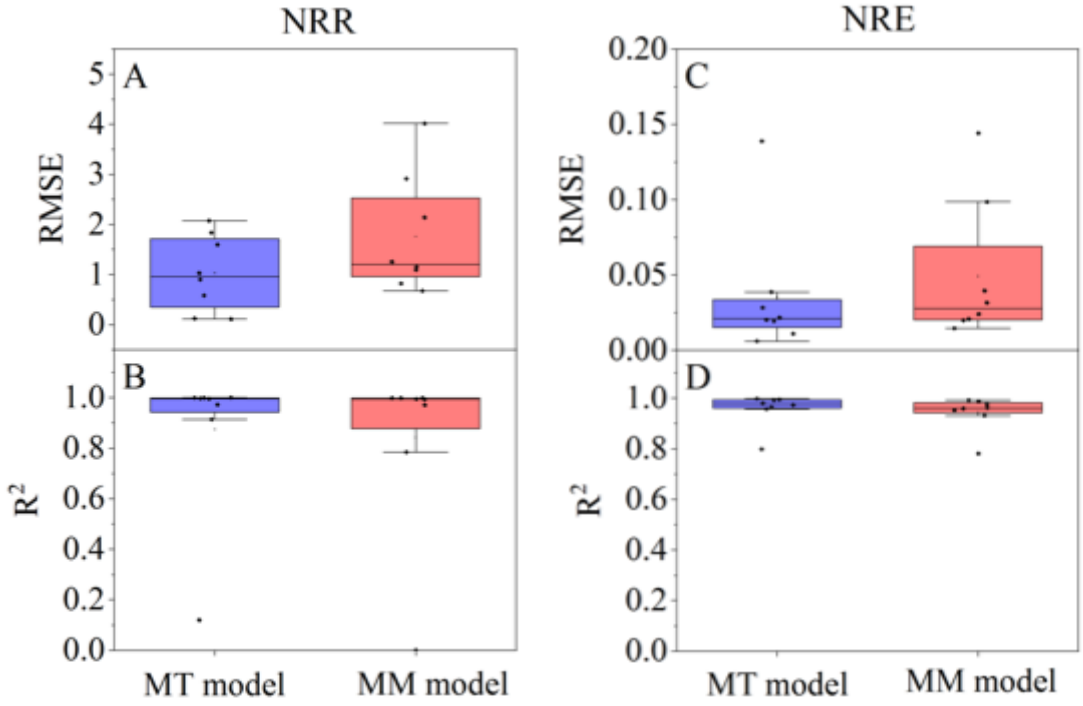

Figure 4.7 A) RMSE and B) R^2 values of NRR by MT and MM model, respectively; C) RMSE and D) R^2 values of NRE by MT and MM model, respectively.

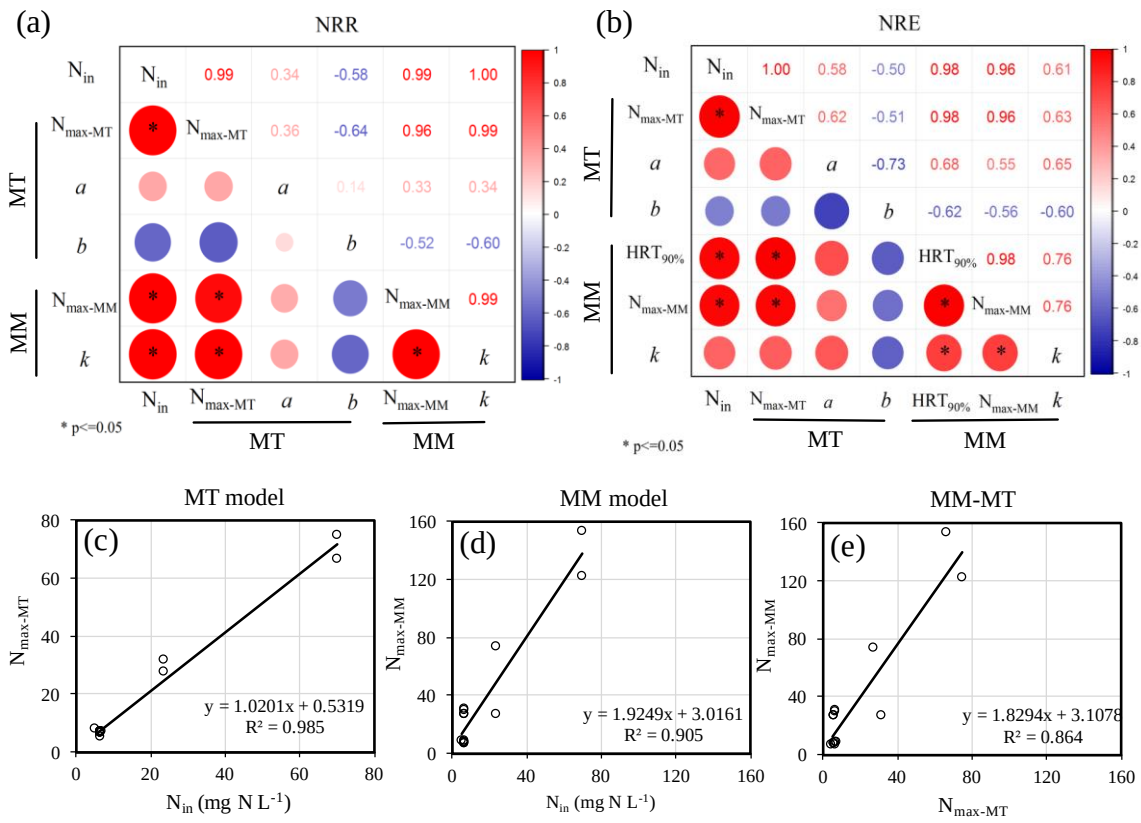

Figure 4.8 a) Pearson correlation of influent nitrate concentration (N_{in}, mg N L^{-1}), $N_{max\text{-}MT}$, *a*, *b*, $N_{max\text{-}MM}$, and *k*; b) Pearson correlation of influent nitrate concentration (N_{in}, mg N L^{-1}), $N_{max\text{-}MT}$, *a*, *b*, $HRT_{90\%}$, $N_{max\text{-}MM}$, and *k*. * represents a significant level (p<0.05). c) $N_{max\text{-}MM}$ versus $N_{max\text{-}MT}$; d) $N_{max\text{-}MT}$ changed with N_{in}; e) $N_{max\text{-}MM}$ changed with N_{in}. N_{in} represents influent nitrate concentration (mg N L^{-1}).

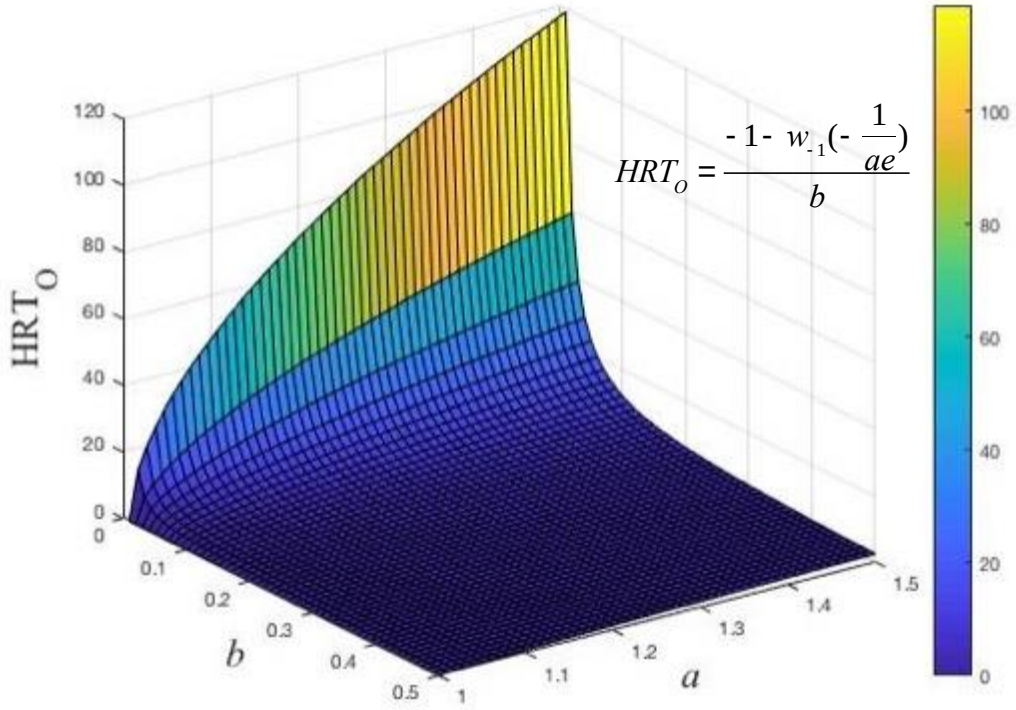

Figure 4.9 HRT_O corresponding to MT's shape parameters *a* and *b*. *a* and b in range 1 to 1.5, and 0 to 0.5, respectively.

CHAPTER V
EVALUATING THE NITRATE REMOVAL PERFORMANCE IN DENITRIFING BIOREACTORS BY INFLOW AND OUTFLOW C/N RATIO

This chapter is based on a manuscript draft by Yuchuan Fan et al.:

A version of this chapter was originally prepared by:

Yuchuan Fan, Jaehoon Lee, Jie Zhuang, Michael Essington, Sindhu Jagadamma, and John Schwartz. Evaluating the nitrate removal performance in denitrifying bioreactors by inflow and outflow C/N ratio.

My primary contributions to the work include (i) designing and implementing experiments, (ii) developing models, (iii) initial writing of the manuscript, and (iv) revising manuscript and coordinating revisions of the manuscript.

Abstract

Denitrifying bioreactors are a cost-effective water management practice used to reduce nitrate concentrations in agricultural drainage and stormwater. The C/N ratio is a critical factor for nitrate removal in denitrifying bioreactors. Due to the characteristics of the denitrifying bioreactors, the C/N ratio within the denitrifying bioreactor itself is difficult to measure given that an anaerobic environment is created in a closed system. The inflow and outflow are easier to access given that they are mostly exposed to the atmosphere. Thus, the objective of this study was to quantitatively understand how the nitrate removal changed with inflow and outflow C/N ratio in denitrifying bioreactors. In this study, a new independent variable (ε), which is the outflow C/N ratio divided by the inflow C/N ratio, was defined. Using a nonlinear model, it was found that ε has a good relationship with nitrate removal efficiency. To verify this model, laboratory and field experiments were conducted under different influent nitrate concentrations (6.8-70 mg N L^{-1}), hydraulic retention times (0.5-24 hours), and media (Woodchip, woodchip+biochar, woodchip+silage leachate, woodchip+biochar+silage leachate). The results showed that the relationship between nitrate removal efficiency and ε can be well described by the nonlinear model. Furthermore, the critical parameter k in this nonlinear model was associated with influent nitrate concentrations, hydraulic retention times, and media. The results

show that *k* could be used as a comprehensive index to evaluate the performance of the denitrifying bioreactor. The greater the *k*, the greater the utilization of C for nitrate removal. Moreover, this nonlinear model can be used as a method to predict the missing values of C and N concentration in inflow and outflow. This study provides greater insights that can be used to understand the changes in nitrate removal with inflow and outflow C/N ratio.

Introduction

The excess leaching of nitrate into soil is a global phenomenon (Padilla et al. 2018). It causes a rise of nitrate discharge from agricultural systems and potentially leads to widespread eutrophication in the water bodies (Liu et al. 2019). Current studies have pointed out that eutrophication is a primary contributor to the low C/N ratio in this water (Wang et al. 2012). Therefore, C/N ratio is an important indicator for nitrate removal in agricultural drainage.

To reduce nitrate in the agricultural system, denitrifying bioreactors (DNBRs) are used as a cost-effective, edge-of-field, management practice with a long service time (Robertson et al. 2008; Schipper et al. 2010; Christianson et al. 2012). The impacts of the C/N ratio in the medium on nitrate removal have been reported. Healy et al. (2012) compared the nitrate removal performance across the different C/N ratio in filling materials, such as lodge pine woodchip (C/N=496), cardboard (C/N=208), lodge pine needles (C/N=46.5), and barley straw (C/N=65.7). Their study reported that cardboard had the highest nitrate removal efficiency (NRE, %). In addition, our meta-analysis of a global-wide database indicated that a higher C/N ratio of the filling materials (>100) showed a higher nitrate removal rate (NRR, g N m^{-3} d^{-1}) (Citing from Chapter 1 of this thesis). Additionally, for the same filling materials (e.g., woodchip), the C/N ratio of

media was also changed along the length of the denitrifying bioreactor (Ghane et al. 2018).

Variations in the C/N ratio of the media also result in variations in the water C/N ratio within the denitrifying bioreactor. For instance, the initial C/N ratio in media will release more dissolved organic carbon (Ghane et al. 2018), which may change the value of the C/N ratio in water. It is widely reported that nitrogen transforming is associated with the C/N ratio in treating water. For example, Bi et al. (2015) observed that the initial C/N ratio of 1.5-2.0 was suitable for heterotrophic denitrification in a batch reactor. Furthermore, van den Berg et al. (2015) conducted experiments using a laboratory reactor and the results indicated that when the COD/N ratio was increased to 7.7, up to 90% of all nitrate was converted to ammonium, which indicates that dissimilatory nitrate reduction to ammonia (DNRA) occurred. The COD/N ratio may also affect the co-existence of Anammox and denitrification (Ni et al. 2012; Miao et al. 2015). In addition to the nitrogen biological process, the C/N ratio of nitrate-laden water may also affect pH values. For example, Nguyen et al. (2018) observed that pH values increased when the C/N ratio rose from 0.5 to 2.5, but decreased with the C/N ratio rose from 2.5 to 10.

The C/N ratio is an important parameter of the denitrification rate. Thus, understanding the relationship between nitrate removal and C/N ratio when treating water can aid in selecting the most appropriate filling materials to optimize the nitrate removal process in denitrifying bioreactors. However, a recent study reported no evidence of a correlation between C/N mass ratio and nitrate removal rate (Cerminara et al. 2020). We believe that the major reason for this finding was that the C/N mass ratio in wastewater cannot serve as a representative parameter because it is not a stable

value in the denitrifying bioreactor. Several studies have reported that C/N mass ratio in wastewater is linked to temporal and spatial changes in the denitrifying bioreactor (Halaburka et al. 2017; Ghane et al. 2018). In addition, sampling wells which are pre-installed in field denitrifying bioreactors are required to measure in situ C/N value. In contrast, the influent C/N ratio and outflow C/N ratio are frequently reported because the inflow and outflow water is always exposed to the atmosphere, so it is easier to set up auto-samplers (e.g., ISCO sampler) before and after the denitrifying bioreactor process. Thus, the inflow and outflow C/N ratio values in water are easily obtained. Nevertheless, few studies reveal how nitrate removal is associated with the inflow and outflow C/N ratio.

Modeling is a useful tool to provide a solid foundation for understanding the relationship between nitrate removal and the C/N ratio in wastewater. Bi et al. (2015) developed mathematical modeling based on batch experiments to study how the C/N ratio and bacterial populations affect nitrogen removal in the simultaneous anammox and heterotrophic denitrification process. However, it may not be easy to apply a similar method to denitrifying bioreactors because the bacterial populations are difficult to control, especially in the field sites. To date, modeling the effects of the C/N ratio on nitrate removal in a denitrifying bioreactor is still lacking. In this study, to model the nitrate removal by inflow and outflow C/N ratio, a new index was proposed as the independent variable, the inflow C/N ratio over outflow C/N ratio, which we termed the C/N magnifying coefficient (ε):

$$\varepsilon = \frac{(C/N)_{out}}{(C/N)_{in}} \quad (1)$$

where $(C/N)_{in}$ represents the influent ratio, and $(C/N)_{out}$ the effluent.

It is well reported that the influent C/N ratio is always kept at a small range (0.5 to 10) (von Ahnen et al. 2021) than effluent (0.01 to 100000) (Bell et al. 2015; Xu et al. 2019; Pluer et al. 2020). We hypothesized that the large difference in the C/N ratio between inflow and outflow is associated with nitrate removal in the denitrifying bioreactors. To verify our hypothesis, a nonlinear model was developed to describe the change in nitrate removal with ε. Our objectives are (1) to verify the developed model and identify the kinetic parameters, and (2) evaluate the model performance by conducting lab- and field-scale experiments under varied ε, media, and influent nitrate concentrations.

Materials and Methods

Experimental set up

Laboratory study

The lab-scale denitrifying bioreactors, one filled with woodchips only (W) and the other three amended with (10% v/v) biochar (W+B), silage leachate (W+S), and biochar and silage leachate (W+B+S). The bioreactors are made from plastic containers (5L volume each), and the size is 0.18 m×0.12 m×0.3 m (W×H×L). The bioreactors consist of a cap and body. The cap part includes a valve, influent pipe, and vent. The vent was installed at the center of the cap to exhaust gases (e.g., N_2, N_2O, CO_2) that are produced. The bottom of the pipe was evenly punched with 6 holes at four directions, and each holes were 0.6 cm far away. The holes can avoid the influent water acting as a point source. The body includes a PVC-made influent dispersion protector, effluent tube, and an outlet. A seal strip between the cap and body was present to provide a relatively closed system for the bioreactor. The reactors

containing biochar contained 10% (v/v), which was filled in the middle of the bioreactor by a filter stand (Width=3 cm) and was placed in direct contact with woodchips. A 2 cm deep layer of coarse sand (diameter<0.5 cm) covered the surface of the woodchip to prevent the woodchip from floating. The woodchips came from the campus mulch. The biochar was obtained from a local company (Proton Power, Inc.). The silage leachate was collected from the UT dairy farm, located at the East Tennessee AgResearch and Education Center (ETREC) at Little River Animal and Environmental Unit (LRAEU). The physical and chemical properties of biochar and silage leachate are provided in the appendix.

Field study

The field DNBR was installed at East Tennessee AgResearch and Education Center (ETREC) at Little River Animal and Environmental Unit (LRAEU) (35°46'14.0"N 83°50'44.9"W). The field barriers consisted of a mixture of sawdust (95%), sand, and soil (5% in volume). The bottom and side of the barriers were lined with commercial grade geosynthetic to prevent groundwater intrusion. The barriers are 1.5 m deep, 2.74 m wide, and 4.5 m long, and receive a discharge from the cropped field in the Unit. The surface of the barriers is covered with a mixture of gravel and soil to hold the fill material in place. There is a total of 12 access tubes in the barrier which are used to collect water monitoring samples. Temperature sensors are also installed at the access ports. The treated drainage is discharged from the outlet located at the end of each barrier by a hydraulic gradient and delivered to nearby grassed waterways. The locations of the barriers were determined based on five years of previous runoff and groundwater monitoring data (Fig. 5.1).

Sampling and analysis methods

The C/N ratios in the influent to the denitrifying bioreactors were calculated from the DOC and NO_3-N concentrations. Other N sources were seldom detected. The influent was sampled from the prepared synthetic solution and controlled at 2.04±0.4, and the effluents were manually sampled from the outflow water. Each outflow sample consisted of one pore volume water of the bioreactor. All samples were filtered with 0.22-μm membrane filters. Filtered subsamples were injected into vials and stored in the refrigerator at 4 ˚C to prepare for NO_3-N measurement within 48 h after the manual sampling (San, Skalar Inc, Dutch). Similarly, filtered subsamples were preserved in glass vials by acidification with HCl before analysis for the DOC content (Shimadzu Inc, Japan).

Developing a nonlinear model to predict nitrate removal efficiency by ε

Based on our analysis, we determined that the relationship between NRE and $ln(\varepsilon)$ can be described by the Mitscherlich model, as reported below (Mitscherlich 1919)

$$NRE = A(1 - Be^{-k\ln e}) \quad (2)$$

where *A*, *B*, and *k* is a shape parameter. *A* is the upper asymptote; *B* is related to the initial value; *k* is a shape parameter and related to the intrinsic growth rate (Richards 1959).

The maximum value for NRE is 100%; thus, the shape parameter *A* is equal to 100%. Under the extreme condition when NRE is equal to zero, it is assumed that there is no change in the C/N ratio in inflow and outflow; thus, the corresponding ε should be 1, and the value of shape parameter *B* is equal to 1. The value of *A* and *B*, when both equal to 1, had to be verified by the experimental data. Datasets from the

literature were fitted to Eq. (2) by the least square method in Matlab, and all the optimized results indicated that parameters *A* and *B* are equal to 1. Therefore, Eq. (2) can be simplified to

$$NRE = 1 - e^{-k \ln e} \tag{3}$$

In this model, ε and *k* can be computed by fitting a set of NRE vs. ε data, where *k* is the fitted parameter. NRE is calculated as

$$NRE = \frac{N_{in} - N_{out}}{N_{in}} \tag{4}$$

Eq. (3) can be written in another form by substituting Eq. (1) and Eq. (4) into Eq. (3) and simplified them as below

$$\left(\frac{N_{out}}{N_{in}}\right)^{1-k} = \left(\frac{C_{in}}{C_{out}}\right)^{k} \tag{5}$$

Eq. (5) is another form of Eq (3), which indicates the balance of C and N mass in the whole bioreactor. When k=1, C_{in} is equal to C_{out}; if k>1, C_{out} is less than C_{in}; and if k<1, C_{out} is greater than C_{in}. The selection of the model form is determined by the need of the user. In this paper, we mainly applied our data to Eq. (3). Eq. (5) can be used to predict one of the missing parameters in C_{out}, C_{in}, N_{in}, and N_{out}. as

Model evaluation and Parameter estimation

The root-mean-squared error (RMSE) and coefficient of determination (R^2) were used to evaluate the performance of the model. RMSE and R^2 were calculated as follows:

$$\mathrm{RMSE} = \sqrt{\sum_{i=1}^{n} \frac{(y_i - x_i)^2}{n}} \tag{6}$$

$$R^2 = 1 - \frac{\sum_{i=1}^{n}(y_i - x_i)^2}{\sum_{i=1}^{n}(y_i - \bar{y}_i)^2} \quad (7)$$

Parameter estimation was performed using the least-square method present in the Excel solver function. Model performance was evaluated using a k-fold cross-validation test. Five data sets were used to train the model, and two data sets were used to test the model. Each model was then parametrized using the two validated data sets and subsequently plotted against the experimental data to validate goodness-of-fit.

Parameter sensitivity analysis

Changes in simulated NRE as a function of ε were tracked while varying the parameter k values by up to 20% using a one-at-a-time (OAT) sampling approach. Then, the relative amount of change that occurs in the outputs as a result of that parameter is calculated using Equation (8), representing the sensitivity of the outputs to the parameters.

$$\frac{\left[\frac{(NRE_{+D} - NRE_{-D})}{NRE_{base}}\right]}{2D} \quad (8)$$

where $NRE_{\pm\Delta}$ is the nitrate removal efficiency when parameter k is increased or decreased by a value of Δ% while NRE_{base} is the NRE calculated at a baseline configuration in which k=1. The OAT method was selected given allows us to obtain a clear idea about the roles of parameter k on the simulation of NRE in a simplistic manner. The other independent variable, ε, was set at the specific values 10, 100, 1000, and 10000, respectively, since ε has a wider range from 1 to 100000.

Results and Discussion

Influent and effluent C/N ratio

As presented in Fig 5.2, the effluent C/N generally has a greater value than influent C/N irrespective of whether the study was performed in a laboratory or field setting. This phenomenon was also consistent with the findings of others (Bell et al. 2015; Xu et al. 2019; Pluer et al. 2020). It should be noted that the effluent C/N ratio is not maintained at the same magnitude with influent C/N. Taken together, the influent and effluent C/N ratio range from 0.01 to 10, and 0.01 to 100,000. Moreover, the mean influent C/N, effluent C/N, and ε were 0.8±0.04, 1220.6±442, and 6299.2±3197, respectively.

The effluent C/N ratio may be greater than influent ratio due to lower nitrate concentrations in the effluent, as well as more organic carbon being released within the bioreactor. We also found that the field data was close to the 1:1 line (ε=1), which indicated that C_{in} equal to C_{out}. In contrast, data obtained from the laboratory study was below the 1:1 line (ε<1), which demonstrated C_{out} is greater than C_{in}.

The relationship between ε, inflow C/N, outflow C/N, and nitrate removal efficiency

Fig 5.3a-5.3c represents how the NRE in the field experiment changed with the influent C/N, effluent C/N, and ε. This suggests that the relationship between ε and NRE can be well fitted by Eq (3) (R^2=0.69). However, NRE did not show a significant trend with influent C/N or effluent C/N ratio. This results implied that ε can be a good independent variable to describe the variations on NRE.

Effects of the influent nitrate concentration on parameter k in the denitrifying bioreactor

Effects of the influent nitrate concentration on nitrate removal, which was fitted by Eq (3), are summarized in Fig 5.4. The confidence band indicates that the fitted nonlinear line was significantly affected by influent nitrate concentration ($p < 0.05$). In addition, increasing influent nitrate concentrations from low N loading (LN) to high N loading (HN) will shift the fitted line from high to low, resulting in a decrease in k from 0.63 to 0.21. It also indicates that increasing the nitrate removal decreases the NRE, which was consistent with previous studies (Cited from Chapter 2 of this thesis). However, increasing influent nitrate concentration shifts the datapoints from right to left, which also means ε decreases. Even though increasing the nitrate concentration will lead to the C/N ratios from inflow and outflow decreasing together, according to the ε calculation the changes of outflow C/N ratios should be larger than the inflow C/N ratios. The increment on ε was likely due to the (1) inflow increasing nitrate concentration cannot keep pace with outflow increasing nitrate concentration, and (2), the outflow C (C_{out}) decreased due to the greater C consumption required to provide electrons for denitrification in the bioreactors.

Effects of the media and hydraulic retention time on parameter k in the denitrifying bioreactor

Fig 5.5 shows that NRE changed with ε according to Eq (3) under different hydraulic retention times (1 h and 6 h) and media (W, W+B, W+S, and W+B+S). After 1 h of HRT, the fitted parameters k for W, W+B, W+S, and W+B+S were 0.21, 0.17, 0.17, and 0.18. While after 6 h of HRT, the fitted parameters k for W, W+B, W+S, and W+B+S were 0.26, 0.31, 0.28, and 0.4. Thus, it showed that increasing HRT would

increase the value of parameters k and ε, which cause changes in the position of the fitted line and data points. Firstly, the fitted line lies closer to the reference line (k=1) and then moves from the bottom to the top. Secondly, the data points move from left to right because ε is increasing. Therefore, 6 h of HRT resulted in a greater NRE than 1 h-HRT. We attributed all these changes to two reasons: 1) a greater HRT may release more C from the media by a relatively slow flow rate; and 2) a greater HRT may reduce more N due to a more adequate reaction time with biofilm on the surface of the woodchip.

It was also found that amending the woodchip bioreactor (W) with biochar (B) and silage leachate (S) increased parameter k and ε, especially after 6 h of HRT. This is not surprising considering that adding biochar and silage leachate can significantly increase the DOC (Cited from Chapter 3 of this thesis).

We also found that data points were always distributed from right to left with time, and these data points at the initial time were always not fitted well by the nonlinear model (Fig. 4a). We suspected that the reason for the data not fitting well at the initial time was probably due to the start-up phenomenon, with it being widely reported that more DOC is released and a higher NRE is observed when first running the denitrifying bioreactors (Maxwell et al. 2019). Thus, the greater amount of C released may cause a greater ε and k, which results in inconsistencies with the stable data points. As such, this implies that it is better to fit the data with Eq. (3) by excluding the initial data.

Sensitivity analysis of parameter k affecting the nitrate removal efficiency

Responses and sensitivity of nitrate removal efficiency corresponding to varying parameters k and ε are presented in Fig 5.6. As highlighted in Fig 5.6a, NRE showed a greater variation at a low value of ε under the different scenarios of k

values. Fig 5.6b also underlines a higher relative sensitivity value when ε is below approximately 60.

Application and evaluation of the nonlinear model

Fitting the nonlinear model with the real data can produce the fitted parameter *k*, which is reflecting the general condition of the denitrifying bioreactor upon C release. The higher *k* indicated that NRE could be higher under the same value of ε. Additionally, our study showed that *k* could be a comprehensive indicator that is able to reflect the relationship between the influent and effluent C because this parameter is also associated with multiple controlling factors, including influent nitrate concentration, hydraulic retention time, and media. Also, to obtain the parameter *k*, the nonlinear model can be applied to predict one of the absent values of C or N in either influent or effluent. For instance, we assumed the values of C_{in}, C_{out}, and N_{in}, based on the calibrated model, while the predicted N_{out} could be calculated according to another form of our nonlinear model (Eq. (5)). As presented in Fig 5.7, this approach estimated the predicted N_{out} rather well. Thus, this nonlinear model can also as an alternative approach to predict N_{out} based on N_{in}, C_{in}, and C_{out}.

Conclusions

An index ε, which is the outflow C/N ratio divided by the inflow C/N ratio, was determined to be an independent variable able to predict nitrate removal efficiency using a nonlinear model. This nonlinear model was verified by laboratory and field experiments. The results indicated that the model could be well fitted for different conditions, including different influent nitrate concentrations, hydraulic retention times,

and media. In addition, it was found that increasing influent nitrate concentration and hydraulic retention time increases the value of the parameter *k*, which can be a comprehensive indicator to reflect the relationship between C concentration in influent and effluent. A greater *k* indicates a higher nitrate removal efficiency. To successfully build upon these results, further work including verification and application, especially in the field, as well as exploring how other important abiotic factors impact *k*, such as temperature and pH, is required.

References

Bell N, Cooke R A, Olsen T, et al. 2015. Characterizing the performance of denitrifying bioreactors during simulated subsurface drainage events[J]. Journal of Environmental Quality, 44(5): 1647-1656.

Bi Z, Takekawa M, Park G, et al. 2015. Effects of the C/N ratio and bacterial populations on nitrogen removal in the simultaneous anammox and heterotrophic denitrification process: mathematic modeling and batch experiments[J]. Chemical Engineering Journal, 280: 606-613.

Cerminara G, Raga R, Hirata O, et al. 2020. Denitrification of low C/N landfill leachate in lab-scale landfill simulation bioreactors[J]. Waste Management, 113: 236-243.

Christianson L E, Bhandari A, Hailers M J. 2012. A Practice-Oriented Review Of Woodchip Bioreactors For Subsurface Agricultural Drainage[J]. Applied Engineering in Agriculture, 28(6): 861-874.

Ghane E, Feyereisen G W, Rosen C J, et al. 2018. Carbon Quality of Four-Year-Old Woodchips in a Denitrification Bed Treating Agricultural Drainage Water[J]. Transactions of the ASABE, 61(3): 995-1000.

Halaburka B J, LeFevre G H, Luthy R G. 2017. Evaluation of Mechanistic Models for Nitrate Removal in Woodchip Bioreactors[J]. Environmental Science & Technology, 51(9): 5156-5164.

Healy M G, Ibrahim T G, Lanigan G J, et al. 2012. Nitrate removal rate, efficiency and pollution swapping potential of different organic carbon media in laboratory denitrification bioreactors[J]. Ecological Engineering, 40: 198-209.

Liu X W, Xu J, Huang J L, et al. 2019. Bacteria-supported iron scraps for the removal of nitrate from low carbon-to-nitrogen ratio wastewater[J]. Rsc Advances, 9(6): 3285-3293.

Maxwell B M, Birgand F, Schipper L A, et al. 2019. Drying–rewetting cycles affect nitrate removal rates in woodchip bioreactors[J]. Journal of Environmental Quality, 48(1): 93-101.

Miao L, Wang S, Cao T, et al. 2015. Optimization of three-stage Anammox system removing nitrogen from landfill leachate[J]. Bioresource Technology, 185: 450-455.

Mitscherlich E A. 1919. Problems of plant growth[J]. Landwirtschaftliche jahrbucher, 53:: 167~182.

Nguyen T N P, Chao S-J, Chen P-C, et al. 2018. Effects of C/N ratio on nitrate removal and floc morphology of autohydrogenotrophic bacteria in a nitrate-containing wastewater treatment process[J]. Journal of Environmental Sciences, 69: 52-60.

Ni S-Q, Ni J-Y, Hu D-L, et al. 2012. Effect of organic matter on the performance of granular anammox process[J]. Bioresource Technology, 110: 701-705.

Padilla F M, Gallardo M, Manzano-Agugliaro F. 2018. Global trends in nitrate leaching research in the 1960–2017 period[J]. Science of The Total Environment, 643: 400-413.

Pluer W T, Walter M T, Steinschneider S. 2020. Understanding Complex Flow Pathways within Lab-Scale Denitrifying Bioreactors with a Conservative Tracer[J]. Transactions of the ASABE, 63(2): 417-427.

Richards F J. 1959. A FLEXIBLE GROWTH FUNCTION FOR EMPIRICAL USE[J]. Journal of Experimental Botany, 10(29): 290-300.
Robertson W D, Vogan J L, Lombardo P S. 2008. Nitrate removal rates in a 15-year-old permeable reactive barrier treating septic system nitrate[J]. Ground Water Monitoring and Remediation, 28(3): 65-72.
Schipper L A, Robertson W D, Gold A J, et al. 2010. Denitrifying bioreactors—An approach for reducing nitrate loads to receiving waters[J]. Ecological Engineering, 36(11): 1532-1543.
van den Berg E M, van Dongen U, Abbas B, et al. 2015. Enrichment of DNRA bacteria in a continuous culture[J]. The ISME Journal, 9(10): 2153-2161.
von Ahnen M, Dalsgaard J, Pedersen P B. 2021. Effect of different C/N ratios and hydraulic retention times on denitrification in saline, recirculating aquaculture system effluents[J]. Aquacultural Engineering, 94: 102170.
Wang S, Zhu G, Peng Y, et al. 2012. Anammox bacterial abundance, activity, and contribution in riparian sediments of the Pearl River estuary[J]. Environmental Science & Technology, 46(16): 8834-8842.
Xu B K, Shi L S, Zhong H, et al. 2019. The performance of pyrite-based autotrophic denitrification column for permeable reactive barrier under natural environment[J]. Bioresource Technology, 290: 10.
Bell N, Cooke R A, Olsen T, et al. 2015. Characterizing the performance of denitrifying bioreactors during simulated subsurface drainage events[J]. Journal of Environmental Quality, 44(5): 1647-1656.
Bi Z, Takekawa M, Park G, et al. 2015. Effects of the C/N ratio and bacterial populations on nitrogen removal in the simultaneous anammox and heterotrophic denitrification process: mathematic modeling and batch experiments[J]. Chemical Engineering Journal, 280: 606-613.
Cerminara G, Raga R, Hirata O, et al. 2020. Denitrification of low C/N landfill leachate in lab-scale landfill simulation bioreactors[J]. Waste Management, 113: 236-243.
Christianson L E, Bhandari A, Hailers M J. 2012. A Practice-Oriented Review Of Woodchip Bioreactors For Subsurface Agricultural Drainage[J]. Applied Engineering in Agriculture, 28(6): 861-874.
Ghane E, Feyereisen G W, Rosen C J, et al. 2018. Carbon Quality of Four-Year-Old Woodchips in a Denitrification Bed Treating Agricultural Drainage Water[J]. Transactions of the ASABE, 61(3): 995-1000.
Halaburka B J, LeFevre G H, Luthy R G. 2017. Evaluation of Mechanistic Models for Nitrate Removal in Woodchip Bioreactors[J]. Environmental Science & Technology, 51(9): 5156-5164.
Healy M G, Ibrahim T G, Lanigan G J, et al. 2012. Nitrate removal rate, efficiency and pollution swapping potential of different organic carbon media in laboratory denitrification bioreactors[J]. Ecological Engineering, 40: 198-209.
Liu X W, Xu J, Huang J L, et al. 2019. Bacteria-supported iron scraps for the removal of nitrate from low carbon-to-nitrogen ratio wastewater[J]. Rsc Advances, 9(6): 3285-3293.
Maxwell B M, Birgand F, Schipper L A, et al. 2019. Drying–rewetting cycles affect nitrate removal rates in woodchip bioreactors[J]. Journal of Environmental Quality, 48(1): 93-101.

Miao L, Wang S, Cao T, et al. 2015. Optimization of three-stage Anammox system removing nitrogen from landfill leachate[J]. Bioresource Technology, 185: 450-455.
Mitscherlich E A. 1919. Problems of plant growth[J]. Landwirtschaftliche jahrbucher, 53:: 167~182.
Nguyen T N P, Chao S-J, Chen P-C, et al. 2018. Effects of C/N ratio on nitrate removal and floc morphology of autohydrogenotrophic bacteria in a nitrate-containing wastewater treatment process[J]. Journal of Environmental Sciences, 69: 52-60.
Ni S-Q, Ni J-Y, Hu D-L, et al. 2012. Effect of organic matter on the performance of granular anammox process[J]. Bioresource Technology, 110: 701-705.
Padilla F M, Gallardo M, Manzano-Agugliaro F. 2018. Global trends in nitrate leaching research in the 1960–2017 period[J]. Science of The Total Environment, 643: 400-413.
Pluer W T, Walter M T, Steinschneider S. 2020. Understanding Complex Flow Pathways within Lab-Scale Denitrifying Bioreactors with a Conservative Tracer[J]. Transactions of the ASABE, 63(2): 417-427.
Richards F J. 1959. A FLEXIBLE GROWTH FUNCTION FOR EMPIRICAL USE[J]. Journal of Experimental Botany, 10(29): 290-300.
Robertson W D, Vogan J L, Lombardo P S. 2008. Nitrate removal rates in a 15-year-old permeable reactive barrier treating septic system nitrate[J]. Ground Water Monitoring and Remediation, 28(3): 65-72.
Schipper L A, Robertson W D, Gold A J, et al. 2010. Denitrifying bioreactors—An approach for reducing nitrate loads to receiving waters[J]. Ecological Engineering, 36(11): 1532-1543.
van den Berg E M, van Dongen U, Abbas B, et al. 2015. Enrichment of DNRA bacteria in a continuous culture[J]. The ISME Journal, 9(10): 2153-2161.
von Ahnen M, Dalsgaard J, Pedersen P B. 2021. Effect of different C/N ratios and hydraulic retention times on denitrification in saline, recirculating aquaculture system effluents[J]. Aquacultural Engineering, 94: 102170.
Wang S, Zhu G, Peng Y, et al. 2012. Anammox bacterial abundance, activity, and contribution in riparian sediments of the Pearl River estuary[J]. Environmental Science & Technology, 46(16): 8834-8842.
Xu B K, Shi L S, Zhong H, et al. 2019. The performance of pyrite-based autotrophic denitrification column for permeable reactive barrier under natural environment[J]. Bioresource Technology, 290: 10.

Appendices

Tables

Table 5.1 Experimental set up

Experiments	Bioreactor type	Scale	Media	N loading (mg N L^{-1})	HRT
Exp1	B1	Lab	W	6.8	0.5, 1, 2, 3, 4, 8, 12, 24
Exp2	B1	Lab	W+B	6.8	0.5, 1, 2, 3, 4, 8, 12, 24
Exp3	B1	Lab	W+S	6.8	0.5, 1, 2, 3, 4, 8, 12, 24
Exp4	B1	Lab	W+B+S	6.8	0.5, 1, 2, 3, 4, 8, 12, 24
Exp5	B2	Lab	W	6.9	1, 2, 4, 6, 8, 12, 18, 24
Exp6	B2	Lab	W	23.7	1, 2, 4, 6, 8, 12, 18, 24
Exp7	B2	Lab	W	70.0	1, 2, 4, 6, 8, 12, 18, 24
Exp8	B3	Field	W	2.8-11.4	Range in 2-50

Figures

Figure 5.1 An aerial view of the East Tennessee AgResearch and Education Center (ETREC) at Little River Animal and Environmental Unit (LRAEU), red circle is the bioreactor location (Source: Google maps). At the LRAEU, Knoxville, TN the climate is hot and humid with an average summer temperature of 25°C (19 °C -31°C) and average winter temperature of 6°C (0°C- 11°C). (1) is the drainage station; (2) is the wetland which details can be seen in Fig 16; (3) is the field denitrifying bioreactors.

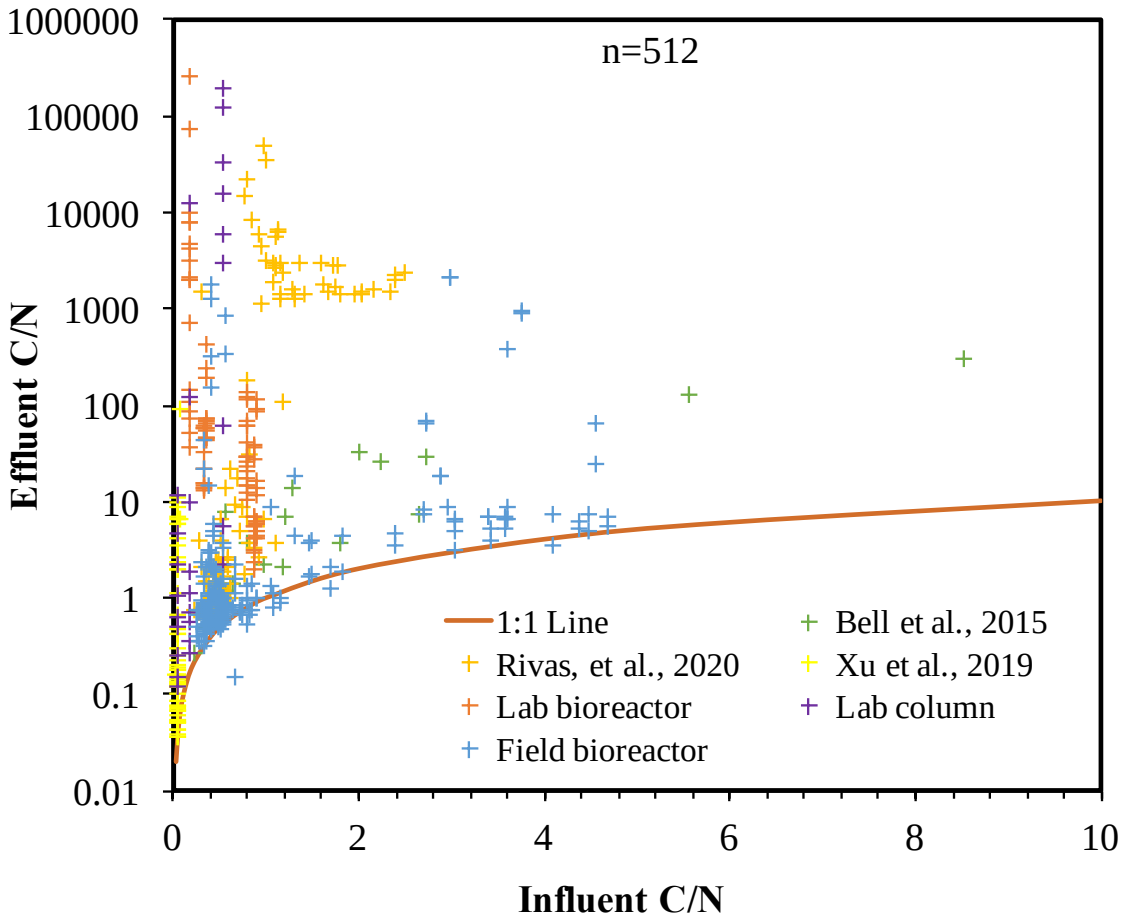

Figure 5.2 Effluent C/N ratio divided by influent C/N ratio. The data were obtained from this study, including laboratory bioreactor experiments, column experiments, and filed bioreactor experiments. Some further data were also considered, including Pluer et al. (2020), Xu et al. (2019), and Bell et al. (2015)

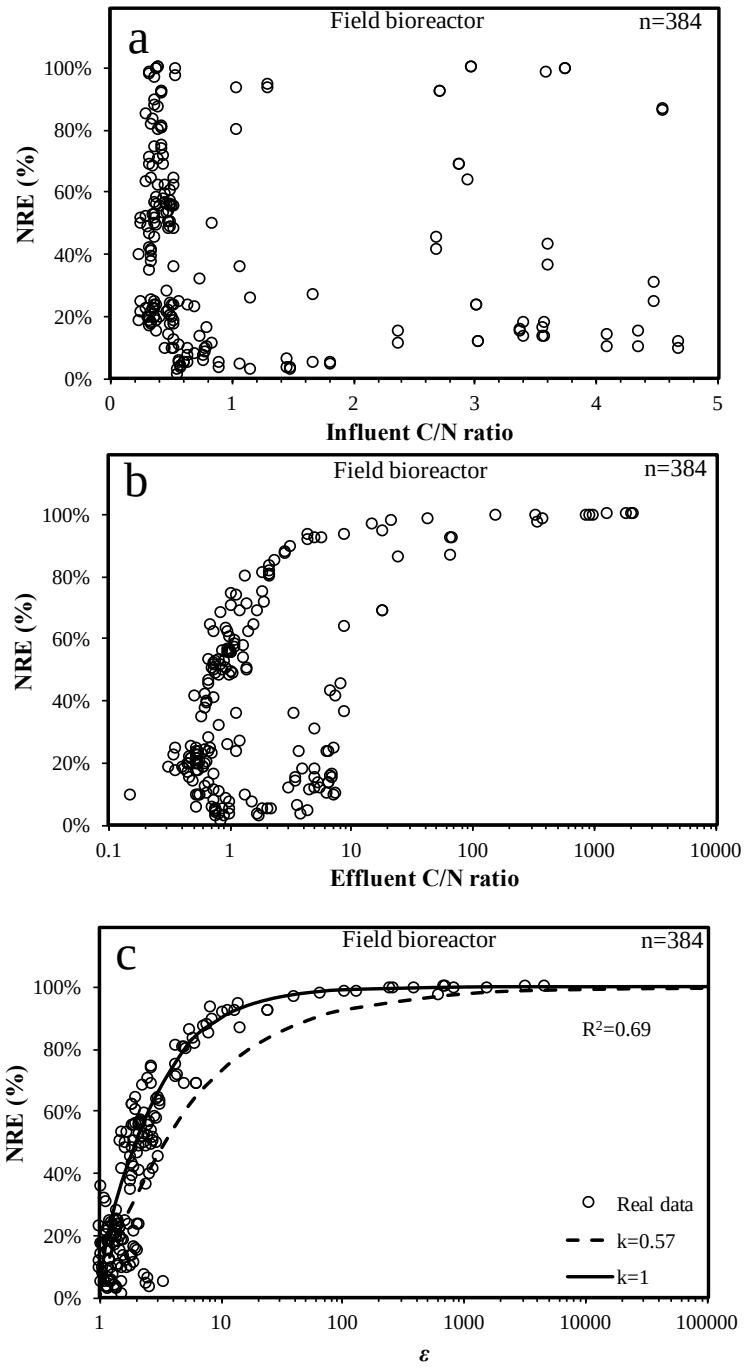

Figure 5.3 Nitrate removal efficiency (NRE, %) corresponding to influent C/N ratio, effluent C/N ratio, and ε, which is the ratio of influent C/N over effluent C/N. *n* represents the number of observations.

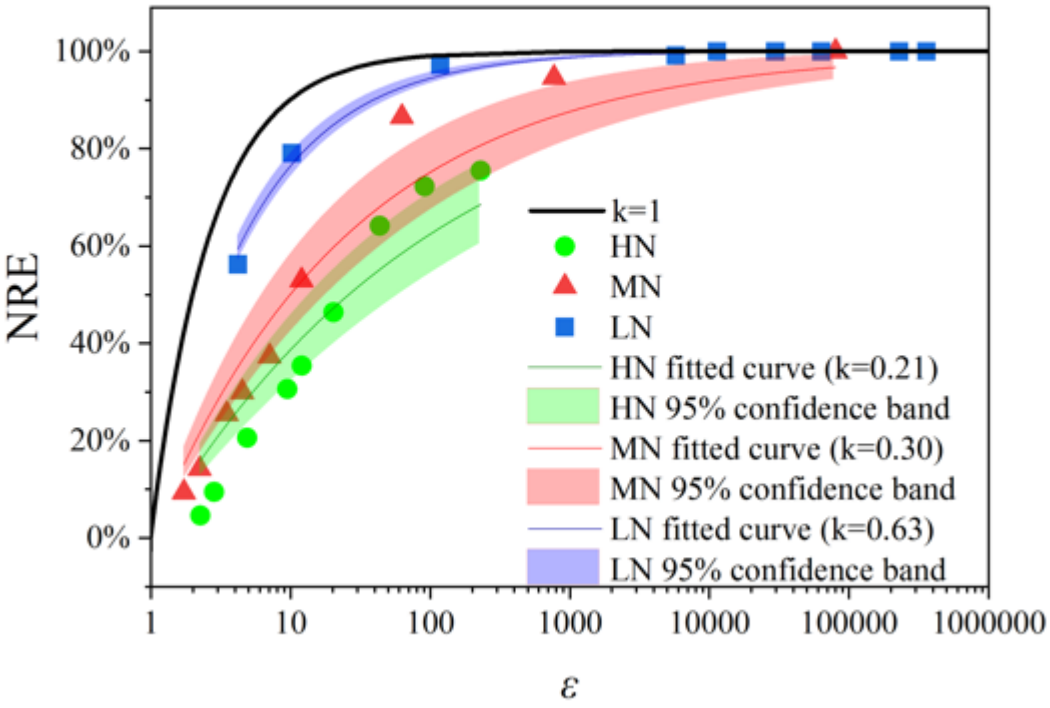

Figure 5.4 Nitrate removal efficiency (NRE) changed with ε (outflow C/N divide inflow C/N) under different influent nitrate concentrations, including low nitrate concentration (LN, 5.4±0.3 mg N L^{-1}), medium nitrate concentration (MN, 15.9±0.4 mg N L^{-1}), and high nitrate concentration (HN, 33±1.5 mg N L^{-1}). The *k* is the critical parameter that is fitted by the nonlinear model. The black real line is the reference line (*k*=1). The different color band represents the 95% confidence interval.

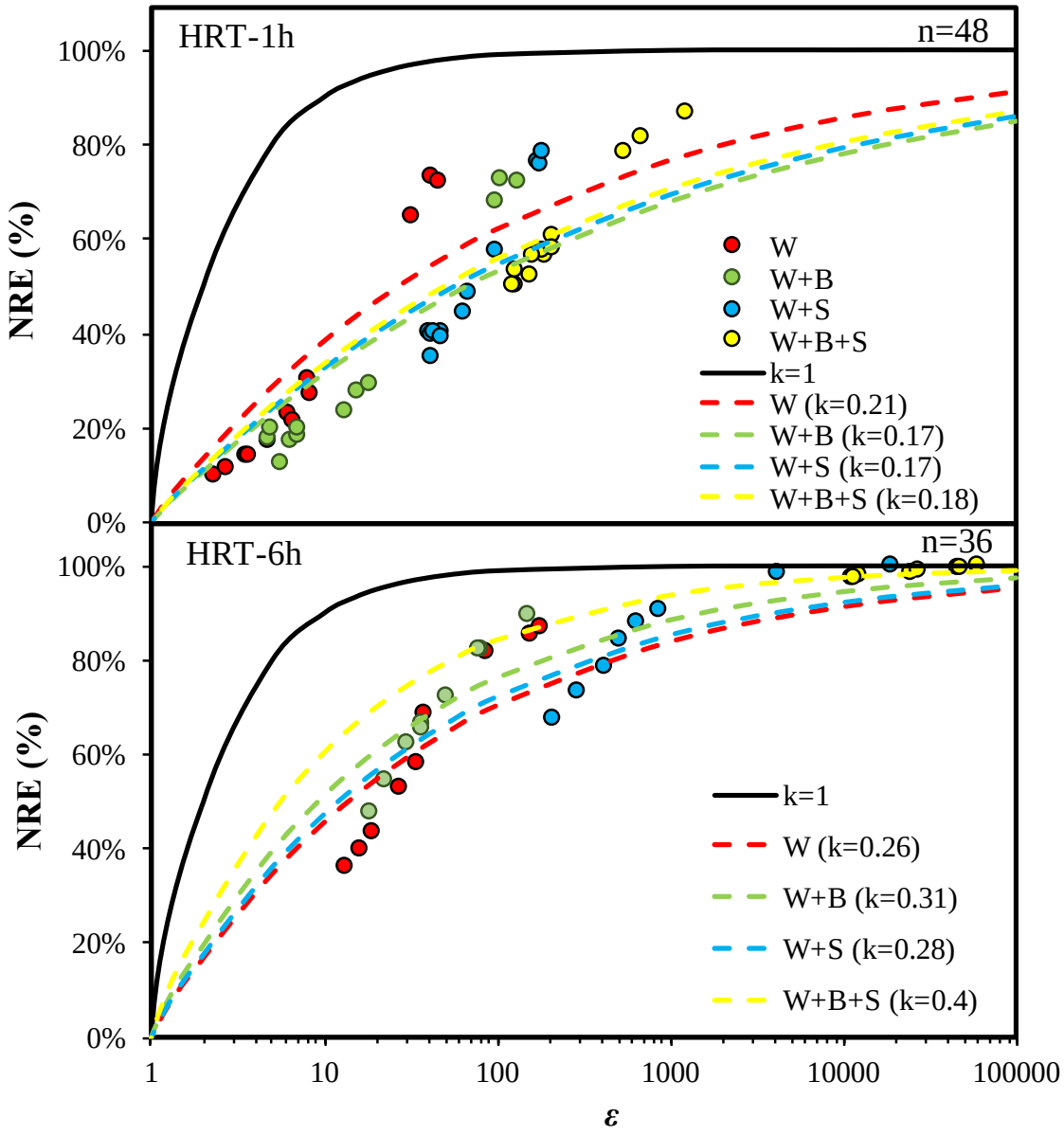

Figure 5.5 Nitrate removal efficiency (NRE) changed with ε (outflow C/N divided by inflow C/N) under different fill-materials, including woodchip (W), woodchip+biochar (W+B), woodchip+silage leachate (W+S), and woodchip+biochar+silage leachate (W+B+S) and conducted at different hydraulic retention time (HRT): a) 1 hour, and b) 6 hour. The influent nitrate concentration was 6.8 mg N L^{-1}. The black real line is a reference (k=1). All the data points were below the reference line.

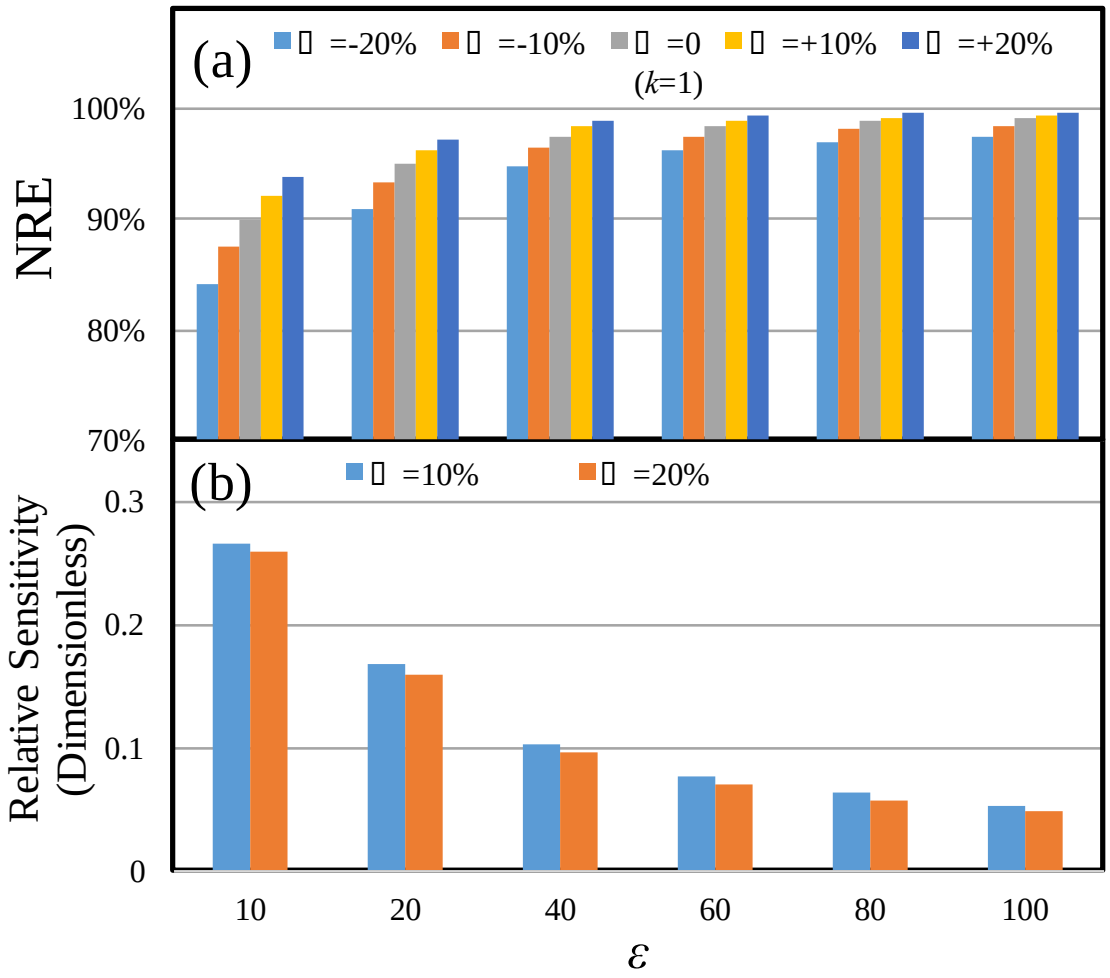

Figure 5.6 (a) Responses and sensitivity of nitrate removal efficiency and (b) relative sensitivity simulated using the nonlinear model which under different values of ε. The base value of RUE was calculated when k=1.

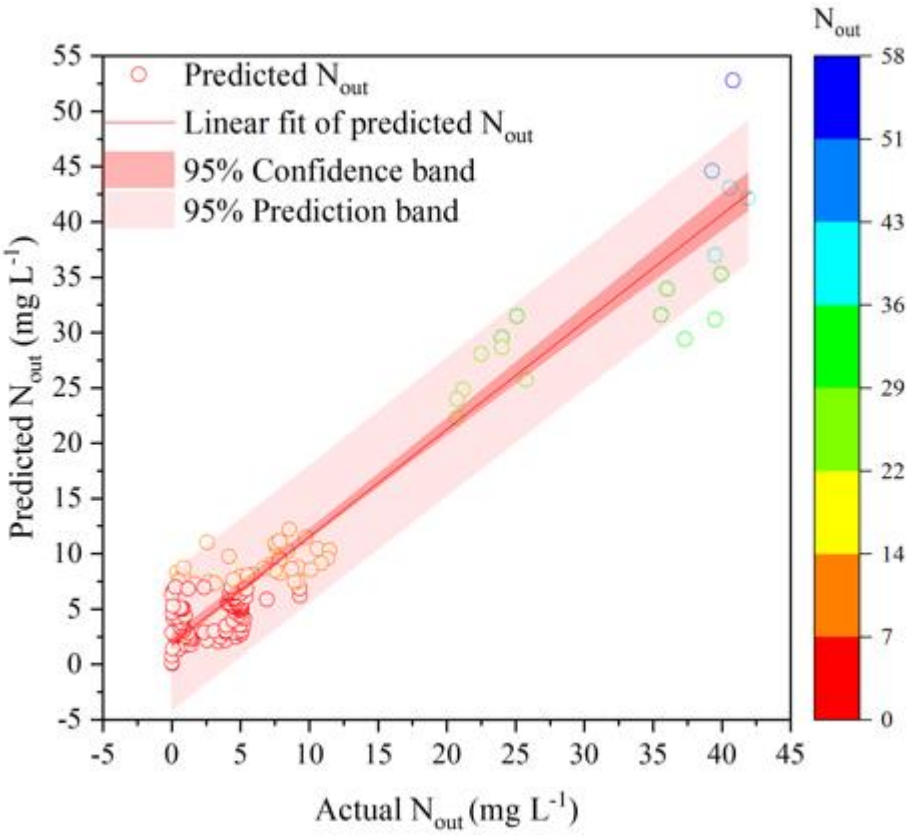

Figure 5.7 The predicted N_{out} (mg NO_3-N L^{-1}) versus experimental N_{out}. 70% of the laboratory and field study data was randomly selected as a calibration, then 30% of the data was used to evaluate the performance of the nonlinear model.

Summary & Conclusion

The five studies described in Chapters 1-5 were designed to improve the nitrate removal performance of denitrifying bioreactors. Bioreactor performance was evaluated relative to the different fill materials and abiotic factors that influence denitrification. Mathematical models were developed to help describe bioreactor efficiency and to identify the abiotic properties that affect efficiency. These models were calibrated using measured data, and tested with data from the peer-reviewed literature.

Chapter 1 systematically reviews 40 types of filling materials, placing them into four main groups: natural carbon (NC), non-natural carbon (NNC), inorganic material (IM), and multi-material (MM). A meta-analysis provided a comparative assessment among the filling materials and indicated that NNC has the highest nitrate removal (NRE & NRR). In addition, the NRR increased with NRE from a holistic review, but a greater uncertainty of NRR was observed when NRE was at a high range (90-100%). The NRR and NRE achieved by the different filling materials in DNBRs varies. We found that nitrate removal is associated with wood types, media C/N ratio, and study scale. Importantly, the ranking order of nitrate removal performance by NRR and NRE is not consistent for the filling materials. Thus, both indexes should be considered in future studies. However, we suggest MM as the optimal material for nitrate removal due to the low cost and wider scope of application. In MMs, adding auxiliary materials into woodchip-based DNBRs was promising for enhancing denitrification and maintaining operation throughout an extended period.

The results presented in Chapter 2 showed that abiotic factors have different interrelationships at lab and field scales, and it was confirmed that pH, DO, HRT, DOC, effective porosity, and media age were the most factors affecting nitrate removal in lab studies. In contrast, temperature, HRT, pH, and effective porosity were the most factors in field studies. Further, a structural equation model (SEM) successfully constructs a framework

to explain how the various abiotic factors, directly and indirectly, affect NRE and NRR (RMSEA=0.008, NFI=0.998).

Chapter 3 illustrated the performance of denitrifying bioreactors amended with biochar and silage leachate. The results showed that adding biochar and silage leachate together could significantly increase NRR, compared with the woodchip bioreactor. Our SEM indicated that this enhancement of nitrate removal could be attributed to the altered physical properties (TOC, pH) induced by biochar addition, as well as the altered physical properties (DO, K_s) induced by silage leachate addition. Thus, adding biochar and silage leachate into a woodchip bioreactor can further benefit bioreactor performance by increasing TOC and decreasing DO, providing a favorable environment for denitrifying bacteria. It was also found that the amended media showed the greatest NRR and NRE at various hydraulic retention times and nitrate loadings. Further, adding biochar and silage leachate alone into woodchip bioreactor could also increase nitrate removal, but removal would primarily be determined by hydraulic retention time and influent nitrate concentration. In addition, we found that biochar addition could increase sulfamethazine and tylosin removal efficiency (RE) at low influent concentrations (<2 mg L^{-1}), while no effects on RE were observed at high antibiotic influent concentrations (25 mg L^{-1}). Future work should evaluate the long-term performance of different fractions of biochar and silage leachate amended woodchip bioreactors for the removal of nitrate and antibiotics.

Chapter 4 characterized the role of hydraulic retention time on the nitrate removal by eight experiments which were conducted under different scales (lab and field), using different media (woodchip, woodchip+biochar, woodchip+silage leachate, woodchip+biochar+silage leachate) and influent nitrate concentration (6.8-70 mg N L^{-1}). Nitrate reduction per length (N_{rd}) was defined and demonstrated to be an acceptable indicator to describe nitrate removal. Two nonlinear models were developed to characterize the N_{rd}, nitrate removal efficiency

(NRE), nitrate removal rate (NRR), and theoretical maximum NRR (NRR_{TM}) by HRT:the Mitscherlich model (MT) and the Michaelis-Menten model (MM). The results showed that N_{rd}, NRR, and NRE could be well fit by the MT and MM models. In contrast, the MT model had a lower RMSE and higher R^2 than the MM model, which indicated that MT performed better than the MM model. In addition, these results indicated that the relationship between NRR and HRT was associated with media, influent nitrate concentration, and scales. The MT model revealed that this change of relationship between NRR and HRT could be determined by fitted parameter *a*, when can be above or below 1. Meanwhile, the optimal HRT (HRT_O) can be predicted by parameters *a* and *b*, which is informative for users of denitrifying bioreactors (DNBRs) when aiming to optimize the nitrate removal performance. Overall, this study provides a tool to characterize nitrate removal as a function of HRT.

Chapter 5 proposed a novel index ε, which is the outflow C/N ratio divided by the inflow C/N ratio. The index was determined to be an independent variable to predict nitrate removal efficiency using a nonlinear model. The nonlinear model was verified by laboratory and field experiments. The results indicated that the model could be used under different conditions, including different influent nitrate concentrations, hydraulic retention times, and media. In addition, it was found that increasing influent nitrate concentration and hydraulic retention time increased the value of the critical parameter *k*, which can be a comprehensive indicator to predict the relationship between C concentration in influent and effluent. The greater *k* will possibly result in a higher nitrate removal efficiency. To successfully build upon these results, further work including verification and application, especially in the field, as well as exploring how other important abiotic factors impact *k*, such as temperature and pH, is required.

APPENDIX

Table S1 Biochar Summary

Feedstock	T (°C)	Yield (%)	Moblie matter (%)	Fixed matter (%)	pH (KCl)	pH (H_2O)	CECa (mmolc kg^{-1})	CECa (molc m^{-2})	C (%)	N (%)	H (%)	O (%)	K (%)	P (%)	Ash b (%)	Volatiles matter (%)[b]	Fixed Cb (%)	C/N ratio	H/C ratioc	O/C ratioc	Aromatic Cd (% of total)	Aromatic clusters	Pore volume(cm^3g^{-1})	SSAe(m^2 g^{-1})	Reference
Broiler litter	350								45.6	4.5	4.0	18.3						10.1	0.09	0.09				60	(Uchimiya et al. 2010)
	700								46.0	2.8	1.4	7.4						16.3	0.03	0.03			0.0018	94	(Uchimiya et al. 2010)
Buffalo weed	300	50	44.2	30.4		8.7			78.1	10.2	4.3	7.4			20.4			7.6	0.05	0.05			0.01	4	(Ahmad et al. 2014)
	700	29	20.9	46.8		12.3			85.0	7.4	1.1	6.6			32.3			11.5	0.01	0.01			0.02	9.3	(Ahmad et al. 2014)
Canola straw	400	27.4							45.7	0.2								240.5							(Tong et al. 2011)
Chicken litter	620	43-49	16	30.8					41.5	2.8	1.2	0.7			53.2			15.0	0.03	0.03					(Ro et al. 2010)
Corn cobs	500	18.9				7.8			77.6	0.9	3.1	5.1			13.3			91.3	0.04	0.04					(Mullen et al. 2010)
Corn stover	600				6.3	6.7	269.4		42.6	0.5	5.5	42.0		0.1	8.8	85.2	6	83.0	1.56	0.74	2	6			(Lehmann et al. 2011)
	350				9.4	9.4	419.3	1.43	60.4	1.2	3.8	23.4		0.2	11.4	48.8	39.8	51.0	0.75	0.29	76.9	19		293	(Lehmann et al. 2011)
	450	15	12.7	28.7					33.2	0.8	1.4	8.6			58.0			41.0	0.04	0.04				12	(Lee et al. 2010)
	500	17				7.2			57.3	1.5	2.9	5.5			32.8			39.0	0.05	0.05				3.1	(Mullen et al. 2010)
	600				9.4	9.4	252.1	0.48	70.6	1.1	2.3	9.4		0.2	16.7	23.5	59.8	66.0	0.39	0.10	88.2	40		527	(Lehmann et al. 2011)
Cottonseed hull	200	83.4	69.3	22.3					51.9	0.6	6.0	40.5			3.1			86.5	0.12	0.12					(Uchimiya et al. 2011)
	350	36.8	34.9	52.6					77.0	1.9	4.5	15.7			5.7			40.5	0.06	0.06				4.7	(Uchimiya et al. 2011)
	500	28.9	18.6	67					87.5	1.5	2.8	7.6			7.9			58.3	0.03	0.03					(Uchimiya et al. 2011)
	650	25.4	13.3	70.3					91.0	1.6	1.3	5.9			8.3			56.9	0.01	0.01				34	(Uchimiya et al. 2011)
	800	24.2	11.4	69.5					90.0	1.9	0.6	7.0			9.2			47.4	0.01	0.01				322	(Uchimiya et al. 2011)
Feed lot	350	51.1	47.9	23.5		9.1			53.3	3.6	4.1	15.7			28.7			14.6	0.08	0.08				1.3	(Cantrell et al. 2012)
	700	32.2	19.8	36.3		10.3			52.4	1.7	0.9	7.2			44.0			30.8	0.02	0.02				145.2	(Cantrell et al. 2012)
Fescue straw	100	99.99	69.6	23.5					48.6	0.6	7.3	44.1			6.9			75.9	0.15	0.15				1.8	(Keiluweit et al. 2010)
	200	96.9	70.7	23.6					47.2	0.6	7.1	45.1			5.7			77.4	0.15	0.15				3.3	(Keiluweit et al. 2010)
	300	75.8	54.4	36.2					59.7	1.0	6.6	32.7			9.4			58.5	0.11	0.11				4.5	(Keiluweit et al. 2010)
	400	37.2	26.8	56.9					77.3	1.2	4.7	16.7			16.3			62.3	0.06	0.06				8.7	(Keiluweit et al. 2010)
	500	31.4	20.3	64.3					82.2	1.1	3.3	13.4			15.4			75.4	0.04	0.04				50	(Keiluweit et al. 2010)

Table S1 continued

	600	29.8	13.5	67.6					89.0	1.0	2.5	7.6		18.9			89.9	0.03	0.03				75	(Keiluweit et al. 2010)
	700	28.8	9.1	71.6					94.2	0.7	1.5	3.6		19.3			134.6	0.02	0.02				139	(Keiluweit et al. 2010)
Oak bark	450		22.8	64.5					71.3	0.5	2.6	13.0		11.1			154.9	0.04	0.04			1.06	1.9	(Mohan et al. 2011)
Oak wood	600				3.2	3.7	182.1		47.1	0.1	5.8	45.2	0.0	0.3	88.6	11.1	444.0	1.48	0.72					(Lehmann et al. 2011)
	350				5.2	4.8	294.2	0.65	74.9	0.2	3.4	20.0	0.0	1.1	60.8	38.1	455.0	0.55	0.20	82.8	18		450	(Lehmann et al. 2011)
	400-450		15.6	78.3					82.8	0.3	2.7	8.1		2.9			267.2	0.03	0.03			0.41	2.7	(Mohan et al. 2011)
	600				7.9	6.4	75.7	0.12	87.5	0.2	2.4	8.2	0.0	1.3	27.5	71.2	489.0	0.33	0.07	86.6	37		642	(Lehmann et al. 2011)
Orange peel	150	82.4							50.6	1.8	6.2	41.0		0.5			28.9	0.12	0.12			0.023	22.8	(Chen and Chen 2009)
	200	61.6							57.9	1.9	5.5	34.4		0.3			30.8	0.10	0.10			0.01	7.8	(Chen and Chen 2009)
	250	48.3							65.1	2.2	5.1	26.5		1.1			29.3	0.08	0.08			0.02	33.3	(Chen and Chen 2009)
	300	37.2							69.3	2.4	4.5	22.2		1.6			29.4	0.07	0.07			0.031	32.3	(Chen and Chen 2009)
	350	33							73.2	2.3	4.2	18.3		2.0			31.8	0.06	0.06			0.01	51	(Chen and Chen 2009)
	400	30							71.7	1.9	3.5	20.8		2.1			37.3	0.05	0.05			0.01	34	(Chen and Chen 2009)
	500	26.9							71.4	1.8	2.3	20.3		4.3			39.0	0.03	0.03			0.019	42.4	(Chen and Chen 2009)
	600	26.7							77.8	1.8	2.0	14.4		4.1			43.2	0.03	0.03			0.008	7.8	(Chen and Chen 2009)
	700	22.2							71.6	1.7	1.8	22.2		2.8			41.6	0.02	0.02			0.035	201	(Chen and Chen 2009)
Paper sludge	105		49.3	17		7.9			45.9	1.5	5.7	46.8		31.5			30.4	0.12	0.12			0.02	4.2	(Ahmad et al. 2014)
	300	65.8	16.6	30.4		7.8			60.0	2.5	3.7	33.8		51.2			24.1	0.06	0.06			0.02	4.3	(Ahmad et al. 2014)
	700	40.3	3.2	21.7		9.9			59.9	1.5	0.7	37.9		73.8			41.0	0.01	0.01			0.07	145.6	(Ahmad et al. 2014)
Peanut shell	300	36.9	60.5	37		7.8			68.3	1.9	3.9	25.9		1.2			35.7	0.06	0.06				3.1	(Ahmad et al. 2012)
	700	21.9	32.7	58.1		10.6			83.8	1.1	1.8	13.3		8.9			73.5	0.02	0.02			0.2	448.2	(Ahmad et al. 2012)
Peanut straw	400	28.2							42.9	1.5							28.6							(Tong et al. 2011)
Pine needles	100	91.2							50.9	0.7	6.2	42.3		1.1			71.6	0.12	0.12				0.7	(Chen and Chen 2009)
	200	75.3							57.1	0.9	5.7	36.3		0.9			64.9	0.10	0.10				6.2	(Chen and Chen 2009)
	250	56.1							61.2	0.9	5.5	32.4		1.2			71.2	0.09	0.09				9.5	(Chen and Chen 2009)
	300	48.6							68.9	1.1	4.3	25.7		1.9			63.8	0.06	0.06				19.9	(Chen and Chen 2009)
	400	30							77.9	1.2	3.0	18.0		2.3			67.1	0.04	0.04			0.044	112.4	(Chen and Chen 2009)
	500	26.1							81.7	1.1	2.3	15.0		2.8			73.6	0.03	0.03			0.095	236.4	(Chen and Chen 2009)

Table S1 continued

	600	20.4							85.4	1.0	1.9	11.8		2.8			87.1	0.02	0.02		0.076	206.7	(Chen and Chen 2009)
	700	14							86.5	1.1	1.3	11.1		2.2			76.6	0.01	0.01		0.186	490.8	(Chen and Chen 2009)
	300	57.6	38.6	54.2		6.4			84.2	3.9	4.4	7.6		7.2			21.7	0.05	0.05			4.1	(Ahmad et al. 2014)
	500	31.8	15.8	72.4		8.1			90.1	4.1	2.1	3.7		11.8			22.0	0.02	0.02		0.015	13.1	(Ahmad et al. 2014)
	700	25	6.2	75		10.6			93.7	3.6	0.6	2.1		18.7			25.7	0.01	0.01		0.12	390.5	(Ahmad et al. 2014)
Pine shaving	100	99.8	77.1	21.7					50.6	0.1	6.7	42.7		1.2			1012.0	0.13	0.13			1.6	(Keiluweit et al. 2010)
	200	95.9	77.1	21.4					50.9	0.0	7.0	42.2		1.5			1272.5	0.14	0.14			2.3	(Keiluweit et al. 2010)
	300	62.2	70.3	28.2					54.8	0.1	6.5	38.7		1.5			1096.0	0.12	0.12			3	(Keiluweit et al. 2010)
	400	35.3	36.4	62.2					74.1	0.1	5.0	20.9		1.1			1235.0	0.07	0.07			28.7	(Keiluweit et al. 2010)
	500	28.4	25.2	72.7					81.9	0.1	3.5	14.5		1.4			1023.8	0.04	0.04			196	(Keiluweit et al. 2010)
	600	23.9	11.1	85.2					89.0	0.1	3.0	8.0		3.7			1483.3	0.03	0.03			392	(Keiluweit et al. 2010)
	700	22	6.3	92					92.3	0.1	1.6	6.0		1.7			1153.8	0.02	0.02			347	(Keiluweit et al. 2010)
Pinewood	700		3.2	57.1		6.6			95.3	0.1	0.8	3.8		38.8			794.2	0.01	0.01		0.13	29	(Liu et al. 2010)
Polar wood	400	32				9.0			67.3	0.8	4.4			3.5			86.3	0.07	0.07			3	(Kloss et al. 2012)
	460					9.2			70.0	1.0	3.5			5.7			73.7	0.05	0.05			8.2	(Kloss et al. 2012)
	525					8.7			77.9	1.1	2.7			6.8			72.8	0.03	0.03			55.7	(Kloss et al. 2012)
Poultry litter	60				7.5	7.5	363		24.6	1.9	3.1	33.8	1.7	36.4	60.5	3.1	13.0	1.51	1.03				(Lehmann et al. 2011)
	350	54.3	42.3	27		8.7			51.1	2.0	1.4	16.0		30.7			26.1	0.03	0.03			3.9	(Cantrell et al. 2012)
	350				9.7	9.7	121.3	2.58	29.3	2.0	16.7	12.0	2.1	51.2	47.2	1.6	15.0	0.57	0.41			47	(Lehmann et al. 2011)
	600				10.3	10.3	58.7	0.63	23.6	0.9	0.4	19.5	2.4	55.8	44.1	0.1	25.0	0.18	0.62			94	(Lehmann et al. 2011)
	700	36.7	18.3	35.5		10.3			45.9	2.1	2.0	10.5		46.2			22.2	0.04	0.04			50.9	(Cantrell et al. 2012)
Poultry manure	300	65.7	19	56.5		8.8			52.9	7.8	3.9	34.7		24.0			6.8	0.07	0.07		0.012	4.3	(Ahmad et al. 2014)
	400	54	8.2	63.8		10.6			51.0	5.4	3.2	39.4		28.0			9.4	0.06	0.06		0.027	11.6	(Ahmad et al. 2014)
	500	72	7.3	68.6		11.0			51.6	5.5	1.9	40.3		24.0			9.4	0.04	0.04		0.022	5.8	(Ahmad et al. 2014)
	600	47	5.4	71.6		11.5			52.3	4.2	1.4	40.3		22.6			12.3	0.03	0.03		0.019	3.7	(Ahmad et al. 2014)
	700	47	4.1	69.6		10.7			56.1	4.2	1.5	37.2		24.2			13.5	0.03	0.03		0.02	6.6	(Ahmad et al. 2014)
Rapeseed plant	400	39.4	27.1	60.7					71.3	1.4	3.9	10.8		12.2			49.9	0.06	0.06		1.244	16	(Karaosmanoğlu et al. 2000)
	500	35.6	17.5	69.6					75.0	1.4	2.6	7.8		12.9			53.2	0.03	0.03		1.15	15.7	(Karaosmanoğlu et al. 2000)

Table S1 continued

	600	32.2	11.5	74.7		78.5	1.5	1.9	3.9			13.9		51.3	0.02	0.02		1.263	17.6	(Karaosmanoğlu et al. 2000)
	700	29.6	9	76.7		79.5	1.4	1.2	3.3			14.4		58.9	0.02	0.02		1.254	19.3	(Karaosmanoğlu et al. 2000)
	800	28.2	6	79.7		79.5	1.5	0.7	2.6			15.3		54.8	0.01	0.01		1.155	19	(Karaosmanoğlu et al. 2000)
	900	27.9	16.1	3.6		79.9	1.6	0.4	1.7					50.9	0.01	0.01		1.323	140.4	(Karaosmanoğlu et al. 2000)
Rice husk	500					42.1	0.5	2.2	12.1			42.2		84.2	0.05	0.05		0.028	34.4	
Rice straw	250	63.2				57.2	1.1			16.9	0.1	20.5	49.6	52.3						(Peng et al. 2011)
	250	53.7				63.5	1.2			18.9	0.2	24.3	41.2	51.0						(Peng et al. 2011)
	250	45.5				63.6	1.6			21.2	0.2	28.5	33.4	39.6						(Peng et al. 2011)
	300	49.2				65.5	1.4			19.8	0.2	28.6	36.5	47.7						(Peng et al. 2011)
	300	46.2				67.6	1.5			19.9	0.2	30.7	36.9	45.9						(Peng et al. 2011)
	300	40.4				65.7	1.7			21.5	0.2	34.6	28.4	38.1						(Peng et al. 2011)
	350	42.2				66.1	1.4			20.7	0.2	32.5	28	47.8						(Peng et al. 2011)
	350	38.9				66.2	1.5			22.2	0.2	35.5	25.3	43.7						(Peng et al. 2011)
	350	31				65.8	1.7			26.1	0.2	45.7	19.4	38.6						(Peng et al. 2011)
	400	37.5				71.3	1.5			24.6	0.2	36.2	24.7	48.9						(Peng et al. 2011)
	400	34.6				69.7	1.3			26.7	0.2	38.8	20.9	55.7						(Peng et al. 2011)
	400	28.9				70.7	1.2			29.9	0.3	47.0	19.6	59.9						(Peng et al. 2011)
	450	34.1				70.6	1.0			26.4	0.2	39.0	12.2	73.6						(Peng et al. 2011)
	450	31.9				72.9	1.1			27.8	0.2	43.5	11	67.5						(Peng et al. 2011)
	450	26				72.0	1.1			31.4	0.3	53.1	10.4	66.1						(Peng et al. 2011)
Saw dust	450		40.1	57.2	5.9	72.0	0.1	3.5	24.4			1.1		900.0	0.05	0.05				(Lin et al. 2012)
	550		13.6	82.6	12.1	85.0	0.3	1.0	13.7			2.8		283.3	0.01	0.01				(Lin et al. 2012)
Sewage sludge	300	70.1	19.8	22.5	6.8	30.7	4.1	3.1	11.2			56.6		7.5	0.10	0.10		0.01	4.5	(Ahmad et al. 2014)
	400	57.4	8.8	23.5	6.6	26.6	4.1	1.9	10.7			67.1		6.5	0.07	0.07		0.02	14.1	(Ahmad et al. 2014)
	500	53.8	7.5	20	7.3	20.2	2.8	1.1	9.8			71.9		7.1	0.05	0.05		0.04	26.2	(Ahmad et al. 2014)
	600	51.2	5.8	19.1	8.3	24.8	2.8	0.8	8.4			74.6		8.9	0.03	0.03		0.04	35.8	(Ahmad et al. 2014)

Table S1 continued

	700	50.3	4.1	16.6	8.1	22.0	1.7	0.6	7.1	76.6	12.7	0.03	0.03	0.05	54.8	(Ahmad et al. 2014)
Soybean stover	300	37	46.3	38.8	7.3	68.8	1.9	4.3	25.0	10.4	36.6	0.06	0.06		5.6	(Ahmad et al. 2012)
	700	21.6	14.7	67.7	11.3	82.0	1.3	1.3	15.5	17.2	63.1	0.02	0.02	0.19	420.3	(Ahmad et al. 2012)
Soybean straw	400	24.7				44.1	2.4				18.5					(Tong et al. 2011)
Spruce wood	400	36			6.9	63.5	1.0	5.5		1.9	62.3	0.09	0.09		1.8	(Kloss et al. 2012)
	460				8.7	79.6	1.2	3.3		3.0	64.2	0.04	0.04		14.2	(Kloss et al. 2012)
	535				8.6	78.3	1.2	3.0		4.7	66.9	0.04	0.04		40.4	(Kloss et al. 2012)
Swine solid	350	62.3	49.8	17.7	8.4	51.5	3.5	4.9	11.1	32.5	14.6	0.10	0.10		0.9	(Cantrell et al. 2012)
	700	36.4	13.4	33.8	9.5	44.1	2.6	0.7	4.0	52.9	16.9	0.02	0.02		4.1	(Cantrell et al. 2012)
	620	43-49	14.1	41.2		50.7	3.3	1.9	<0.01	44.7	15.6	0.04	0.04			(Ro et al. 2010)
Tire rubber	200	93.5				74.7		6.4	3.9	15.0		0.09	0.09			(Lian et al. 2011)
	400	59.3				77.7		3.6	3.3	15.4		0.05	0.05	0.08	24.2	(Lian et al. 2011)
	600	54.5				81.3		1.7	1.4	15.6		0.02	0.02	0.12	51.5	(Lian et al. 2011)
	800	43				86.0	0.5	0.9	2.2	10.5	183.0	0.01	0.01	0.11	50	(Lian et al. 2011)
Turkey litter	350	58.1	42.1	23.1	8.0	49.3	4.1	3.6	15.4	34.8	12.1	0.07	0.07		2.6	(Cantrell et al. 2012)
	700	39.9	20.8	29.2	9.9	44.8	1.9	0.9	5.8	49.9	23.1	0.02	0.02		66.7	(Cantrell et al. 2012)
Wheat straw	400	34			9.1	65.7	1.1	4.1		9.7	62.6	0.06	0.06		4.8	(Kloss et al. 2012)
	460				8.7	72.4	1.1	3.2		12.0	67.7	0.04	0.04		2.8	(Kloss et al. 2012)
	525				9.2	72.4	1.0	2.8		12.7	69.6	0.04	0.04		14.2	(Kloss et al. 2012)

Table S2 Silage leachate summary

No	Reference	Source	Leachate Source	Site	pH	NO_3^- (mg/L)	NH_4^+ (mg/L)	Cl^- (mg/L)	BOD_5 (mg/L)	COD (mg/L)	TOC (mg/L)	TP (mg/L)	TN (mg/L)	SRP (mg/L)	TKN (mg/L)
1	(Holly et al. 2018)	Bunker silos	Dairy Silage	Wisconsin, USA	6.36				1451	2997		28		20	83
2	(Holly et al. 2018)	Bunker silos	Dairy Silage	Wisconsin, USA	5.44				2733	6827		50		35	102
3	(Holly et al. 2018)	Bunker silos	Dairy Silage	Wisconsin, USA	4.24				2288	5899		44		39	177
4	(Holly et al. 2018)	Bunker silos	Dairy Silage	Wisconsin, USA	5.41					8848		71		67	270
5	(Holly et al. 2018)	Bunker silos	Dairy Silage	Wisconsin, USA	5.34					5220		37		31	175
6	(Holly et al. 2018)	Bunker silos	Dairy Silage	Wisconsin, USA	5.25					6225		46		38	205
7	(Holly et al. 2018)	Bunker silos	Dairy Silage	Wisconsin, USA	5.53					3427		26		21	119
8	(Holly et al. 2018)	Bunker silos	Dairy Silage	Wisconsin, USA	5.54					5140		32		27	199
9	(Holly et al. 2018)	Bunker silos	Dairy Silage	Wisconsin, USA	5.08					4800		35		31	204
10	(Chiumenti et al. 2018)		Corn Silage	Gorizia, northeastern Italy	4.08										4.1
11	(Chiumenti et al. 2018)		Rye Grass	Gorizia, northeastern Italy	4.16										14
12	(Chiumenti et al. 2018)		Alfalfa	Gorizia, northeastern Italy											16.05

Table S2 continued

13	(Chiumenti et al. 2018)	Triticale	Gorizia, northeastern Italy	4.04					5.4
14	(Chiumenti et al. 2018)	Straw	Gorizia, northeastern Italy						5.3
15	(Chiumenti et al. 2018)	Input mix	Gorizia, northeastern Italy	7.84		204.4			5.05
16	(Chiumenti et al. 2018)	Leachate	Gorizia, northeastern Italy	8.45		29.5			4.93
17	(Chiumenti et al. 2018)	Digestate	Gorizia, northeastern Italy	9.07		133.6			5.26
18	(Arnold et al., 2000)	Grass silage		5.8		80960	21400		
19	(Arnold et al., 2000)	Grass silage		3.7		34440	22970		
20	(Arnold et al., 2000)	Grass silage		4.2		16410	6320		
21	(Deans and Svoboda, 1992)	Grass silage		4.2	33800	46200		2920	
22	(Deans and Svoboda, 1992)	Grass silage		4.2	37900	49400		2750	
23	(Deans and Svoboda, 1992)	Grass silage		3.9	46400	71600		3340	

Table S2 continued

24	(Galanos et al., 1995)	Grass silage	4.5	68500	800	4010
25	(Galanos et al., 1995)	Grass silage	4.7	72500	850	4120
26	(Galanos et al., 1995)	Grass silage	4.2	61800	740	3620
27	(Galanos et al., 1995)	Grass silage	4.4	61800	840	3870
28	(O'Donnell et al., 1995)	Unwilted grass silage	4.4			
29	(O'Donnell et al., 1995)	Unwilted grass silage	4			
30	(O'Donnell et al., 1995)	Unwilted grass silage	4			
31	(O'Donnell et al., 1995)	Unwilted grass silage	3.8			
32	(Faulkner et al. 2011)	Corn and hay Silage		4		
33	(Faulkner et al. 2011)	Corn and hay Silage		1		

Table S2 continued

34	(Stephens et al., 1997)		Grass silage				44000		
35	(Stephens et al., 1997)		Grass silage				64000		
36	(Faulkner et al. 2011)	Bunker silos	Maize silage	Western New York, USA	1.7	60	96		0.08
37	(Faulkner et al. 2011)	Bunker silos	Maize silage	Western New York, USA	0.9	38.5	69		3.03
38	(Faulkner et al. 2011)	Bunker silos	Maize silage	Western New York, USA	5.2	7.2	53		0.25
39	(Faulkner et al. 2011)	Bunker silos	Maize silage	Western New York, USA	1	4	13		0.39
40	(Faulkner et al. 2011)	Bunker silos	Maize silage	Western New York, USA	1.8	12.5	34		0.12
41	(Faulkner et al. 2011)	Bunker silos	Maize silage	Western New York, USA	0.3	3.4	73		0.05
42	(Faulkner et al. 2011)	Bunker silos	Maize silage	Western New York, USA	0.3	18.4	56		1.22
43	(Faulkner et al. 2011)	Bunker silos	Maize silage	Western New York, USA	5.4	3.7	44		0.25

Table S2 continued

44	(Faulkner et al. 2011)	Bunker silos	Maize silage	Western New York, USA	1.1	1.6	20	0.15
45	(Faulkner et al. 2011)	Bunker silos	Maize silage	Western New York, USA	12	2.4	4	0.11
46	(Faulkner et al. 2011)	Bunker silos	Maize silage	Western New York, USA	0.3	227.8	106	13.91
47	(Faulkner et al. 2011)	Bunker silos	Maize silage	Western New York, USA	0.1	115.4	101	9.88
48	(Faulkner et al. 2011)	Bunker silos	Maize silage	Western New York, USA	0.3	55.6	78	1.23
49	(Faulkner et al. 2011)	Bunker silos	Maize silage	Western New York, USA	9	2.2	21	0.67
50	(Faulkner et al. 2011)	Bunker silos	Maize silage	Western New York, USA	4.3	1.8	8	0.08
51	(Faulkner et al. 2011)	Bunker silos	Maize silage	Western New York, USA	0.1	6.6	53	0.07
52	(Faulkner et al. 2011)	Bunker silos	Maize silage	Western New York, USA	0.1	25.5	51	0.51
53	(Faulkner et al. 2011)	Bunker silos	Maize silage	Western New York, USA	0.2	53.8	78	0.75

Table S2 continued

54	(Faulkner et al. 2011)	Bunker silos	Maize silage	Western New York, USA	0.3	9.1	50	0.05
55	(Faulkner et al. 2011)	Bunker silos	Maize silage	Western New York, USA	7.5	4.4	56	0.43
56	(Faulkner et al. 2011)	Bunker silos	Maize silage	Western New York, USA	1.2	72.6	86	11.27
57	(Faulkner et al. 2011)	Bunker silos	Maize silage	Western New York, USA	2.2	33.1	62	2.83
58	(Faulkner et al. 2011)	Bunker silos	Maize silage	Western New York, USA	0.7	9.9	31	2.48
59	(Faulkner et al. 2011)	Bunker silos	Maize silage	Western New York, USA	1.1	9	23	2.3
60	(Faulkner et al. 2011)	Bunker silos	Maize silage	Western New York, USA	3.6	2.3	109	0.15
61	(Faulkner et al. 2011)	Bunker silos	Maize silage	Western New York, USA	0.4	61.3	105	4.79
62	(Faulkner et al. 2011)	Bunker silos	Maize silage	Western New York, USA	0.8	28.8	72	1.99
63	(Faulkner et al. 2011)	Bunker silos	Maize silage	Western New York, USA	0.3	16.3	48	1.04

Table S2 continued

64	(Faulkner et al. 2011)	Bunker silos	Maize silage	Western New York, USA	1.3	9.2	40					0.4
65	(Tikkisetty and Kuperus 2004)		Silage leachate	New Zealand				60000		1000	23000	

Table S3 Details of meta-analysis by the effect size of NRR

Carbon type	No	Wood type	Nation	Scale	Year	Reference	T-number	T-mean	T-SD
NC_1	1	S	New zealand	L	2010	(Cameron and Schipper 2010)	15	8.32	3.26
NC_1	2	H	New zealand	L	2010	(Cameron and Schipper 2010)	15	7.79	2.90
NC_1	3	S	New zealand	L	2010	(Cameron and Schipper 2010)	15	9.69	3.67
NC_1	4	H	New zealand	L	2010	(Cameron and Schipper 2011)	15	11.77	2.16
NC_1	5	H	New zealand	L	2010	(Cameron and Schipper 2011)	20	5.97	3.15
NC_1	6		USA	F	2016	(David et al. 2016)	221	18.38	20.07
NC_1	7		Canada	F	2006	(Van Driel et al. 2006)	44	3.18	3.14
NC_1	8		Canada	F	2006	(Van Driel et al. 2006)	28	3.24	1.62
NC_1	9		USA	L	2015	(Easton et al. 2015)	48	1.31	0.57
NC_1	10		USA	L	2015	(Easton et al. 2015)	48	1.38	0.50
NC_1	11		USA	L	2015	(Easton et al. 2015)	48	1.46	0.42
NC_1	12		USA	L	2015	(Easton et al. 2015)	48	1.43	0.47
NC_1	13	S	New zealand	F	2011	(Long et al. 2011)	21	1.67	0.92
NC_1	14	H	USA	L	2016	(Pluer et al. 2016)	6	6.09	1.11
NC_1	15	H	Danmark	F	2020	(Aalto et al. 2020)	6	5.55	2.52
NC_1	16	S	Ireland	L	2012	(Healy et al. 2012)	22	0.93	0.16
NC_1	17	S	Ireland	L	2012	(Healy et al. 2012)	22	0.93	0.16
NC_1	18	S	Ireland	L	2012	(Healy et al. 2012)	22	0.91	0.16

Table S3 continued

NC_1	19	S	New zealand	F	2011	(Warneke et al. 2011a)	7	6.54	3.50
NC_1	20		USA	F	2010	(Woli et al. 2010)	35	0.55	0.37
NC_1	21	S	New zealand	F	2010	(Schipper et al. 2010)	35	13.68	6.40
NC_1	22	S	New zealand	F	2010	(Schipper et al. 2010)	71	3.03	2.50
NC_1	23	S	New zealand	F	2010	(Schipper et al. 2010)	30	0.94	1.14
NC_1	24	S	Canada	L	2010	(Robertson 2010)	20	16.24	19.97
NC_1	25	S	Canada	L	2010	(Robertson 2010)	24	8.75	10.96
NC_1	26	S	Canada	L	2010	(Robertson 2010)	24	7.30	4.17
NC_1	27	S	Canada	L	2010	(Robertson 2010)	24	4.26	1.68
NC_1	28	S	New zealand	L	2011	(Warneke et al. 2011b)	2	1.44	0.12
NC_1	29	S	New zealand	L	2011	(Warneke et al. 2011b)	2	2.57	0.64
NC_1	30	H	New zealand	L	2011	(Warneke et al. 2011b)	2	1.65	0.02
NC_1	31	S	New zealand	L	2011	(Warneke et al. 2011b)	2	2.36	0.24
NC_1	32	H	New zealand	L	2011	(Warneke et al. 2011b)	2	2.93	0.39
NC_1	33	S	Canada	F	2010	(Elgood et al. 2010)	30	0.79	0.56
NC_1	34	S	New zealand	F	1998	(Schipper and Vojvodic-Vukovic 1998)	6	0.36	0.22
NC_1	35	S	New zealand	F	1998	(Schipper and Vojvodic-Vukovic 1998)	10	0.13	0.13
NC_1	36		Ireland	L	2007	(Healy et al. 2007)	71	0.90	0.70

Table S3 continued

NC_1	37		USA	L	2018	(Roser et al. 2018)	12	5.17	2.74
NC_1	38		Canada	F	2009	(Robertson et al. 2009)	91	2.73	1.81
NC_1	39		Canada	F	2009	(Robertson and Merkley 2009)	61	3.31	2.38
NC_1	40		USA	F	2015	(Bell et al. 2015)	21	16.12	9.51
NC_1	41	H	USA	L	2016	(Feyereisen et al. 2016)	54	1.69	0.69
NC_1	42	H	USA	L	2016	(Feyereisen et al. 2016)	49	3.23	1.98
NC_1	43		USA	L	2015	(Hoover et al. 2015)	99	2.14	2.24
NC_1	44	H	USA	L	2015	(Lepine et al. 2015)	78	30.59	14.64
NC_1	45	H	USA	L	2015	(Lepine et al. 2015)	78	17.28	8.91
NC_1	46	H	USA	L	2015	(Lepine et al. 2015)	78	11.40	6.66
NC_1	47	H	USA	L	2015	(Lepine et al. 2015)	78	9.22	5.17
NC_1	48	H	USA	L	2009	(Greenan et al. 2009)	144	2.12	1.17
NC_1	49	H	USA	L	2009	(Greenan et al. 2009)	109	2.67	0.96
NC_1	50	H	USA	L	2009	(Greenan et al. 2009)	131	2.57	0.94
NC_1	51	H	USA	L	2016	(Hua et al. 2016)	41	9.97	0.01
NC_1	52	H	USA	L	2016	(Hua et al. 2016)	46	18.68	1.40
NC_1	53		USA	F	2012	(Schmidt and Clark 2012)	30	2.12	0.21
NC_1	54		USA	F	2012	(Schmidt and Clark 2012)	30	0.95	0.12
NC_1	55		USA	F	2012	(Schmidt and Clark 2012)	30	3.34	0.65
NC_1	56		USA	F	2015	(Bock et al. 2015b)	8	2.08	1.29

Table S3 continued

NC_1	57	S	Lithuania	F	2020	(Povilaitis and Matikienė 2020)	126	1.61	1.03
NC_1	58	S	New zealand	L	2012	(Cameron and Schipper 2012)	2	3.60	1.98
NC_1	59	S	New zealand	L	2012	(Cameron and Schipper 2012)	2	4.10	0.93
NC_1	60	S	New zealand	L	2012	(Cameron and Schipper 2012)	2	4.20	1.56
NC_1	61	S	New zealand	L	2012	(Cameron and Schipper 2012)	2	4.45	1.20
NC_1	62	S	New zealand	L	2012	(Cameron and Schipper 2012)	2	3.75	0.64
NC_1	63	H	New zealand	L	2012	(Cameron and Schipper 2012)	2	3.95	1.34
NC_1	64		USA	L	2015	(Bock et al. 2015a)	3	4.44	0.63
NC_1	65		USA	L	2015	(Easton et al. 2015)	33	3.81	2.98
NC_1	66	S	Canada	F	2016	(Choudhury et al. 2016)	27	1.09	1.96
NC_1	67	S	Canada	F	2016	(Choudhury et al. 2016)	15	0.21	0.51
NC_1	68	S	Ireland	L	2015	(Healy et al. 2015)	64	1.49	0.62
NC_1	69		USA	F	2017	(Rosen and Christianson 2017)	65	1.47	0.64
NC_1	70		USA	F	2017	(Rosen and Christianson 2017)	52	0.69	0.62
NC_1	71		USA	L	2019	(Maxwell et al. 2019b)	658	15.66	6.53
NC_1	72		USA	L	2019	(Maxwell et al. 2019a)	1752	7.81	3.88
NC_1	73		USA	L	2018	(Li et al. 2018)	42	39.18	9.78
NC_1	74	S	USA	L	2013	(Schmidt and Clark 2013)	52	2.68	2.14
NC_1	75		USA	L	2011	(Christianson et al. 2011)	12	4.44	2.80

Table S3 continued

NC_1	76	S	New zealand	F	2020	(Rivas et al. 2020)	39	0.55	0.49
NC_1	77	S	New zealand	F	2020	(Rivas et al. 2020)	86	1.47	1.85
NC_1	78	H	USA	F	2019	(Pluer et al. 2019)	19	40.01	53.88
NC_1	79	H	USA	F	2019	(Pluer et al. 2019)	16	10.59	10.17
NC_1	80	S	New zealand	F	2020	(Corbett et al. 2020)	12	22.62	6.48
NC_1	81	S	New zealand	F	2020	(Corbett et al. 2020)	9	2.09	0.79
NC_1	82	S	China	L	2015	(Liang et al. 2015)	14	3.93	0.81
NC_1	83	H	Canada	F	2008	(Robertson et al. 2008)	30	3.12	1.87
NC_1	84	H	Finland	L	2020	(Kiani et al. 2020)	26	16.46	7.48
NC_1	85	H	USA	L	2020	(Pluer et al. 2020)	20	22.88	11.54
NC_1	86	H	USA	L	2020	(Pluer et al. 2020)	22	23.03	12.50
NC_1	87	H	USA	L	2020	(Pluer et al. 2020)	22	24.23	15.22
NC_1	88	H	USA	L	2019	(Coleman et al. 2019)	40	12.22	2.53
NC_1	89	H	USA	L	2019	(Coleman et al. 2019)	36	12.63	2.58
NC_1	90	H	USA	L	2019	(Coleman et al. 2019)	48	12.18	2.00
NC_1	91	H	USA	L	2019	(Coleman et al. 2019)	37	12.09	1.85
NC_1	92	H	USA	L	2019	(Coleman et al. 2019)	32	14.32	4.16
NC_1	93	H	USA	L	2019	(Coleman et al. 2019)	35	14.58	4.09
NC_1	94	H	USA	L	2019	(Coleman et al. 2019)	31	4.83	0.55
NC_1	95	H	USA	L	2019	(Coleman et al. 2019)	26	4.89	0.46

Table S3 continued

NC_1	96	H	USA	L	2019	(Coleman et al. 2019)	32	8.68	1.14
NC_1	97	H	USA	L	2019	(Coleman et al. 2019)	23	11.17	0.74
NC_1	98	H	USA	L	2019	(Coleman et al. 2019)	33	11.91	2.91
NC_1	99	H	USA	L	2019	(Coleman et al. 2019)	39	12.06	2.48
NC_2	1		USA	L	2016	(Feyereisen et al. 2016)	54	5.70	1.87
NC_2	2		USA	L	2016	(Feyereisen et al. 2016)	49	21.51	5.08
NC_3	1		Ireland	L	2012	(Healy et al. 2012)	12	0.96	0.11
NC_3	2		Ireland	L	2012	(Healy et al. 2012)	12	0.96	0.11
NC_3	3		Ireland	L	2012	(Healy et al. 2012)	12	0.96	0.11
NC_3	4		USA	L	2016	(Feyereisen et al. 2016)	54	5.43	1.87
NC_3	5		USA	L	2016	(Feyereisen et al. 2016)	49	22.51	7.14
NC_3	6		Ireland	L	2015	(Healy et al. 2015)	33	1.32	0.55
NC_4	1		China	L	2012	(Liu et al. 2015)	16	1.58	0.78
NC_4	2		China	L	2015	(Liang et al. 2015)	14	5.53	0.51
NC_4	3		China	L	2015	(Liang et al. 2015)	17	6.52	2.13
NC_4	4		China	L	2015	(Liang et al. 2015)	14	8.50	3.50
NC_4	5		China	L	2015	(Liang et al. 2015)	8	0.39	0.24
NC_4	6		China	L	2015	(Liang et al. 2015)	14	3.32	1.78
NC_4	7		China	L	2015	(Liang et al. 2015)	17	6.57	2.17
NC_4	8		China	L	2015	(Liang et al. 2015)	17	6.53	2.15

Table S3 continued

NC_5	1	New zealand	L	2010	(Cameron and Schipper 2010)	15	17.13	11.43
NC_5	2	New zealand	L	2010	(Cameron and Schipper 2010)	15	19.79	9.39
NC_5	3	New zealand	L	2011	(Warneke et al. 2011b)	4	4.18	1.06
NC_5	4	New zealand	L	2012	(Cameron and Schipper 2012)	2	9.15	1.91
NC_6	1	New zealand	L	2010	(Cameron and Schipper 2010)	15	28.51	11.39
NC_6	2	New zealand	L	2011	(Warneke et al. 2011b)	4	5.05	0.44
NC_6	3	USA	L	2018	(Roser et al. 2018)	12	14.84	7.01
NC_6	4	USA	L	2016	(Feyereisen et al. 2016)	54	7.74	2.28
NC_6	5	USA	L	2016	(Feyereisen et al. 2016)	49	33.33	4.69
NC_6	6	New zealand	L	2011	(Cameron and Schipper 2011)	43	23.39	13.29
NC_6	7	New zealand	L	2011	(Cameron and Schipper 2011)	42	24.67	10.56
NC_6	8	New zealand	L	2012	(Cameron and Schipper 2012)	2	17.40	3.39
NC_6	9	USA	L	2016	(Sharrer et al. 2016)	48	37.72	7.01
NC_6	10	USA	L	2016	(Sharrer et al. 2016)	53	7.32	1.46
NC_7	1	New zealand	L	2011	(Warneke et al. 2011b)	4	4.12	0.74
NC_7	2	New zealand	L	2010	(Cameron and Schipper 2010)	15	14.79	7.35
NC_7	3	New zealand	L	2012	(Cameron and Schipper 2012)	2	6.80	1.41
NC_8	1	Ireland	L	2015	(Healy et al. 2015)	21	1.01	0.13
NC_8	2	Ireland	L	2015	(Healy et al. 2015)	21	0.98	0.13
NC_8	3	Ireland	L	2015	(Healy et al. 2015)	21	1.00	0.13

Table S3 continued

NC_9	1	China	L	2019	(Yao et al. 2019)	90	10.05	4.98
NC_9	2	China	L	2019	(Yao et al. 2019)	90	13.11	5.35
NC_9	3	China	L	2019	(Yao et al. 2019)	90	15.02	1.94
NNC_1	1	Ireland	L	2012	(Healy et al. 2012)	23	0.93	0.16
NNC_1	2	Ireland	L	2012	(Healy et al. 2012)	23	0.92	0.16
NNC_1	3	Ireland	L	2012	(Healy et al. 2012)	23	0.93	0.16
NNC_1	4	Ireland	L	2015	(Healy et al. 2015)	29	1.81	0.79
NNC_2	1	USA	L	2015	(Easton et al. 2015)	45	9.46	10.99
NNC_3	1	Germany	L	2000	(Boley et al. 2000)	13	1433.5	750.71
NNC_4	2	Germany	L	2000	(Boley et al. 2000)	13	767.33	511.91
NNC_4	4	Japan	L	2002	(Honda and Osawa 2002)	30	72.09	21.53
NNC_5	3	Germany	L	2000	(Boley et al. 2000)	13	1104.8	900.67
NNC_5	5	China	L	2009	(Zhou et al. 2009)	58	273.73	129.79
IM_1	1	USA	L	2015	(Easton et al. 2015)	45	6.71	5.83
IM_2	1	USA	L	2015	(Easton et al. 2015)	45	7.30	6.23
IM_3	1	China	L	2019	(Xu et al. 2019)	61	2.75	1.46
MM_1	1	Canada	L	1994	(Blowes et al. 1994)	12	0.66	0.26
MM_2	1	Canada	L	1994	(Blowes et al. 1994)	12	1.28	0.48
MM_3	1	China	L	2017	(Li et al. 2017)	23	20.10	2.80
MM_4	1	USA	L	2018	(Roser et al. 2018)	4	20.48	9.48

Table S3 continued

MM_4	2	USA	L	2018	(Roser et al. 2018)	4	7.65	1.77
MM_4	3	USA	L	2018	(Roser et al. 2018)	4	20.25	7.82
MM_5	1	USA	L	2018	(Roser et al. 2018)	4	16.33	5.83
MM_5	2	USA	L	2018	(Roser et al. 2018)	4	6.40	0.43
MM_5	3	USA	L	2018	(Roser et al. 2018)	4	19.83	7.72
MM_6	1	USA	L	2016	(Sharrer et al. 2016)	48	45.94	8.39
MM_6	2	USA	L	2016	(Sharrer et al. 2016)	53	9.46	1.70
MM_7	1	Iran	L	2017	(Tangsir et al. 2017)	19	35.78	7.50
MM_7	2	Iran	L	2017	(Tangsir et al. 2017)	20	11.08	2.02
MM_8	1	China	L	2009	(Ruan et al. 2009)	45	0.40	0.15
MM_9	1	USA	L	2016	(Hua et al. 2016)	87	11.32	4.07
MM_{10}	1	USA	L	2016	(Pluer et al. 2016)	6	7.31	1.65
MM_{10}	2	USA	L	2018	(Roser et al. 2018)	12	3.54	2.47
MM_{10}	3	USA	L	2018	(Bock et al. 2018)	149	0.88	1.80
MM_{10}	4	USA	L	2015	(Bock et al. 2015b)	8	2.19	1.25
MM_{10}	5	Lithuania	F	2020	(Povilaitis and Matikienė 2020)	119	1.81	1.13
MM_{10}	6	USA	L	2015	(Bock et al. 2015a)	24	12.15	7.18
MM_{10}	7	USA	L	2019	(Pluer et al. 2019)	16	24.31	40.49
MM_{10}	8	USA	L	2019	(Pluer et al. 2019)	13	12.54	11.19

Table S3 continued

MM_{10}	9	Finland	L	2020	(Kiani et al. 2020)	26	15.16	6.80
MM_{10}	10	USA	L	2019	(Coleman et al. 2019)	41	10.68	3.19
MM_{10}	11	USA	L	2019	(Coleman et al. 2019)	42	11.86	2.27
MM_{10}	12	USA	L	2019	(Coleman et al. 2019)	46	9.79	2.27
MM_{10}	13	USA	L	2019	(Coleman et al. 2019)	43	14.18	3.88
MM_{10}	14	USA	L	2019	(Coleman et al. 2019)	48	12.52	8.87
MM_{10}	15	USA	L	2019	(Coleman et al. 2019)	32	15.22	4.23
MM_{10}	16	USA	L	2019	(Coleman et al. 2019)	42	13.44	7.55
MM_{10}	17	USA	L	2019	(Coleman et al. 2019)	40	14.83	2.02
MM_{10}	18	USA	L	2019	(Coleman et al. 2019)	32	17.73	9.75
MM_{10}	19	USA	L	2019	(Coleman et al. 2019)	36	24.88	8.19
MM_{10}	20	USA	L	2019	(Coleman et al. 2019)	25	15.46	4.35
MM_{10}	21	USA	L	2019	(Coleman et al. 2019)	35	22.19	9.63
MM_{10}	22	USA	L	2019	(Coleman et al. 2019)	25	5.47	0.32
MM_{10}	23	USA	L	2019	(Coleman et al. 2019)	17	5.62	0.23
MM_{10}	24	USA	L	2019	(Coleman et al. 2019)	31	5.19	0.50
MM_{10}	25	USA	L	2019	(Coleman et al. 2019)	25	5.30	0.56
MM_{10}	26	USA	L	2019	(Coleman et al. 2019)	36	7.52	2.22
MM_{10}	27	USA	L	2019	(Coleman et al. 2019)	37	8.09	2.54
MM_{10}	28	USA	L	2019	(Coleman et al. 2019)	38	8.28	2.04

Table S3 continued

MM_{10}	29	USA	L	2019	(Coleman et al. 2019)	44	7.18	2.51
MM_{10}	30	USA	L	2019	(Coleman et al. 2019)	33	9.82	1.54
MM_{10}	31	USA	L	2019	(Coleman et al. 2019)	25	11.63	3.71
MM_{10}	32	USA	L	2019	(Coleman et al. 2019)	37	10.85	3.49
MM_{10}	33	USA	L	2019	(Coleman et al. 2019)	29	9.83	2.93
MM_{11}	1	USA	L	2018	(Roser et al. 2018)	12	30.68	29.89
MM_{12}	1	Lithuania	F	2020	(Povilaitis and Matikienė 2020)	134	1.61	1.06
MM_{13}	1	Denmark	L	2016	(Bruun et al. 2016)	8	1.37	0.92
MM_{14}	1	Denmark	L	2016	(Bruun et al. 2016)	8	1.85	1.22
MM_{15}	1	Ireland	L	2007	(Healy et al. 2007)	86	0.68	0.31
MM_{15}	2	Ireland	L	2007	(Healy et al. 2007)	55	2.18	0.22
MM_{15}	3	Ireland	L	2007	(Healy et al. 2007)	96	2.74	1.05
MM_{15}	4	Ireland	L	2007	(Healy et al. 2007)	79	0.86	0.36
MM_{15}	5	Ireland	L	2007	(Healy et al. 2007)	60	1.12	0.51
MM_{16}	1	USA	L	2016	(Feyereisen et al. 2016)	54	7.19	1.81
MM_{16}	2	USA	L	2016	(Feyereisen et al. 2016)	49	28.85	5.14
MM_{17}	1	USA	L	2018	(Li et al. 2018)	14	19.57	2.16
MM_{17}	2	USA	L	2018	(Li et al. 2018)	14	23.41	2.24
MM_{17}	3	USA	L	2018	(Li et al. 2018)	14	14.33	1.68

Table S3 continued

MM_{18}	1	Finland	L	2020	(Kiani et al. 2020)	26	15.25	7.47
MM_{19}	1	Finland	L	2020	(Kiani et al. 2020)	26	20.54	10.08
Soil	1	Ireland	L	2012	(Healy et al. 2012)	13	0.08	0.77
Soil	2	Ireland	L	2012	(Healy et al. 2012)	13	0.19	0.76
Soil	3	Ireland	L	2015	(Healy et al. 2015)	41	0.28	0.30
Soil	4	Iran	L	2017	(Tangsir et al. 2017)	20	9.64	1.32

Note: NC represents natural carbon; NNC represents non-natural carbon; IM represents inorganic materials; MM represents multi-materials, and the subscript number represents the different types of media; The No represents the sequential number of the independent bioreactor unit in the group, details of the fill materials can be seen in Table S1; H represents hardwood; S represents softwood. L represents lab scale; F represents field scale; T-number, T-mean and T-SD represents the number of data points, mean value of the data points, and standard deviation of the data points respectively.

Table S4 Details of meta-analysis by the effect size of NRE

Carbon type	No	Wood type	Nation	Scale	Year	Reference	T-number	T-mean	T-SD
NC_1	1	S	New zealand	L	2010	(Cameron and Schipper 2010)	15	0.16	0.06
NC_1	2	H	New zealand	L	2010	(Cameron and Schipper 2010)	15	0.15	0.05
NC_1	3	S	New zealand	L	2010	(Cameron and Schipper 2010)	15	0.21	0.08

Table S4 continued

NC_1	4	H	New zealand	L	2010	(Cameron and Schipper 2011)	15	0.25	0.05
NC_1	5	H	New zealand	L	2010	(Cameron and Schipper 2011)	20	0.12	0.07
NC_1	6		USA	F	2016	(David et al. 2016)	221	0.44	0.36
NC_1	7		Canada	F	2006	(Van Driel et al. 2006)	44	0.51	0.34
NC_1	8		Canada	F	2006	(Van Driel et al. 2006)	28	0.25	0.12
NC_1	9		USA	L	2015	(Easton et al. 2015)	48	0.71	0.31
NC_1	10		USA	L	2015	(Easton et al. 2015)	48	0.79	0.29
NC_1	11		USA	L	2015	(Easton et al. 2015)	48	0.87	0.25
NC_1	12		USA	L	2015	(Easton et al. 2015)	48	0.84	0.28
NC_1	13	S	New zealand	F	2011	(Long et al. 2011)	21	0.68	0.17
NC_1	14	H	USA	L	2016	(Pluer et al. 2016)	6	0.51	0.15
NC_1	15	H	Danmark	F	2020	(Aalto et al. 2020)	6	0.50	0.15
NC_1	16	S	Ireland	L	2012	(Healy et al. 2012)	22	1.00	0.00
NC_1	17	S	Ireland	L	2012	(Healy et al. 2012)	22	1.00	0.00
NC_1	18	S	Ireland	L	2012	(Healy et al. 2012)	22	0.99	0.02
NC_1	19	S	New zealand	F	2011	(Warneke et al. 2011a)	7	0.51	0.09
NC_1	20		USA	F	2010	(Woli et al. 2010)	35	0.50	0.30
NC_1	21	S	New zealand	F	2010	(Schipper et al. 2010)	35	0.48	0.19

Table S4 continued

NC_1	22	S	New zealand	F	2010	(Schipper et al. 2010)	71	0.81	0.25
NC_1	23	S	New zealand	F	2010	(Schipper et al. 2010)	30	0.85	0.26
NC_1	24	S	Canada	L	2010	(Robertson 2010)	20	0.80	0.23
NC_1	25	S	Canada	L	2010	(Robertson 2010)	24	0.64	0.32
NC_1	26	S	Canada	L	2010	(Robertson 2010)	24	0.57	0.32
NC_1	27	S	Canada	L	2010	(Robertson 2010)	24	0.49	0.35
NC_1	28	S	New zealand	L	2011	(Warneke et al. 2011b)	2	0.29	0.02
NC_1	29	S	New zealand	L	2011	(Warneke et al. 2011b)	2	0.51	0.13
NC_1	30	H	New zealand	L	2011	(Warneke et al. 2011b)	2	0.33	0.00
NC_1	31	S	New zealand	L	2011	(Warneke et al. 2011b)	2	0.33	0.03
NC_1	32	H	New zealand	L	2011	(Warneke et al. 2011b)	2	0.40	0.05
NC_1	33	S	Canada	F	2010	(Elgood et al. 2010)	30	0.63	0.28
NC_1	34	S	New zealand	F	1998	(Schipper and Vojvodic-Vukovic 1998)	6	0.81	0.14
NC_1	35	S	New zealand	F	1998	(Schipper and Vojvodic-Vukovic 1998)	10		
NC_1	36		Ireland	L	2007	(Healy et al. 2007)	71	0.39	0.31
NC_1	37	S	UK	L	2008	(Gibert et al. 2008)	30	0.90	0.22
NC_1	38	H	UK	L	2008	(Gibert et al. 2008)	30	0.90	0.21
NC_1	39		UK	L	2008	(Gibert et al. 2008)	30	0.91	0.20

Table S4 continued

NC_1	40	H	UK	L	2008	(Gibert et al. 2008)	30	0.85	0.23
NC_1	41		USA	L	2018	(Roser et al. 2018)	12	0.26	0.25
NC_1	42		Canada	F	2009	(Robertson et al. 2009)	91	0.48	0.32
NC_1	43		Canada	F	2009	(Robertson and Merkley 2009)	61	0.79	0.20
NC_1	44		USA	F	2015	(Bell et al. 2015)	21	0.63	0.27
NC_1	45	H	USA	L	2016	(Feyereisen et al. 2016)	54	0.04	0.02
NC_1	46	H	USA	L	2016	(Feyereisen et al. 2016)	49	0.07	0.04
NC_1	47		USA	L	2015	(Hoover et al. 2015)	99	0.28	0.18
NC_1	48	H	USA	L	2015	(Lepine et al. 2015)	78	0.68	0.24
NC_1	49	H	USA	L	2015	(Lepine et al. 2015)	78	0.73	0.22
NC_1	50	H	USA	L	2015	(Lepine et al. 2015)	78	0.81	0.20
NC_1	51	H	USA	L	2015	(Lepine et al. 2015)	78	0.85	0.15
NC_1	52	H	USA	L	2009	(Greenan et al. 2009)	144	0.88	0.16
NC_1	53	H	USA	L	2009	(Greenan et al. 2009)	109	0.66	0.22
NC_1	54	H	USA	L	2009	(Greenan et al. 2009)	131	0.41	0.22
NC_1	55	H	USA	L	2016	(Hua et al. 2016)	41	1.00	0.00
NC_1	56	H	USA	L	2016	(Hua et al. 2016)	46	0.75	0.06
NC_1	57		USA	F	2012	(Schmidt and Clark 2012)	30	0.99	0.02
NC_1	58		USA	F	2012	(Schmidt and Clark 2012)	30	0.99	0.02

Table S4 continued

NC_1	59		USA	F	2012	(Schmidt and Clark 2012)	30	0.74	0.10
NC_1	60		USA	F	2015	(Bock et al. 2015b)	8		
NC_1	61	S	Lithuania	F	2020	(Povilaitis and Matikienė 2020)	126		
NC_1	62	S	New zealand	L	2012	(Cameron and Schipper 2012)	2		
NC_1	63	S	New zealand	L	2012	(Cameron and Schipper 2012)	2		
NC_1	64	S	New zealand	L	2012	(Cameron and Schipper 2012)	2		
NC_1	65	S	New zealand	L	2012	(Cameron and Schipper 2012)	2		
NC_1	66	S	New zealand	L	2012	(Cameron and Schipper 2012)	2		
NC_1	67	H	New zealand	L	2012	(Cameron and Schipper 2012)	2		
NC_1	68		USA	L	2015	(Bock et al. 2015a)	3	0.50	0.31
NC_1	69		USA	L	2015	(Easton et al. 2015)	33	0.73	0.28
NC_1	70	S	Canada	F	2016	(Choudhury et al. 2016)	27	0.55	0.28
NC_1	71	S	Canada	F	2016	(Choudhury et al. 2016)	15	0.29	0.27

Table S4 continued

NC_1	72	S	Ireland	L	2015	(Healy et al. 2015)	64		
NC_1	73		USA	F	2017	(Rosen and Christianson 2017)	65	0.99	
NC_1	74		USA	F	2017	(Rosen and Christianson 2017)	52	0.98	0.04
NC_1	75		USA	L	2019	(Maxwell et al. 2019b)	658		
NC_1	76		USA	L	2019	(Maxwell et al. 2019a)	1752	0.42	0.21
NC_1	77		USA	L	2018	(Li et al. 2018)	42	0.69	0.18
NC_1	78	S	USA	L	2013	(Schmidt and Clark 2013)	52	0.65	0.36
NC_1	79		USA	L	2011	(Christianson et al. 2011)	12	0.36	0.30
NC_1	80	S	New zealand	F	2020	(Rivas et al. 2020)	39	1.00	0.00
NC_1	81	S	New zealand	F	2020	(Rivas et al. 2020)	86	0.50	0.25
NC_1	82	H	USA	F	2019	(Pluer et al. 2019)	19	0.79	0.29
NC_1	83	H	USA	F	2019	(Pluer et al. 2019)	16		
NC_1	84	S	New zealand	F	2020	(Corbett et al. 2020)	12	1.00	0.00
NC_1	85	S	New zealand	F	2020	(Corbett et al. 2020)	9	0.94	0.02
NC_1	86	S	China	L	2015	(Liang et al. 2015)	14	0.35	0.07
NC_1	87	H	Canada	F	2008	(Robertson et al. 2008)	30		
NC_1	88	H	Finland	L	2020	(Kiani et al. 2020)	26	0.79	0.23
NC_1	89	H	USA	L	2020	(Pluer et al. 2020)	20	0.70	0.05

Table S4 continued

NC_1	90	H	USA	L	2020	(Pluer et al. 2020)	22	0.68	0.05
NC_1	91	H	USA	L	2020	(Pluer et al. 2020)	22	0.69	0.06
NC_1	92	H	USA	L	2019	(Coleman et al. 2019)	40	0.57	0.12
NC_1	93	H	USA	L	2019	(Coleman et al. 2019)	36	0.59	0.12
NC_1	94	H	USA	L	2019	(Coleman et al. 2019)	48	0.29	0.05
NC_1	95	H	USA	L	2019	(Coleman et al. 2019)	37	0.28	0.04
NC_1	96	H	USA	L	2019	(Coleman et al. 2019)	32	0.17	0.05
NC_1	97	H	USA	L	2019	(Coleman et al. 2019)	35	0.17	0.05
NC_1	98	H	USA	L	2019	(Coleman et al. 2019)	31	0.81	0.09
NC_1	99	H	USA	L	2019	(Coleman et al. 2019)	26	0.82	0.08
NC_1	100	H	USA	L	2019	(Coleman et al. 2019)	32	0.73	0.10
NC_1	101	H	USA	L	2019	(Coleman et al. 2019)	23	0.94	0.06
NC_1	102	H	USA	L	2019	(Coleman et al. 2019)	33	0.50	0.12
NC_1	103	H	USA	L	2019	(Coleman et al. 2019)	39	0.51	0.10
NC_2	1		USA	L	2016	(Feyereisen et al. 2016)	54	0.12	0.04
NC_2	2		USA	L	2016	(Feyereisen et al. 2016)	49	0.47	0.10
NC_3	1		Ireland	L	2012	(Healy et al. 2012)	12	1.00	0.00
NC_3	2		Ireland	L	2012	(Healy et al. 2012)	12	1.00	0.01
NC_3	3		Ireland	L	2012	(Healy et al. 2012)	12	1.00	0.00
NC_3	4		USA	L	2016	(Feyereisen et al. 2016)	54	0.11	0.04

Table S4 continued

NC_3	5	USA	L	2016	(Feyereisen et al. 2016)	49	0.48	0.17
NC_3	6	Ireland	L	2015	(Healy et al. 2015)	33		
NC_4	1	China	L	2012	(Liu et al. 2015)	16	0.25	0.12
NC_4	2	China	L	2015	(Liang et al. 2015)	14	0.96	0.02
NC_4	3	China	L	2015	(Liang et al. 2015)	17	0.53	0.18
NC_4	4	China	L	2015	(Liang et al. 2015)	14	0.41	0.16
NC_4	5	China	L	2015	(Liang et al. 2015)	8	0.05	0.03
NC_4	6	China	L	2015	(Liang et al. 2015)	14	0.08	0.05
NC_4	7	China	L	2015	(Liang et al. 2015)	17	0.11	0.08
NC_4	8	China	L	2015	(Liang et al. 2015)	17	0.53	0.17
NC_5	1	New zealand	L	2010	(Cameron and Schipper 2010)	15	0.32	0.22
NC_5	2	New zealand	L	2010	(Cameron and Schipper 2010)	15	0.42	0.20
NC_5	3	New zealand	L	2011	(Warneke et al. 2011b)	4	0.69	0.13
NC_5	4	New zealand	L	2012	(Cameron and Schipper 2012)	2		
NC_6	1	New zealand	L	2010	(Cameron and Schipper 2010)	15	0.54	0.21
NC_6	2	New zealand	L	2011	(Warneke et al. 2011b)	4	0.85	0.16

Table S4 continued

NC_6	3	USA	L	2018	(Roser et al. 2018)	12	0.58	0.34
NC_6	4	USA	L	2016	(Feyereisen et al. 2016)	54	0.17	0.05
NC_6	5	USA	L	2016	(Feyereisen et al. 2016)	49	0.73	0.08
NC_6	6	New zealand	L	2011	(Cameron and Schipper 2011)	43		
NC_6	7	New zealand	L	2011	(Cameron and Schipper 2011)	42		
NC_6	8	New zealand	L	2012	(Cameron and Schipper 2012)	2		
NC_6	9	USA	L	2016	(Sharrer et al. 2016)	48	0.73	0.09
NC_6	10	USA	L	2016	(Sharrer et al. 2016)	53	0.16	0.04
NC_7	1	New zealand	L	2011	(Warneke et al. 2011b)	4	0.72	0.27
NC_7	2	New zealand	L	2010	(Cameron and Schipper 2010)	15	0.28	0.14
NC_7	3	New zealand	L	2012	(Cameron and Schipper 2012)	2		
NC_8	1	Ireland	L	2015	(Healy et al. 2015)	21	0.99	0.01
NC_8	2	Ireland	L	2015	(Healy et al. 2015)	21	0.99	0.04
NC_8	3	Ireland	L	2015	(Healy et al. 2015)	21	1.00	0.00
NC_9	1	China	L	2019	(Yao et al. 2019)	90	0.74	0.34

Table S4 continued

NC_9	2	China	L	2019	(Yao et al. 2019)	90	0.80	0.31
NC_9	3	China	L	2019	(Yao et al. 2019)	90	0.91	0.12
NC_{10}	1	UK	L	2008	(Gibert et al. 2008)	30	0.92	0.22
NC_{11}	1	UK	L	2008	(Gibert et al. 2008)	30	0.63	0.48
NC_{11}	2	UK	L	2008	(Gibert et al. 2008)	30	0.89	0.22
NNC_1	1	Ireland	L	2012	(Healy et al. 2012)	23	1.00	0.00
NNC_1	2	Ireland	L	2012	(Healy et al. 2012)	23	1.00	0.00
NNC_1	3	Ireland	L	2012	(Healy et al. 2012)	23	1.00	0.00
NNC_1	4	Ireland	L	2015	(Healy et al. 2015)	29		
NNC_2	1	USA	L	2015	(Easton et al. 2015)	45	0.93	0.12
NNC_3	1	Germany	L	2000	(Boley et al. 2000)	13	0.65	0.22
NNC_4	2	Germany	L	2000	(Boley et al. 2000)	13	0.66	0.37
NNC_4	4	Japan	L	2002	(Honda and Osawa 2002)	30	0.79	0.23
NNC_5	3	Germany	L	2000	(Boley et al. 2000)	13	0.50	0.32
NNC_5	5	China	L	2009	(Zhou et al. 2009)	58	0.66	0.31
IM_1	1	USA	L	2015	(Easton et al. 2015)	45	0.85	0.21
IM_2	1	USA	L	2015	(Easton et al. 2015)	45	0.89	0.19
IM_3	1	China	L	2019	(Xu et al. 2019)	61	0.55	0.29
MM_1	1	Canada	L	1994	(Blowes et al. 1994)	12	0.94	0.16
MM_2	1	Canada	L	1994	(Blowes et al. 1994)	12	0.93	0.12

Table S4 continued

MM_3	1	China	L	2017	(Li et al. 2017)	23	0.81	0.11
MM_4	1	USA	L	2018	(Roser et al. 2018)	4	0.72	0.33
MM_4	2	USA	L	2018	(Roser et al. 2018)	4	0.63	0.33
MM_4	3	USA	L	2018	(Roser et al. 2018)	4	0.31	0.20
MM_5	1	USA	L	2018	(Roser et al. 2018)	4	0.29	0.19
MM_5	2	USA	L	2018	(Roser et al. 2018)	4	0.74	0.36
MM_5	3	USA	L	2018	(Roser et al. 2018)	4	0.75	0.36
MM_6	1	USA	L	2016	(Sharrer et al. 2016)	48	0.87	0.09
MM_6	2	USA	L	2016	(Sharrer et al. 2016)	53	0.21	0.04
MM_7	1	Iran	L	2017	(Tangsir et al. 2017)	19	0.37	0.26
MM_7	2	Iran	L	2017	(Tangsir et al. 2017)	20	0.37	0.25
MM_8	1	China	L	2009	(Ruan et al. 2009)	45		
MM_9	1	USA	L	2016	(Hua et al. 2016)	87	0.91	0.09
MM_{10}	1	USA	L	2016	(Pluer et al. 2016)	6	0.59	0.16
MM_{10}	2	USA	L	2018	(Roser et al. 2018)	12	0.20	0.21
MM_{10}	3	USA	L	2018	(Bock et al. 2018)	149	0.16	0.29
MM_{10}	4	USA	L	2015	(Bock et al. 2015b)	8		
MM_{10}	5	Lithuania	F	2020	(Povilaitis and Matikienė 2020)	119		
MM_{10}	6	USA	L	2015	(Bock et al. 2015a)	24	0.98	0.04

Table S4 continued

MM_{10}	7	USA	L	2019	(Pluer et al. 2019)	16	1.00	0.00
MM_{10}	8	USA	L	2019	(Pluer et al. 2019)	13		
MM_{10}	9	Finland	L	2020	(Kiani et al. 2020)	26	0.73	0.27
MM_{10}	10	USA	L	2019	(Coleman et al. 2019)	41	0.50	0.15
MM_{10}	11	USA	L	2019	(Coleman et al. 2019)	42	0.56	0.11
MM_{10}	12	USA	L	2019	(Coleman et al. 2019)	46	0.46	0.11
MM_{10}	13	USA	L	2019	(Coleman et al. 2019)	43	0.67	0.18
MM_{10}	14	USA	L	2019	(Coleman et al. 2019)	48	0.29	0.21
MM_{10}	15	USA	L	2019	(Coleman et al. 2019)	32	0.36	0.10
MM_{10}	16	USA	L	2019	(Coleman et al. 2019)	42	0.32	0.18
MM_{10}	17	USA	L	2019	(Coleman et al. 2019)	40	0.35	0.05
MM_{10}	18	USA	L	2019	(Coleman et al. 2019)	32	0.21	0.11
MM_{10}	19	USA	L	2019	(Coleman et al. 2019)	36	0.29	0.10
MM_{10}	20	USA	L	2019	(Coleman et al. 2019)	25	0.18	0.05
MM_{10}	21	USA	L	2019	(Coleman et al. 2019)	35	0.26	0.11
MM_{10}	22	USA	L	2019	(Coleman et al. 2019)	25	0.92	0.05
MM_{10}	23	USA	L	2019	(Coleman et al. 2019)	17	0.95	0.04
MM_{10}	24	USA	L	2019	(Coleman et al. 2019)	31	0.87	0.08
MM_{10}	25	USA	L	2019	(Coleman et al. 2019)	25	0.89	0.09
MM_{10}	26	USA	L	2019	(Coleman et al. 2019)	36	0.63	0.19

Table S4 continued

MM_{10}	27	USA	L	2019	(Coleman et al. 2019)	37	0.68	0.21
MM_{10}	28	USA	L	2019	(Coleman et al. 2019)	38	0.70	0.17
MM_{10}	29	USA	L	2019	(Coleman et al. 2019)	44	0.60	0.21
MM_{10}	30	USA	L	2019	(Coleman et al. 2019)	33	0.41	0.06
MM_{10}	31	USA	L	2019	(Coleman et al. 2019)	25	0.49	0.16
MM_{10}	32	USA	L	2019	(Coleman et al. 2019)	37	0.46	0.15
MM_{10}	33	USA	L	2019	(Coleman et al. 2019)	29	0.41	0.12
MM_{11}	1	USA	L	2018	(Roser et al. 2018)	12	0.85	0.28
MM_{12}	1	Lithuania	F	2020	(Povilaitis and Matikienė 2020)	134		
MM_{13}	1	Denmark	L	2016	(Bruun et al. 2016)	8		
MM_{14}	1	Denmark	L	2016	(Bruun et al. 2016)	8		
MM_{15}	1	Ireland	L	2007	(Healy et al. 2007)	86	0.30	0.14
MM_{15}	2	Ireland	L	2007	(Healy et al. 2007)	55	0.95	0.10
MM_{15}	3	Ireland	L	2007	(Healy et al. 2007)	96	0.36	0.14
MM_{15}	4	Ireland	L	2007	(Healy et al. 2007)	79	0.11	0.05
MM_{15}	5	Ireland	L	2007	(Healy et al. 2007)	60	0.15	0.07
MM_{16}	1	USA	L	2016	(Feyereisen et al. 2016)	54	0.16	0.04
MM_{16}	2	USA	L	2016	(Feyereisen et al. 2016)	49	0.63	0.09
MM_{17}	1	USA	L	2018	(Li et al. 2018)	14	0.85	0.07

Table S4 continued

MM_{17}	2	USA	L	2018	(Li et al. 2018)	14	0.50	0.05
MM_{17}	3	USA	L	2018	(Li et al. 2018)	14	0.88	0.09
MM_{18}	1	Finland	L	2020	(Kiani et al. 2020)	26	0.70	0.25
MM_{19}	1	Finland	L	2020	(Kiani et al. 2020)	26	0.87	0.17
Soil	1	Ireland	L	2012	(Healy et al. 2012)	13	0.06	0.76
Soil	2	Ireland	L	2012	(Healy et al. 2012)	13	0.17	0.71
Soil	3	Ireland	L	2015	(Healy et al. 2015)	41		
Soil	4	Iran	L	2017	(Tangsir et al. 2017)	20	0.37	0.25

Note: NC represents natural carbon; NNC represents non-natural carbon; IM represents inorganic materials; MM represents multi-materials, and the subscript number represents the different types of media; The No represents the sequential number of the independent bioreactor unit in the group, details of the fill materials can be seen in Table S1; H represents hardwood; S represents softwood. L represents lab scale; F represents field scale; T-number, T-mean and T-SD represents the number of data points, mean value of the data points, and standard deviation of the data points respectively.

References for Table 1. 5 and 1.6

Aalto S L, Suurnäkki S, von Ahnen M, et al. 2020. Nitrate removal microbiology in woodchip bioreactors: A case-study with full-scale bioreactors treating aquaculture effluents[J]. Science of The Total Environment: 138093.

Ahmad M, Lee S S, Dou X, et al. 2012. Effects of pyrolysis temperature on soybean stover- and peanut shell-derived biochar properties and TCE adsorption in water[J]. Bioresource Technology, 118: 536-544.

Ahmad M, Rajapaksha A U, Lim J E, et al. 2014. Biochar as a sorbent for contaminant management in soil and water: A review[J]. Chemosphere, 99(Supplement C): 19-33.

Bell N, Cooke R A, Olsen T, et al. 2015. Characterizing the performance of denitrifying bioreactors during simulated subsurface drainage events[J]. Journal of Environmental Quality, 44(5): 1647-1656.

Blowes D W, Robertson W D, Ptacek C J, et al. 1994. Removal of agricultural nitrate from tile-drainage effluent water using in-line bioreactors[J]. Journal of Contaminant Hydrology, 15(3): 207-221.

Bock E, Smith N, Rogers M, et al. 2015a. Enhanced Nitrate and Phosphate Removal in a Denitrifying Bioreactor with Biochar[J]. Journal of Environmental Quality, 44(2): 605-613.

Bock E M, Coleman B, Easton Z M. 2015b. Effect of Biochar on Nitrate Removal in a Pilot-Scale Denitrifying Bioreactor[J]. Journal of Environmental Quality, 45(3): 762-771.

Bock E M, Coleman B S L, Easton Z M. 2018. Performance of an under-loaded denitrifying bioreactor with biochar amendment[J]. Journal of Environmental Management, 217: 447-455.

Boley A, Müller W R, Haider G. 2000. Biodegradable polymers as solid substrate and biofilm carrier for denitrification in recirculated aquaculture systems[J]. Aquacultural Engineering, 22(1): 75-85.

Bruun J, Hoffmann C C, Kjaergaard C. 2016. Nitrogen Removal in Permeable Woodchip Filters Affected by Hydraulic Loading Rate and Woodchip Ratio[J]. Journal of Environmental Quality, 45(5): 1688-1695.

Cameron S G, Schipper L A. 2010. Nitrate removal and hydraulic performance of organic carbon for use in denitrification beds[J]. Ecological Engineering, 36(11): 1588-1595.

Cameron S G, Schipper L A. 2011. Evaluation of passive solar heating and alternative flow regimes on nitrate removal in denitrification beds[J]. Ecological Engineering, 37(8): 1195-1204.

Cameron S G, Schipper L A. 2012. Hydraulic properties, hydraulic efficiency and nitrate removal of organic carbon media for use in denitrification beds[J]. Ecological Engineering, 41: 1-7.

Cantrell K B, Hunt P G, Uchimiya M, et al. 2012. Impact of pyrolysis temperature and manure source on physicochemical characteristics of biochar[J]. Bioresource Technology, 107: 419-428.
Chen B, Chen Z. 2009. Sorption of naphthalene and 1-naphthol by biochars of orange peels with different pyrolytic temperatures[J]. Chemosphere, 76(1): 127-133.
Chiumenti A, da Borso F, Limina S. 2018. Dry anaerobic digestion of cow manure and agricultural products in a full-scale plant: Efficiency and comparison with wet fermentation[J]. Waste Management, 71: 704-710.
Choudhury T, Robertson W D, Finnigan D S. 2016. Suspended Sediment and Phosphorus Removal in a Woodchip Filter System Treating Agricultural Wash Water[J]. Journal of Environmental Quality, 45(3): 796-802.
Christianson L E, Hanly J A, Hedley M J. 2011. Optimized denitrification bioreactor treatment through simulated drainage containment[J]. Agricultural Water Management, 99(1): 85-92.
Coleman B S L, Easton Z M, Bock E M. 2019. Biochar fails to enhance nutrient removal in woodchip bioreactor columns following saturation[J]. Journal of Environmental Management, 232: 490-498.
Corbett T D W, Dougherty H, Maxwell B, et al. 2020. Utility of 'Diffusive Gradients in Thin-Films' for the measurement of nitrate removal performance of denitrifying bioreactors[J]. Science of The Total Environment, 718: 135267.
David M B, Gentry L E, Cooke R A, et al. 2016. Temperature and Substrate Control Woodchip Bioreactor Performance in Reducing Tile Nitrate Loads in East-Central Illinois[J]. Journal of Environmental Quality, 45(3): 822-829.
Easton Z M, Rogers M, Davis M, et al. 2015. Mitigation of sulfate reduction and nitrous oxide emission in denitrifying environments with amorphous iron oxide and biochar[J]. Ecological Engineering, 82: 605-613.
Elgood Z, Robertson W D, Schiff S L, et al. 2010. Nitrate removal and greenhouse gas production in a stream-bed denitrifying bioreactor[J]. Ecological Engineering, 36(11): 1575-1580.
Faulkner J W, Zhang W, Geohring L D, et al. 2011. Nutrient transport within three vegetative treatment areas receiving silage bunker runoff[J]. Journal of Environmental Management, 92(3): 587-595.
Feyereisen G W, Moorman T B, Christianson L E, et al. 2016. Performance of agricultural residue media in laboratory denitrifying bioreactors at low temperatures[J]. Journal of Environmental Quality, 45(3): 779-787.
Gibert O, Pomierny S, Rowe I, et al. 2008. Selection of organic substrates as potential reactive materials for use in a denitrification permeable reactive barrier (PRB)[J]. Bioresource Technology, 99(16): 7587-7596.

Greenan C M, Moorman T B, Parkin T B, et al. 2009. Denitrification in wood chip bioreactors at different water flows[J]. Journal of Environmental Quality, 38(4): 1664-1671.
Healy M G, Barrett M, Lanigan G J, et al. 2015. Optimizing nitrate removal and evaluating pollution swapping trade-offs from laboratory denitrification bioreactors[J]. Ecological Engineering, 74: 290-301.
Healy M G, Ibrahim T G, Lanigan G J, et al. 2012. Nitrate removal rate, efficiency and pollution swapping potential of different organic carbon media in laboratory denitrification bioreactors[J]. Ecological Engineering, 40: 198-209.
Healy M G, Rodgers M, Mulqueen J. 2007. Denitrification of a nitrate-rich synthetic wastewater using various wood-based media materials[J]. Journal of Environmental Science and Health Part A, 41(5): 779-788.
Holly M A, Larson R A, Cooley E T, et al. 2018. Silage storage runoff characterization: Annual nutrient loading rate and first flush analysis of bunker silos[J]. Agriculture, Ecosystems & Environment, 264: 85-93.
Honda Y, Osawa Z. 2002. Microbial denitrification of wastewater using biodegradable polycaprolactone[J]. Polymer Degradation and Stability, 76(2): 321-327.
Hoover N L, Bhandari A, Soupir M L, et al. 2015. Woodchip denitrification bioreactors: Impact of temperature and hydraulic retention time on nitrate removal[J]. Journal of Environmental Quality, 45(3): 803-812.
Hua G, Salo M W, Schmit C G, et al. 2016. Nitrate and phosphate removal from agricultural subsurface drainage using laboratory woodchip bioreactors and recycled steel byproduct filters[J]. Water Research, 102: 180-189.
Karaosmanoğlu F, Işığıgür-Ergüdenler A, Sever A. 2000. Biochar from the straw-stalk of rapeseed plant[J]. Energy & Fuels, 14(2): 336-339.
Keiluweit M, Nico P S, Johnson M G, et al. 2010. Dynamic molecular structure of plant biomass-derived black carbon (biochar)[J]. Environmental Science & Technology, 44(4): 1247-1253.
Kiani S, Kujala K, T. Pulkkinen J, et al. 2020. Enhanced nitrogen removal of low carbon wastewater in denitrification bioreactors by utilizing industrial waste toward circular economy[J]. Journal of Cleaner Production, 254: 119973.
Kloss S, Zehetner F, Dellantonio A, et al. 2012. Characterization of slow pyrolysis biochars: Effects of feedstocks and pyrolysis temperature on biochar properties[J]. Journal of Environmental Quality, 41(4): 990-1000.
Lee J W, Kidder M, Evans B R, et al. 2010. Characterization of biochars produced from cornstovers for soil amendment[J]. Environmental Science & Technology, 44(20): 7970-7974.
Lehmann J, Rillig M C, Thies J, et al. 2011. Biochar effects on soil biota – A review[J]. Soil Biology & Biochemistry, 43(9): 1812-1836.

Lepine C, Christianson L, Sharrer K, et al. 2015. Optimizing hydraulic retention times in denitrifying woodchip bioreactors treating recirculating aquaculture system wastewater[J]. Journal of Environmental Quality, 45(3): 813-821.
Li R, Feng C P, Xi B D, et al. 2017. Nitrate removal efficiency of a mixotrophic denitrification wall for nitrate-polluted groundwater in situ remediation[J]. Ecological Engineering, 106: 523-531.
Li S, Cooke R A, Huang X, et al. 2018. Evaluation of fly ash pellets for phosphorus removal in a laboratory scale denitrifying bioreactor[J]. Journal of Environmental Management, 207: 269-275.
Lian F, Huang F, Chen W, et al. 2011. Sorption of apolar and polar organic contaminants by waste tire rubber and its chars in single- and bi-solute systems[J]. Environmental Pollution, 159(4): 850-857.
Liang X Q, Lin L M, Ye Y S, et al. 2015. Nutrient removal efficiency in a rice-straw denitrifying bioreactor[J]. Bioresource Technology, 198: 746-754.
Lin Y, Munroe P, Joseph S, et al. 2012. Water extractable organic carbon in untreated and chemical treated biochars[J]. Chemosphere, 87(2): 151-157.
Liu F, Wang Y, Xiao R, et al. 2015. Influence of substrates on nutrient removal performance of organic channel barriers in drainage ditches[J]. Journal of Hydrology, 527: 380-386.
Liu Z, Zhang F-S, Wu J. 2010. Characterization and application of chars produced from pinewood pyrolysis and hydrothermal treatment[J]. Fuel, 89(2): 510-514.
Long L M, Schipper L A, Bruesewitz D A. 2011. Long-term nitrate removal in a denitrification wall[J]. Agriculture Ecosystems & Environment, 140(3-4): 514-520.
Maxwell B M, Birgand F, Schipper L A, et al. 2019a. Drying–rewetting cycles affect nitrate removal rates in woodchip bioreactors[J]. Journal of Environmental Quality, 48(1): 93-101.
Maxwell B M, Birgand F, Schipper L A, et al. 2019b. Increased duration of drying–rewetting cycles increases nitrate removal in woodchip bioreactors[J]. Agricultural & Environmental Letters, 4.
Mohan D, Rajput S, Singh V K, et al. 2011. Modeling and evaluation of chromium remediation from water using low cost bio-char, a green adsorbent[J]. Journal of Hazardous Materials, 188(1): 319-333.
Mullen C A, Boateng A A, Goldberg N M, et al. 2010. Bio-oil and bio-char production from corn cobs and stover by fast pyrolysis[J]. Biomass and Bioenergy, 34(1): 67-74.
Peng X, Ye L L, Wang C H, et al. 2011. Temperature- and duration-dependent rice straw-derived biochar: Characteristics and its effects on soil properties of an Ultisol in southern China[J]. Soil and Tillage Research, 112(2): 159-166.

Pluer W T, Geohring L D, Steenhuis T S, et al. 2016. Controls influencing the treatment of excess agricultural nitrate with denitrifying bioreactors[J]. Journal of Environmental Quality, 45(3): 772-778.
Pluer W T, Morris C K, Walter M T, et al. 2019. Denitrifying bioreactor response during storm events[J]. Agricultural Water Management, 213: 1109-1115.
Pluer W T, Walter M T, Steinschneider S. 2020. Understanding Complex Flow Pathways within Lab-Scale Denitrifying Bioreactors with a Conservative Tracer[J]. Transactions of the ASABE, 63(2): 417-427.
Povilaitis A, Matikienė J. 2020. Nitrate removal from tile drainage water: The performance of denitrifying woodchip bioreactors amended with activated carbon and flaxseed cake[J]. Agricultural Water Management, 229: 105937.
Rivas A, Barkle G, Stenger R, et al. 2020. Nitrate removal and secondary effects of a woodchip bioreactor for the treatment of subsurface drainage with dynamic flows under pastoral agriculture[J]. Ecological Engineering, 148: 105786.
Ro K S, Cantrell K B, Hunt P G. 2010. High-temperature pyrolysis of blended animal manures for producing renewable energy and value-added biochar[J]. Industrial & Engineering Chemistry Research, 49(20): 10125-10131.
Robertson W D. 2010. Nitrate removal rates in woodchip media of varying age[J]. Ecological Engineering, 36(11): 1581-1587.
Robertson W D, Merkley L C. 2009. In-Stream Bioreactor for Agricultural Nitrate Treatment All rights reserved. No part of this periodical may be reproduced or transmitted in any form or by any means, electronic or mechanical, including photocopying, recording, or any information storage and retrieval system, without permission in writing from the publisher[J]. Journal of Environmental Quality, 38(1): 230-237.
Robertson W D, Ptacek C J, Brown S J. 2009. Rates of Nitrate and Perchlorate Removal in a 5-Year-Old Wood Particle Reactor Treating Agricultural Drainage[J]. Ground Water Monitoring and Remediation, 29(2): 87-94.
Robertson W D, Vogan J L, Lombardo P S. 2008. Nitrate removal rates in a 15-year-old permeable reactive barrier treating septic system nitrate[J]. Ground Water Monitoring and Remediation, 28(3): 65-72.
Rosen T, Christianson L. 2017. Performance of Denitrifying Bioreactors at Reducing Agricultural Nitrogen Pollution in a Humid Subtropical Coastal Plain Climate[J]. Water, 9(2): 16.
Roser M B, Feyereisen G W, Spokas K A, et al. 2018. Carbon Dosing Increases Nitrate Removal Rates in Denitrifying Bioreactors at Low-Temperature High-Flow Conditions[J]. Journal of Environmental Quality, 47(4): 856-864.

Ruan Y J, Luo G Z, Tan H X, et al. 2009. Nitrate and phosphate removal in sulphur-coral stone autotrophic denitrification packed-bed reactors[J]. Canadian Journal of Civil Engineering, 36(5): 923-932.
Schipper L, Vojvodic-Vukovic M. 1998. Nitrate removal from groundwater using a denitrification wall amended with sawdust: Field trial[J]. Journal of Environmental Quality, 27(3): 664-668.
Schipper L A, Cameron S C, Warneke S. 2010. Nitrate removal from three different effluents using large-scale denitrification beds[J]. Ecological Engineering, 36(11): 1552-1557.
Schmidt C A, Clark M W. 2012. Efficacy of a denitrification wall to treat continuously high nitrate loads[J]. Ecological Engineering, 42: 203-211.
Schmidt C A, Clark M W. 2013. Deciphering and modeling the physicochemical drivers of denitrification rates in bioreactors[J]. Ecological Engineering, 60: 276-288.
Sharrer K L, Christianson L E, Lepine C, et al. 2016. Modeling and mitigation of denitrification 'woodchip' bioreactor phosphorus releases during treatment of aquaculture wastewater[J]. Ecological Engineering, 93: 135-143.
Tangsir S, Moazed H, Naseri A A, et al. 2017. Investigation on the performance of sugarcane bagasse as a new carbon source in two hydraulic dimensions of denitrification beds[J]. Journal of Cleaner Production, 140: 1176-1181.
Tikkisetty B, Kuperus W. Environmentally friendly silage management[C]//Environmentally friendly silage management. Proceedings of SIDE Conference. South Island Dairy Event.
Tong X-j, Li J-y, Yuan J-h, et al. 2011. Adsorption of Cu(II) by biochars generated from three crop straws[J]. Chemical Engineering Journal, 172(2): 828-834.
Uchimiya M, Chang S, Klasson K T. 2011. Screening biochars for heavy metal retention in soil: Role of oxygen functional groups[J]. Journal of Hazardous Materials, 190(1): 432-441.
Uchimiya M, Wartelle L H, Lima I M, et al. 2010. Sorption of deisopropylatrazine on broiler litter biochars[J]. Journal of Agricultural and Food Chemistry, 58(23): 12350-12356.
Van Driel P, Robertson W, Merkley L. 2006. Denitrification of agricultural drainage using wood-based reactors[J]. Transactions of the ASABE, 49(2): 565-573.
Warneke S, Schipper L A, Bruesewitz D A, et al. 2011a. Rates, controls and potential adverse effects of nitrate removal in a denitrification bed[J]. Ecological Engineering, 37(3): 511-522.
Warneke S, Schipper L A, Matiasek M G, et al. 2011b. Nitrate removal, communities of denitrifiers and adverse effects in different carbon substrates for use in denitrification beds[J]. Water Research, 45(17): 5463-5475.

Woli K P, David M B, Cooke R A, et al. 2010. Nitrogen balance in and export from agricultural fields associated with controlled drainage systems and denitrifying bioreactors[J]. Ecological Engineering, 36(11): 1558-1566.
Xu B K, Shi L S, Zhong H, et al. 2019. The performance of pyrite-based autotrophic denitrification column for permeable reactive barrier under natural environment[J]. Bioresource Technology, 290: 10.
Yao Z B, Wang C L, Song N, et al. 2019. Development of a hybrid biofilm reactor for nitrate removal from surface water with macrophyte residues as carbon substrate[J]. Ecological Engineering, 128: 1-8.
Zhou H, Zhao X, Wang J. 2009. Nitrate removal from groundwater using biodegradable polymers as carbon source and biofilm support[J]. International Journal of Environment and Pollution, 38(3): 339-348.
Aalto S L, Suurnäkki S, von Ahnen M, et al. 2020. Nitrate removal microbiology in woodchip bioreactors: A case-study with full-scale bioreactors treating aquaculture effluents[J]. Science of The Total Environment: 138093.
Ahmad M, Lee S S, Dou X, et al. 2012. Effects of pyrolysis temperature on soybean stover- and peanut shell-derived biochar properties and TCE adsorption in water[J]. Bioresource Technology, 118: 536-544.
Ahmad M, Rajapaksha A U, Lim J E, et al. 2014. Biochar as a sorbent for contaminant management in soil and water: A review[J]. Chemosphere, 99(Supplement C): 19-33.
Bell N, Cooke R A, Olsen T, et al. 2015. Characterizing the performance of denitrifying bioreactors during simulated subsurface drainage events[J]. Journal of Environmental Quality, 44(5): 1647-1656.
Blowes D W, Robertson W D, Ptacek C J, et al. 1994. Removal of agricultural nitrate from tile-drainage effluent water using in-line bioreactors[J]. Journal of Contaminant Hydrology, 15(3): 207-221.
Bock E, Smith N, Rogers M, et al. 2015a. Enhanced Nitrate and Phosphate Removal in a Denitrifying Bioreactor with Biochar[J]. Journal of Environmental Quality, 44(2): 605-613.
Bock E M, Coleman B, Easton Z M. 2015b. Effect of Biochar on Nitrate Removal in a Pilot-Scale Denitrifying Bioreactor[J]. Journal of Environmental Quality, 45(3): 762-771.
Bock E M, Coleman B S L, Easton Z M. 2018. Performance of an under-loaded denitrifying bioreactor with biochar amendment[J]. Journal of Environmental Management, 217: 447-455.
Boley A, Müller W R, Haider G. 2000. Biodegradable polymers as solid substrate and biofilm carrier for denitrification in recirculated aquaculture systems[J]. Aquacultural Engineering, 22(1): 75-85.
Bruun J, Hoffmann C C, Kjaergaard C. 2016. Nitrogen Removal in Permeable Woodchip Filters Affected by Hydraulic Loading Rate and Woodchip Ratio[J]. Journal of Environmental Quality, 45(5): 1688-1695.

Cameron S G, Schipper L A. 2010. Nitrate removal and hydraulic performance of organic carbon for use in denitrification beds[J]. Ecological Engineering, 36(11): 1588-1595.
Cameron S G, Schipper L A. 2011. Evaluation of passive solar heating and alternative flow regimes on nitrate removal in denitrification beds[J]. Ecological Engineering, 37(8): 1195-1204.
Cameron S G, Schipper L A. 2012. Hydraulic properties, hydraulic efficiency and nitrate removal of organic carbon media for use in denitrification beds[J]. Ecological Engineering, 41: 1-7.
Cantrell K B, Hunt P G, Uchimiya M, et al. 2012. Impact of pyrolysis temperature and manure source on physicochemical characteristics of biochar[J]. Bioresource Technology, 107: 419-428.
Chen B, Chen Z. 2009. Sorption of naphthalene and 1-naphthol by biochars of orange peels with different pyrolytic temperatures[J]. Chemosphere, 76(1): 127-133.
Chiumenti A, da Borso F, Limina S. 2018. Dry anaerobic digestion of cow manure and agricultural products in a full-scale plant: Efficiency and comparison with wet fermentation[J]. Waste Management, 71: 704-710.
Choudhury T, Robertson W D, Finnigan D S. 2016. Suspended Sediment and Phosphorus Removal in a Woodchip Filter System Treating Agricultural Wash Water[J]. Journal of Environmental Quality, 45(3): 796-802.
Christianson L E, Hanly J A, Hedley M J. 2011. Optimized denitrification bioreactor treatment through simulated drainage containment[J]. Agricultural Water Management, 99(1): 85-92.
Coleman B S L, Easton Z M, Bock E M. 2019. Biochar fails to enhance nutrient removal in woodchip bioreactor columns following saturation[J]. Journal of Environmental Management, 232: 490-498.
Corbett T D W, Dougherty H, Maxwell B, et al. 2020. Utility of ‘Diffusive Gradients in Thin-Films’ for the measurement of nitrate removal performance of denitrifying bioreactors[J]. Science of The Total Environment, 718: 135267.
David M B, Gentry L E, Cooke R A, et al. 2016. Temperature and Substrate Control Woodchip Bioreactor Performance in Reducing Tile Nitrate Loads in East-Central Illinois[J]. Journal of Environmental Quality, 45(3): 822-829.
Easton Z M, Rogers M, Davis M, et al. 2015. Mitigation of sulfate reduction and nitrous oxide emission in denitrifying environments with amorphous iron oxide and biochar[J]. Ecological Engineering, 82: 605-613.
Elgood Z, Robertson W D, Schiff S L, et al. 2010. Nitrate removal and greenhouse gas production in a stream-bed denitrifying bioreactor[J]. Ecological Engineering, 36(11): 1575-1580.

Faulkner J W, Zhang W, Geohring L D, et al. 2011. Nutrient transport within three vegetative treatment areas receiving silage bunker runoff[J]. Journal of Environmental Management, 92(3): 587-595.
Feyereisen G W, Moorman T B, Christianson L E, et al. 2016. Performance of agricultural residue media in laboratory denitrifying bioreactors at low temperatures[J]. Journal of Environmental Quality, 45(3): 779-787.
Gibert O, Pomierny S, Rowe I, et al. 2008. Selection of organic substrates as potential reactive materials for use in a denitrification permeable reactive barrier (PRB)[J]. Bioresource Technology, 99(16): 7587-7596.
Greenan C M, Moorman T B, Parkin T B, et al. 2009. Denitrification in wood chip bioreactors at different water flows[J]. Journal of Environmental Quality, 38(4): 1664-1671.
Healy M G, Barrett M, Lanigan G J, et al. 2015. Optimizing nitrate removal and evaluating pollution swapping trade-offs from laboratory denitrification bioreactors[J]. Ecological Engineering, 74: 290-301.
Healy M G, Ibrahim T G, Lanigan G J, et al. 2012. Nitrate removal rate, efficiency and pollution swapping potential of different organic carbon media in laboratory denitrification bioreactors[J]. Ecological Engineering, 40: 198-209.
Healy M G, Rodgers M, Mulqueen J. 2007. Denitrification of a nitrate-rich synthetic wastewater using various wood-based media materials[J]. Journal of Environmental Science and Health Part A, 41(5): 779-788.
Holly M A, Larson R A, Cooley E T, et al. 2018. Silage storage runoff characterization: Annual nutrient loading rate and first flush analysis of bunker silos[J]. Agriculture, Ecosystems & Environment, 264: 85-93.
Honda Y, Osawa Z. 2002. Microbial denitrification of wastewater using biodegradable polycaprolactone[J]. Polymer Degradation and Stability, 76(2): 321-327.
Hoover N L, Bhandari A, Soupir M L, et al. 2015. Woodchip denitrification bioreactors: Impact of temperature and hydraulic retention time on nitrate removal[J]. Journal of Environmental Quality, 45(3): 803-812.
Hua G, Salo M W, Schmit C G, et al. 2016. Nitrate and phosphate removal from agricultural subsurface drainage using laboratory woodchip bioreactors and recycled steel byproduct filters[J]. Water Research, 102: 180-189.
Karaosmanoğlu F, Işığıgür-Ergüdenler A, Sever A. 2000. Biochar from the straw-stalk of rapeseed plant[J]. Energy & Fuels, 14(2): 336-339.
Keiluweit M, Nico P S, Johnson M G, et al. 2010. Dynamic molecular structure of plant biomass-derived black carbon (biochar)[J]. Environmental Science & Technology, 44(4): 1247-1253.
Kiani S, Kujala K, T. Pulkkinen J, et al. 2020. Enhanced nitrogen removal of low carbon wastewater in denitrification bioreactors by utilizing industrial waste toward circular economy[J]. Journal of Cleaner Production, 254: 119973.

Kloss S, Zehetner F, Dellantonio A, et al. 2012. Characterization of slow pyrolysis biochars: Effects of feedstocks and pyrolysis temperature on biochar properties[J]. Journal of Environmental Quality, 41(4): 990-1000.
Lee J W, Kidder M, Evans B R, et al. 2010. Characterization of biochars produced from cornstovers for soil amendment[J]. Environmental Science & Technology, 44(20): 7970-7974.
Lehmann J, Rillig M C, Thies J, et al. 2011. Biochar effects on soil biota – A review[J]. Soil Biology & Biochemistry, 43(9): 1812-1836.
Lepine C, Christianson L, Sharrer K, et al. 2015. Optimizing hydraulic retention times in denitrifying woodchip bioreactors treating recirculating aquaculture system wastewater[J]. Journal of Environmental Quality, 45(3): 813-821.
Li R, Feng C P, Xi B D, et al. 2017. Nitrate removal efficiency of a mixotrophic denitrification wall for nitrate-polluted groundwater in situ remediation[J]. Ecological Engineering, 106: 523-531.
Li S, Cooke R A, Huang X, et al. 2018. Evaluation of fly ash pellets for phosphorus removal in a laboratory scale denitrifying bioreactor[J]. Journal of Environmental Management, 207: 269-275.
Lian F, Huang F, Chen W, et al. 2011. Sorption of apolar and polar organic contaminants by waste tire rubber and its chars in single- and bi-solute systems[J]. Environmental Pollution, 159(4): 850-857.
Liang X Q, Lin L M, Ye Y S, et al. 2015. Nutrient removal efficiency in a rice-straw denitrifying bioreactor[J]. Bioresource Technology, 198: 746-754.
Lin Y, Munroe P, Joseph S, et al. 2012. Water extractable organic carbon in untreated and chemical treated biochars[J]. Chemosphere, 87(2): 151-157.
Liu F, Wang Y, Xiao R, et al. 2015. Influence of substrates on nutrient removal performance of organic channel barriers in drainage ditches[J]. Journal of Hydrology, 527: 380-386.
Liu Z, Zhang F-S, Wu J. 2010. Characterization and application of chars produced from pinewood pyrolysis and hydrothermal treatment[J]. Fuel, 89(2): 510-514.
Long L M, Schipper L A, Bruesewitz D A. 2011. Long-term nitrate removal in a denitrification wall[J]. Agriculture Ecosystems & Environment, 140(3-4): 514-520.
Maxwell B M, Birgand F, Schipper L A, et al. 2019a. Drying–rewetting cycles affect nitrate removal rates in woodchip bioreactors[J]. Journal of Environmental Quality, 48(1): 93-101.
Maxwell B M, Birgand F, Schipper L A, et al. 2019b. Increased duration of drying–rewetting cycles increases nitrate removal in woodchip bioreactors[J]. Agricultural & Environmental Letters, 4.

Mohan D, Rajput S, Singh V K, et al. 2011. Modeling and evaluation of chromium remediation from water using low cost bio-char, a green adsorbent[J]. Journal of Hazardous Materials, 188(1): 319-333.
Mullen C A, Boateng A A, Goldberg N M, et al. 2010. Bio-oil and bio-char production from corn cobs and stover by fast pyrolysis[J]. Biomass and Bioenergy, 34(1): 67-74.
Peng X, Ye L L, Wang C H, et al. 2011. Temperature- and duration-dependent rice straw-derived biochar: Characteristics and its effects on soil properties of an Ultisol in southern China[J]. Soil and Tillage Research, 112(2): 159-166.
Pluer W T, Geohring L D, Steenhuis T S, et al. 2016. Controls influencing the treatment of excess agricultural nitrate with denitrifying bioreactors[J]. Journal of Environmental Quality, 45(3): 772-778.
Pluer W T, Morris C K, Walter M T, et al. 2019. Denitrifying bioreactor response during storm events[J]. Agricultural Water Management, 213: 1109-1115.
Pluer W T, Walter M T, Steinschneider S. 2020. Understanding Complex Flow Pathways within Lab-Scale Denitrifying Bioreactors with a Conservative Tracer[J]. Transactions of the ASABE, 63(2): 417-427.
Povilaitis A, Matikienė J. 2020. Nitrate removal from tile drainage water: The performance of denitrifying woodchip bioreactors amended with activated carbon and flaxseed cake[J]. Agricultural Water Management, 229: 105937.
Rivas A, Barkle G, Stenger R, et al. 2020. Nitrate removal and secondary effects of a woodchip bioreactor for the treatment of subsurface drainage with dynamic flows under pastoral agriculture[J]. Ecological Engineering, 148: 105786.
Ro K S, Cantrell K B, Hunt P G. 2010. High-temperature pyrolysis of blended animal manures for producing renewable energy and value-added biochar[J]. Industrial & Engineering Chemistry Research, 49(20): 10125-10131.
Robertson W D. 2010. Nitrate removal rates in woodchip media of varying age[J]. Ecological Engineering, 36(11): 1581-1587.
Robertson W D, Merkley L C. 2009. In-Stream Bioreactor for Agricultural Nitrate Treatment All rights reserved. No part of this periodical may be reproduced or transmitted in any form or by any means, electronic or mechanical, including photocopying, recording, or any information storage and retrieval system, without permission in writing from the publisher[J]. Journal of Environmental Quality, 38(1): 230-237.
Robertson W D, Ptacek C J, Brown S J. 2009. Rates of Nitrate and Perchlorate Removal in a 5-Year-Old Wood Particle Reactor Treating Agricultural Drainage[J]. Ground Water Monitoring and Remediation, 29(2): 87-94.

Robertson W D, Vogan J L, Lombardo P S. 2008. Nitrate removal rates in a 15-year-old permeable reactive barrier treating septic system nitrate[J]. Ground Water Monitoring and Remediation, 28(3): 65-72.
Rosen T, Christianson L. 2017. Performance of Denitrifying Bioreactors at Reducing Agricultural Nitrogen Pollution in a Humid Subtropical Coastal Plain Climate[J]. Water, 9(2): 16.
Roser M B, Feyereisen G W, Spokas K A, et al. 2018. Carbon Dosing Increases Nitrate Removal Rates in Denitrifying Bioreactors at Low-Temperature High-Flow Conditions[J]. Journal of Environmental Quality, 47(4): 856-864.
Ruan Y J, Luo G Z, Tan H X, et al. 2009. Nitrate and phosphate removal in sulphur-coral stone autotrophic denitrification packed-bed reactors[J]. Canadian Journal of Civil Engineering, 36(5): 923-932.
Schipper L, Vojvodic-Vukovic M. 1998. Nitrate removal from groundwater using a denitrification wall amended with sawdust: Field trial[J]. Journal of Environmental Quality, 27(3): 664-668.
Schipper L A, Cameron S C, Warneke S. 2010. Nitrate removal from three different effluents using large-scale denitrification beds[J]. Ecological Engineering, 36(11): 1552-1557.
Schmidt C A, Clark M W. 2012. Efficacy of a denitrification wall to treat continuously high nitrate loads[J]. Ecological Engineering, 42: 203-211.
Schmidt C A, Clark M W. 2013. Deciphering and modeling the physicochemical drivers of denitrification rates in bioreactors[J]. Ecological Engineering, 60: 276-288.
Sharrer K L, Christianson L E, Lepine C, et al. 2016. Modeling and mitigation of denitrification ‘woodchip’ bioreactor phosphorus releases during treatment of aquaculture wastewater[J]. Ecological Engineering, 93: 135-143.
Tangsir S, Moazed H, Naseri A A, et al. 2017. Investigation on the performance of sugarcane bagasse as a new carbon source in two hydraulic dimensions of denitrification beds[J]. Journal of Cleaner Production, 140: 1176-1181.
Tikkisetty B, Kuperus W. Environmentally friendly silage management[C]//Environmentally friendly silage management. Proceedings of SIDE Conference. South Island Dairy Event.
Tong X-j, Li J-y, Yuan J-h, et al. 2011. Adsorption of Cu(II) by biochars generated from three crop straws[J]. Chemical Engineering Journal, 172(2): 828-834.
Uchimiya M, Chang S, Klasson K T. 2011. Screening biochars for heavy metal retention in soil: Role of oxygen functional groups[J]. Journal of Hazardous Materials, 190(1): 432-441.
Uchimiya M, Wartelle L H, Lima I M, et al. 2010. Sorption of deisopropylatrazine on broiler litter biochars[J]. Journal of Agricultural and Food Chemistry, 58(23): 12350-12356.

Van Driel P, Robertson W, Merkley L. 2006. Denitrification of agricultural drainage using wood-based reactors[J]. Transactions of the ASABE, 49(2): 565-573.
Warneke S, Schipper L A, Bruesewitz D A, et al. 2011a. Rates, controls and potential adverse effects of nitrate removal in a denitrification bed[J]. Ecological Engineering, 37(3): 511-522.
Warneke S, Schipper L A, Matiasek M G, et al. 2011b. Nitrate removal, communities of denitrifiers and adverse effects in different carbon substrates for use in denitrification beds[J]. Water Research, 45(17): 5463-5475.
Woli K P, David M B, Cooke R A, et al. 2010. Nitrogen balance in and export from agricultural fields associated with controlled drainage systems and denitrifying bioreactors[J]. Ecological Engineering, 36(11): 1558-1566.
Xu B K, Shi L S, Zhong H, et al. 2019. The performance of pyrite-based autotrophic denitrification column for permeable reactive barrier under natural environment[J]. Bioresource Technology, 290: 10.
Yao Z B, Wang C L, Song N, et al. 2019. Development of a hybrid biofilm reactor for nitrate removal from surface water with macrophyte residues as carbon substrate[J]. Ecological Engineering, 128: 1-8.
Zhou H, Zhao X, Wang J. 2009. Nitrate removal from groundwater using biodegradable polymers as carbon source and biofilm support[J]. International Journal of Environment and Pollution, 38(3): 339-348.

Vita

Yuchuan Fan was grow up at city of Chengdu in southwest of China. He received his B.S. degree in Environmental Science from Southwest University. He received his M.S. degree in Soil Science from China Agricultural University. His master's thesis is titled: Effects of elevated CO_2 and nitrogen supply level on radiation use efficiency of wheat. This research prompted his early interests in the agricultural science and basic skills in laboratory and field studies.

Yuchuan served as a graduate student, and recipient of the "U.S and China Food-Energy-Water Ph.D. Innovative Program" fellowship, while obtaining his Ph.D. in Biosystems Engineering and Soil Science. His dissertation research was primarily focused on improving the nitrate removal performance in denitrifying bioreactors from vary perspectives, including filling materials, abiotic factors, and developing reliable models. His research was in water resources and hydrology with interests including water quantity/quality, nutrients and wastes management, and field-in-edge practices. He is also interested in Food-Energy-Water nexus and irrigation optimization under climate change.

Yuchuan has been actively participating in national and international conferences to present his research. He won the first place in the soils and environmental quality poster competition at the ASA-CSSA-SSSA international conference. He is a member of the Soil Science Society of America (SSSA), the American Society of Agronomy (ASA), the Crop Science Society of America (CSSA), and the International Biochar Initiative (IBI).